Modelling Soil Erosion, Flash Flood Prediction and Evapotranspiration in Northern Vietnam

DISSERTATION

for the award of the degree

"Doctor rerum naturalium" (Dr.rer.nat.)

of the Georg-August-Universität Göttingen

within the doctoral program of Geoscience/Geography

of the Georg-August University School of Science (GAUSS)

Submitted by

Nguyen Hong Quang

From Vietnam

Göttingen, February 2016

Thesis Committee

Prof. Dr. Martin Kappas, Department of Cartography, GIS and Remote Sensing, Institute of Geography, University of Göttingen

Prof. Dr. Ralph Mitlöhner, Tropical Silviculture and Forest Ecology, Burckhardt-Institute, University of Göttingen

Members of the Examination Board

Reviewer: Prof. Dr. Martin Kappas, Department of Cartography, GIS and Remote Sensing, Institute of Geography, University of Göttingen

Second Reviewer: Prof. Dr. Ralph Mitlöhner, Tropical Silviculture and Forest Ecology, Burckhardt-Institute, University of Göttingen

Further members of the Examination Board:

Prof. Dr. Hans Ruppert, Dept. of Sedimentology & Environmental Geology, Geoscience Center, University of Göttingen

Prof. Dr. Joachim Saborowski, Department Ecoinformatics, Biometrics and Forest Growth, Büsgeninstitut, University of Göttingen

Prof. Dr. Daniela Sauer, Department of Physical Geography, Institute of Geography, University of Göttingen

PD Dr. Rüdiger Schaldach, Center for Environmental Systems Research (CESR), University of Kassel

Date of the oral examination: 17.02.2016

To my father; Nguyen Ngoc Ban, my dear wife; Dang Thi Thu Hien, and my son; Nguyen Duc Vinh

Acknowledgments

Firstly, I would like to express my sincere gratitude to my supervisor Prof. Dr. Martin Kappas for his continuous support of my PhD study, especially in the embryo stage before I had got the financial support from the KAAD, as well as for his patience, motivation and immense knowledge. His guidance has helped me throughout my research as well as with the writing of papers and with this thesis as well. My special thanks go to my second supervisor, Dr. Stefan Erasmi, for his able guidance and support during my stay at the institute.

Besides my supervisor, I would like to thank the rest of my thesis committee; Prof. Dr. Ralph Mitlöhner, Prof. Dr. Hans Ruppert, Prof. Dr. Joachim Saborowski, Dr. Daniela Sauer, and PD Dr. Rüdiger Schaldach for their insightful comments and encouragement, but also for the hard questions which motivated me to broaden my research from various perspectives.

My great thanks go to all my colleagues at the Department of Cartography, GIS and Remote Sensing, Institute of Geography, Goettingen University for supporting and assisting me spiritually and academically during my study time in Germany, namely Dr. Ammar Rafiei Eman, Dr. Jan Degener, Dr. Michael Klinge, Dr. Nguyen Khanh Linh and MSc. Elbek Erdanaev for their incorporation, many valuable discussions and proofreading the papers and the thesis. My sincere thanks go to the secretary Mrs. Martina Beck, who is always smiling and who helped me with all the documents and facilities I needed.

My research would not have been possible without various data sources. I would like to thank very much the Vietnamese Environment and Resources Corporation, the Vietnamese National Center for Hydro-Meteorological Forecasting for providing topographical and meteorological data, respectively, and the Numerical Terradynamic Simulation Group (NTSG) at the University of Montana for providing the MOD16 ET datasets.

Gratefully, I would like to acknowledge Katholisher Akademischer Ausländer–Dienst (KAAD) for not only their financial support but also the opportunities to attend conferences and seminars held by KAAD, all of which helped me very much to overcome the hardest stages of my study by exchanging experiences with the people in the KAAD scholar's circle.

Last but not least, none of this would have been possible without the love of and patience of my family. No words can express how grateful I am to my parents for giving birth to me and supporting me spiritually in my life. I would like to express my heartfelt gratitude to my parents in law for their enormous care and encouragement. This dissertation would not have been completed without the abundant love and continuous support of my wife Dang Thi Thu Hien and my son Nguyen Duc Vinh.

Preface

The present thesis “Modelling Soil Erosion, Flash Flood Prediction and Evapotranspiration in Northern Vietnam” has been submitted in partial fulfilment of the requirements for the Ph.D. degree at the University of Göttingen (Germany). The main supervisor was Prof. Dr. Martin Kappas and the second supervisor was Dr. Stefan Erasmi.

The thesis consists of an introduction to the research objectives and questions, a general literature review, a brief of the study site’s characteristics, five manuscripts and a summary and conclusion.

The study was conducted at the Department of Cartography, GIS and Remote Sensing from April 2012 to February 2016.

Göttingen, February 2016
Nguyen Hong Quang

Table of Content

List of figures

List of tables

Abbreviations

Acronyns	Definition
AMP	Annual Mean Precipitation
ANSWERS	Areal Nonpoint Source Watershed Environmental Response Simulation
ARMA	AutoRegressive Moving Average model
BEACH	Bridge Event And Continuous Hydrological model
CN	Curve Number method
CSA	Critical Source Area
DEM	Digital Elevation Model
DWD	German National Meteorological Service
DWSM	Dynamic Watershed Simulation Model
E	Evaporation
Ea	actual Evaporation
ET	EvapoTranspiration
ET_0	potential EvapoTranspiration
ETa	actual EvapoTranspiration
FAO/UNESCO	Food and Agriculture Organization of the United Nations Educational, Scientific and Cultural Organization
FF	Flash Flood
FFGS	Flash Flood Guidance Systems
FV	Flow Velocity
GIS	Geographical Information System
GSM	Global Spectral Model
HEC-RAS	Hydrologic Engineering Center's River Analysis System
HOF	Horton Overland Flow
HRM	High Resolution Model
HRU	Hydrologic Response Unit
HSPF	Hydrologic Simulation Program–FORTRAN
JMA	Japan Meteorological Agency
KINREOS2	KINEmatic Runoff and erOSion model
LOX WFO	Los Angeles-Oxnard Weather Forecast Office
LULC	Land Use/Land Cover
MAD	Mean Absolute Difference
MODIS	Moderate Resolution Imaging Spectroradiomete
MSs	Meteorological ground Stations
MUSLE	Modified Universal Soil Loss Equation
NCHMF	Vietnam National Centre for Hydro-Meteorological Forecasting
NIAPP	National Institute of Agricultural Planning and Projection
NSE	Nash-Sutcliffe Efficiency coefficient

NWP	Numerical Weather Prediction
NWS	National Weather Services
P	streamflow Power
PhD	Doctor of Philosophy
Q	River Discharge
RAD-P	RADar-based Precipitation
RC	coRrelation Coefficient
RMSE	Root-Mean-Square Error
ROCE	RunOff Coefficient Error
RS	River cross Section
SAT-P	SATellite-based Precipitation
SCS-CN	Soil Conservation Service-Curve Number
SeF	Sediment Flow
SGs	Stream Gauges
SHE	Systeme Hydrologique European
SR	Surface Runoff
ST	Sediment Transport
SWAT	Soil Water Assessment Tool
SY	Sediment Yield
TIN	Triangulated Irregular Network
TSeF	Total Sediment Flow
USLE	Universal Soil Loss Equation
Vinanren	Vietnam Natural Resources and Environment Corporation
VNERCAIPD	Vietnam Resource Centre-Agricultural Institute of Plan and Design
WASMOD	WAter and Snow Balance MODelling System
WB	Water Balance error
WEPP	Water Erosion Prediction Projection
WL	Water Level
WSE	Water-induced Soil Erosion
YBS	Yen Bai custom Soil map

Abstract

Water-induced soil erosion (WSE) is a main factor of land degradation in many parts of the world and reported as a main threat to agriculture compared to the second largest risk by wind. Some parts of Vietnam have been suffering WSE rates of over 50 t ha year^{-1} (t ha^{-1} y^{-1}), (particularly in the North) which has negative effects on the agriculture. In addition, Vietnam is a developing country and most of the resident livelihoods are based on agriculture. However, due to a lack of information about both spatial and rates of WSE in the region, the soil erosion mitigation efforts seem to be inadequate. Furthermore, far too little attention has been paid to soil erosion modelling in the tropics in general and in the North of Vietnam in particular.

In the first part of this research, surface runoff investigation and WSE evaluation were targeted employing the hydrological modelling methodology and the so-called "regionalization approach" for generating the results of calibrated watersheds to uncalibrated ones. This makes a regional scale (for the SWAT application) from watershed scale. The KINEROS2 model was also used for modelling WSE at finer event-based and watershed scale. In the results of model calibration and validation, both the SWAT and KINEROS2 presented their capabilities to generate simulated discharge matching closely to observed data. Although the mean estimated WSE rate was 4.1 t ha^{-1} y^{-1}, approximately 15% of the Yen Bai province was computed at the rate of 8.5 t ha^{-1} y^{-1}. Attention was given to the changes in land use/land cover (LULC) conditions (2002-2009) which have had a growth of the WSE rate from 0.2 to 3.3 t ha^{-1} y^{-1} in some areas of the province. This scenario was also found in the results of the KINEROS2 model but for the LULC conditions in 2002 and 2007.The KINEROS2 parameter sensitivity tests indicated that the model's outputs were very sensitive to the antecedent soil moisture condition (θ_{ant}) and the hydraulic conductivity (Ksat). This reveals a need of estimates θ_{ant} for later applications of the model such as for flash flood (FF) prediction.

Flash flooding is responsible for severe loss of life and property in lots of countries. Increases of the surface runoff not only speed up the erosive processes, but also intensify the FF risk. Many parts of Vietnam have been confronted with increasing FF consequences but the situation is much worse in northern Vietnam. Due to the fact that FF often occur in small streams and are linked to short, but heavy rains, much previous research has suggested methods to identify FF occurrences early in order to mitigate their impacts.

Approaches with assembled and coupling hydrological models were used for the aim of FF prediction. The assembly of the SWAT, BEACH and KINEROS2 models filled up the hole of lacking θ_{ant} and defined well the boundary conditions for the KINEROS2's runs. The model sensitivity tests played a crucial role due to its shortening the model calibration and validation

processes. To implement the latter method, the results of the KINEROS2 models serve the HEC-RAS inputs such as the hydrographs, river depths, initial flow and Manning's n coefficient. What is interesting is that I also used several rainfall sources (satellite, radar, NWP, and gauge) to test and compare their abilities of application with the aim of FF forecast.

With the calibrated parameters the KINEROS2 model computed the river discharge (Q) fitting well to observed data (average NSE $\approx$ 0.78, $R^2 \approx$ 0.93). The daily soil moisture calculated by BEACH was very helpful for the assembly because changing of the θ_{ant}, Ksat, and N varied the model outputs dramatically. Remarkably, KINEROS2 predicted the Q (in streams and overland) using GSM and HRM rainfalls revealed a good possibility to predict the time, magnitude and location of approaching FFs. The most surprising result is that the use of radar rainfall produced less accurate Q compared to the use of satellite precipitation.

The results of coupling the KINEROS2 and HEC-RAS models provide a more in-depth analysis of FF behaviour based not only on river discharge but also on flood water level (WL) or stage, flow velocity (FV) and power (P) at river cross sections (RSs). First, the models were calibrated and validated for four rainfall events for the Q and WL with satisfactory results (mean NSE $\approx$ 0.85, $R^2 \approx$ 0.91 for the Q, and mean NSE $\approx$ 0.82, $R^2 \approx$ 0.90 for the stage). A comparison between the rating curves and river banks showed the stream flow was approximately two metres over the banks during the rain on 23rd June 2011 at the outlet of the Nam Kim e.g. relationships between FV and channel slope, between top width, flow area and FV were analysed in detail. The most striking result to emerge from the HEC-RAS forecasted outputs is that the predicted Q and WL agreed basically with the *in situ* measurements but there have been some false/missing alarms. There is also much valuable discussion on uncertainty, methodical efficiency.

The last objective is focusing on modelling evapotranspiration (ET). The ET is considered to have played a crucial role in the hydrological cycle linking as well to the above-mentioned issues of WSE and flash flooding. The modelled ET data were compared to MODIS ET. The BEACH's parameters were calibrated for the 2001-2004 periods and validated for 2005-2012 periods using observed evaporation. Although the MODIS ET was higher than the SWAT and BEACH ET, a general fine agreement between them was found based on both monthly and yearly ET. A slightly downward trend of all ET in the 2001-2012 periods has been shown in the trend analysis. However, longer investigation of trend analysis might be needed to verify this trend (40 years for example).

CHAPTER 1

Introduction

"Most of the fundamental ideas of science are essentially simple, and may, as a rule, be expressed in a language comprehensible to everyone."

- Albert Einstein

1.1 General Introduction

In recent years, there has been increasing interest in water-induced soil erosion, flash flooding and evapotranspiration which are all results and parts of surface water processes and closely linked to the water cycle elements.

Land is considered to be the most basic geographic component in the growth and development of the earth's biophysical resources (Bakimchandra, 2011). Consequences of soil erosion increase the risk of declining land availability and fresh water available per capita. Therefore, food security and sustainable development are important problems in the low available land per capita countries (Dercon et al., 2012) such as in Vietnam. The main causes of soil erosion are environmental degradation, such as deforestation, intensified land use, and the increasing world population (Ahmed et al., 2010), climate and morphological conditions, for instance high intensive rainfall, steep hillslopes. Formerly in tropical regions, the top soil layer was often protected by dense vegetation cover, root systems (Kefi et al., 2011). However, the impact of land cover changes and unsustainable agricultural practices in recent decades appear as the main effects on land degradation (Baja et al., 2009, Cerda et al., 2007) and which has been estimated increasingly in recent decades. Soil erosion presents the main threat to agriculture in Yen Bai province, Vietnam, where most people's livelihoods are based on cultivation and the population density is statistically about 104.5 people per km^2 in 1997, according to the (Vn-Atlas, 1997). Despite all the important aspects of soil erosion, few modelling attempts have focused on the tropics, particularly in developing countries where available data is often sparse and much work needs to be done for the better understanding of soil erosion processes in tropical regions (Ndomba et al., 2008).

Soil erosion is not only an environmental problem in Vietnam as a whole and in Yen Bai province in particular, but also flash flooding is a major threat to human life and property damage. Flash floods are defined here as extreme floods produced by intense precipitation

over quickly responding catchments and happen within six hours of the causal rainfall events. They have recently drawn increased attention, both from the scientific community and from the media due to their devastating consequences (Brauer et al., 2011, Gupta, 2006, Unkrich et al., 2010). In general, FFs are rare and variable in time, space and the magnitude of occurrences and therefore prediction methods which are based on extensive rainfall-runoff information are hardly satisfactory (El-Hames and Richards, 1998) or subjected to uncertainty and a failure in the predictive behaviours of FFs of exiting models is not rare (Garcia-Pintado et al., 2009). However, in the tropical climate regions of Vietnam, FFs have been occurring more frequently. Among 29 provinces in Northern Vietnam, eighteen have extensively occurred, leading to more than 500 people dead or missing. Additionally, thousands of people have been made homeless, millions of tons of fertile soil, properties, crops and livestock have been lost over the last two decades, according to the report of (NCHMF, 2011). Although the uncertainty in FF prediction remains, thanks to more data availability (Bloschl et al., 2008), the advancement of GIS and hydrological-distributed models are able to provide FF predictors with a tool that can forecast the timing (near/real-time) and magnitude of peak flows in high-risk zones better which determine the FF occurrence (Carpenter et al., 1999; Lin et al., 2002; Platt and Cahail, 1987; Unkrich et al., 2010; Yatheendradas, 2008). On the one hand, many studies have been conducted on modelling flash floods and have attempted to forecast them (Borga et al., 2014, Naulin et al., 2013, Versini, 2012) to name a few, however, far too little attention has been paid to tropical-mountainous catchments (Khavich and Benzvi, 1995) which may be explained by the complex characteristics of FF and data scarcity obstacles (Montz and Gruntfest, 2002).

Globally, more than half of the solar energy is used to evaporate the surface water to the atmosphere (Jung et al., 2010) from a bare surface, from water bodies (evaporation) and from the trees (transpiration). Evapotranspiration is defined as the combination of these two processes (Kisi et al., 2015). As ET plays as a key role in the water and energy cycles (Vanderhoof and Williams, 2015), changes in ET can directly result in altering stream discharge (Likens et al., 1994), air temperature (Tian et al., 2013, Sun et al., 2012) and cloud development (Bala et al., 2007). Besides, there is still an increased demand for research into ET at different scales (global to local) as it is related to other fields such as agronomy, agrology, meteorology and hydrology.

Why are the study objectives of soil erosion, flash flood and ETa becoming more important? Land use/land cover changes including deforestation, agricultural practices,

climate change and urbanization have had a direct influence on hydraulic response such as the increase of surface runoff (intensively effecting soil erosion and flash flooding) (Suriya and Mudgal, 2012, Kefi et al., 2011, Benito et al., 2003), reducing infiltration and soil moisture (Parise and Cannon, 2012, Ziegler et al., 2007) (effecting a decline of ET) etc. The situation is much worse in North Vietnam where cultivation shifting and unsustainable agricultural practices are taking place. Hence, the study objectives are especially motivated. This aim of this research includes the following objectives.

1.2 Research Objectives

The main goal of this research is to model long-term and event-based water-induced soil erosion, flash flooding and evapotranspiration using hydrological models.

Specific objectives are:

a. Evaluating long-term annual soil erosion and surface runoff rates employing the SWAT model for the study site, mapping soil erosion patterns and their changes due to land use/land cover changes in a 12-year period, from 2001 to 2012.
b. Modelling event-based soil erosion, downscaling to small and medium watershed scale applying the KINEROS2 model.
c. Predicting flash flood occurrence in gauged and ungauged watersheds using the KINEROS2 model and forecast rainfall.
d. Downscaling FF prediction in river reaches based on simulated river discharge, water levels, flow velocity and stream power by coupling the KINEROS2 and HEC-RAS models.
e. Modelling daily actual evapotranspiration using the SWAT, the BEACH and comparing the estimated monthly and yearly ETa with the MODIS product.

1.3 Research Questions

This research seeks to address the following questions:

- What were the annual soil erosion and surface runoff rates in the Yen Bai province from 2001 to 2012 and were they increasing in that time period?
- Can the hydrologic models of the SWAT and KINEROS2 be calibrated and validated for a tropical region (they were originally developed for arid climate regions) and are they applicable for soil erosion modelling purposes in the tropics (noted that few attempts have been made for tropics)?

- Which model parameters of the SWAT and KINEROS2 are sensitive to surface runoff and sediment yield?
- Could flash floods in complex mountainous watersheds be forecasted using the modelling approach (referring to using the SWAT, KINEROS2 and HEC-RAS models)?
- What are the rates of evapotranspiration in the Nam Kim watershed?
- Are there any correlations between the SWAT, BEACH and MODIS ET and what is the overall trend of the ET?

1.4 Overview of the Thesis

This section provides an overview of the content of each chapter and a quick snapshot to understand how the study objectives are accomplished and, in addition, a study framework is demonstrated in the Fig. 1-1. This dissertation is a cumulative version and divided into eight chapters (chapters 3 to 7 have been written in the scientific manuscript structure).

Chapter 1: This chapter presents the basic background in the research proposal development. An overall introduction of research problems, objectives and questions is addressed. In addition, the fundamental concept, literature and approaches are also introduced.

Chapter 2: This chapter provides information about the study area including location, land use, climate, and some relevant social information.

Chapter 3: An application of the SWAT model for the aim of modelling surface runoff and soil erosion and sediment yield for watersheds in Yen Bai province. Input data preparation, model calibration and validation[1], model parameters sensitivity test, result analyses of runoff and maps of changes in soil erosion affected by different LULC conditions are presented in this chapter. The results are discussed and compared to relevant literature[2].

Chapter 4: This chapter provides a deeper look at erosive process in two medium watersheds in Yen Bai province by modelling one rain event using the KINEROS2 model. Satellite and radar rainfalls were input for testing the effect of different rainfall sources on estimated sediment yield. Some sensitive variables of relative saturation index, plane and stream

[1, 2] these tasks also have been done in the next chapters of 4,5,6 and 7, therefore, they are not repeated in this section

roughness coefficients and model resolution were examined to gauge to what extent their impact had on sediment yield and transport. Finally, different LULC conditions in 2002 and 2007 which affected sediment yield were mapped and compared.

Chapter 5: First, in this chapter the past flash flooding event was modelled using the KINEROS2 model and then abilities of the model were investigated in forecasting flash floods based on modelling forecasted river hydrographs and discharge, and historical thresholds. Different flooding scenarios with different satellite, radar and forecast rainfalls were modelled. As antecedent soil moisture was extremely sensitive to modelling discharge, the BEACH model was used to obtain this significant information.

Chapter 6: Downscaling flash flooding modelling aims to look closely at flooding behaviours in streams such as flow velocity, water levels, flow power and shear stress can be found in this chapter. The method of coupling the KINEROS2 and HEC-RAS models and relationships between discharge and water levels, between flow velocities, channel slope and top width and between flow velocity, power and shear stress are represented. The results of coupling the models reveal an opportunity to predict FF occurrences using forecast rainfalls.

Chapter 7: This chapter presents the daily modelled evapotranspiration by the SWAT and BEACH models and comparisons between them and MODIS ET are also depicted. In the 2001-2012 periods, the overall trend monthly of the SWAT, BEACH and MODIS ET was analysed.

Chapter 8: This section will summarize the results and state some research contributions, limitations and recommendations for the future work.

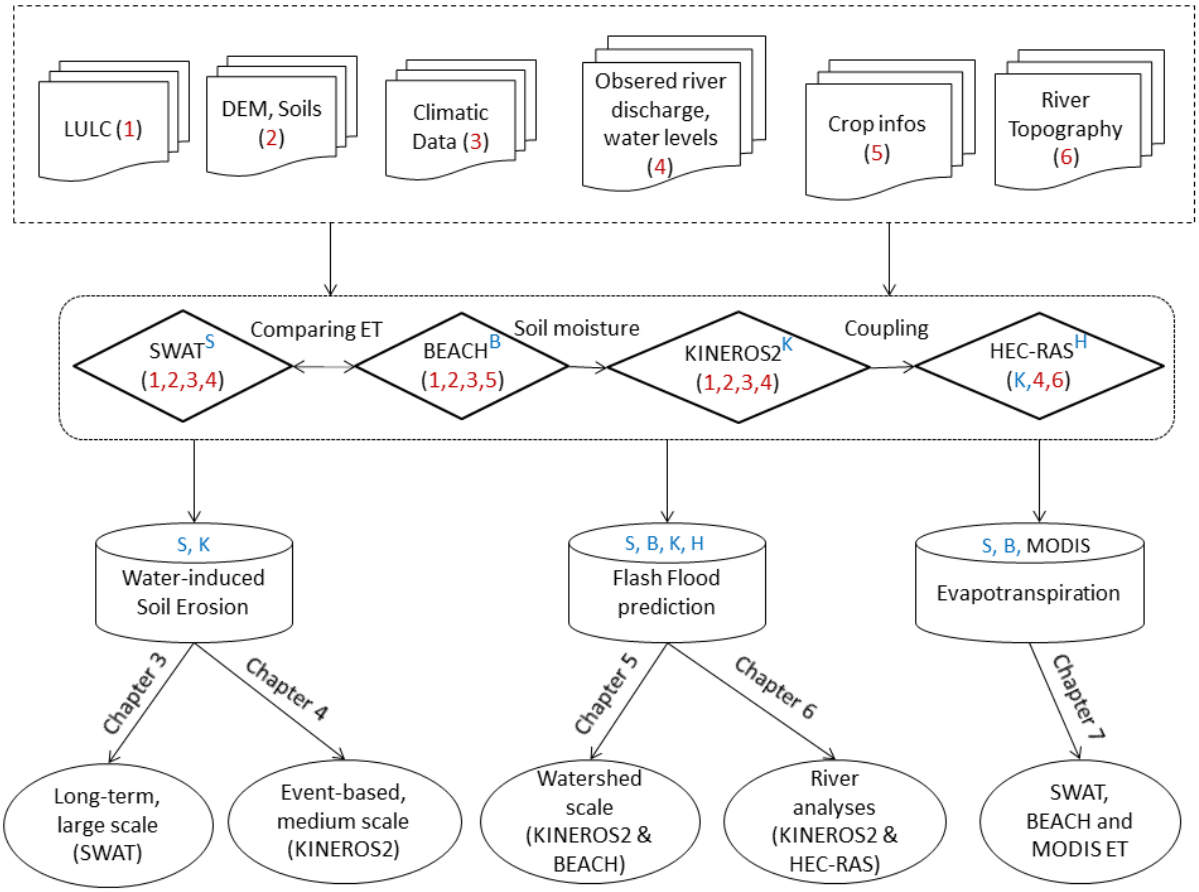

Figure 1-1. The overarching study flowchart of the modelling soil erosion, flash flooding and evapotranspiration.

1.5 Concept, Literature Review and Methodology

The methodology, concept and literature about the study objectives and relevance are discussed in more detail in the following chapters; hence hereby an overview is highlighted only.

1.5.1 Soil Erosion

The problem of soil erosion was certainly recognized a long time ago by local farmers cultivating their soils in Burkina Faso They had already used a “runoff-farming” technique by canalizing rainfall water (Schmitt, 1987). The detachment, transport and disposition of soil particles by the erosive forces of rainfall and surface flow are known as processes of water erosion (Batjes, 1996). To date, soil erosion science has been advanced and the physical and dynamic processes of soil erosion have been analysed, modelled at different scales ranging from the minimum laboratory scale (Fister et al., 2012, Momber, 1998), plot/slope scale (Anh et al., 2014, Bryan, 2000), small (Starkloff and Stolte, 2014, Cooper et al., 2012, Momber,

1998), large basin (Mchunu and Chaplot, 2012) to global scale (Pham et al., 2003, Batjes, 1996). The smaller scales might be feasible for on-site or direct measurement approaches but with larger scales indirect methods such as modelling, using remote sensing or other indicators of soil erosion could be more appropriate. The latter approach would be costly, time consuming and sometimes implementable if applied to large areas and long-term assessment.

Referring to ***cautions*** of soil erosion, previous literature has shown two sources of wind and water (runoff and waves) and both types of soil erosion are related to land degradation (Borrelli et al., 2014). However, the wind erosion assessment is out of the scope of this research. Not only the short-term activities (agricultural practices), medium alternations (changing of land use structure), but also the long-term change of the climate resulting in more extreme rainfall events have been contributing to the soil erosion exaggeration (Routschek et al., 2014) and all these changes are considered linked to the human-induced activities.

In the ***general background*** in Europe, the risk of soil erosion is predicted to increase to about 80% of the area of European agricultural land by the year 2050 (EEA, 1999) and this is seen as the main cause of land degradation (David et al., 2014). In developing countries like in Asia, Africa and South America, the soil erosion rate is approximately 30-40 t ha^{-1} $year^{-1}$ (t ha^{-1} y^{-1}) (Barrow, 1991). However, Asia suffered the rate of 138 t ha^{-1} y^{-1} (Sfeir-Younis, 1986). In Vietnam, the soil redistributions varied from area to area but in the North the problem seems to be more serious in general. There have been some studies on soil erosion conducted for regions of Vietnam (Anh et al., 2014, Ranzi et al., 2012) and others on runoff (Vu et al., 2012, Ziegler et al., 2007, Ziegler et al., 2006, Ziegler et al., 2004). Unfortunately, there is no study (at finer scale) or measurement of soil erosion conducted in Yen Bai province (the study area of this research).

1.5.2 Land Degradation, Land Use Changes and Climate Change

These aspects are reviewed here due to their strong relationships to the study objectives. The term “land degradation” is understood as a decrease in the capacity of biological and economic productivity of the land both by human and natural impacts. The land degradation is accelerating worldwide, but in the developing countries the rates are double the global average (UNCCD, 2013). Wherein, water erosion plays the most important role in land degradation, and this is followed by wind erosion, chemical and physical degradation (Batjes, 1996). In addition, the land has been pushed under the pressure of an increasing world

population, expected to reach 9.3 billion by the year 2050 which leads to the serious problem of food security, inadequate infrastructure and scarcity of freshwater resources (Dercon et al., 2012). While the world population has increased 3.8 times since the beginning of this century, Vietnam's population increased 5.8 times and this pressure of population growth on land is getting to a critical threshold (Huyen, 1993).

LULC information (including characteristics and distribution) is widely used and is an indispensable data for monitoring environmental problems and their risks (Bakimchandra, 2011). Changes in LULC are mostly due to human-made activities and they could have significant impacts on hydraulic behaviours such as surface runoff, infiltration, transpiration and eventually on soil erosion and flooding. Many studies focus on the impact of the changes to environmental degradation but less research have been done for mitigation because of gaps between politics and sciences, between sustainable and economic developments, especially in developing countries. One of these research objectives is to investigate to what extent the LULC changes will affect estimated soil erosion and surface runoff rates.

More extreme precipitation events resulting in an increase in flooding risk is commonly known due to climate change (Tripathi et al., 2014). In addition, many studies have been carried out using statistical approaches to evaluate hydrological responses. However, climate change is altering annual hydrological routines like flooding routine in both global and local scales (Moradkhani et al., 2010). This might increase the uncertainty of the statistical method in the future. Nonetheless, physical-based approaches could be appropriate such as physical-based distributed modelling particularly for flood prediction (Reed et al., 2007) in comparison with lumped models.

1.5.3 Flash Flooding

The concept of flash flood is defined as rapid surface water responses to precipitation from intense thunderstorms or an unexpected release of water from a dike or ice jam[3] (Calianno et al., 2013). Typically, FFs occur in quick response watersheds for two main reasons of short concentration time and fast responding runoff processes (Versini, 2012), a few hours after rainfall peaks (4 to 6) and are the deadliest and costliest natural disasters worldwide (Kourgialas et al., 2012). One of the effective mitigations is to predict location and time of FF occurrence (Looper and Vieux, 2012) for emergency responders. That is why we need to predict FF occurrence.

[3] FF caused by dam break or ice jam is out of this study scope

The common term related to FF mitigation effort is from Flash Flood Guidance Systems (FFGS) such as those of the USA, France, and Italia. They are in cooperation with National Weather Services (NWS). Basically, the FFGS are working and relying on an advance rainfall estimation technique (Satellite, Radar for example), Numerical Weather Models (NWM) forecasting precipitation, and hydrological models, for example.

Due to the complexity of FF processes (highly non-linear) and short lag time, questions of ***uncertainty*** are often addressed when it comes to FF prediction. The errors could come from many sources but virtually from estimated rainfall, hydrological models and evaluated thresholds (Quintero et al., 2012). The USA national average value of FF accuracy is 69 percent (31 percent for false/missing alarm) but the best system was of the Los Angeles-Oxnard Weather Forecast Office (LOX WFO) with 79 percent (Smith et al., 2005).

Vietnam is reported to be a nation which has a high frequency of FF events and is under pressure of fatal loss and economic damage. Despite this, officially, there has been no FF early warning system established in Vietnam. The local people deal with the FFs in their own way of "dodging" based on their own experiences. However, as mentioned above, the climate change and LULC changes are affecting the flooding behaviours (Nguyen Van Tai et al., 2009) resulting in difficulty for local people to adapt. Most attempts have paid attention to paleoflood and their impacts on social aspects such as (Schad et al., 2012, Wickramanayake, 1994). On the other hand, very little research (based on current search engines) has been conducted for flash flood prediction in Vietnam.

1.5.4 Evapotranspiration

Evapotranspiration (ET) can be defined as water from the soil transferring to vapour in the atmosphere. ET consists of two processes of evaporation from a non-vegetation surface and transpiration from crops (Allen et al., 1998). Evapotranspiration plays a crucial role in the hydrological cycle such as accurate estimates of ET could be important data sources for runoff, soil moisture and crop productivity prediction (Zhan et al., 2015). In addition, accurate information of temporal and spatial variations in ET and rainfall might help to improve the understanding of interactions between the atmosphere and land surfaces. In ET estimation expectation, there are two methods of direct measurement and indirect evaluation of ET. Field measurements reveal a limitation at point observations and are costly when conducted for a large area, nevertheless gain higher accuracy. In contrast, indirect approaches such as the use of a remote sensing technique and modelling can be conducted for larger scales at lower cost. However, due to the low level of observed ET availability, it is extremely difficult to validate

the estimates of the second method. Once this obstacle is overcome, the results could be valuable (as in this study).

1.5.5 Study Methodology in an Overview

As details of methodology/applied models to achieve specific objectives are indicated in following chapters of 4, 5, 6 and 7, this section will provide general information regarding the modelling approach.

Hydrological Modelling History at a Glance

The real world system related to hydrology could be simply represented by a hydrological model (Moradkhani and Sorooshian, 2008). The first generation of hydrologic models was in the middle of the 19th century with a focus on three types of engineering problem: (1) urban sewer, (2) land reclamation drainage system, and (3) reservoir spillway designs. In the early 20th century, the first basic rainfall-runoff model based on a transfer function was developed to cope with non-uniform distribution, in space and time of rainfall and catchment characters. In the middle of the 20th century, it was the time of the conceptual models' development and in the 1950s hydrologists revolved the "unit hydrograph" problem introduced by the American engineer Sherman in 1932 (for more details see (Xu, 2002a)). At the beginning of the 1980s advances in three-dimensional modelling by linking physically-based distributed-parameter models with Digital Elevation Model (DEM) solved the problems of hydrological forecast, effects of land use changes and spatially variable inputs and outputs, and hydraulic responses of ungauged catchments etc. Finally, from the late 1980s up to the current situation, hydrological modellers have been attempting to deal with macro-scale hydrological models for various fields. However, many studies focus on mitigation, management of natural hazards/resources with interactions of GIS and remote sensing techniques (Xu, 2002).

Hydrological Model Classification

There are a vast number of hydrological models and they could be classified into three groups based on process description, spatial representation and randomness (Fig. 1-2). However, models could be a mixture of these groups. Empirical or black-box models work are based on observations or experience (Solomatine and Wagener, 2011) and do not aid in physical understanding such as the ARMA (autoregressive moving average) model developed by (Gave and Lewis, 1980). In intermediation between theoretical and empirical models are conceptual models and they are sometimes called grey-box models, the Water and Snow Balance Modelling System (WASMOD) developed by Xu et al., (1996) cited by (Xu, 2002b)

is an instance of a stochastic-conceptual hydrological model. Physically-based models compute flows and energy fluxes from prevailing partial equations and they could be semi/ fully distributed-parameter deterministic models and applied for meso or regional scales. The Systeme Hydrologique European (SHE) (Abbott et al., 1986), TOPMODEL (Beven and Kirkby, 1977) and KINEROS (Smith et al., 1995) are some examples of physically-based, distributed models. While lumped parameter models present an entire river basin in one unit, the spatial variability of the basin is represented by distributed parameter models like the SWAT model (Arnold, 1994, Arnold and Williams, 1995), etc.

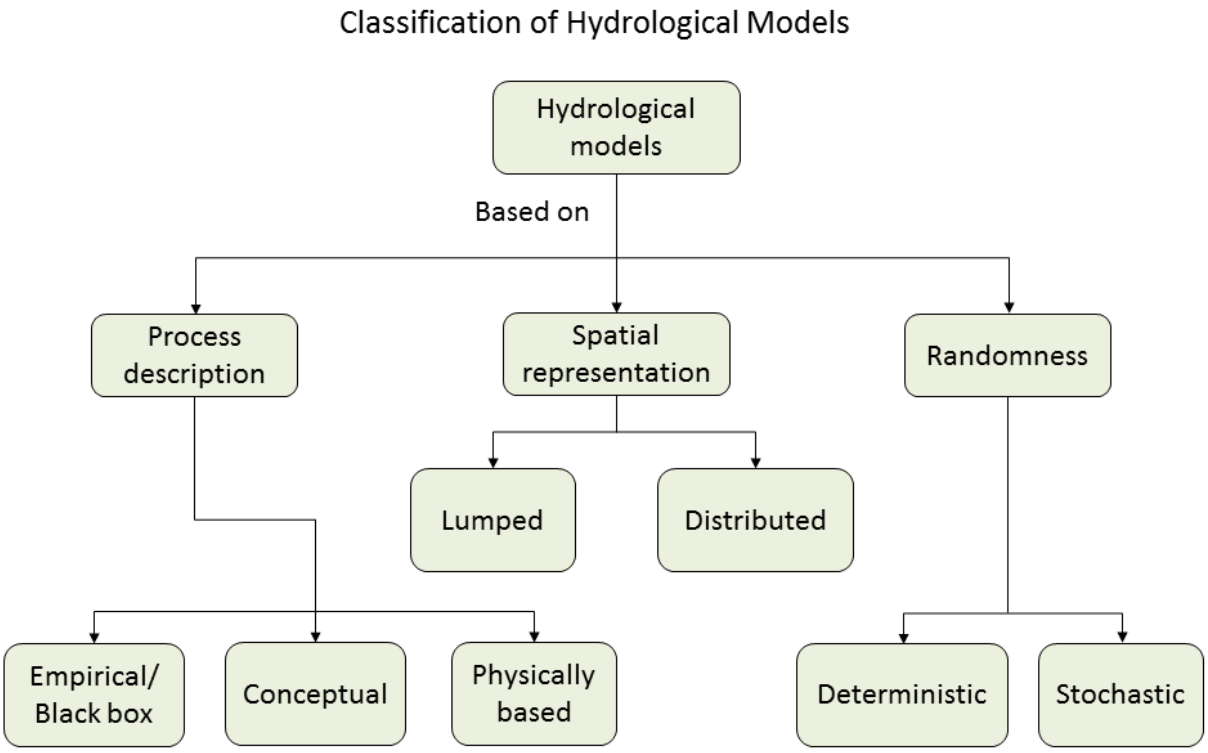

Figure 1-2. Hydrological model classification

Uncertainty

As mentioned earlier, hydrological models represent simply real hydraulic systems, the errors of which therefore exist naturally. Uncertainty could be understood similarly to some terms such as doubtful, questionable, vague, liable to vary or change, not steady or constant and varying (Solomatine and Wagener, 2011). However, what is an acceptable uncertainty. It might depend on the aims of the modelling. Absolutely, we need to examine. Therefore, uncertainty analyses are necessary for every modelling implementation. The uncertainties are often induced from the input and forcing data, initial and boundary conditions, model

structure and parameters. Song et al., (2015) showed the dependency of the model structure, input and parameter uncertainty on the model complexity (Fig. 1-3).

Recently, a number of approaches have been introduced in the literature to evaluate model uncertainty of hydrological model applications. According to Solomatine and Wagener (2011), they could be classified into several categories of; (1) analytical methods (e.g. Tung, 1995); (2) approximation methods such as first-order second moment method of Melching (1992); (3) simulation and sampling-based (Monte Carlo) methods like the GLUE method (Beven and Binley, 1992); (4) approach based on the past model error analysis and either employing distribution transforms or building a forecast machine learning of uncertainty (Shrestha and Solomatine, 2008); and (5) approach based on fuzzy set theory (e.g. Maskey et al., 2004). In addition, some common uncertainty analysis objectives are absolute relative bias (ARE), Mean Absolute Difference (MAD), Nash-Sutcliffe efficiency coefficient (NSE), correlation coefficient (RC), root-mean-square error (RMSE), Runoff coefficient error (ROCE), water balance error (WB) and the model coefficient of determination (R^2).

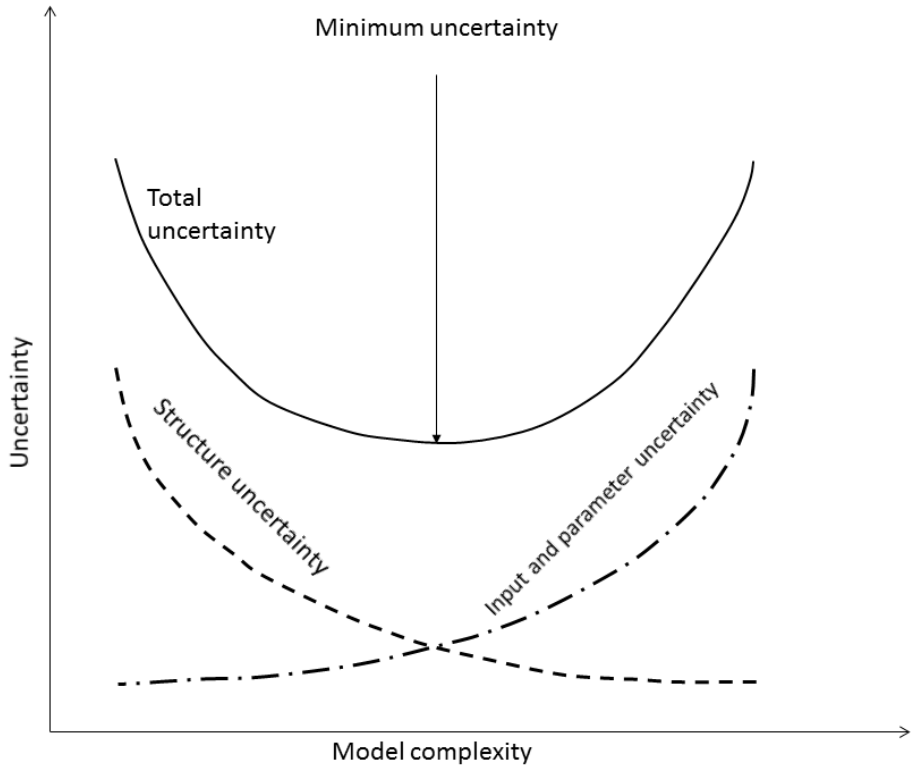

Figure 1-3. Dependency of model structure, input and parameter uncertainty on the model complexity (Adopted from Solomatine and Wagener (2011)).

Hydrological Models Applied for this Research

Hydrological modelling is considered a valuable approach (e.g. soil erosion estimates, flooding prediction) and applied thoroughly in this PhD research. The hydrological modelling method has not only been a long-term development but has been widely used. Using this approach also could satisfy the research needs of long-term assessments, various temporal and spatial assessments and prediction operations as well. Choosing appropriate models meeting research needs is a challenge, especially as they could be "interactive" with each other as in the Fig. 1-1. Furthermore, regarding the uncertainty evaluation and data availability (Figs 1-3 and 4), I selected the four models (summarized in Table 1-1) for achieving the research goals. In this study, the NSE, R^2 and graphical comparison were firmly used for accuracy assessments.

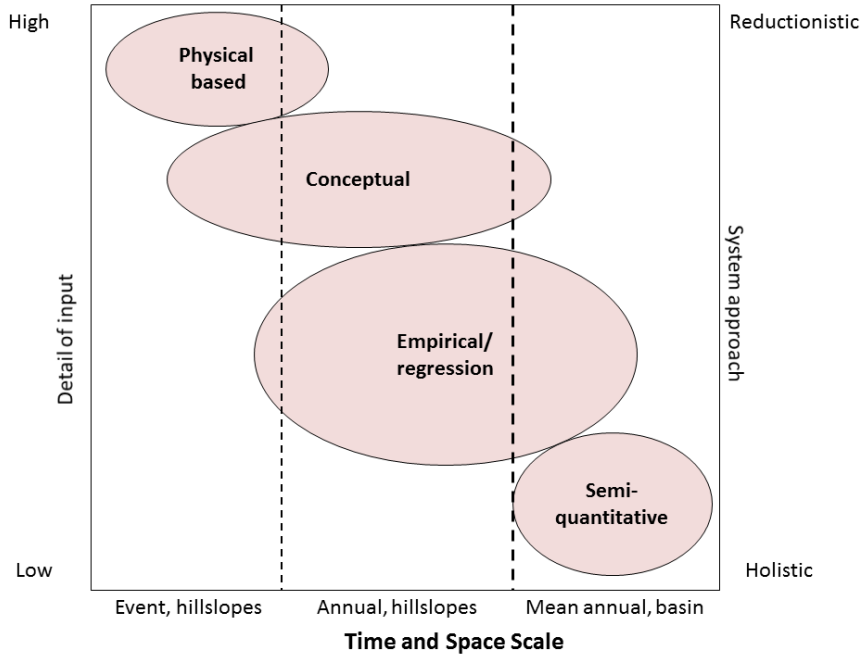

Figure 1-4. Hydrological model classification based on input requirement, system approach and time and space scale (Adopted from de Vente and Poesen (2005)).

General Introduction to the Models Used in this Research

The Table 1-1 shows information about three widely-used models of the SWAT, KINEROS2 and HEC-RAS and the BEACH model. It should be noted that this information was derived from collected literature and could be changed in the future due to quick upgrading of the models. The applications of each model in this research are clearly shown in the Fig. 1-1. In addition, some Numerical Weather Prediction (NWP) models of the Global Spectral Model (GSM) (Krishnamurti et al., 2006) and the High Resolution Model (HRM) (Majewski, 2009)

were used for flash flood prediction stage in terms of providing the forecast rainfalls. Some ArcGIS-ModelBuilder-based models developed by this study's author were used for processing the satellite and radar-based rainfalls.

Table 1-1. Meta data of the SWAT, KINEROS2, BEACH and HEC-RAS models.

Models	**Descriptions**	**Developers**	**Types**	**Time and space scale**	**Main related outputs**
SWAT	Soil Water Assessment Tool	Arnold, 1994, Arnold and Williams, 1995	Physically based, Semi-distributed	➢ Hourly, daily, annual, long-term. ➢ River basin, watershed, scale	Runoff, sediment yield, ET, percolation, transmission loss, etc.
KINEROS2	KINEmatic Runoff and erOSion model	(Smith et al., 1995)	Physically based, Semi-distributed	➢ Event-based (a minute). ➢ Small and medium watersheds	Runoff, sediment yield, infiltration, sediment discharge
BEACH	Bridge Event And Continuous Hydrological model	(Sheikh et al., 2009)	Physically based, distributed	➢ Daily. ➢ Hillslope, small watershed	Soil moisture, ET, runoff
HEC-RAS	Hydrologic Engineering Center's River Analysis System	(Brunner, 2010)	Engineering, physically-based river analysis model	➢ A minute to a year. ➢ Individual or net of reaches	Steady/unsteady analyses, sediment transport, water quality simulation

Temporal and Spatial Downscales

All the study objectives were designed to achieve from larger to finer scales. This is shown in the ellipses of the Fig. 1-1 and the "time and space scale" column of the Table 1-1. Specifically, annual soil erosion maps were mapped at *provincial scale* using the SWAT, after that event-based sediment yield was estimated for planes and channels of two small *watersheds* (the Nam Kim and the Nam Khat). The flash flooding prediction was firstly modelled at watershed scale (positioning locations where FFs were likely to occur within the watersheds). Afterward, the KINEROS2 was coupled with the HEC-RAS in order to analyse the flash flood behaviour at *river cross sections (reach)*. Finally, ET data were extracted from global datasets and modelled from *river basin* (SWAT) to *hillslope* (BEACH) scales. This

downscaling technique often provides knowledge from overviews and trends (with larger scale) to details (smaller scale) for users.

Roles of Remote Sensing and GIS Techniques

Remote sensing played indispensable roles in this study regarding data sources of required LULC, rainfall and ET data of the models. Most data preparation/analyses were made thanks to the advancements of the GIS software. In addition, the SWAT and KINEROS2 were run on ArcMap's interfaces and some models for rainfall processing were created in the ArcMap-ArcInfo environment.

Model Integration

What makes the method used in this research convincing? This research did not simply use the existing models coherently for achieving the study objectives but the meteorological and hydrological models were combined with the others. This helps to increase the accuracy of the outputs (the soil moisture of the BEACH defined boundary condition for the KINEROS2, for example), to solve lack of data in poorly gauged areas (outputs of the KINEROS2 used for inputs of the HEC-RAS), and to compare models' outcomes. Furthermore, the interactions between the NWP models (GSM and HRM) and the hydrological models (the KINEROS2 and HEC-RAS models) served crucial forecast discharge, flooding water level and velocity etc. for the flash flood prediction stage.

1.6 References

Abbott, M., Bathurst, J., Cunge, J., O'connell, P., & Rasmussen, J. (1986). An introduction to the European Hydrological System—Systeme Hydrologique Europeen,"SHE", 2: Structure of a physically-based, distributed modelling system. *Journal of Hydrology, 87*(1), 61-77.

Ahmed M. Y, Biswajeet P, & Abdallah M. H. (2010). Flash flood risk estimation along the St. Katherine road, southern Sinai, Egypt using GIS based morphometry and satellite imagery. *Environ Earth Sci (2011) 62*:611–623.

Allen, R. G., Pereira, L. S., Raes, D., & Smith, M. (1998). Crop evapotranspiration: guidelines for computing cropwater requirements. In: Irrigation and Drainage. *Paper 56. FAO, Rome*.

Anh, P. T. Q., Gomi, T., MacDonald, L. H., Mizugaki, S., Van Khoa, P., & Furuichi, T. (2014). Linkages among land use, macronutrient levels, and soil erosion in northern Vietnam: A plot-scale study. *Geoderma, 232–234*(0), 352-362. doi: http://dx.doi.org/10.1016/j.geoderma.2014.05.011

Arnold, J. G., J.R. Williams, R. Srinivasan, K.W. King, and R.H. Griggs. (1994). SWAT: Soil Water Assessment Tool. *U. S. Department of Agriculture, Agricultural Research Service, Grassland, Soil and Water Research Laboratory.* Temple, TX.

Arnold, J. G., & Williams, J. R. (1995). SWRRB-A watershed scale model for soil and water resources management. p. 847-908, In V.P. Singh (ed)(*Computer models of watershed hydrology. Water Resources Publications*).

Baja, S., Ramli, M., & Lias, S. A. (2009). Spatial-based assessment of land use, soil erosion, and water protection in the Jeneberang valley, *Indonesia. Biologia, 64*(3), 522-526. doi: DOI 10.2478/s11756-009-0074-y

Bakimchandra, O. (2011). Integrated Fuzzy-GIS approach for assessing regional soil erosion risks. *Universitsty of Stuttgart, Germany.* PhD thesis.

Bala, G., Caldeira, K., Wickett, M., Phillips, T. J., Lobell, D. B., Delire, C., & Mirin, A. (2007). Combined climate and carbon-cycle effects of large-scale deforestation. *Proceedings of the National Academy of Sciences, 104*(16), 6550-6555. doi: 10.1073/pnas.0608998104

Barrow, C. J. (1991). Land Degradation. *Cambridge University Press, Cambridge*.

Batjes, N. H. (1996). Global assessment of land vulnerability to water erosion on a 1/2 degrees by 1/2 degrees grid. *Land Degradation & Development, 7*(4), 353-365. doi: Doi 10.1002/(Sici)1099-145x(199612)7:4<353::Aid-Ldr239>3.0.Co;2-N

Benito, E., Santiago, J. L., De Blas, E., & Varela, M. E. (2003). Deforestation of water-repellent soils in Galicia (NW Spain): Effects on surface runoff and erosion under simulated rainfall. *Earth Surface Processes and Landforms, 28*(2), 145-155. doi: Doi 10.1002/Esp.431

Beven, K., & Binley, A. (1992). The future role of distributed models: model calibration and predictive uncertainty. *Hydrological Processes, 6*, 279-298.

Beven, K., & Kirkby, M. (1977). Towards a Simple, Physically-based, Variable Contributing Area Model of Catchment Hydrology: *University of Leeds, School of Geography*.

Bloschl, G., Reszler, C., & Komma, J. (2008). A spatially distributed flash flood forecasting model. *Environmental Modelling & Software, 23*(4), 464-478. doi: DOI 10.1016/j.envsoft.2007.06.010

Borga, M., Stoffel, M., Marchi, L., Marra, F., & Jakob, M. (2014). Hydrogeomorphic response to extreme rainfall in headwater systems: Flash floods and debris flows. *Journal of Hydrology, 518, Part B*, 194-205. doi: http://dx.doi.org/10.1016/j.jhydrol.2014.05.022

Borrelli, P., Ballabio, C., Panagos, P., & Montanarella, L. (2014). Wind erosion susceptibility of European soils. *Geoderma, 232–234*(0), 471-478. doi: http://dx.doi.org/10.1016/j.geoderma.2014.06.008

Brauer, C. C., Teuling, A. J., Overeem, A., Velde, Y. v. d., Hazenberg, P., Warmerdam, P. M. M., & Uijlenhoet, R. (2011). Anatomy of extraordinary rainfall and flash flood in a Dutch lowland catchment. *Hydrology and Earth System Sciences, Hydrol. Earth Syst. Sci., 15*, 1991–2005, 2011. doi: doi:10.5194/hess-15-1991-2011

Brunner, G. W. (2010). HEC-RAS, River Analysis System Hydraulic Reference Manual. *Hydrological Engineering Center, US Army Corps of Engineers, Davis, CA*, Version 4.1 January 2010(Approved for Public Release. Distribution Unlimited. CPD-69).

Bryan, R. B. (2000). Soil erodibility and processes of water erosion on hillslope. *Geomorphology, 32*(3-4), 385-415. doi: Doi 10.1016/S0169-555x(99)00105-1

Calianno, M., Ruin, I., & Gourley, J. J. (2013). Supplementing flash flood reports with impact classifications. *Journal of Hydrology, 477*, 1-16. doi: DOI 10.1016/j.jhydrol.2012.09.036

Carpenter, T. M., Sperfslage, J. A., Georgakakos, K. P., Sweeney, T., & Fread, D. L. (1999). National threshold runoff estimation utilizing GIS in support of operational flash flood warning systems. *Journal of Hydrology, 224*(1–2), 21-44. doi: 10.1016/s0022-1694(99)00115-8

Cerda, A., Imeson, A. C., & Poesen, J. (2007). Soil water erosion in rural areas - Preface. *CATENA, 71*(2), 191-192. doi: DOI 10.1016/j.catena.2007.03.002

Cooper, J. R., Wainwright, J., Parsons, A. J., Onda, Y., Fukuwara, T., Obana, E., . . . Hargrave, G. H. (2012). A new approach for simulating the redistribution of soil particles by water erosion: A marker-in-cell model. *Journal of Geophysical Research-Earth Surface, 117*. doi: Artn F04027 Doi 10.1029/2012jf002499

David, M., Follain, S., Ciampalini, R., Le Bissonnais, Y., Couturier, A., & Walter, C. (2014). Simulation of medium-term soil redistributions for different land use and landscape design scenarios within a vineyard landscape in Mediterranean France. *Geomorphology, 214*(0), 10-21. doi: http://dx.doi.org/10.1016/j.geomorph.2014.03.016

de Vente, J., & Poesen, J. (2005). Predicting soil erosion and sediment yield at the basin scale: Scale issues and semi-quantitative models. *Earth-Science Reviews, 71*(1–2), 95-125. doi: http://dx.doi.org/10.1016/j.earscirev.2005.02.002

Dercon, G., Mabit, L., Hancock, G., Nguyen, M. L., Dornhofer, P., Bacchi, O. O. S., . . . Zhang, X. (2012). Fallout radionuclide-based techniques for assessing the impact of soil conservation measures on erosion control and soil quality: an overview of the

main lessons learnt under an FAO/IAEA Coordinated Research Project. *Journal of environmental radioactivity, 107*(0), 78-85. doi: 10.1016/j.jenvrad.2012.01.008

EEA. (1999). Environment in the European Union at the Turn of the Century. ISBN: 92 9157-202-0, pp. 183–202.

El-Hames, A. S., & Richards, K. S. (1998). An integrated, physically based model for arid region flash flood prediction capable of simulating dynamic transmission loss. *Hydrological Processes, 12*(8), 1219-1232. doi: Doi 10.1002/(Sici)1099-1085(19980630)12:8<1219::Aid-Hyp613>3.0.Co;2-Q

Fister, W., Iserloh, T., Ries, J. B., & Schmidt, R. G. (2012). A portable wind and rainfall simulator for in situ soil erosion measurements. *CATENA, 91*, 72-84. doi: 10.1016/j.catena.2011.03.002

Garcia-Pintado, J., Barbera, G. G., Erena, M., & Castillo, V. M. (2009). Calibration of structure in a distributed forecasting model for a semiarid flash flood: Dynamic surface storage and channel roughness. *Journal of Hydrology, 377*(1-2), 165-184. doi: DOI 10.1016/j.jhydrol.2009.08.024

Gave, D. P., & Lewis, P. A. W. (1980). First-order autoregressive gamma sequences and point processes. *Adv. Appl. Probab. 12* 727-745.

Gupta, H. 2006 Development of a site-specific flash flood forecasting model for the Western Region- Final Report for COMET proposal. *University of Arizona: Tucson, AZ, USA*. Available online: http://www.comet.ucar.edu/outreach/abstract_final/0344674_AZ.pdf (accessed on 20th November 2014)

Huyen, T. G. (1993). Country profile: Land use in Vietnam: Facts and figures. *Sustainable Development, 1*(3), 4-7. doi: 10.1002/sd.3460010304

Jung, M., Reichstein, M., Ciais, P., Seneviratne, S., Sheffield, J., Goulden, M., . . . Zhang, K. (2010). Recent decline in the global land evapotranspiration trend due to limited moisture supply. *Nature 467*, 951–954.

Kefi, M., Yoshino, K., Setiawan, Y., Zayani, K., & Boufaroua, M. (2011). Assessment of the effects of vegetation on soil erosion risk by water: a case of study of the Batta watershed in Tunisia. *Environmental Earth Sciences, 64*(3), 707-719. doi: DOI 10.1007/s12665-010-0891-x

Khavich, V., & Benzvi, A. (1995). Flash-Flood Forecasting-Model for the Ayalon Stream, Israel. *Hydrological Sciences Journal-Journal Des Sciences Hydrologiques, 40*(5), 599-613. doi: Doi 10.1080/02626669509491447

Kisi, O., Sanikhani, H., Zounemat-Kermani, M., & Niazi, F. (2015). Long-term monthly evapotranspiration modeling by several data-driven methods without climatic data. *Computers and Electronics in Agriculture, 115,* 66-77. doi: http://dx.doi.org/10.1016/j.compag.2015.04.015

Kourgialas, N. N., Karatzas, G. P., & Nikolaidis, N. P. (2012). Development of a thresholds approach for real-time flash flood prediction in complex geomorphological river basins. *Hydrological Processes, 26*(10), 1478-1494. doi: Doi 10.1002/Hyp.8272

KrishnamurtiT.N., Bedi, H. S., Hardiker, V. M., & Ramaswamy, L. (2006). An Introduction to Global Spectral Modeling. 2nd Revised and Enlarged Edition, *Springer, Atmospheric and Oceanographic Sciences Library*.

Likens, G. E., Driscoll, C. T., Buso, D. C., Siccama, T. S., Johnson, C. E., Lovett, G. M., . . . Reiners, W. A. (1994). The biogeochemistry of potassium at Hubbard Brook. *Biogeochemistry 25,* 61–125.

Lin, C. A., Wen, L., Beland, M., & Chaumont, D. (2002). A coupled atmospheric-hydrological modeling study of the 1996 Ha! Ha! River basin flash flood in Quebec, Canada. *Geophysical Research Letters, 29*(2). doi: Artn 1026 Doi 10.1029/2001gl013827

Looper, J. P., & Vieux, B. E. (2012). An assessment of distributed flash flood forecasting accuracy using radar and rain gauge input for a physics-based distributed hydrologic model. *Journal of Hydrology, 412,* 114-132. doi: DOI 10.1016/j.jhydrol.2011.05.046

Majewski, D. 2009 HRM – User's Guide for the HRM with the SSO scheme (Vrs. 2.5 and higher). *Deutscher Wetterdienst, Press and Public Relations:* Offenbach, Germany. Available online: http://www.dwd.de/SharedDocs/downloads/DE/modelldokumentationen/nwv/hrm/HRM_users_guide.pdf?__blob=publicationFile&v=2 (accessed on 4th November 2014)

Maskey, S., Guinot, V., & Price, R. K. (2004). Treatment of precipitation uncertainty in rainfall-runoff modelling: a fuzzy set approach. *Advances in Water Resources, 27*(9), 889-898.

Mchunu, C., & Chaplot, V. (2012). Land degradation impact on soil carbon losses through water erosion and CO2 emissions. *Geoderma, 177,* 72-79. doi: DOI 10.1016/j.geoderma.2012.01.038

Melching, C. (1992). An improved first-order reliability approach for assessing uncertainties in hydrologic modeling. *Journal of Hydrology, 132*(1), 157-177.

Momber, A. W. (1998). The kinetic energy of wear particles generated by abrasive-water-jet erosion. *Journal of Materials Processing Technology, 83*(1-3), 121-126. doi: Doi 10.1016/S0924-0136(98)00050-8

Montz, B. E., & Gruntfest, E. (2002). Flash flood mitigation: recommendations for research and applications. Global Environmental Change Part B: *Environmental Hazards, 4*(1), 15-22. doi: 10.1016/s1464-2867(02)00011-6

Moradkhani, H., Baird, R. G., & Wherry, S. A. (2010). Assessment of climate change impact on floodplain and hydrologic ecotones. *Journal of Hydrology, 395*(3–4), 264-278. doi: http://dx.doi.org/10.1016/j.jhydrol.2010.10.038

Moradkhani, H., & Sorooshian, S. (2008). General review of rainfall-runoff modeling: model calibration, data assimilation, and uncertainty analysis. *Hydrological modelling and the water cycle* (pp. 1-24): Springer.

Naulin, J. P., Payrastre, O., & Gaume, E. (2013). Spatially distributed flood forecasting in flash flood prone areas: Application to road network supervision in Southern France. *Journal of Hydrology, 486*(0), 88-99. doi: http://dx.doi.org/10.1016/j.jhydrol.2013.01.044

NCHMF. (2011). Vietnamese National Center for Hydrological Forecasting http://www.nchmf.gov.vn/web/vi-VN/71/29/45/Default.aspx. (accessed on 7th March 2014).

Ndomba, P., Mtalo, F., & Killingtveit, A. (2008). SWAT model application in a data scarce tropical complex catchment in Tanzania. *Physics and Chemistry of the Earth, Parts A/B/C, 33*(8–13), 626-632. doi: http://dx.doi.org/10.1016/j.pce.2008.06.013

Nguyen Van Tai, Kim Thi Tuy Ngoc, Phan Tuan Hung, Le Thi Le Quyen, Nguyen Thi Ngoc Anh, Anna Stabrawa, . . . Cuong, N. M. (2009). Vietnam Assessment Report on Climate Change (VARCC). Institute of Strategy and Policy on natural resources and environment (ISPONRE), *Viet Nam Van hoa - Thong tin Publishing House,* 0-893507-779124, 893112-893115.

Parise, M., & Cannon, S. H. (2012). Wildfire impacts on the processes that generate debris flows in burned watersheds. *Natural Hazards, 61*(1), 217-227. doi: 10.1007/s11069-011-9769-9

Pham, T. N., Dawen, Y., Shinjiro, K., Taikan, O., & Katumi, M. (2003). Global Soil Loss Estimate Using RUSLE Model: The Use of Global Spatial Datasets on Estimating Erosive Parameters. *Geoinformatics, vol.14, no.1,* pp.49-53, 2003.

Platt, R. H., & Cahail, S. A. (1987). Automated Flash-Flood Warning Systems. *Applied Geography, 7*(4), 289-301. doi: Doi 10.1016/0143-6228(87)90021-X

Quintero, F., Sempere-Torres, D., Berenguer, M., & Baltas, E. (2012). A scenario-incorporating analysis of the propagation of uncertainty to flash flood simulations. *Journal of Hydrology, 460,* 90-102. doi: DOI 10.1016/j.jhydrol.2012.06.045

Ranzi, R., Le, T. H., & Rulli, M. C. (2012). A RUSLE approach to model suspended sediment load in the Lo river (Vietnam): Effects of reservoirs and land use changes. *Journal of Hydrology, 422–423*(0), 17-29. doi: http://dx.doi.org/10.1016/j.jhydrol.2011.12.009

Reed, S., Schaake, J., & Zhang, Z. Y. (2007). A distributed hydrologic model and threshold frequency-based method for flash flood forecasting at ungauged locations. *Journal of Hydrology, 337*(3-4), 402-420. doi: DOI 10.1016/j.jhydrol.2007.02.015

Routschek, A., Schmidt, J., Enke, W., & Deutschlaender, T. (2014). Future soil erosion risk — Results of GIS-based model simulations for a catchment in Saxony/Germany. *Geomorphology, 206*(0), 299-306. doi: http://dx.doi.org/10.1016/j.geomorph.2013.09.033

Schad, I., Schmitter, P., Saint-Macary, C., Neef, A., Lamers, M., Nguyen, L., . . . Hoffmann, V. (2012). Why do people not learn from flood disasters? Evidence from Vietnam's northwestern mountains. *Natural Hazards, 62*(2), 221-241.

Schmitt. (1987). System zur Nutzung der Flutwelle eines Erosionsgully (Systembeschreibung und Versuchsbericht 1986). *Sahel-Info des Deutschen Sahelprogramms*, GTZ, Eschborn.

Sfeir-Younis, A. (1986). Soil Conservation in Developing Countries. Western Africa Projects Department, *The World Bank,* Washington, DC.

Sheikh, V., Visser, S., & Stroosnijder, L. (2009). A simple model to predict soil moisture: Bridging Event and Continuous Hydrological (BEACH) modelling. *Environmental Modelling & Software, 24*(4), 542-556. doi: http://dx.doi.org/10.1016/j.envsoft.2008.10.005

Shrestha, D. L., & Solomatine, D. P. (2008). Data-driven approaches for estimating uncertainty in rainfall-runoff modelling. *International Journal of River Basin Management, 6*(2), 109-122.

Smith, P. L., Ana Barros, v. Chandrasekar, Greg Forbes, Eve Gruntfest, Witold Krajewski, . . . Galinis, E. (2005). Flash flood forecasting over complex terrain With An Assessment Of The Sulphur Mountain NEXRAD In Southern California. *The National Academies Press, DC 20001;* 800-624-6242.

Smith, R., Goodrich, D., Woolhiser, D., Unkrich, C., & Singh, V. (1995). KINEROS-A kinematic runoff and erosion model. *Computer models of watershed hydrology.*, 697-732.

Solomatine, D. P., & Wagener, T. (2011). 2.16 - Hydrological Modeling. *In P. Wilderer (Ed.), Treatise on Water Science* (pp. 435-457). Oxford: Elsevier.

Song, X., Zhang, J., Zhan, C., Xuan, Y., Ye, M., & Xu, C. (2015). Global sensitivity analysis in hydrological modeling: Review of concepts, methods, theoretical framework, and applications. *Journal of Hydrology, 523*, 739-757. doi: http://dx.doi.org/10.1016/j.jhydrol.2015.02.013

Starkloff, T., & Stolte, J. (2014). Applied comparison of the erosion risk models EROSION 3D and LISEM for a small catchment in Norway. *CATENA, 118*(0), 154-167. doi: http://dx.doi.org/10.1016/j.catena.2014.02.004

Sun, J., Salvucci, G. D., & Entekhabi, D. (2012). Estimates of evapotranspiration from MODIS and AMSR-E land surface temperature and moisture over the Southern Great Plains. *Remote Sensing of Environment, 127*, 44-59. doi: http://dx.doi.org/10.1016/j.rse.2012.08.020

Suriya, S., & Mudgal, B. V. (2012). Impact of urbanization on flooding: The Thirusoolam sub watershed – A case study. *Journal of Hydrology, 412–413*(0), 210-219. doi: http://dx.doi.org/10.1016/j.jhydrol.2011.05.008

Tian, F., Qiu, G., Yang, Y., Lü, Y., & Xiong, Y. (2013). Estimation of evapotranspiration and its partition based on an extended three-temperature model and MODIS products. *Journal of Hydrology, 498*, 210-220. doi: http://dx.doi.org/10.1016/j.jhydrol.2013.06.038

Tripathi, R., Sengupta, S. K., Patra, A., Chang, H., & Jung, I. W. (2014). Climate change, urban development, and community perception of an extreme flood: A case study of Vernonia, Oregon, USA. *Applied Geography, 46*(0), 137-146. doi: http://dx.doi.org/10.1016/j.apgeog.2013.11.007

Tung, Y.-K. (1995). Uncertainty and reliability analysis. Water resources handbook.

UNCCD secretariat. (2013). A Stronger UNCCD for a Land-Degradation Neutral World. *Issue Brief, Bonn, Germany*.

Unkrich, C. L., Michael Schaffner, Chad Kahler, David C. Peter Troch, Hoshin Gupta, Thorsten Wagener, & Yatheendradas, S. (2010). Real-time Flash Flood Forecasting Using Weather Radar and Distributed Rainfall-Runoff Model. *2nd Joint Federal Interagency Conference, Las Vegas, NV*.

Vanderhoof, M. K., & Williams, C. A. (2015). Persistence of MODIS evapotranspiration impacts from mountain pine beetle outbreaks in lodgepole pine forests, south-central

Rocky Mountains. *Agricultural and Forest Meteorology, 200*, 78-91. doi: http://dx.doi.org/10.1016/j.agrformet.2014.09.015

Versini, P. A. (2012). Use of radar rainfall estimates and forecasts to prevent flash flood in real time by using a road inundation warning system. *Journal of Hydrology, 416*, 157-170. doi: DOI 10.1016/j.jhydrol.2011.11.048

Vn-Atlas. (1997). Atlas of national physical maps of 66 fields. *Viet Nam Publishing House of Natural Resources, Environment and Cartography*, 1997. http://www.bando.com.vn/en/default.aspx.

Vu, M. T., Raghavan, S. V., & Liong, S. Y. (2012). SWAT use of gridded observations for simulating runoff - a Vietnam river basin study. *Hydrology and Earth System Sciences, 16*(8), 2801-2811. doi: DOI 10.5194/hess-16-2801-2012

Wickramanayake, E. (1994). Flood Mitigation Problems in Vietnam. *Disasters, 18*(1), 81-86.

Xu, C. Y. (2002). Textbook of Hydrological Models. *Uppsala University Department of Earth Sciences Hydrology*, edition 2002.

Xu, C. (2002). WASMOD–The WAter and Snow balance MODelling system. Mathematical models of small watershed. *Hydrology and applications*, pp555-590 ISBN 1-887201-35-1.

Yatheendradas, S. W., T. Gupta, H. Unkrich, C. Goodrich, D. Schaffner, M. Stewart, A. (2008). Understanding uncertainty in distributed flash flood forecasting for semiarid regions. *Water Resources Research, 44*(5). Doi 10.1029/2007wr005940

Zhan, C., Yin, J., Wang, F., & Dong, Q. (2015). Regional estimation and validation of remotely sensed evapotranspiration in China. *CATENA, 133*, 35-42. doi: http://dx.doi.org/10.1016/j.catena.2015.04.018

Ziegler, A. D., Giambelluca, T. W., Plondke, D., Leisz, S., Tran, L. T., Fox, J., . . . Tran Duc, V. (2007). Hydrological consequences of landscape fragmentation in mountainous northern Vietnam: Buffering of Hortonian overland flow. *Journal of Hydrology, 337*(1–2), 52-67. doi: http://dx.doi.org/10.1016/j.jhydrol.2007.01.031

Ziegler, A. D., Giambelluca, T. W., Tran, L. T., Vana, T. T., Nullet, M. A., Fox, J., . . . Evett, S. (2004). Hydrological consequences of landscape fragmentation in mountainous northern Vietnam: evidence of accelerated overland flow generation. *Journal of Hydrology, 287*(1–4), 124-146. doi: http://dx.doi.org/10.1016/j.jhydrol.2003.09.027

Ziegler, A. D., Tran, L. T., Giambelluca, T. W., Sidle, R. C., Sutherland, R. A., Nullet, M. A., & Vien, T. D. (2006). Effective slope lengths for buffering hillslope surface runoff in fragmented landscapes in northern Vietnam. *Forest Ecology and Management, 224*(1–2), 104-118. doi: http://dx.doi.org/10.1016/j.foreco.2005.12.011

CHAPTER 2

Overall Introduction to the Study Area

"Destroying rainforest for economic gain is like burning a Renaissance painting to cook a meal."

-E. O. Wilson

As the topographic, social and climatic characteristics of Yen Bai province and the three study watersheds of Nam Kim, Nam Khat and Ngoi Hut will be discussed in detail in the following chapters, this chapter will provide the general information of location and geographic characteristics, climate, LULC and data availability of Vietnam and the Yen Bai province.

2.1 Location and Geographic Characteristics

Vietnamese territory consists of the mainland of approximately 332,000 km^2, the East Sea and thousands of islands of various sizes in the East Sea. The mainland is located from 102^o 10' 00'' (in the Lai Chau province) to 109^o 24' 00'' (in the Khanh Hoa province) East and from 8^o 30' 00'' (in the Ca Mau province) to 23^o 22' 00'' (in the Ha Giang province) North. Vietnam has five main terrain groups of mountains, karst, valleys and mountainous hollows, sedimentary deltas and coasts. The mountainous terrain could be divided into seven forms including high mountains (over 2,500 m) concentrated in the North-West, average mountains (1,000 to 2,500 m) in the North-East, North-West, North/South Central, low mountains (500 to 1000 m) located in the Central Highlands and North-West, the highlands concentrated in the North east, hills in the North-East, and semi-plains located in the middle of Vietnam. There are three kinds of agglomerate deltas including a horizontal narrow mountain-based delta located in central Vietnam, an eroded-agglomerated/terraced delta, and deltas consolidated by rivers in the North and the South (Nguyen Van Tai et al., 2009). There is a dense drainage network with nine major river systems namely the Bang Giang-Ky Cung, Thai Binh, Red, Ma, Ca, Thu Bon, Ba, Dong Nai-Vam Co and Mekong and each river basin occupies more than 10,000 km^2.

This study focuses on the North of Vietnam located from 102^o 20' 00'' to 108^o 00' 00'' East and from 17^o 00' 00'' and 23^o 22' 00''North (Fig. 2-1). The Yen Bai province and three watersheds in the province were chosen for model implementations and which have a mean slope angle of approximately 24.4 degree and short slope lengths due to the partitioned

surface and a wide range of altitude (from 18 to 2016 m a.s.l). The terrain is higher in the West and lower in the East of the province and this mainly forms the flow direction from the West to the East.

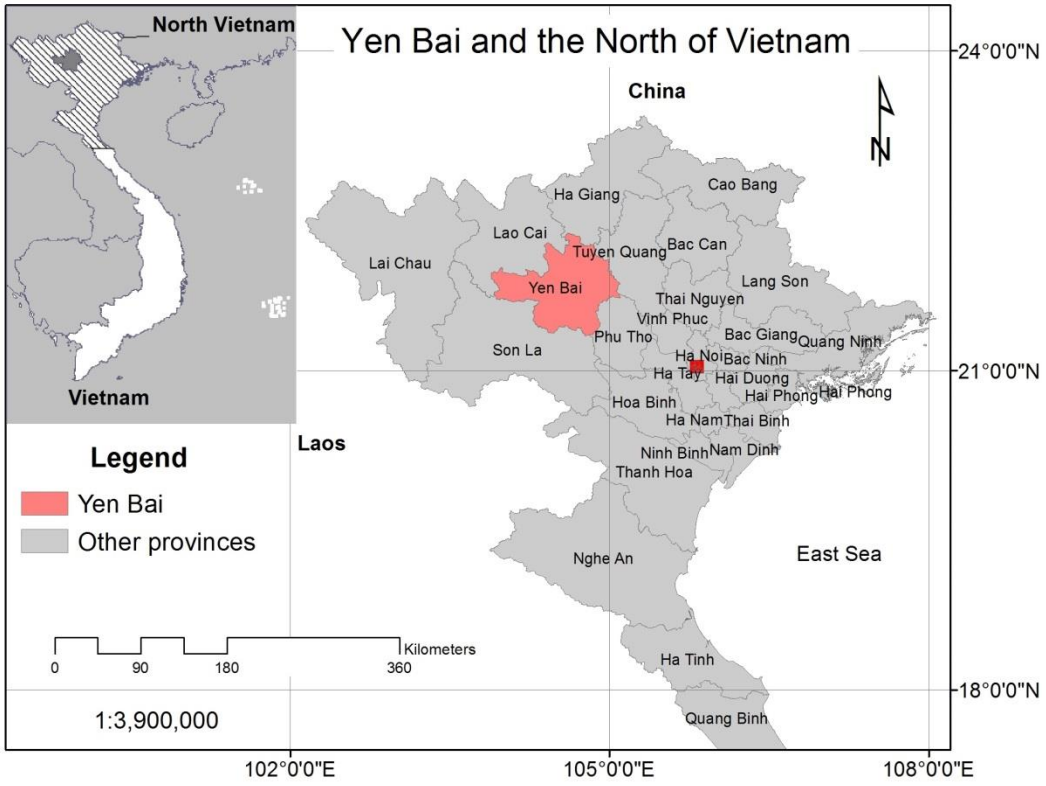

Figure 2-1. Location of Yen Bai province and the North of Vietnam.

2.2 Climate

Vietnam's atmospheric circulation is in the Southeast-Asian-monsoon circulation and is affected by three distinct features of the South/Northeast monsoon, tropical/sub-tropical and temperature circulation of the North/South hemisphere, and the Pacific equatorial sea in winter and summer. The monsoon circulation forms two main seasons of summer (May to September) and winter (November to March) and two transitional seasons of spring (April) and fall (October). The mean annual temperature of Vietnam is 20.7 ˚C and the mean annual maximum and minimum temperatures are 25.3 and 16.1 ˚C, respectively. In the South, the temperature is higher than in the North. The temperature map is indicated in the Fig. 2-2. The map shows the Northwest (including the study site) has the lowest annual temperature. The daily average relative humidity is approximately 80%. The annual precipitation of the region varies from 1365 to 1570 mm but the rainfall patterns vary considerably across the country (Fig. 2-2). Approximately 85 percent of total rainfall is recorded in the summer time. The

mean daily solar radiation is estimated to be very high at 14.5 (MJ m^{-2} day^{-1}) and the mean wind speed is 1.23 (m s^{-1}). This factual climatic information is calculated from seven methodological gauges inside and surrounding the study site. Convective storms with 150 to 200 mm occur frequently in the rainy season.

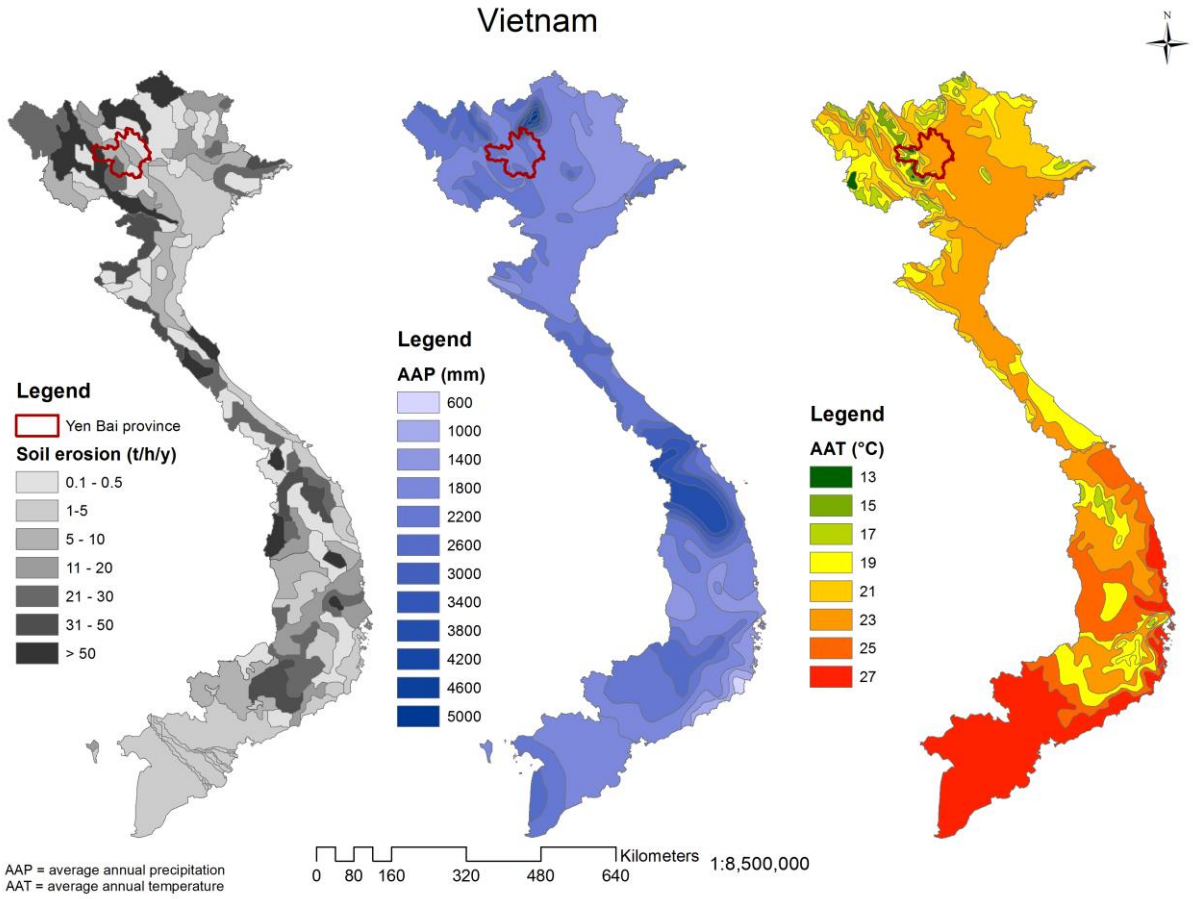

Figure 2-2. Average annual soil erosion, precipitation and temperature maps of Vietnam (Mapped from Vn-Atlas 1997).

2.3 Land Use/Population in Vietnam and in Yen Bai

Vietnam is considered to have a large population but a small land area (≈332,000 km²) (Huyen, 1993). Vietnam is under increasing pressure of population growth (Fig. 2-3) (slightly over 3.7 times from 1950 to 2015), which has also put the pressure on the LULC in particular and on economic development in general. However, the population growth rate has declined since the peak of 3.08 in 1960 to 1.0 in 2005. This rate is predicted to remain unchanged in the near future.

In Vietnam, there are 7.0 million hectares of agricultural land which are used for rice cultivation accounting for 4.0, cash and long-term crops for 1.1, pastures and hydro-culture

for 0.3 million hectares. The agricultural land is expected to enlarge in the near future. The forest land is approximately 9.3 million hectares and nearly 93 percent constitutes natural forest. During the last five years, forestry resources have been deleted at the rate of 2.6 percent. Reforestation programmes are deemed insufficient to recoup the annual forest loss (Huyen, 1993).

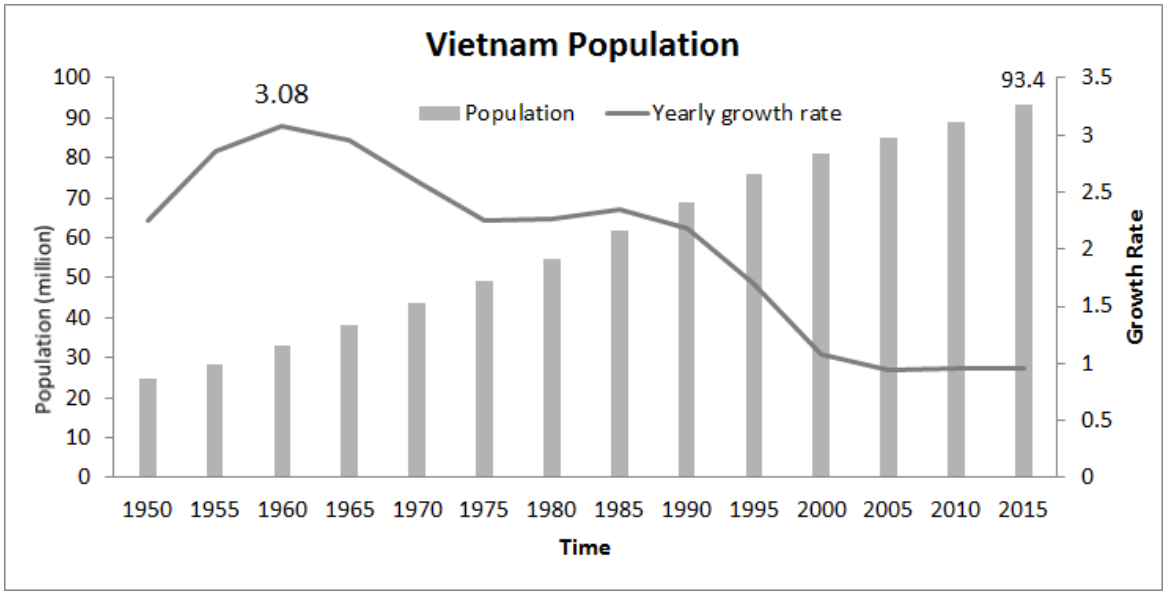

Figure 2-3. Vietnam population growth

(Data derived from www.Worldometers.info).

Yen Bai is a medium-sized province with a small city of 108.2 km^2 with 96,000 residents (in 2008) and which was named after the province. Most industrial zones are in and surrounding the city. Nonetheless, the urbanized and industrialized development is considered to be slow. There is a large electronic power reservoir in the Yen Binh district and a number of ponds distributed in the eastern districts. The total water area covers 2.8% of the province (February, 2009). Beside the population growth, the changing LULC from conservation of forested land to shrub land and agricultural fields (see Fig. 2-4) might also be negatively altering the hydraulic responses in the river basins such as reduction of infiltration, increase of runoff (Ranzi et al., 2012).

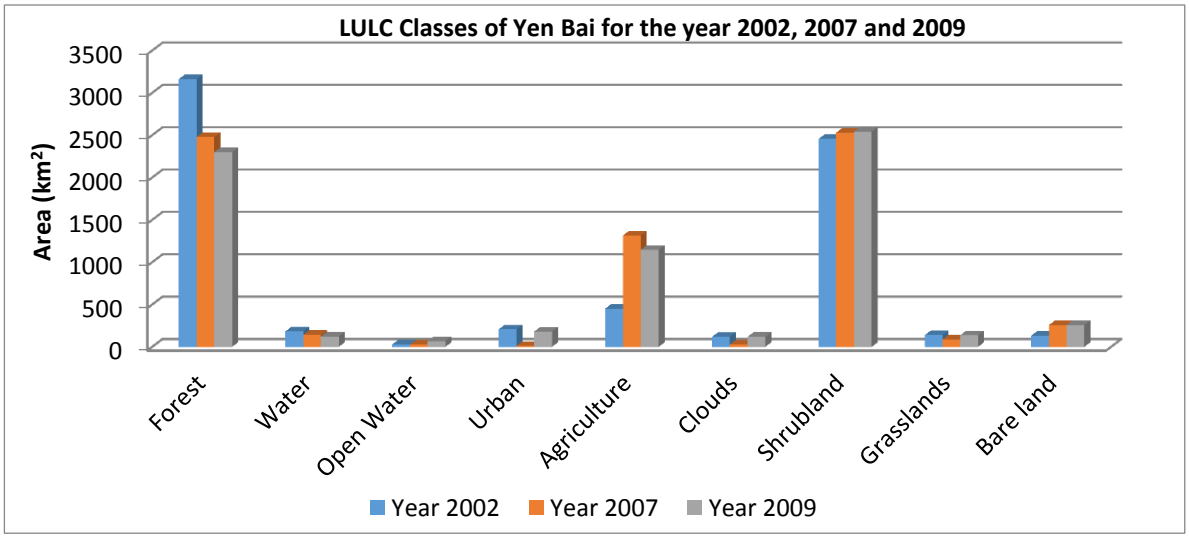

Figure 2-4. Landsat-based LULC statistics for the Yen Bai province.

Important natural problems in the North of Vietnam are soil erosion, flooding (also flash flood), and landslides. Yen Bai is located in the highest soil erosion rate in the Northwest of Vietnam (Fig. 2-2) with the average rate of approximately 25 t ha^{-1} y^{-1}. Among the 29 provinces in the region, 18 provinces have experienced flash floods. The flash flooding problem is globally well-known and reported by studies (Table 2-1 reports some losses of some past events).

Table 2-1. Losses to FFs
(quoted from Montz and Gruntfest (2002))

Date	Location	Deaths	Other losses	Additional information
July, 1997	Fort Collins, CO, USA	5	$200 M in damages ($100 M to Colo. State Univ.)	
✂✂ ✂	✂✂✂	✂✂	✂✂✂	✂✂✂
July, 199	Switzerland	21	"Conyoning" group	
July/August, 1999	**Vietnam**	**40**	22,000 evacuated or lost homes; ~$19.5 M in damage	
✂✂✂	✂✂✂	✂✂	✂✂✂	✂✂✂
May, 2000	St. Louis, MO USA	2	Hundreds of people evacuated, flash flood also hit Tulsa other Oklahoma communities	14 inches of rain over night
July, 2000	**Vietnam**	**24**	Five homes, 250 m of canals, 20 irrigation systems and 7 power pylons	Flash flood and landslides
✂✂✂	✂✂✂	✂✂	✂✂✂	✂✂✂

Source: Flash flood lab, Clorado State University, 2000 and news reports.

2.4 Data Availability

Hydrological modelling often requires data from several sources. However, the data consumption depends on what kinds of applied models and the aims of modelling. Basically, physically-based distributed parameter models are based heavily on spatial input data (sometimes time series data). Besides some sources of remote sensing datasets, global meteorological data are now available, we still need finer data of meteorological ground stations (MSs), and stream gauges (SGs), for example, for the model's runs at finer scale modelling. The figure 2-5 shows numbers (108 MSs, 251 SGs, and 3 radar stations) and locations of MSs and SGs set up in the North of Vietnam for obtaining various types of data such as rainfall, temperature, humidity, wind speed evaporation, river discharge and water levels etc. The density of the stations is considered insufficient for finer scales (basin, watershed scales) of modelling. In Yen Bai province, there were only three MSs and nine SGs, for example. The three radar ground stations (RSs) (Viet Tri, Phu Lien and Vinh) with a scanning diameter of 600 km cannot cover the whole region, particularly the Northwest which has high mountains. They are all the old radar technology of the 1970s.

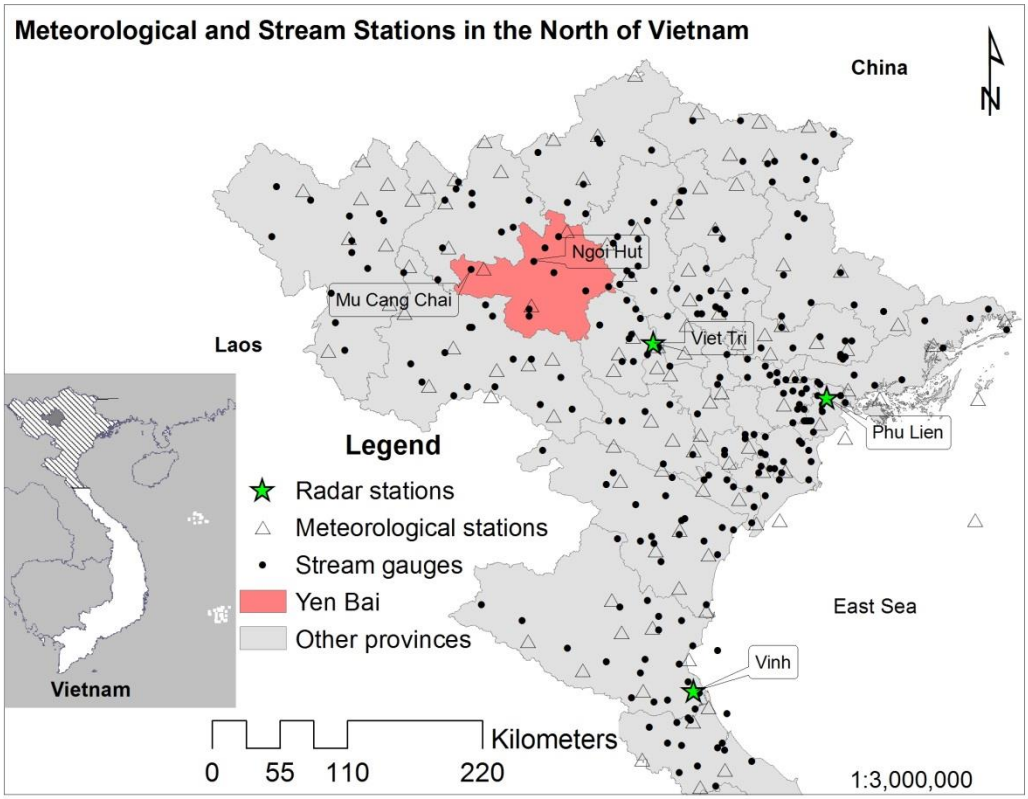

Figure 2-5. Weather and hydraulic stations established in the North of Vietnam (source: (Vn-Atlas, 1997)).

The Vietnam National Centre for Hydro-Meteorological Forecasting (NCHMF) has been co-operating with the German National Meteorological Service (DWD) and the Japan Meteorological Agency (JMA) to produce meteorological products including forecast rainfall (for any regional grid) employing the Numerical Weather Prediction (NWP) models of the Global Spectral Model (GSM) and High resolution Regional Model (HRM). This research used predicted rainfall of the two models. To obtain the forecast rainfalls in the province, the GSM and HRM stations were established as shown in the Fig. 2-6.

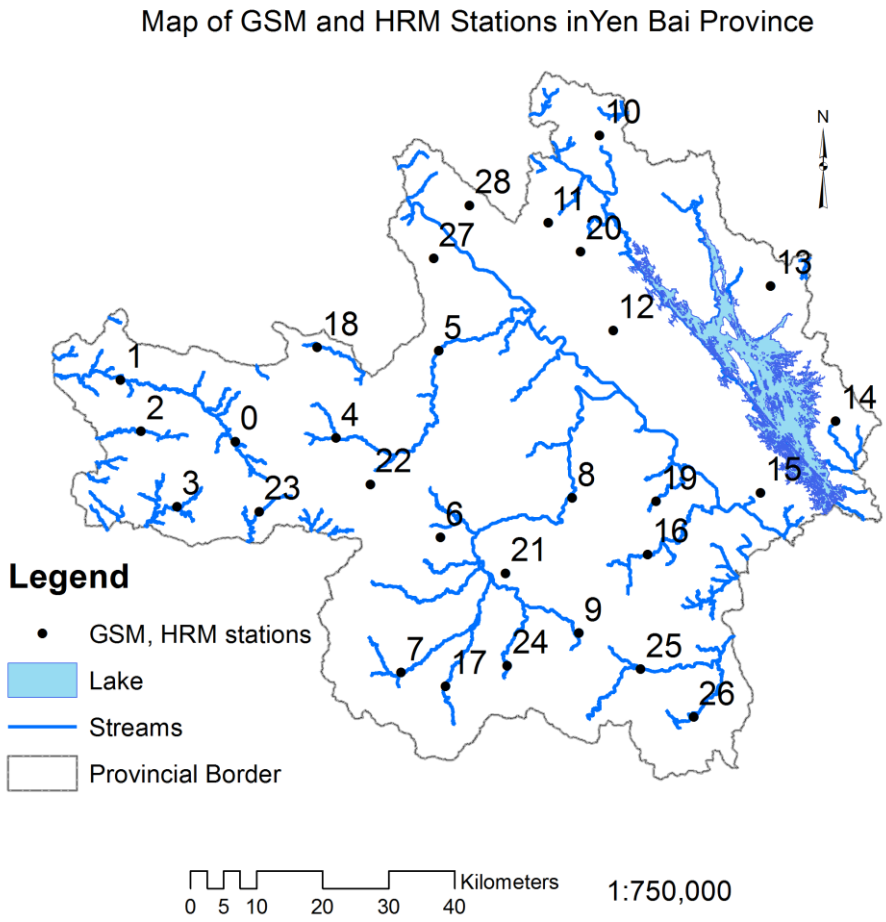

Figure 2-6. Stations designed for forecasting rainfall using GSM and HRM models.

Since 2008, basic geographical geodatabases (scale 1:10,000) and digital terrain models (the same scale, in vectors) of all Vietnamese provinces have been made by the Department of Survey and Mapping and the Vietnam Natural Resources and Environment Corporation (Vinanren) - Ministry of Natural Resources and Environment. These could be potential data sources for the purposes of this research. In addition, global soil datasets provided by the FAO/UNESCO are freely used. In this research, a custom soil map of Yen Bai province mapped by the Centre for Resources and Environment, National Institute of Agricultural Planning and Projection (NIAPP, 1996) and the FAO soils were used for the model parameterizations.

2.5 References

Huyen, T. G. (1993). Country profile: Land use in Vietnam: Facts and figures. *Sustainable Development, 1*(3), 4-7. doi: 10.1002/sd.3460010304

Montz, B. E., & Gruntfest, E. (2002). Flash flood mitigation: recommendations for research and applications. Global Environmental Change Part B: *Environmental Hazards, 4*(1), 15-22. doi: 10.1016/s1464-2867(02)00011-6

Nguyen Van Tai, Kim Thi Tuy Ngoc, Phan Tuan Hung, Le Thi Le Quyen, Nguyen Thi Ngoc Anh, Anna Stabrawa, . . . Cuong, N. M. (2009). Vietnam Assessment Report on Climate Change (VARCC). Institute of Strategy and Policy on natural resources and environment (ISPONRE), *Viet Nam Van hoa - Thong tin Publishing House,* 0-893507-779124, 893112-893115.

NIAPP. (1996). Yen Bai Soil Map Report. National Institute of Agricultural Planning and Projection (NIAPP)-*Centre for Resources and Environment*, Hanoi, Vietnam.

Ranzi, R., Le, T. H., & Rulli, M. C. (2012). A RUSLE approach to model suspended sediment load in the Lo river (Vietnam): Effects of reservoirs and land use changes. *Journal of Hydrology, 422–423*(0), 17-29. doi: http://dx.doi.org/10.1016/j.jhydrol.2011.12.009

Vn-Atlas. (1997). Atlas of national physical maps of 66 fields. *Viet Nam Publishing House of Natural Resources, Environment and Cartography*, 1997. http://www.bando.com.vn/en/default.aspx.

CHAPTER 3

Modelling Surface Runoff and Soil Erosion in Yen Bai Province, Vietnam Using the Soil and Water Assessment Tool (SWAT)[4]

"Climate change is a terrible problem, and it absolutely needs to be solved. It deserves to be a huge priority."

-Bill Gates

Abstract

Applications of the Soil and Water Assessment Tool (SWAT) are common. However, few attempts have focused on the tropics like in the Yen Bai province, Vietnam. Annual water-induced soil erosion (WSE) rates and surface runoff (SR) were estimated. We tested the sensitivity of the spatial resolution of the digital terrain model and the contributing source area to the model outputs. Correlations between precipitation, land covers, surface runoff and WSE were indicated. Although the estimated average WSE (4.1 t ha^{-1} $year^{-1}$ (t ha^{-1} y^{-1})) was moderate, some steep-bare areas were suffering serious soil loss of 26 t ha^{-1} y^{-1} and 15% of the province was calculated at the rate of 8.5 t ha^{-1} y^{-1}. We found that the changes in WSE significantly correlated with land use changes. As calibrated SR matched closely with the measured data, we recommend the use of the SWAT for long-term soil erosion assessments in the tropics.

[4] This paper is under review in the Hydrology and Earth System Sciences (HESS), Copernicus Publications

3.1 Introduction

Soil denudation intensity is one of the most favoured topics (Ananda and Herath, 2003) in whole soil erosion and water-induced soil erosion (WSE) (Lopez-Vicente et al., 2013), in particular. The consequences of surface runoff (SR) and soil erosion increase the risk of declining land availability (Dercon et al., 2012) and downstream water quality (Arnhold et al., 2014). Therefore, food security and sustainable development are the main problems in the reduced availability of land per capita countries (Dercon et al., 2012) such as in Vietnam with 2542 m^2 per capita in 1930 and 437 m^2 per capita in 2011 (VEM, 2012). However, land cover change and unsustainable agricultural practices in recent decades appear to be the main impact on land degradation (Baja et al., 2009; Bakimchandra, 2011; Cerda et al., 2007). This has been estimated increasingly in recent decades and is due to inappropriate agricultural practices and social development. Since the 1960s, WSE has been studied by various approaches (Evans, 2005). However, only a few studies have focused on the tropics. Formerly in the tropical region of northern Vietnam, the top soil layer was well-protected by dense vegetation cover and well-developed root systems (Andreu et al., 1994). This is one reason why only a little research has focused on SR and WSE in the tropical regions. On the other hand, WSE presents the main threat to agriculture in the Yen Bai province of Vietnam, where most people's livelihoods are based on cultivation. The population density in 1997 was 104.5 persons per km^2 (statistics from VN-Atlas, 1997). Although the local communities are extremely vulnerable to soil degradation, it appears that proactively in the study site there is no evidence of a soil erosion mitigation effort. Whereas some unintentional activities such as industrial tea planting and agricultural practices result in an increase of runoff and eventually in magnification of erosive processes (Anh et al., 2014).

The linkage between SR, WSE amplification, intensive land uses and deforestation has been analysed by various scientists, for example Benito et al., (2003), David et al., (2014), Davidson and Harrison (1995), de Aguiar et al., (2010), Mchunu and Chaplot (2012) and Lopez-Vicente et al., (2013). In the study site there was an unsustainable agricultural practice by local residents of cutting down trees for crop planting on soils with low fertility. When the soil becomes degraded after such a short-term use, they change to another place. This action is called "shifting cultivation of wandering hill tribes". Thanks to the efforts of the government, the situation has been ameliorated but a large area of forest has been converted to scrubland or even barren land (123 km^2, from 2002 to 2009 -based on our data statistics of land use classification). Since the vegetative cover has been reduced, the soil protection index (SPI-

which is a function of land use/land cover (LULC) and Normalized Difference Vegetation Index) has been decreased (Bakimchandra, 2011) or the soil has become less resistant to the erosive force of rain drops and runoff. These result in increasing run off, lower infiltration and eventually soil erosion exaggeration (Andrade et al., 2010; Benito et al., 2003). The reduction of vegetative cover and overgrazing make the region more prone to soil erosion (Baja et al., 2009; Blavet et al., 2009) and play an important role in soil erosion and consequently in sediments deposition in reservoirs as well (Butt et al., 2010).

Many recent studies have focused on impacts of climate change on WSE intensity by increases of annual rainfall, temperature and extreme events (De Munck et al., 2008; Nunes et al., 2008). However, Mukundan et al., (2013) found that soil erosion and sediment yield (SY) appeared to decrease due to the increase in soil moisture deficit and evapotranspiration. We hypothesized that the rates of soil erosion and sediment transport in Yen Bai would rise mainly due to the decline in vegetative cover.

Water-induced soil erosion assessments by modelling at hill-slope scale or larger have been conducted by many scientists e.g. Cooper et al., (2012), Gumiere et al., (2011), Hessel and Tenge (2008), Kefi et al., (2012), Nearing et al., (1989) and Routschek et al., (2014). The SWAT model is known worldwide and there are also many works using the SWAT model to investigate soil erosion by water, or to examine the precision of the model such as the studies of Zhang et al., (2008) and Zhang et al., (2009). Conversely, there have been only a few attempts which have tested the abilities of the SWAT model to the tropical regions. Although the SWAT was developed for dry areas, the algorithm inside the SWAT are able to be implemented in tropical regions and this was proven by the studies of Tibebe (2011), Fukunaga et al., (2015) and Ndomba et al., (2008). While there are many existing modelling approaches to water-induced soil erosion (Brazier et al., 2000) such as semi-quantitative, empirical regression, conceptual and physical based models, according to the model classification of Blinkov and Kostadinov (2010), it is difficult to choose and judge one model over others (Bakimchandra, 2011). After considering the model's requirements and scale and the issue of some common physically-based models, for instance the Areal Nonpoint Source Watershed Environmental Response Simulation (ANSWERS) (Huggins and Monke, 1966), Water Erosion Prediction Projection (WEPP) (Foster et al., 1995), Kinematic Runoff and Erosion (KINEROS) (Smith et al., 1995), Hydrologic Simulation Program–FORTRAN (HSPF) (Bicknell et al., 2001) and Dynamic Watershed Simulation Model (DWSM) (Borah et al., 2002), the SWAT was considered suitable and was selected for the long-term soil

erosion assessment of this study. We took advantages of GIS and remote sensing techniques for the aim of WSE assessment. This was supported by Batjes (1996), Cyr et al., (1995), Jurgens and Fander (1993), Kefi et al., (2012) and Schmengler (2010) with global, hill-slope, national, regional and catchment scale, respectively.

In the results section, the SWAT showed its ability to generate river discharge matching closely with observed data. Unfortunately, daily measured SY was not available for model validation but the simulated WSE was compared with data from an existing map. The results also revealed the capacity of the model's application for the tropics with reliable outputs and this has also been done by Fukunaga et al., (2015), Ndomba et al., (2008) and Tibebe (2011) even for regions of Vietnam by Vu et al., (2012).

3.2 Study Site

The study site is located within the Yen Bai province of Vietnam (Fig. 3-1), which is located in north-western Vietnam. The central coordinates that indicate the locality of the watershed are 104°30'9.0" E and 21°35'26.7" N. The area is 6883.5 square kilometres, with the mean elevation of 902 meters above the Bien Dong Sea level. Although the soil erosion rate of Yen Bai is not seen as the highest within the north of Vietnam, the region was chosen as a study area for this research project because of several dominant aspects that were taken into account, such as the typical climatic conditions, representative morphological characteristics, availability of data and the upward trend of WSE. Hydrologically, the province is in the three river basins of Da, Hong and Chay.

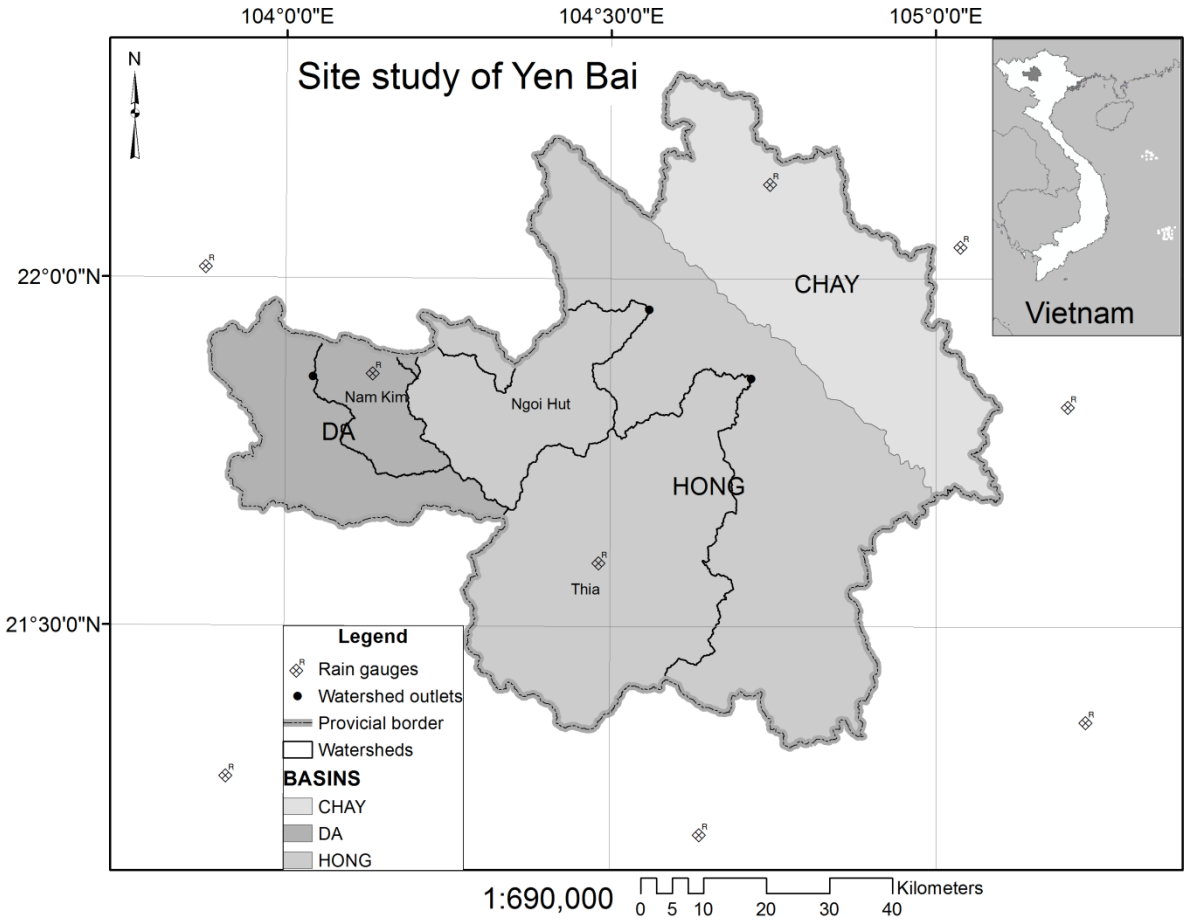

Figure 3-1. Yen Bai province and three watersheds chosen for model calibration, validation and sensitive test.

The site has an annual average precipitation (no snow) of 1,638 mm and the rainfall covers mostly 85 percentage of the total value only in the rainy season from May to September (based on our acquired rainfall data from the 9 rain gauges). Additionally, the terrain of the study area is partitioned by dense stream networks and the average slope gradient was estimated to be 24.4 degrees (statistics from the Yen Bai digital elevation model (DEM) – Fig. 3-2). Morphologically, the site is considered as an area with good soil erosion occurrence possibilities.

3.3 Materials and Methods

To achieve the study goals, the study site (the whole province) was divided into 32 watersheds (Fig. 3-2) in the SWAT watershed delineations. As measured discharge data was recorded for the Nam Kim and Ngoi Hut watershed, they were chosen for model calibration and validation. The Thia watershed was selected for the parameter sensitive test due to its representative characteristics such as presentation of all LULC classes; variations of slope gradients and being the biggest one (see the study site). Due to our assumption that the

climatic condition in the province was not much different from the watersheds to the watersheds, we used the approach of proximity used by Makungo et al., (2010) for the rest of the watersheds and then made up the provincial scale.

Although the SWAT model was developed for arid regions, we tested the flexibility of the equations describing the hydraulic relationships for the tropics by adjusting sensitive parameters. This has also been done by Fukunaga et al., (2015) and Tibebe (2011). The main mathematical relationships employed in the SWAT are presented as following.

3.3.1 Modified Soil Loss Equation

Soil erosion and SY are calculated for each hydrologic response unit (HRU) with the Modified Universal Soil Loss Equation (MUSLE) (Williams, 1975). Whilst within the Universal Soil Loss Equation (USLE) (Wischmeier and Smith, 1965, 1978) precipitation is used as an indicatory force of erosive energy, MUSLE however employs the amount of runoff to estimate erosion and SY (Neitsch et al., 2009).

Soil loss is estimated by means of the following equation (Williams, 1995):

$$sed = 11.8 \cdot \left(Q_{\text{surf}} \cdot q_{\text{peak}} \cdot area_{\text{hru}}\right)^{0.56} \cdot K_{\text{USLE}} \cdot C_{\text{USLE}} \cdot P_{\text{USLE}} \cdot LS_{\text{USLE}} \cdot CFRG \qquad (3\text{-}1)$$

where sed refers to the SY on any given day (t), Q_{surf} is the volume of surface runoff (mm h^{-1}), q_{peak} is the peak runoff rate ($m^3 s^{-1}$), $area_{\text{hru}}$ is the area of the HRU (ha). K_{USLE}, C_{USLE}, P_{USLE} and LS_{USLE} are the USLE soil erodibility factor, cover and management factor, support practice factor and topographic factor, respectively. The $CFRG$ indicates the coarse fragment factor of the soil.

3.3.1.1 Soil Erodibility Factor

The soil erodibility factor as used in the model for this research was originally developed by Wischmeier and Smith (1978) and it presents the Soil Loss Rate per Erosion Index of specified soils as measured on a unit plot. The equation is defined as follows:

$$K_{USLE} = \frac{0.00021 \cdot M^{1.14}(12 - OM) + 3.25 \cdot (c_{soilstr} - 2) + 2.5 \cdot \left(c_{perm} - 3\right)}{100} \qquad (3\text{-}2)$$

where K_{USLE} refers to the soil erodibility factor, M is the particle-size parameter, OM is the percentage of organic matter (%), $c_{soilstr}$ is the soil structure code used in soil classification

and c_{perm} is the soil-profile permeability class. The authors also emphasized that in referring to whether the corresponding increase in the sand fraction or clay fraction, a soil type, normally becomes more erodibility-resistant with a decline in silt fraction.

3.3.1.2 Cover and Management Factor

Wischmeier and Smith (1978) defined the C_{USLE} as the ratio of soil loss, from cropped land cropped under specified conditions, to the corresponding soil detachment from clean-tilled, continuously fallow soil. The SWAT model updates the C_{USLE} on a daily basis (refer to Equation 3-3) due to the variation of plant cover being present during the growth cycle of different plant species.

$$C_{USLE} = exp\left(\left[\ln(0.8) - \ln(C_{USLE,mm})\right] \cdot exp\left[-0.00115 \cdot rsd_{surf}\right] + ln\left[C_{USLE,mm}\right]\right) \quad (3\text{-}3)$$

where $C_{USLE,mm}$ is the minimum value for the cover and management factor for the land cover, and rsd_{surf} is the amount of residue on the soil surface (kg/ha). The $C_{USLE,mm}$ is calculated from the known annual cover factor ($C_{USLE,aa}$) using the following equation (Arnold and Williams, 1995).

$$C_{USLE,mm} = 1.463\ ln\left[C_{USLE,aa}\right] + 0.1034 \quad (3\text{-}4)$$

3.3.1.3 Support Practice Factor (P_{USLE})

The P_{USLE} can be explained as the ratio of soil loss with a specific support practice to corresponding loss with variation of slope-length. Support practices consist of contour tillage, strip-cropping along the contour, as well as the terrace system (Neitsch et al., 2009). The values of the P_{USLE} were estimated and tabulated based on the support practice by (Wischmeier and Smith, 1978).

3.3.1.4 Topographic Factor (LS_{USLE})

The factor is defined as ratio of soil loss per unit area from slope to that from 22.1 m in length of uniform 9 per cent under otherwise the same condition and calculated as the following equation.

$$LS_{USLE} = \left(\frac{L_{hill}}{22.1}\right)^{m} \cdot (65.41 \cdot \sin^2(\alpha_{hill}) + 4.56 \cdot \sin \alpha_{hill} + 0.065) \quad (3\text{-}5)$$

where L_{hill} is the slope length (m), m is the exponential term, and $hill$ is the angle of the slope. The exponential term, m is calculated:

$$m = 0.6 \cdot (1 - exp[-35.835 \cdot slp]) \quad (3\text{-}6)$$

where slp is the slope of the HRU expressed as rise over run (m m^{-1}). The correlation between α_{hill} and slp is defined as:

$$slp = \tan \alpha_{hill} \quad (3\text{-}7)$$

3.3.1.5 Coarse Fragment Factor ($CFRG$)

The $CFRG$ value is calculated from the per cent of rock in the first soil layer and expressed by:

$$CFRG = \exp(-0.053 \cdot rock) \quad (3\text{-}8)$$

where $rock$ is the percentage rock within the first soil class (%).

3.3.2 SCS-Curve Number Method

The surface runoff can be estimated by one of the following two provided methods. These include the SCS-CN (Soil Conservation Service-Curve Number) method (USDA-SCS, 1972) and the Green–Ampt infiltration method (Green and Ampt, 1911). The CN is broadly employed and estimated based on the area's hydrologic soil group, land use, treatment and hydrologic condition. The CN range is from 30 to 100; lower values indicate low runoff potential while larger numbers show higher runoff potential. The higher CN values indicate the greater ability of infiltration (USDA-SCS, 1986). The direct runoff from a rainfall event in a particular area is determined efficiently using CN.

In this study, the former approach (USDA-SCS, 1972) has been used. The run-off value can be calculated as:

$$Q_{\text{surf}} = \frac{\left(R_{\text{day}} - I_{\text{a}}\right)^2}{\left(R_{\text{day}} - I_{\text{a}} - S\right)} \quad (3\text{-}9)$$

where Q_{surf} refers to the accumulated runoff or rainfall excess (mm), R_{day} is the rainfall depth for the specific day (mm), I_{a} is the initial abstractions, which includes surface-water storage, interception and infiltration prior to runoff (mm) and S indicates the retention parameter (mm). Equation (3-9) indicates that the runoff will only occur when the $R_{\text{day}} > I_{\text{a}}$. The changing soils, land use practices, management regimes and slope, will temporally result in the varying of the S -value, because of changes in soil-water content.

The retention parameter can be calculated as follows:

$$S = 25.4\left(\frac{1000}{CN} - 10\right) \quad (3\text{-}10)$$

where CN refers to the curve number for the day. The initial abstractions, I_{a} is frequently estimated as 0.2 S and the equation (3-9) is rewritten as:

$$Q_{\text{surf}} = \frac{\left(R_{\text{day}} - 0.2S\right)^2}{\left(R_{\text{day}} + 0.8S\right)} \quad (3\text{-}11)$$

3.3.3 Model Inputs

The model requires various inputs including topography, land use/land cover (LULC), soils and time-series information of daily precipitation and temperature.

3.3.3.1 Topography and River Network

The morphological dataset used for watershed delineations, discretization, delineated drainage network (Fig. 3-2b) and morphologic parameterizations was a 10 × 10 m DEM extracted from a Yen Bai geodatabase (Fig. 3-2a) (30 × 30 and 50 × 50 m DEMs were reductions of the original). The DEM was produced by Vietnam Resources and Environment Corporation in 2009 employing Aerial Photogrammetry technology from the Intergraph Corporation, USA.

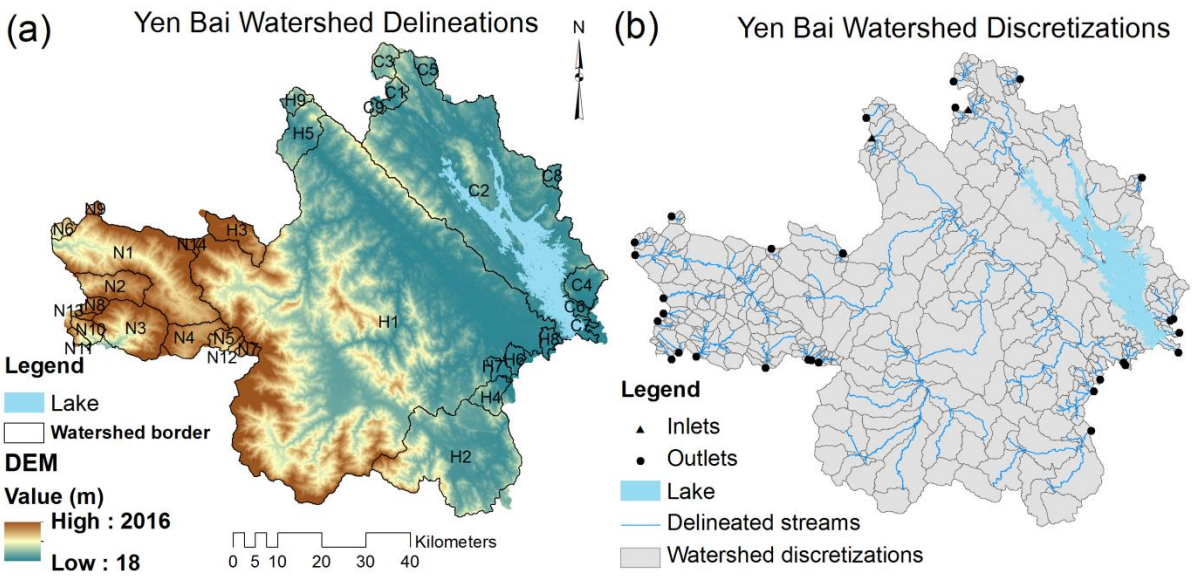

Figure 3-2. DEM and modelled sub-watersheds/HRUs in Yen Bai province.

3.3.3.2 Land Use/Land Cover (LULC)

Different LULC maps of the study site were prepared from Landsat TM imagery acquired on 28th January 2002, 26th March 2007 and 30th September 2009 for testing the impacts of land use changes on surface runoff and SY. The ground control points and ground-truth data were extracted from the Yen Bai geodatabase for geometric corrections and the supervised maximum likelihood classified method (with considering seasonal effects) using the ENVI 4.7, respectively.

The LULC was classified into nine classes for each map as shown in the Fig. 3-3. The Kappa statistics (Berry, 1992) producer accuracy and user accuracy were assessed for each class of the maps and written in Table 3-1. The average Kappa statistic of 0.7 was calculated and asserted a substantial agreement based on Viera & Garrett (2005).

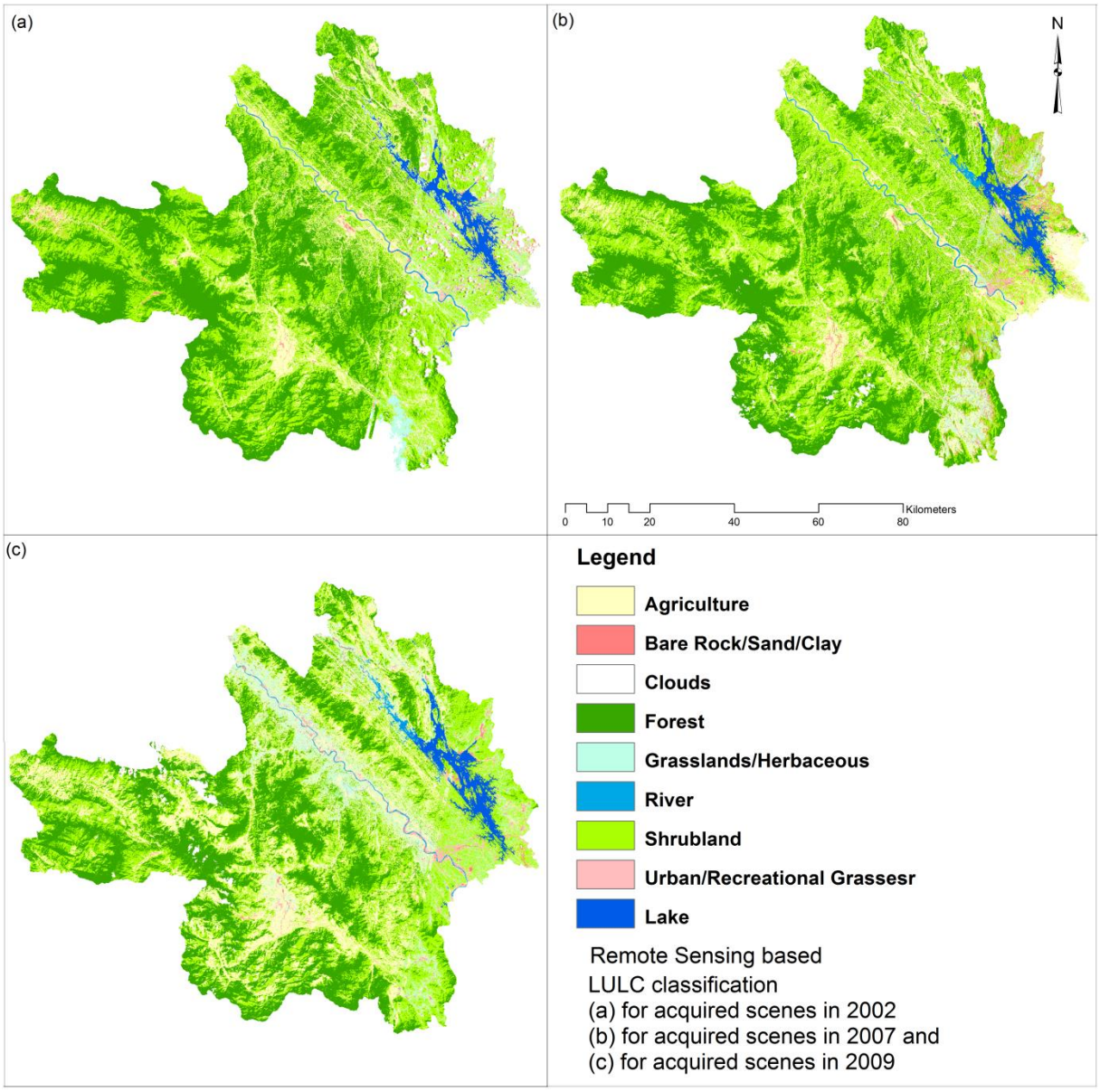

Figure 3-3. Maps of LULC mapped from Lansat TM scenes for Yen Bai province.

Table 3-1. LULC classification accuracy assessment.

LULC (year)	P/U (%)	Forest	Lake	River	Urban	Agriculture	Shrubland	Grassland	Barren	O (%)	Kappa
2002	P	78.0	82.4	57.5	73.6	61.1	61.8	61.5	76.2	69.3	0.65
	U	72.1	73.9	61.1	73.3	65.6	65.0	63.7	77.2		
2007	P	79.1	87.8	70.0	70.2	71.4	63.5	61.0	78.6	73.2	0.69
	U	76.9	80.4	69.0	75.6	68.5	67.8	66.6	77.7		
2009	P	86.2	88.8	76.3	72.3	73.4	73.8	64.0	74.7	76.8	0.73
	U	86.5	82.7	74.7	75.2	68.8	73.1	73.3	78.7		

P= Producer accuracy, U= User accuracy, O= Overall accuracy, and Kappa is the kappa statistic or kappa coefficient.

3.3.3.3 Soils

The Yen Bai custom soil (YBS) map below generated in the MapInfo software in 1996 and set by the FAO/UNESCO norms for quality. Fifteen soil types (Fig. 3-4) were classified with their characteristics such as gradient (4 level of 0−8°, 8°−15°, 15°−25° and above 25°), soil thicknesses, soil texture, profiles etc. and divided into 6 major soil groupings including fluvisols, calcisols, ferralsols, alisols, acrisols and gleysols. The two dominant soils are Plinthic Ferralsols and Gleyic Alisols with distribution of 3855.8 and 998.6 km^2, respectively.

Secondly, the FAO Digitized Soil (FAO soils) Map of the World, version 3.6, was completed January 2003. It was provided by the Food and Agriculture Organization of the United Nations. Based on the FAO soils, only the two soil types are identified in the study region namely Ferric Acrisols and Orthic Acrisols.

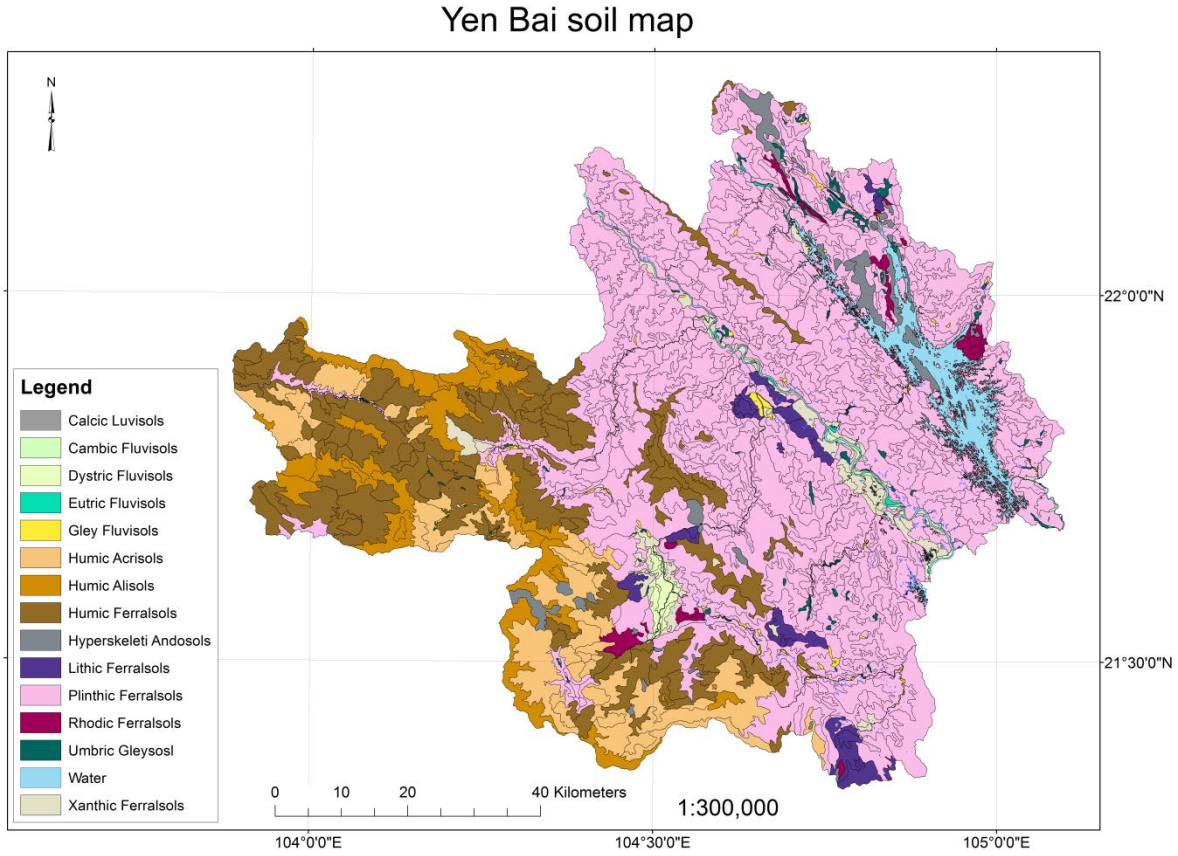

Figure 3-4. Soil map of Yen Bai province.

3.3.3.4 Precipitation and Temperature

Point measurements of daily rainfall and temperature were recorded by nine gauges (see Fig. 3-1) conducted inside the province and surroundings. The twelve-year daily data (from 01.01.2001 to 31.12.2012) was acquired and processed in Excel environment in order to

generate the precipitation and temperature inputs for the SWAT model. Some short missing data was interpolated using the inverse-distance weighted equation (Shepard, 1986). Distributed data of precipitation and temperature were generated from gauged data using the Thiessen polygon method (Thiessen, 1911).

3.3.4 Parameter Sensitive Test

As the most sensitive parameter to surface runoff and SY of curve number was tested by others such as Shen et al., (2009) and Tibebe (2011), we thus tested other parameters of the model spatial resolution by changing the Contributing Source Areas (CSAs) from 2.5 (≈3900 hectares), 5 (≈7800 hectares), and 10 % (≈15,600 hectares) of the watershed area and the DEM resolution from 10 × 10 to 30 × 30 and to 50 × 50 m to the modelled sediment yield. The CSA defines the numbers of elements (HRUs) of the watershed, hence determines the spatial resolution of the model. The Thia watershed was chosen for the analyses as it is big enough to represent the climatic and morphological conditions of the others.

3.3.5 Model Calibration, Validation and Simulation

Model calibration was done manually "by changing sensitive parameters" employing 5-year gauged data (daily and monthly) from 2001 to 2005. Some model sensitive parameters such as the CN, base flow recession and soil evaporation compensation were adjusted at this stage. Both the model calibration and validation (7-year periods of 2006-2012) were done for the Nam Kim and Ngoi Hut watersheds and the top-ten sensitive parameters are tabularised in the Table 3-2. The model performance was investigated by using the coefficient of determination (R^2), Nash–Sutcliffe coefficient of simulation efficiency (NSE) (Nash & Sutcliffe, 1970).

Table 3-2. SWAT initial and final calibrated parameters (NK = Nam Kim, NH =Ngoi Hut).

Parameter	Description	Unit	Range	Initial value	Final value (NK)	Final value (NH)
CN2	Curve number condition 2	–	35–98	35	54.1	48.7
Alpha_Bf	Baseflow recession constant	days	0–1	0.04	0.4	0.5
Ch_K2	Effective hydraulic conductivity in channel	mm hr^{-1}	−0.01–500	50	75	50
Sol_K	Saturated hydraulic conductivity	mm hr^{-1}	0–2,000	2	4.30	16.03
Ch_N2	Manning's n value for the main channel	–	−0.01–0.3	0.015	0.05	0.05
Surlag	Surface runoff lag coefficient	–	1–24	4	2.5	5.6
Sol_Awc	Available water capacity	mm mm^{-1}	0–1	0.22	0.31	0.35
Gw_Revap	Revap coefficient	–	0.02–0.2	0.02	0.2	0.2
Esco	Soil evaporation compensation factor	–	0-1	0	0.95	0.95
Gwqmin	Threshold water level in shallow aquifer for base flow	mm	0–5,000	0	1500	2000

Model parameter simulations with different LULC and soil data were done for the 32 watersheds (N1 to N14, H1 to H9 and C1 to C9 shown in Fig. 3-2a) in Yen Bai province (summarized for the basins (Chay, Hong and Da) written in Table 3-3).

Table 3-3. Parameterization for river basins.

RS	Morphological parameters				Land cover and soil parameters								AMP (mm)
							Mean CN (YBSs)			Mean cover			
	Area (1000 ha)	M_E (m)	A_S ($m\ m^{-1}$)	SMFL (km)	YB soils (YBSs)	FAO soils	LULC 2002	LULC 2007	LULC 2009	LULC 2002	LULC 2007	LULC 2009	
Chay	153	206	0.3	96	Plinthic Ferralsols, Lithosols, Humic Ferralsols, Acric Ferralsols, Xanthic Ferralsols	Ferric Acrisols ,Orthic Acrisols	68	76	76	25	29	28	1731
Hong	439	504	0.4	170	Humic Ferralsols, Plinthic Ferralsols, Acric Ferralsols, Humic Alisols, Dystric Fluvisols, Humic Acrisols	Ferric Acrisols ,Orthic Acrisols	71	76	73	28	31	28	1515
Da	90	1556	0.6	48	Humic Acrisols, Humic Alisol, Acric Ferralsols, Plinthic Ferralsols, Humic Ferralsols	Orthic Acrisols	77	80	76	27	28	27	1669

RS = River Subbasin; M_E = mean elevation; A_S = Average Slope; SMFL = Simulated Maximum Flow Length; and AMP = Annual Mean Precipitation

3.4 Results and Dissection

3.4.1 Test the Model Sensitivity to Spatial Resolution

The results of spatial examination showed the variety of estimated soil loss rates and the accumulative sediment transport (ST) in streams while the CSAs and the DEM grid sizes were changed. Generally speaking, the higher value (in hectares) of CSAs tended to estimate more significance of the erosion problem, except for the cases of CSA 5% of the watershed area and 30 × 30 and 50 × 50 m DEMs. On the contrary, the reduction of DEM resolution produced the lower erosion rates. There was a remarkable jump of the rates of around ten thousand tons per year when the CAS varied from 2.5 to 5% of the watershed area. The maps (Fig. 3-5) indicate the changes of calculated SY patterns. It is clearly shown that the smaller CSAs generated finer maps. Some areas with an erosion rate of 0−1 t ha^{-1} y^{-1} in the centre of the watershed were generalized with higher rates in the rougher DEMs used.

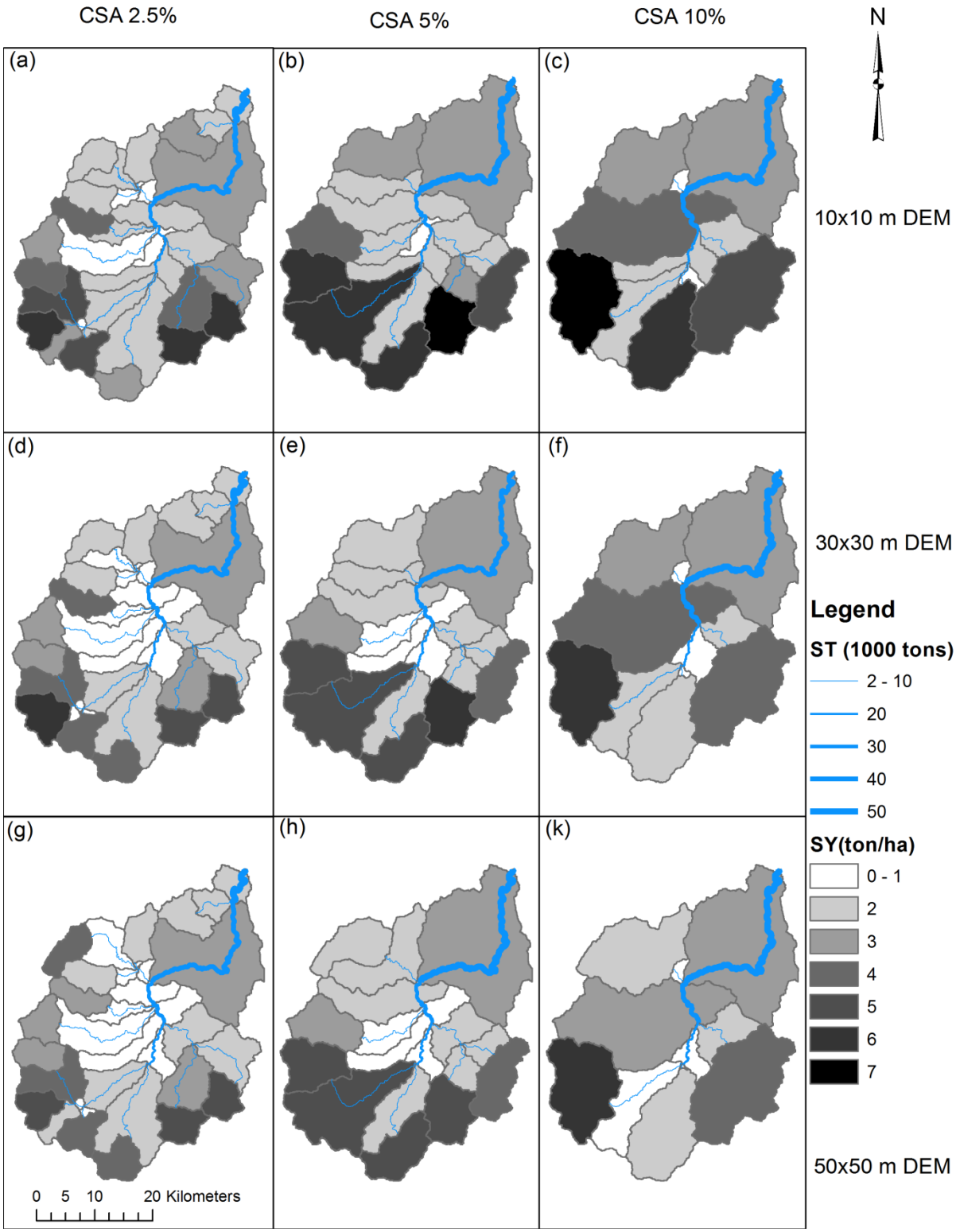

Figure 3-5. Maps of model spatial tests for the Thia watershed.
(SY= sediment yield; ST = sediment transport in channels)

3.4.2 Monthly Surface Runoff

The Fig. 3-6 presents the 5-year results of the model calibration of monthly outflow from 2001 to 2005. Before model calibration (Figs 3-6a and b), basically there were underestimates of base flows and the peaks for both the Nam Kim (NSE=0.3, R^2 = 0.81) and Ngoi Hut (NSE = 0.1, R^2 = 0.39). On the other hand, the model performed well with the calibrated discharge matching closely with the measured data for both the watersheds, verified by evaluating NSEs of 0.86, R^2= 0.87 for the Nam Kim and NSEs of 0.81, R^2= 0.76 for the Ngoi Hut (Figs 3-6c and d), respectively. It was a result of alternation of the base flow recession, inter flow and other parameters.

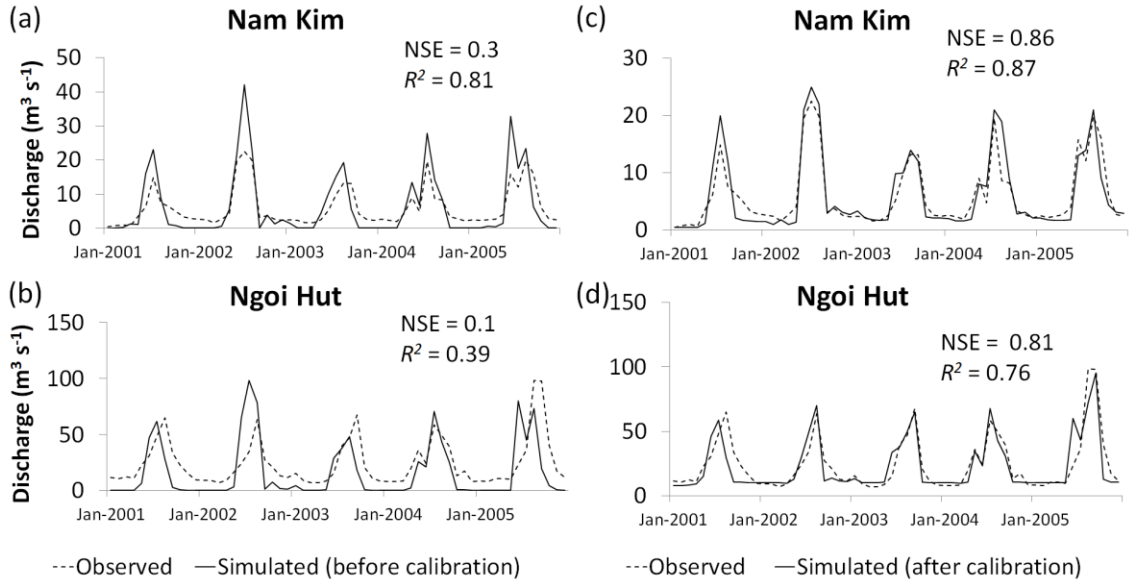

Figure 3-6. Observed and simulated monthly surface runoff before calibration (a and b) and after calibration (c and d) (January 2001-December 2005).

The good model results of monthly validation during the seven years from 2006 to 2012 were illustrated in Fig. 3-7 for the Nam Kim and Ngoi Hut. Based on the NSE and R^2 values, the model performed better with the smaller watershed (the Nam Kim-Fig. 3-7a with both the NSE and R^2 of 0.87) compared to the bigger one of the Ngoi Hut (Fig. 3-7b with NSE of 0.78, R^2 of 0.8). The figure also showed variations of runoff in rainy and dry seasons in quite big ranges of about 40 and 80 m^3 s^{-1} for the Nam Kim and Ngoi Hut and the very consistent time of peaks in July (also in the calibration period). The two-year driest periods were from 2010 to 2011 in the Nam Kim and from 2009 to 2010 in the Ngoi Hut.

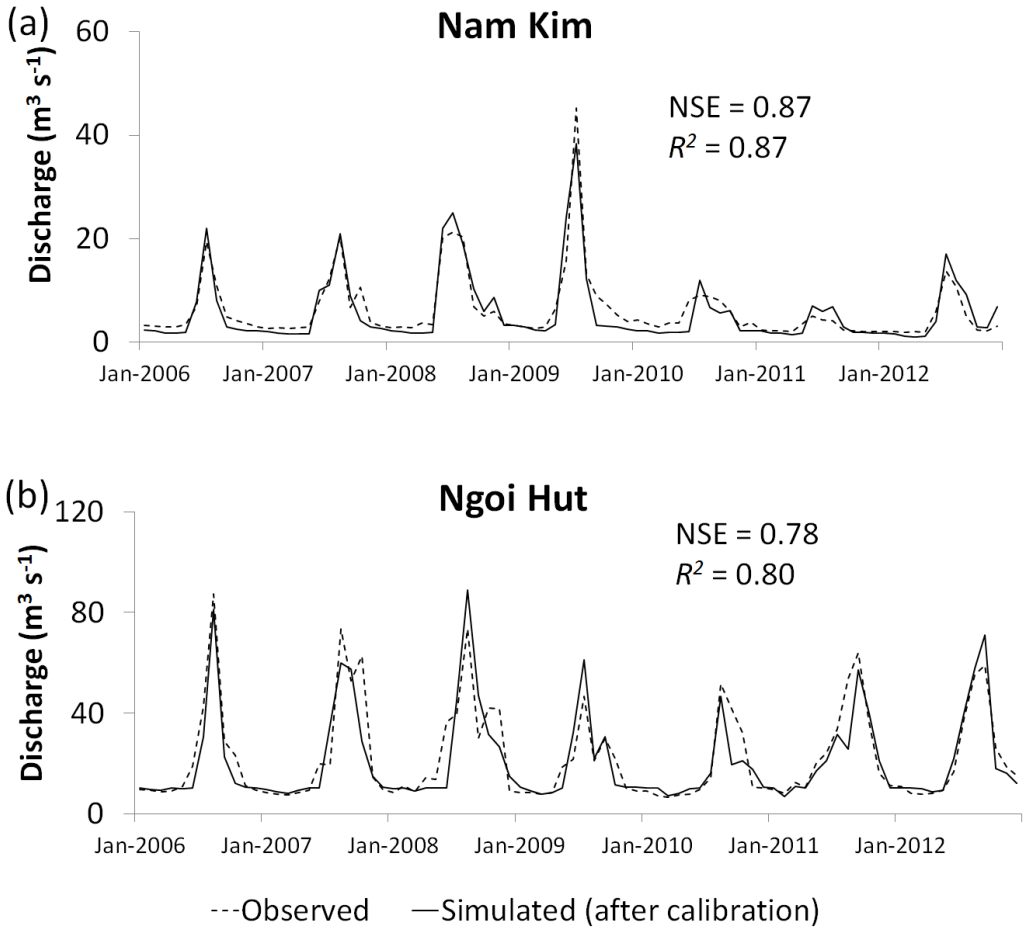

Figure 3-7. Observed and simulated monthly surface runoff for model validation (a) the Nam Kim (b) the Ngoi Hut (January 2006-December 2012).

3.4.3 Daily Surface Runoff

Model calibration has also been done with daily climatic data (rainfall, temperature, etc.) for the 2001-2005 periods. Again the base flow was underestimated before calibration stage and this made the correlation coefficient and determination very low of −0.4 and −0.3 of NSE and 0.5 and 0.2 of R^2 calculated for the Nam Kim and Ngoi Hut (Figs 3-8a and c), respectively. The daily rainfall is depicted in the figure showing the relation of the runoff to the rainfall (runoff coefficient).

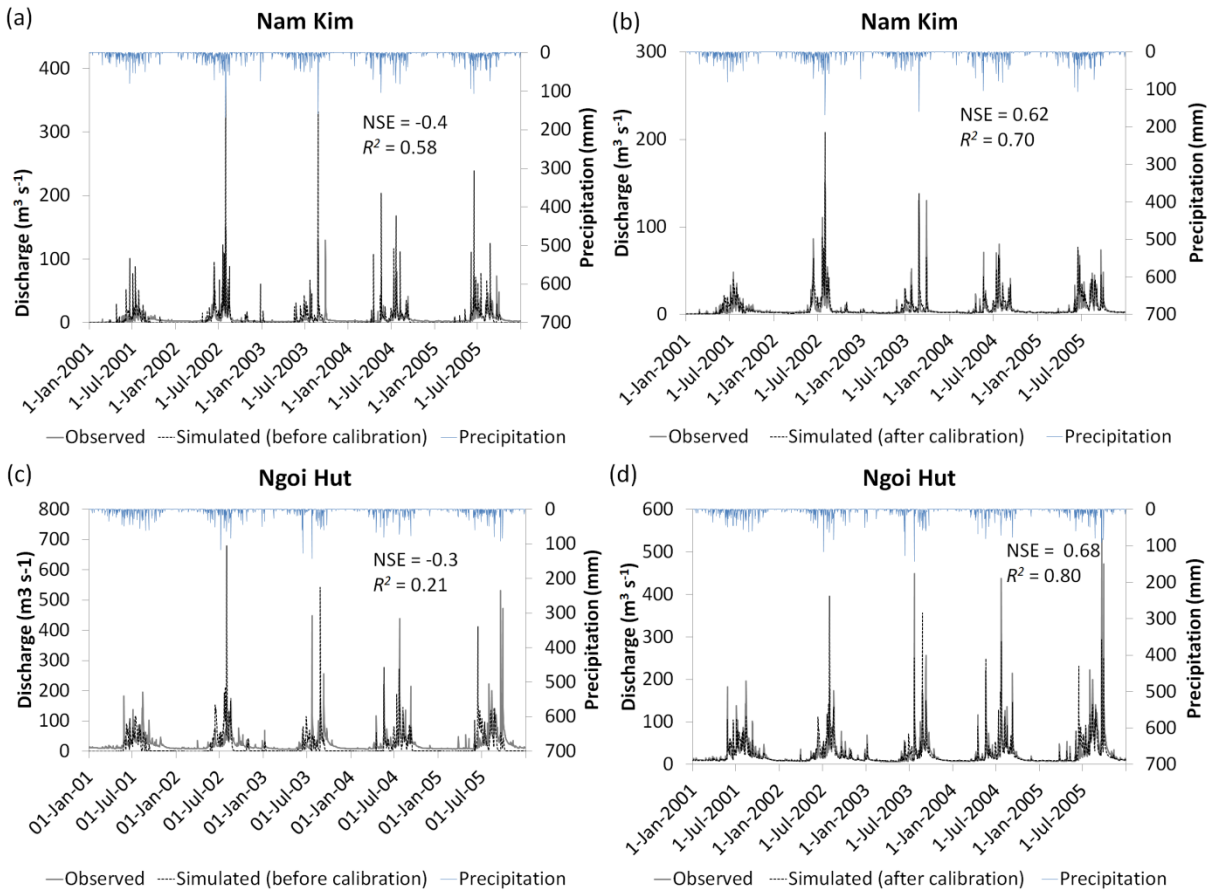

Figure 3-8. Daily observed and simulated runoff for model calibration (January 2001-December 2005).

The daily calibrated discharge matched well with computed data verified by NSEs of 0.65 and 0.62 (Figs 3-8b and d) and R^2 of 0.8 and 0.7 for the two watersheds. What is interesting on the graphs is the runoff coefficient, particularly of the post-calibrated graphs with very high flow peaks resulting from heavy rains.

Figure 3-9 presents observed and simulated daily surface runoff for the validated period from 2006 to 2012 and also the rainfall on the upper X axis for graphical comparisons. Although the NSEs were not very high (0.65 for the Nam Kim-Fig. 3-9a and 0.58 for the Ngoi Hut-Fig. 3-9b) but asserted a good level according to Santhi et al., (2001) and Moriasi et al., (2007). However, the R^2 of 0.88 and 0.79 for the Nam Kim and Ngoi Hut showed the satisfaction of the model performance.

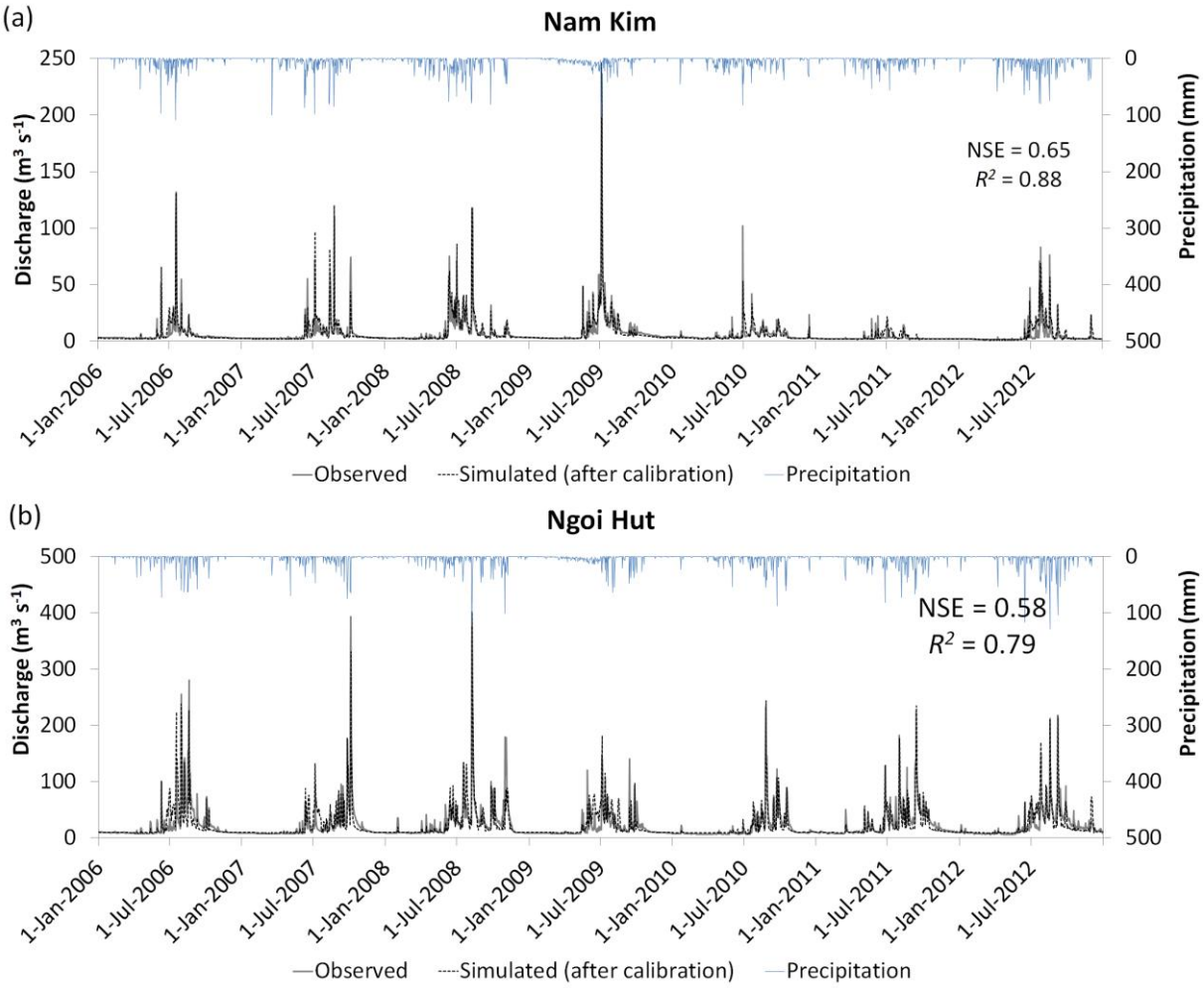

Figure 3-9. Daily observed and simulated runoff for model validation (January 2006-December 2012).

3.4.4 Relationships between Annual Precipitation, Simulated Surface Runoff and Sediment Yield

In general, there were significant positive correlations between annual rainfall, surface runoff and SY in the three basins (Fig. 3-10) calculated for the 2001−2012 period indicated by coefficient of determinations. All of the R^2 values were larger than 0.65 (particularly 0.91 for the relationship between runoff and SY in the Hong basin). These results might reveal that the model estimates were possibly reasonable.

The figure also shows the simulated surface runoff and SY values for the three basins. Although the Chay had the highest AMP (about 1800 mm), the average runoff (43 mm) and SY(1.7 t ha^{-1} y^{-1}) were not much higher than in the Hong basin (mean runoff of 36 (mm) and SY of 1.5 t ha^{-1} y^{-1}) with AMP of around 1400 (mm). The Da basin presented the most eroded region with an annual mean rate of over 4 (t ha^{-1} y^{-1}) and runoff of 60 (mm) but the AMP was 100 mm less than in the Chay. The high SR and SY rates of the Da could be

explained by a positive proportional linkage between slopes (slope length and gradient, see the DEM (Fig. 3-2a) and SR and SY values (Oliveira et al., 2013).

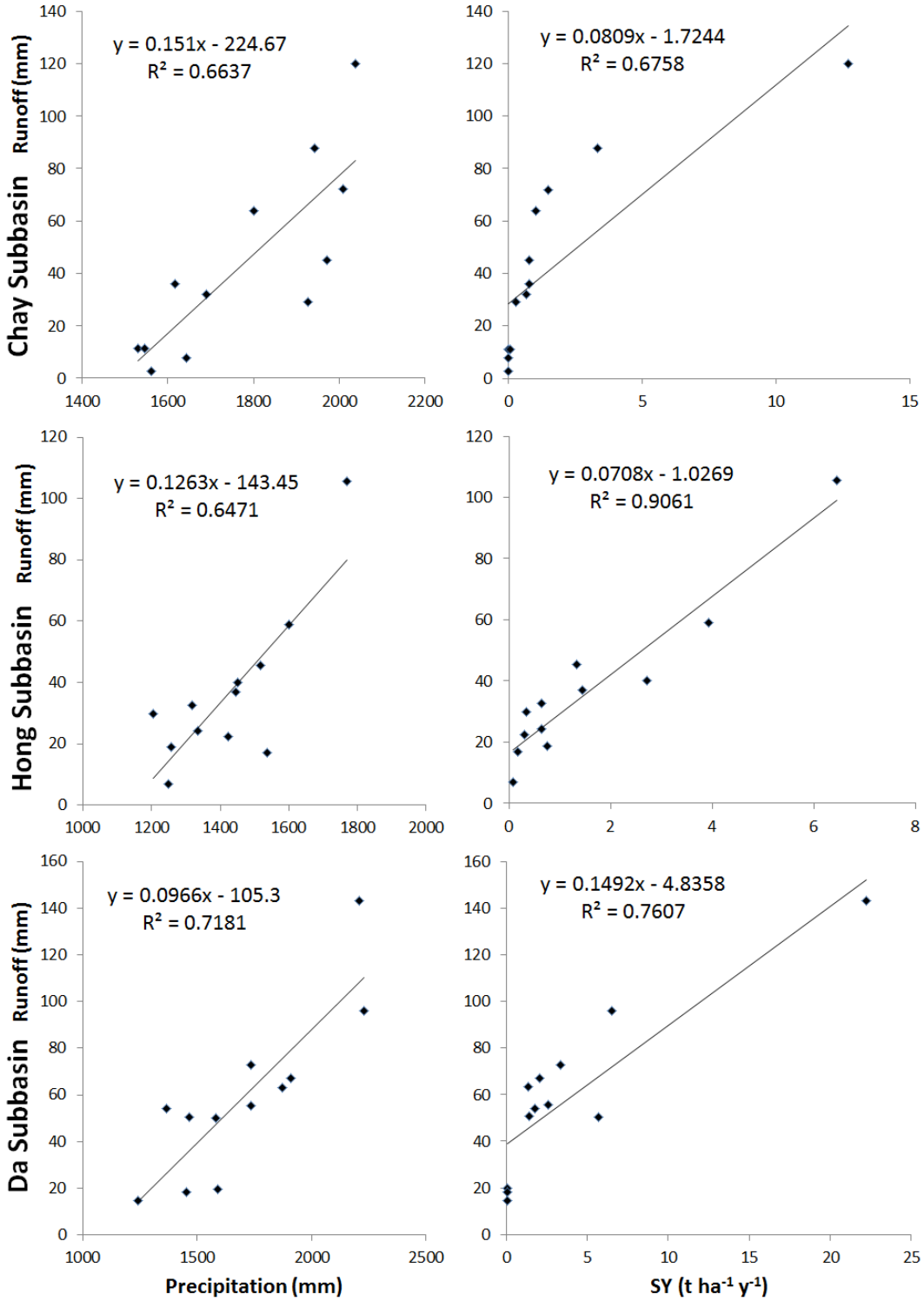

Figure 3-10. Correlations between annual rainfall, simulated surface runoff and sediment yield.

The figure 3-10 also indicates that in some wet years (AMP > 1800 mm) both the runoff and SY rates were higher than 60 (mm) and 5 (t ha^{-1} y^{-1}), respectively and particularly in the

Da basin. On the other hand, in some dry years when the runoff rates were estimated less than 20 (mm), the SY values were nearly zero. That proved the changes in runoff and SY over the years were significant.

3.4.5 Estimated Soil Loss for Districts Comparing with Data from the Vn-Atlas, 1997

Mean soil loss rates were calculated for the 12-year period from 2001 to 2012 for seven districts of the province employing LULC 2002, 2007 and 2009 and different soil data of Yen Bai soils and FAO soils (Table 3-4). During the calculated period, the soil loss rates increased about 0.56 t ha^{-1} y^{-1} for the use of YBSs and 0.51 t ha^{-1} y^{-1} for the use of FAO soils. The first four districts in Table 3-4 were classified into the low SY rates (1-5 t ha^{-1} y^{-1}) and the highest rates were calculated for the Tram Tau and Mu Cang Chai districts (5-8 t ha^{-1} y^{-1}) and categorized to moderate value. It is noted that the statistics on the table were averaged from distributed small elements of the watersheds, and that there were some areas in the region classified into very high erosion rates of about 27 t ha^{-1} y^{-1} (see Fig. 3-10). The most striking result to emerge from the table is that the simulated soil loss matched closely with data from the Vn-Atlas, 1997 in general, except slightly underestimated for the Tram Tau and Mu Cang Chai and a bit overestimated for the Luc Yen.

The employment of the soil data of FAO on the whole produced the higher SY rates than the use of the YBSs, remarkably in the areas which have many reservoirs and ponds such as in Yen Binh, Tran Yen and Luc Yen districts.

Table 3-4. Mean simulated soil loss for seven districts of Yen Bai province using LU2002, LU200, LU2009, YBSs and FAO soils.

Districts	Area (km^2)	Area (%)	Soil erosion rates (t ha^{-1} y^{-1}) using YBSs and			Soil erosion rates (t ha^{-1} y^{-1}) using FAO soils and			Vn-Atlas, 1997
			LU2002	LU2007	LU2009	LU2002	LU2007	LU2009	
Tran Yen	716.8	9.6	1.2	1.7	1.9	2.5	3.0	3.3	2.1
Van Tran	1225.8	16.4	2.0	2.3	2.5	3.4	3.7	3.8	3.6
Yen Binh	753.9	10.1	2.4	2.9	3.1	2.5	3.0	3.3	2.3
Luc Yen	1481.1	19.8	2.3	2.7	2.9	4.3	4.7	4.9	1.9
Van Yen	1389.9	18.6	2.5	2.9	3.1	4.5	4.8	5.0	3.8
Tram Tau	743.1	9.9	4.4	4.3	5.1	6.7	6.5	6.8	9.5
MCC	1177.9	15.7	7.6	7.8	7.9	7.7	8.0	8.1	12.1

MCC = Mu Cang Chai, LU = Land use/land cover, FAO = the Food and Agriculture Organization

Figure 3-11 shows estimated annual mean soil erosion rates (12-year simulation) using different LULC and soil data compared with soil erosion map extracted from the Vn-Atlas, 1997. The significant soil erosion areas were in Mu Cang Chai and Tram Tau districts and the moderate erosive areas were in the remaining districts in all cases. The maps also indicated the changes of land use (Figs 3-11a and b) effect on the soil erosion patterns. Some noted

increases can be seen in the Mu Cang Chai, Van Yen and Van Chan districts with the dark-blue colours. The use of FAO soils (Fig. 3-11d) produced the coarse maps or some areas could be combined into one zone. On the other hand, the employment of the YBSs generated finer maps and is recommended to be used for provincial scale. Intuitively, the soil loss distributions shown on the map correlated well with the coarse map of the Vn-Atlas, 1997 (Fig. 3-11c) even if they were in different scales.

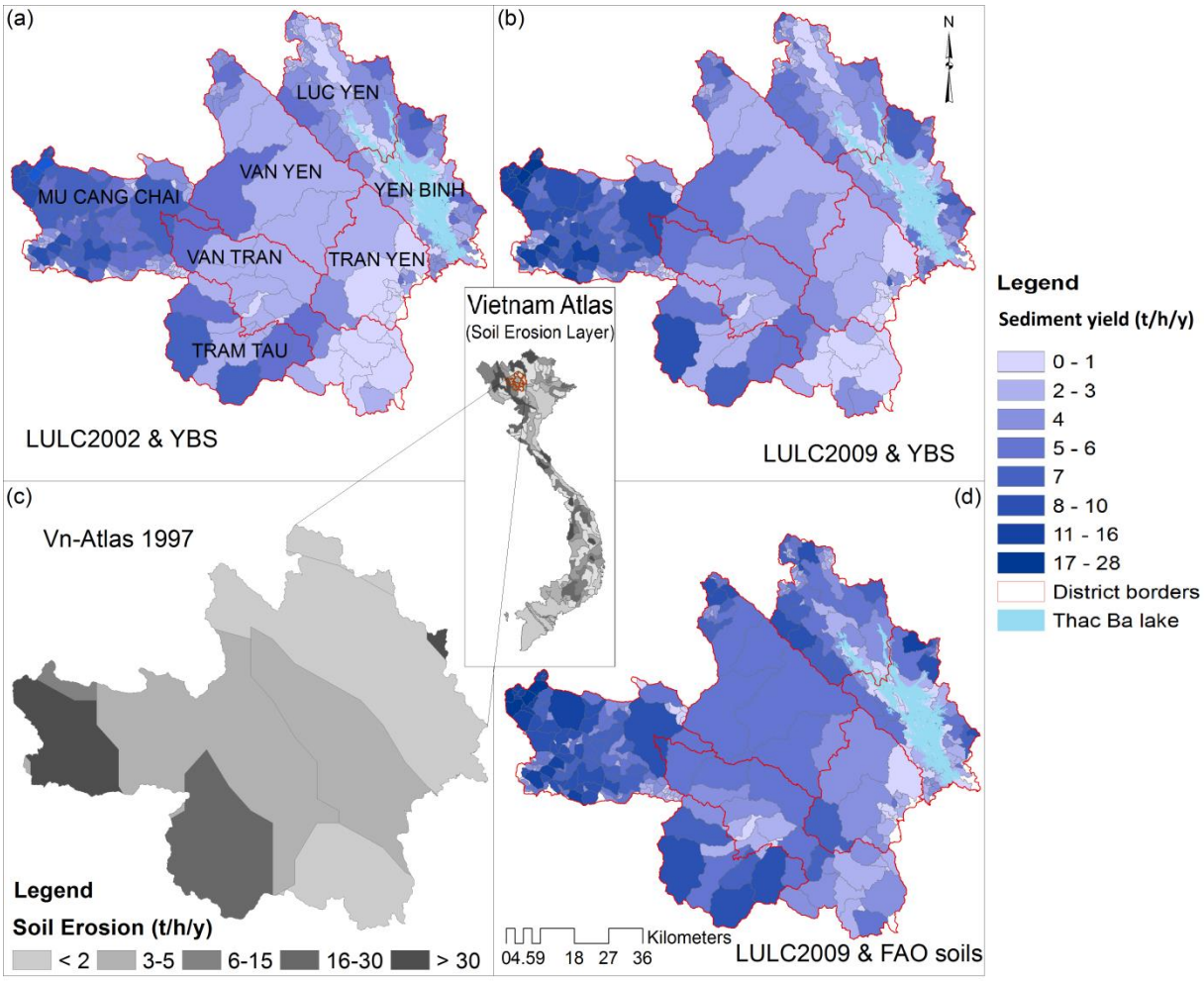

Figure 3-11. Maps of SWAT soil erosion comparing with the Vn-Atlas 1997 map.

3.4.6 Land Use Changes Effect on Soil Erosion Distributions

One of the important assessments of this study is to evaluate to what extent the changes in LULC affect the annual mean soil erosion values. The results (Fig. 3-12) illustrated that reduction of the vegetative cover increased soil erosion rates and most of the red areas (increased from one to 3.3 t ha^{-1} y^{-1}) were the results of vegetation reductions and the increase in available agricultural land (compared with Fig. 3-3). Conversely, some areas were well protected by vegetative cover (in blue and light blue), possibly due to afforestation and decline in bare land.

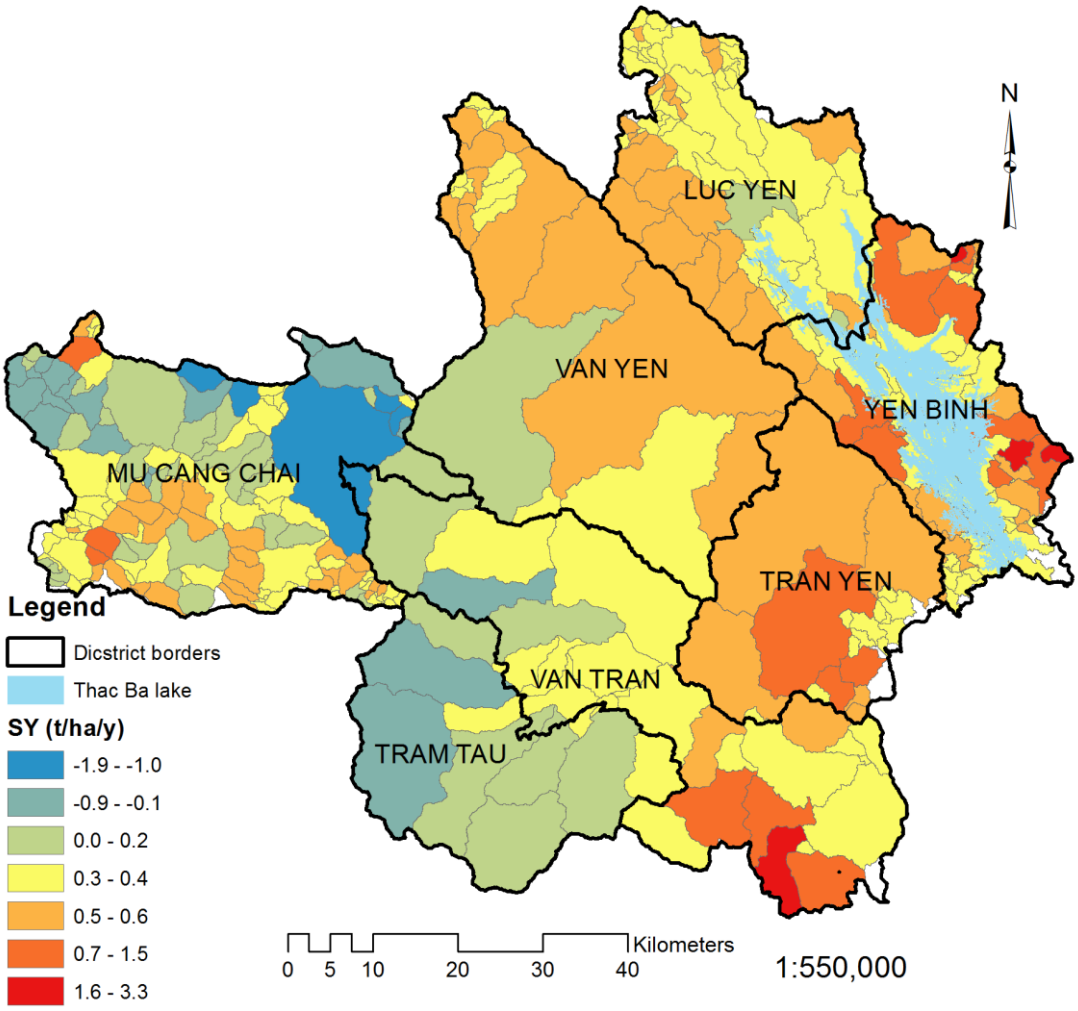

Figure 3-12. Map of soil erosion changes based on LULC2002 and 2009 inputs.

3.5 Discussion and Conclusions

The results of sensitivity of the model simulation to its spatial resolution illustrated significant variations of model outputs. It is clear that distributed models integrate spatial variability by dividing the landscape into individual components (Schmengler, 2010) and the higher the number of model element, the larger the number of single processes can be reflected and a higher spatial representation is achieved (Grayson and Blöschl, 2000). Unfortunately, increasing model resolution is not enough to ensure model precision, but it also depends on a variety of parameters such as boundary condition, effective parameter and model structure (Brazier et al., 2000). Therefore, chosen spatial data input (referring to DEMs) and model divisions (referring to CSAs) should be done with care (consideration of precision and computational time).

At the model pre-calibration, the model underestimated the base flow and overestimated the peaks as well. A possible explanation for this might be that the model was originally developed for arid regions with low in flow and low soil moisture but computed for the

tropics. However, the results of 5-year calibration and 7-year validation revealed that the monthly and daily simulated runoff matched closely with the measured discharge. This might indicate the flexibility of the model and that it could be adopted for the tropics in respect of surface runoff estimates. The study results could be archived better, if the input climate data were recorded for 20 years (Neitsch et al., 2009) or longer. For this remote-developing study site, the use of 12-year climatic data is acceptable but longer time-series climatic data is still needed for better accurate WSE estimation. In addition, the observed SY data is not available in the study site. Therefore, there is a need for *in situ* observations of model validation.

Beside the climatic and topographic aspects, the LULC plays an important role in shaping the soil erosion distributions. The reason for the increase of SY shown on the maps (Fig. 3-12) could be a reduction of vegetative cover during 2002 to 2009. This vegetative cover decrease led to higher estimated soil loss rates and this finding is in agreement with the findings of Baja et al., (2009), Bakimchandra (2011) and Cerda et al., (2007). The increase in WSE rates might cause an increase in agricultural land and bare land, especially in the uplands (Abaci and Papanicolaou, 2009) of the region as well. As this role is significant, seasonal effects on LULC classification have to be taken in to account for classification accuracy and later on resulted in evaluating WSE (Cerda, 2007; Karambiri et al., 2003 and Kefi et al., 2011). In the tropics, such as in the north of Vietnam, the agricultural land is cultivated very intensively, three or even more crops per year. This makes different reflectance on satellite scenes with different kinds of crops and, thus, sufficient ground-truth data (number of samples and being representative) has to be derived for the agricultural class. In addition, the annual soil erosion map derived from the Vn-Atlas, 1997 was assumingly not fine enough but it could somewhat verify the model's results. Remarkably, with the same inputs of the larger scale FAO soil map the model estimated a slightly higher SY rate. This was possibly due to a disappearance of water bodies in the map and in these areas the deposition processes are often more dominant rather than the erosive stages (Butt et al., 2010; Christiansson, 1979; Schmengler, 2010 and Touaibia et al., 1999).

An important finding is that the close linkages between annual rainfall, SR and SY were investigated for the 2001−2012 period and shown by the scattered graphs and equations. The equations and the R^2 values explained the logically good correlation between these factors. Surprisingly, the Da basin was found to be the most eroded area with precipitation lower than in the Chay. This rather contradictory result may be due to the strong linkage between slope, runoff and SY (the Da has the highest slope length and gradient). This relationship can also easily be seen in the equations 3-1and 2 and explained more in Neitsch et al., (2009).

In conclusion, the study objectives of modelling surface runoff and soil erosion for the tropical areas of Vietnam have been done using the SWAT model. The model simulation was found sensitive to the DEM mesh sizes and CSAs. The results also show that the model could simulate the SR and SY to a good level of accuracy. Both the daily and monthly simulated runoff closely matched with those collected from gauged measurements affirmed by the agreement coefficients (NSE and R^2).

Generally, the positive proportional linkages between AMP, SR and SY were found from those simulated results for the three basins. Significantly, soil erosion rates were estimated by the model, summarized and mapped with a consideration of LULC changes. Although the on-site SY measurement was not available for model validation, equivalent rates and distribution between simulated and existing map data have been presented. From all these, the SWAT model provides an effective tool to estimate SR and WSE for tropical regions.

3.6 References

Abaci, O., & Papanicolaou, A. N. T., 2009. Long-term effects of management practices on water-driven soil erosion in an intense agricultural sub-watershed: monitoring and modelling. *Hydrological Processes, 23*(19), 2818-2837. doi: Doi 10.1002/Hyp.738

Ananda, J., & Herath, G., 2003. Soil erosion in developing countries: a socio-economic appraisal. *Journal of Environmental Management 68, 343–353.*

Andrade, O., Kappas, M., & Erasmi, S., 2010. Assemment of Erosion Hazard in Torres Municipality of Lara State (Venezuela) based on GIS. *Asociación Interciencia Venezuela, Interciencia, Vol. 35, Núm. 5, mayo-sin mes, 2010, pp. 348-356.*

Andreu, V., Rubio, J. L., & Cerni, R., 1994. Use of a Shrub (Medicago-Arborea) to Control Water Erosion on Steep Slopes. *Soil Use and Management, 10*(3), 95-99. doi: DOI 10.1111/j.1475-2743.1994.tb00466.x

Anh, P. T. Q., Gomi, T., MacDonald, L. H., Mizugaki, S., Van Khoa, P., & Furuichi, T., 2014. Linkages among land use, macronutrient levels, and soil erosion in northern Vietnam: A plot-scale study. *Geoderma, 232–234*(0), 352-362. doi: http://dx.doi.org/10.1016/j.geoderma.2014.05.011

Arnhold, S., Lindner, S., Lee, B., Martin, E., Kettering, J., Nguyen, T. T., . . . Huwe, B., 2014. Conventional and organic farming: Soil erosion and conservation potential for row crop cultivation. *Geoderma, 219–220*(0), 89-105. doi: http://dx.doi.org/10.1016/j.geoderma.2013.12.023

Baja, S., Ramli, M., & Lias, S. A., 2009. Spatial-based assessment of land use, soil erosion, and water protection in the Jeneberang valley, Indonesia. *Biologia, 64*(3), 522-526. doi: DOI 10.2478/s11756-009-0074-y

Bakimchandra, O., 2011. Integrated Fuzzy-GIS approach for assessing regional soil erosion risks. *Universitsty of Stuttgart, Germany*. PhD thesis.

Batjes, N. H., 1996. Global assessment of land vulnerability to water erosion on a 1/2 degrees by 1/2 degrees grid. *Land Degradation & Development, 7*(4), 353-365. doi: Doi 10.1002/(Sici)1099-145x(199612)7:4<353::Aid-Ldr239>3.0.Co;2-N

Benito, E., Santiago, J. L., De Blas, E., & Varela, M. E., 2003. Deforestation of water-repellent soils in Galicia (NW Spain): Effects on surface runoff and erosion under simulated rainfall. *Earth Surface Processes and Landforms, 28*(2), 145-155. doi: Doi 10.1002/Esp.431

Berry, C. C., 1992. The kappa statistic. *Journal of the American Medical Association, 268(18):2513*.

Bicknell, B. R., Imhoff, J. C., J.L. Kittle, J., Jobes, T. H., & A.S. Donigian, J., 2001. Hydrologic Simulation Program – FORTRAN (HSPF). *user's manual for version 12.0 : USEPA, Athens, GA, 30605*.

Blavet, D., De Noni, G., Le Bissonnais, Y., Leonard, M., Maillo, L., Laurent, J. Y., . . . Roose, E., 2009. Effect of land use and management on the early stages of soil water erosion in French Mediterranean vineyards. *Soil & Tillage Research, 106*(1), 124-136. doi: DOI 10.1016/j.still.2009.04.010

Blinkov, I., & Kostadinov, S., 2010. Applicability of Various Erosion Risk Assessment Methods for Engineering Purposes. *Fourth International Scientific Conference, BALWOIS (Balkan Water Observation and Information System for Balkan countries), Ohrid, Republic of Macedonia,25-29 May 2010*

Borah, D. K., Xia, R., & Bera, M., 2002. Chapter 5: DWSM − A dynamic watershed simulation model. In Mathematical Models of Small Watershed. *Hydrology and Applications, 113−166. V. P*(Singh and D. K. Frevert, eds. Highlands Ranch, Colo.: Water Resources Publications).

Brazier, R. E., Beven, K. J., Freer, J., & Rowan, J. S., 2000. Equifinality and uncertainty in physically based soil erosion models: Application of the glue methodology to WEPP-the water erosion prediction project-for sites in the UK and USA. *Earth Surface Processes and Landforms, 25*(8), 825-845. doi: Doi 10.1002/1096-9837(200008)25:8<825::Aid-Esp101>3.0.Co;2-3

Butt, M. J., Waqas, A., Mahmood, R., & Cshrg., 2010. The Combined Effect of Vegetation and Soil Erosion in the Water Resource Management. *Water Resources Management, 24*(13), 3701-3714. doi: DOI 10.1007/s11269-010-9627-7

Cerda, A., 2007. Soil water erosion on road embankments in eastern Spain. *Science of The Total Environment, 378*(1-2), 151-155. doi: DOI 10.1016/j.sciotenv.2007.01.041

Cerda, A., Imeson, A. C., & Poesen, J., 2007. Soil water erosion in rural areas - Preface. *CATENA, 71*(2), 191-192. doi: DOI 10.1016/j.catena.2007.03.002

Christiansson, C., 1979. Imagi Dam - Study of Soil-Erosion, Reservoir Sedimentation and Water-Supply at Dodoma, Central Tanzania. *Geografiska Annaler Series a-Physical Geography, 61*(3-4), 113-145. doi: Doi 10.2307/520908

Cooper, J. R., Wainwright, J., Parsons, A. J., Onda, Y., Fukuwara, T., Obana, E., . . . Hargrave, G. H., 2012. A new approach for simulating the redistribution of soil particles by water erosion: A marker-in-cell model. *Journal of Geophysical Research-Earth Surface, 117*. doi: Artn F04027 Doi 10.1029/2012jf002499

Cyr, L., Bonn, F., & Pesant, A., 1995. Vegetation Indexes Derived from Remote-Sensing for an Estimation of Soil Protection against Water Erosion. *Ecological Modelling, 79*(1-3), 277-285. doi: Doi 10.1016/0304-3800(94)00182-H

David, M., Follain, S., Ciampalini, R., Le Bissonnais, Y., Couturier, A., & Walter, C., 2014. Simulation of medium-term soil redistributions for different land use and landscape

design scenarios within a vineyard landscape in Mediterranean France. *Geomorphology, 214*(0), 10-21. doi: http://dx.doi.org/10.1016/j.geomorph.2014.03.016

Davidson, D. A., & Harrison, D. J., 1995. The Nature, Causes and Implications of Water Erosion on Arable Land in Scotland. *Soil Use and Management, 11*(2), 63-68. doi: DOI 10.1111/j.1475-2743.1995.tb00498.x

de Aguiar, M. I., Maia, S. M. F., Xavier, F. A. D., Mendonca, E. D., Araujo, J. A., & de Oliveira, T. S., 2010. Sediment, nutrient and water losses by water erosion under agroforestry systems in the semi-arid region in northeastern Brazil. *Agroforestry Systems, 79*(3), 277-289. doi: DOI 10.1007/s10457-010-9310-2

De Munck, C. S., Hutchings, T. R., & Moffat, A. J., 2008. Impacts of climate change and establishing a vegetation cover on water erosion of contaminated spoils for two contrasting United Kingdom regional climates: a case study approach. *Integr Environ Assess Manag, 4*(4), 443-455. doi: 10.1897/IEAM_2008-016.1

Dercon, G., Mabit, L., Hancock, G., Nguyen, M. L., Dornhofer, P., Bacchi, O. O. S., . . . Zhang, X., 2012. Fallout radionuclide-based techniques for assessing the impact of soil conservation measures on erosion control and soil quality: an overview of the main lessons learnt under an FAO/IAEA Coordinated Research Project. *Journal of environmental radioactivity, 107*(0), 78-85. doi: 10.1016/j.jenvrad.2012.01.008

Evans, R., 2005. Monitoring water erosion in lowland England and Wales - A personal view of its history and outcomes. *CATENA, 64*(2-3), 142-161. doi: DOI 10.1016/j.catena.2005.08.003

Foster, G. R., Flanagan, D. C., Nearing, M. A., Lane, L. J., Risse, L. M., & Finkner, S. C., 1995. Hillslope erosion component, in Water Erosion Prediction Project. *Hillslope Profile and Watershed Model Documentation, USDA NSERL Rep. 10, edited by D. C. Flanagan and M. Nearing* (chap. 11, 11.1–11.12, Natl. Soil Erosion Res. Lab., Agric. Res. Serv., U.S. Dep. of Agric., West Lafayette, Indiana.).

Fukunaga, D. C., Cecílio, R. A., Zanetti, S. S., Oliveira, L. T., & Caiado, M. A. C., 2015. Application of the SWAT hydrologic model to a tropical watershed at Brazil. *CATENA, 125*(0), 206-213. doi: http://dx.doi.org/10.1016/j.catena.2014.10.032

Grayson, R., & Blöschl, G., 2000. Spatial modelling of catchment dynamics. In: Grayson R, Blöschl G (eds) Spatial patterns in catchment hydrology. Observation and modeling. *Cambridge University Press, Cambridge, pp51-81*

Green, W. H., & Ampt, G. A., 1911. Studies on soil physics, 1. The flow of air and water through soils. *Journal of Agricultural Sciences 4:11-24*.

Gumiere, S. J., Raclot, D., Cheviron, B., Davy, G., Louchart, X., Fabre, J. C., . . . Le Bissonnais, Y., 2011. MHYDAS-Erosion: a distributed single-storm water erosion model for agricultural catchments. *Hydrological Processes, 25*(11), 1717-1728. doi: Doi 10.1002/Hyp.7931

Hessel, R., & Tenge, A., 2008. A pragmatic approach to modelling soil and water conservation measures with a catchment scale erosion model. *CATENA, 74*(2), 119-126. doi: DOI 10.1016/j.catena.2008.03.018

Huggins, L. F., & Monke, E. J., 1966. The mathematical simulation of small watersheds. *Technical Report 1. Water Resources Research Center, Purdue University. West Lafayette, IN. 130 p*.

Jurgens, C., & Fander, M., 1993. Soil-Erosion Assessment by Means of Landsat-Tm and Ancillary Digital Data in Relation to Water-Quality. *Soil Technology, 6*(3), 215-223. doi: Doi 10.1016/0933-3630(93)90011-3

Karambiri, H., Ribolzi, O., Delhoume, J. P., Ducloux, J., Coudrain-Ribstein, A., & Casenave, A., 2003. Importance of soil surface characteristics on water erosion in a small grazed Sahelian catchment. *Hydrological Processes, 17*(8), 1495-1507. doi: Doi 10.1002/Hyp.1195

Kefi, M., Yoshino, K., & Setiawan, Y., 2012. Assessment and mapping of soil erosion risk by water in Tunisia using time series MODIS data. *Paddy and Water Environment, 10*(1), 59-73. doi: DOI 10.1007/s10333-011-0265-3

Kefi, M., Yoshino, K., Setiawan, Y., Zayani, K., & Boufaroua, M., 2011. Assessment of the effects of vegetation on soil erosion risk by water: a case of study of the Batta watershed in Tunisia. *Environmental Earth Sciences, 64*(3), 707-719. doi: DOI 10.1007/s12665-010-0891-x

Lopez-Vicente, M., Poesen, J., Navas, A., & Gaspar, L., 2013. Predicting runoff and sediment connectivity and soil erosion by water for different land use scenarios in the Spanish Pre-Pyrenees. *CATENA, 102*, 62-73. doi: DOI 10.1016/j.catena.2011.01.001

Makungo, R., Odiyo, J. O., Ndiritu, J. G., & Mwaka, B. (2010). Rainfall–runoff modelling approach for ungauged catchments: A case study of Nzhelele River sub-quaternary catchment. *Physics and Chemistry of the Earth, Parts A/B/C, 35*(13–14), 596-607. doi: http://dx.doi.org/10.1016/j.pce.2010.08.001

Mchunu, C., & Chaplot, V., 2012. Land degradation impact on soil carbon losses through water erosion and CO2 emissions. *Geoderma, 177*, 72-79. doi: DOI 10.1016/j.geoderma.2012.01.038

Moriasi, D. N., Arnold, J. G., Van Liew, M.W., Bringer, R. L., Harmel, R. D.&Veith, T. L., 2007. Model evaluation guidelines for systematic quantification of accuracy in watershed simulations. *Am. Soc. Agric. Biol. Eng. 50* (3), 885–900.

Mukundan, R., Pradhanang, S. M., Schneiderman, E. M., Pierson, D. C., Anandhi, A., Zion, M. S., . . . Steenhuis, T. S., 2013. Suspended sediment source areas and future climate impact on soil erosion and sediment yield in a New York City water supply watershed, USA. *Geomorphology, 183*, 110-119. doi: DOI 10.1016/j.geomorph.2012.06.021

Nash, J. E., & Sutcliffe, J. V., 1970. River flow forecasting through conceptual models 1: a discussion of principles. *Journal of Hydrology 10* (3), *282–290.*

Ndomba, P., Mtalo, F., & Killingtveit, A., 2008. SWAT model application in a data scarce tropical complex catchment in Tanzania. *Physics and Chemistry of the Earth, Parts A/B/C, 33*(8–13), 626-632. doi: http://dx.doi.org/10.1016/j.pce.2008.06.013

Nearing M. A., G. R. Foster, L. J. Lane, & Finkner, S. C., 1989. A Process-Based Soil Erosion Model for USDA - Water Erosion Prediction Project Technology. *The American Society of Agricultural Engineers* Vol. 32(5): 09-10.1989

Neitsch, S. L., J.G. Arnold, J.R. Kiniry , & Williams, J. R., 2009. Soil and Water Assessment Tool Theoretical Documentation, Version 2009. *Texas Water Resources Institute Technical Report No. 406*.

Nunes, J. P., Seixas, J., & Pacheco, N. R., 2008. Vulnerability of water resources, vegetation productivity and soil erosion to climate change in Mediterranean watersheds. *Hydrological Processes, 22*(16), 3115-3134. doi: Doi 10.1002/Hyp.6897

Oliveira, A. H., Silva, M. L. N., Curi, N., Avanzi, J. C., Neto, G. K., & Araujo, E. F., 2013. Water Erosion in Soils under Eucalyptus Forest as Affected by Development Stages and Management Systems. *Ciencia E Agrotecnologia, 37*(2), *159-169.*

Routschek, A., Schmidt, J., Enke, W., & Deutschlaender, T., 2014. Future soil erosion risk — Results of GIS-based model simulations for a catchment in Saxony/Germany. *Geomorphology, 206*(0), 299-306. doi: http://dx.doi.org/10.1016/j.geomorph.2013.09.033

Santhi, C., Arnold, J. G., Williams, J. R., Dugas,W. A., Srinivasan, R. & Hauck, L. M., 2001. Validation of the SWAT model on a large river basin with point and nonpoint sources. J. Am. *Water Resour. Assoc. 37* (5), 1169–1188.

Schmengler, A. C., 2010. Modeling soil erosion and reservoir sedimentation at hill and catchment scale in semi-arid Burkina Faso. *Rheinischen Friedrich-Wilhelms-Universität zu Bonn*. PhD thesis.

Shen, Z. Y., Gong, Y. W., Li, Y. H., Hong, Q., Xu, L., & Liu, R. M., 2009. A comparison of WEPP and SWAT for modeling soil erosion of the Zhangjiachong Watershed in the Three Gorges Reservoir Area. *Agricultural Water Management, 96*(10), 1435-1442. doi: DOI 10.1016/j.agwat.2009.04.017

Shepard, D., 1986. A two-dimensional interpolation function for irregularly spaced data. *In Proceedings of the 1968 23rd ACM National Conference, 517–523*.

Smith, R. E., Goodrich, D. C., Woolhiser, D. A., & Unkrich, C. L., 1995. KINEROS – A kinematic runoff and erosion model; Chapter 20 in V.P. Singh (editor), Computer Models of Watershed Hydrology. *Water Resources Publications, Highlands Ranch, Colorado, 1130 pp*.

Thiessen, A. H., 1911. PRECIPITATION AVERAGES FOR LARGE AREAS. *Monthly Weather Review, 39*(7), 1082-1089. doi: 10.1175/1520-493(1911)39<1082b:PAFLA>2.0.CO;2

Tibebe, D. B., W., 2011. Surface Runoff and Soil Erosion Estimation Using the Swat Model in the Keleta Watershed, Ethiopia. *Land Degradation & Development, 22*(6), 551-564. doi: Doi 10.1002/Ldr.1034

Touaibia, B., Dautrebande, S., Gomer, D., & Aidaoui, A., 1999. Quantitative approach to water erosion at different spatial scales: basin of Oued Mina. *Hydrological Sciences Journal-Journal Des Sciences Hydrologiques, 44*(6), 973-986. doi: Doi 10.1080/02626669909492292

USDA-SCS (United States Department of Agriculture–Soil Conservation Service). (1972). *National Engineering Handbook, Section 4 Hydrology*. Washington, DC.

USDA-SCS., 1986. Technical Release 55, Urban hydrology for small watersheds. (Chapter 9 and 10). *United States Department of Agriculture, Soil Conservation Service*. http://www.wcc.nrcs.usda.gov/hydro//hydro-tools-models-tr55.html.

VEM, V. E. M., 2012. Chính sách đất đai phát triển "tam nông": Những vấn đề đặt ra. http://www.tapchitaichinh.vn/Trao-doi-Binh-luan/Chinh-sach-dat-dai-phat-trien-tam-nong-Nhung-van-de-dat-ra/14637.tctc.

Vn-Atlas., 1997. Atlas of national physical maps of 66 fields. *Viet Nam Publishing House of Natural Resources, Environment and Cartography*, 1997. http://www.bando.com.vn/en/default.aspx

Viera, A. J., & Garrett, J. M., 2005. Understanding Interobserver Agreement: The Kappa Statistic. *Family Medicine, Fam Med 2005;37*(5):360-3.

Vu, M. T., Raghavan, S. V., & Liong, S. Y., 2012. SWAT use of gridded observations for simulating runoff - a Vietnam river basin study. *Hydrology and Earth System Sciences, 16*(8), 2801-2811. doi: DOI 10.5194/hess-16-2801-2012

Williams, J. R., 1975. Sediment-yield prediction with universal equation using runoff energy factor. In Present and prospective technology for predicting sediment yield and sources: *Proceedings of the sediment-yield workshop, USDA Sedimentation Lab., Oxford, MS, p. 244-252, November 28-30, 1972. ARS-S-40.*

Williams, J. R., 1995. Chapter 25: The EPIC model. *p. 909-1000. In V.P. Singh (ed.) Computer models of watershed hydrology.* Water Resources Publications.

Wischmeier, W. H., & Smith, D. D., 1965. Predicting rainfall-erosion losses from cropland east of the Rocky Mountains. *Agriculture Handbook 282.* USDA-ARS.

Wischmeier, W. H., & Smith, D. D., 1978. Predicting rainfall erosion losses: a guide to conservation planning. *Agriculture Handbook 282.* USDA-ARS.

Zhang, X., R. Srinivasan, & Liew, M. V., 2008. Multi-site Calibration of the SWAT Model for Hydrological Modelling. *Soil & Water Division of ASABE, Vol. 51*(6): 2039-2049

Zhang, X., Raghavan Srinivasan, & Bosch, D., 2009. Calibration and uncertainty analysis of the SWAT model using Genetic Algorithms and Bayesian Model Averaging. *Journal of Hydrology*. *S0022-1694*(09), 00354-0. doi: 10.1016/j.jhydrol.2009.06.023

CHAPTER 4

Event-based, Water-induced Soil Erosion Modelling for Medium Watersheds in Yen Bai Province, Vietnam Using the KINEROS2 Model[5]

"The nation that destroys its soil destroys itself."

-Franklin D. Roosevelt

SUMMARY

The problem of water and soil erosion has become an important issue in the North of Vietnam. Modelling its processes might help in understanding and quantifying the development of erosion better. Based on data availability, climate condition and scale (medium watershed and event-based rain) we decided to use the KINEROS2 model for this research. The changing land use practices have a significant impact on the reduction of saturated hydraulic conductivity (Ks), thus, increasing the Horton overland flow (HOF) and eventually exaggerating soil erosion. On the model simulation stage, we found that the boundary conditions and the parameter sensitive tests were crucial for estimation of model outputs and these converged to measured data. Interestingly, the use of the finer temporal resolution (5 minutes) of radar rainfall (accumulative 144 mm) produced much lower sediment yield (SY) rates compared to satellite precipitation (30 minutes, accumulative 138 mm). Although each tested variable had different effects on model outputs, the Ks presented the most sensitive parameter to SY in both channels and on planes, followed by soil saturation index (S) and hillslope roughness (R). The geomorphological resolutions based on critical source area (CSA) defining modelling resolutions were found to be remarkable for soil loss estimation and must be determined with care. Finally, changing land uses which resulted in soil erosion were mapped with significant increases in SY for the whole Man Kim and for some areas in the Nam Khat watershed.

[5] This paper is published in the conference proceedings of the FIG conference, 17th - 21st, May 2015, Sofia, Bulgaria.
http://www.fig.net/resources/proceedings/fig_proceedings/fig2015/papers/ts05a/TS05A_mguyen_kappas_7589.pdf

4.1 Introduction

Land degradation, including soil erosion has become one of the most serious problems (da Silva et al., 2012; Kefi et al., 2011; Pham Thai NAM, 2003) and has affected sustainable development (Kefi et al., 2012), particularly in developing countries with low cultivated land per capita as in Vietnam. Information about the rate of soil erosion could help in better understanding the development of the land (Parsons et al., 2004) and is useful for determining the sustainability of agricultural practices (Cooper et al., 2012). Effective soil erosion modelling can provide important data on soil erosion patterns and trends (Millington, 1986).

In northern Vietnam, the problem of land degradation has reportedly become worse due to the reduction of canopy, mostly the decline of forested land (shifting agriculture and timber removal by ethnic groups) (Tuan, 1993), and forest fragmentation (Ziegler et al., 2006). This has reduced the saturated hydraulic conductivity (Ks) of the lands (forest land has highest Ks among the others), and thus, increased the Hortonian overland flow (HOF, occurs when the rainfall rate exceeds infiltration capacity and surface storage; (Horton, 1933)). Two watersheds named Nam Kim and Nam Khat, both located in the Mu Cang Chai district of Yen Bai province Vietnam, were chosen for the case study based on the high rates of soil erosion (about 5-10 t ha^{-1} y^{-1}).

There are various existing methods of approaching the erosion issue (Guzman et al., 2013), including direct and indirect approaches. Modelling is one of the options which might have some advantages in terms of time consuming cost and trend analyses. The KINEROS2 model accounts separately for soil erosion caused by rain drop energy and by flowing water (Woolhiser et al., 1990). On the other hand, the (SWAT (Arnold, 1994) model accounts for only runoff causing erosion, the WEPP model divides erosion process into rill and interill erosion (Nearing et al., 1989)). In the KINEROS2, some key parameters are taken into account like Ks, Manning's n, splash, and cover, soil profiles (fraction of sand, silk and clay) etc. Although each variable differs to some extent in sensitivity to the model's outputs, all these parameters must be well-prepared in order to gain the best model estimations. Additionally, observed data is crucial and a prerequisite for validating the model. We applied the KINEROS2 for modelling sediment yield on hill slopes and sediment transport in channels of two medium-sized watersheds with model validation, sensitivity tests and trend analysis of different LULCs. While this KINEROS2 was developed for small semi-arid watersheds (Burns et al., 2008), it was employed for the tropics which are similar to our study

site in a study by Ziegler et al., (2007). Furthermore, based on our study aim of spatial and temporal scale of modelling, we decided to use the model.

In this study, we investigated the ability of the KINEROS2 to model medium-sized (74-268 km^2) catchment areas with acceptable results. Herein, we (i) calibrated channel discharge at the outlets and compared gauged data with different uses of rainfall data sources; (ii) parameter sensitive test for some variables; (iii) analysis of the effect of LULC inputs on sediment yield in watershed's elements and streams. The results indicated that the model was validated by producing the discharge closely to field measured data for both uses of satellite and radar rainfalls. What is more, we found that the tests for parameter sensitivities were crucial for understanding the behaviour of the model and what aspects each variable had in influencing hydraulic responses in the watersheds. Therefore, we recommend the use of the KINEROS2 for similar study objectives.

4.2 Study Site

The study watersheds are located in Yen Bai province, Vietnam (Fig. 4-1) and are a part of typical tropics in North-Western Vietnam. The areas of the watershed are 268 km^2 and 74 km^2 for the Nam Kim and the Nam Khat watershed, respectively. The central coordinates of the province are 104°30'9.0" E and 21°35'26.7" N and the mean elevation is about 900 meters above the Bien Dong Sea level. The annual precipitation in the region varies from 1,365 to 1,570 mm and approximately 85 percent of the total rainfall is recorded in the summer time. The mean daily solar radiation is estimated very high at 14.5 (MJ m^{-2} day^{-1}) and the mean wind speed is 1.23 (m s^{-1}). We chose these watersheds for the case study because of their representation of rapid eroded processes and their representative morphological characteristics for the whole region.

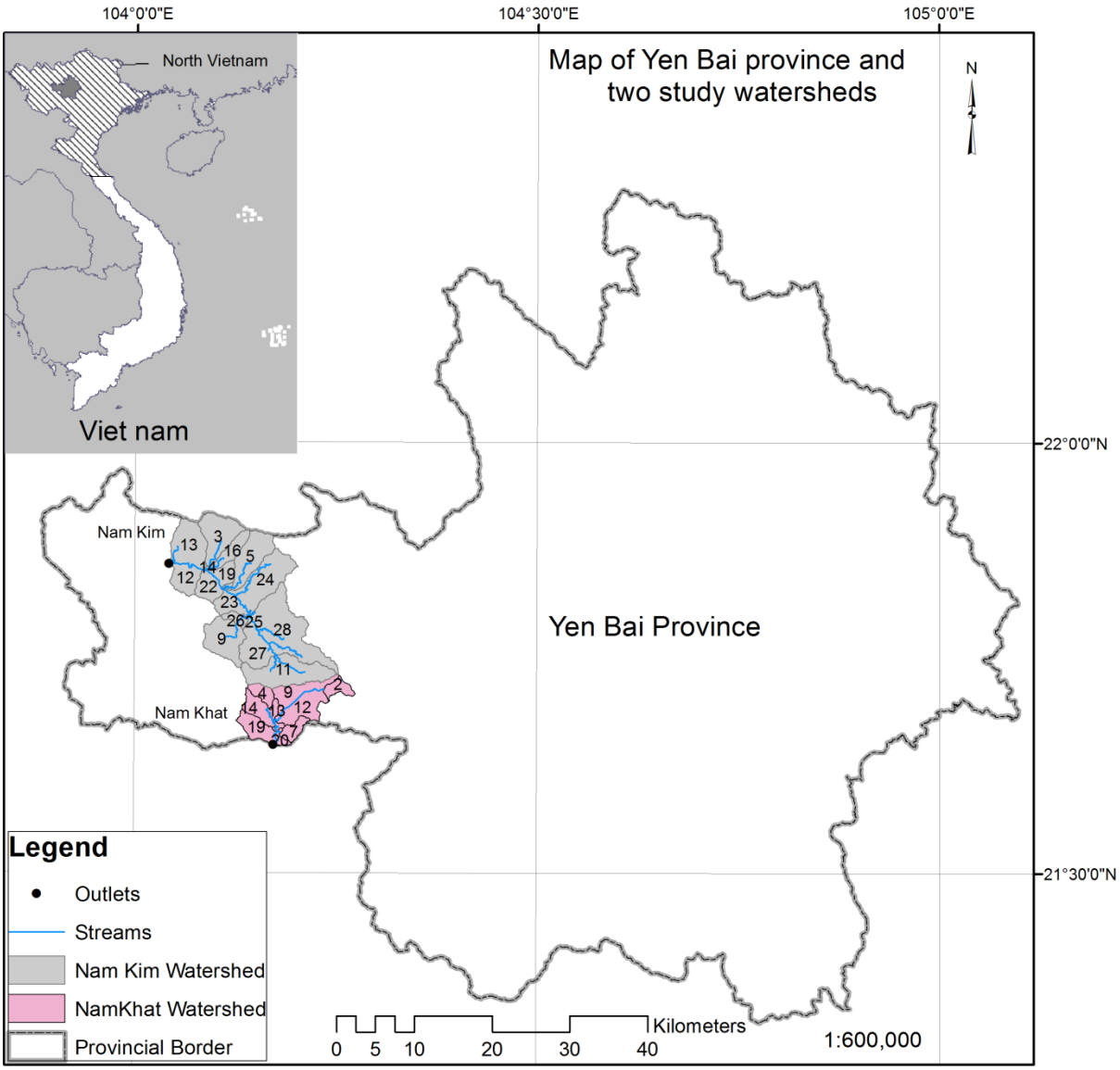

Figure 4-1. Study site - the Nam Kim and the Nam Khat watershed of Yen Bai province, Vietnam.

4.3 Materials and Method

4.3.1 Soil Erosion Equations Used in the KINEROS2 Model

The KINEROS2 (Smith et al., 1995) is a modified model of the original model of KINEROS (Woolhiser et al., 1990) and is an event-based model rather than a continuous simulation model (Smith et al., 1999). It is a model of Hortonian hydrology and simulates saturation overland flow when the top soil layer lying above a restrictive layer becomes saturated. While the SWAT model calculates sediment yield based on the amount of runoff and employs the equation of (Williams, 1995), KINEROS2 estimates sediment transport based on both rain-drop energy and surface runoff. The soil erosion and sediment transport rate are determined by the solution to the sediment balance as in the following relation (Smith et al., 1999);

$$\frac{\partial(AC_S)}{\partial t} + \frac{\partial(QC_S)}{\partial x} - we(x,t,C_s) = q_c(x,t) \quad (4\text{-}1)$$

where A is local cross sectional area of flow (m^2), Q is local discharge rate $m^3\ s^{-1}$, t is time (s), x is distance along the flow path (m), w indicates local flow width (m), q is rainfall exceed (m s^{-1}), C_s is the sediment concentration ($m^3\ m^{-3}$), e indicates the local rate of erosion or deposition ($m^3\ s^{-1}\ m^{-2}$) and q_c refers to the rate of sediment inflow, as for lateral inflow to a channel (m s^{-1}).

In which, the KINEROS2 estimates runoff by dynamic routing of rainfall excess;

$$q_{(t)} = r_{(t)} - f_{(t)} \quad (4\text{-}2)$$

where $r_{(t)}$ is rainfall runoff pattern (mm s^{-1}), $f_{(t)}$ indicates infiltration pattern usually more effectively related to infiltrate depth (mm s^{-1}).

In addition, the erosion rate is computed from rain splash erosion $e_s(r,h)$ and hydraulic erosion, e_h, rain flash erosion is directly linked to rain energy and related to rain intensity in a unit of area. The KINEROS2 links e_s with the precipitation rate (r), the fraction of covered soil (y) and the min runoff depth ($\bar{h}$).

Splash erosion is determined as follows;

$$e_s = Spl\,(1-y)\cdot exp\left(-c_d\bar{h}\right)r^2 \quad (4\text{-}3)$$

The soil vulnerability to rainfall detachment is determined by parameter Spl and c_d is indicating the effect of water depth in damping splash energy. A reduction in splash erosion with a raising depth of surface water is expressed by the exponent function and reflects its dampening effect on splash energy.

The hydraulic erosion is calculated as in relation;

$$e_h = Ch_{vs}\,(C_m - C_s) \quad (4\text{-}4)$$

where C_m is transport capacity, a concentration is presented and is estimated in KINEROS2 by a modified form of the Engelund and Hansen relation (Engelund & Hansen, 1967). The Ch is a coefficient and inversely related to soil cohesion or any other restriction on soil entrainment by flowing water. It is set to 1.0 during the deposition process ($C_s > C_m$). Schematic illustration of the geometric subdivision of a hypothetical catchment and other components of the model can be referenced in the literature of (Woolhiser et al., 1990).

4.3.2 Data for the Model Parameterizations

4.3.2.1 The Digital Elevation Model (DEM)

A DEM extracted from a Yen Bai database (produced by the Vietnam Natural Resources and Environment Corporation in 2009) was used for morphological input data. This is a 10 × 10 m grid-based DEM and produced using Photogrammetry technology (Image Stations of Intergraph Corporation, USA).

4.3.2.2 Land Use/Land Cover (LULC) Datasets

We used Landsat TM imagery for LULC classifications and the ground control points and ground-truth data were extracted from the Yen Bai geodatabase for geometric corrections and the supervised maximum likelihood classified method using the ENVI 4.7, respectively. Two Landsat TM scenes acquired on 28th January 2002 and 26th March 2007 were processed and analysed for seven LULC categories (Fig. 4-8) and accuracy assessment (kappa statistics producer accuracy and user accuracy).

Mean producer accuracy of classes of LULC2002 is 69.0%, of LULC2007 is 72.7%. Average user accuracy calculated for LULC2002 and 2007 are 68.9 and 72.8% and overall accuracies are 69.3 and 72.2%, respectively. The kappa statistics were also estimated at 0.65 for LULC2002 and 0.69 for LULC2007. The reductions of vegetation cover presented in the watersheds during 2002-2007 period can be seen within the Fig. 4-8. This, on the one hand, is illustrated most clearly in the Nam Kim and less, on the other hand, in the Nam Khat watershed.

4.3.2.3 Soil Data

Soil profiles of the study site were derived from the Yen Bai custom soil map scale 1: 600,000 produced by the Environment and Resource Centre-Agricultural Institute of Plan and Design, Vietnam. The soils were mapped in MapInfo software in 1996 and categorized into 6 major soil groupings including fluvisols, calcisols, ferralsols, alisols, acrisols and gleysols. However, the humic ferralsols and humic acrisols are dominant in the Nam Kim and Nam Khat watersheds.

4.3.2.4 Satellite-based and Radar Rainfall Data

MTSAT images with fifteen-minute and 4 × 4 km temporal and spatial resolutions were provided by the Vietnam National Centre for Hydro-Meteorological Forecasting (NCHMF, 2011) for the rainfall input to the model in order to assess the rain event on 23rd June 2011.

The radar rainfall with five-minute, 2 × 2 km rainfall images from the NCHMF were used for the precipitation input for the same day.

4.3.2.5 Observed Discharge for Model Validation

Only discharge data from the hydrological gauge at the outlet of the Nam Kim watershed called Mu Cang Chai station was available and collected for the model validation. There was another gauge at Hut's outlet, but the Hut basin is too large (≈ 617 km^2) and considered not appropriate for a KINEROS2 application due to the scale problem.

4.3.3 Application of the Model

4.3.3.1 Watershed Delineations and Parameterizations

The two watersheds were parameterized using above inputs and the tabular summaries are indicated within Tables 4-1 and 2. The information within the two tables used LULC2007 and the CSAs were set at 7.5% of the area for the Nam Kim and 5% for the Nam Khat watershed.

4.3.3.2 Testing Model Parameter Sensitivity

As based on previous literature, the K_s- saturated hydraulic conductivities of hill slopes were found to be most sensitive to surface runoff (Memarian et al., 2013). The sensitivities of the relative saturation index (R) and the critical source area (CSA) are considered to have significant effects on the model outputs (Kalin et al., 2003). Therefore, we tested these parameters for our study zones.

4.3.3.3 Model Calibration and Validation

The watersheds were calibrated with a slope adjustment for the curve number (CN) of the nine land use types of both LULC2002 and 2007 for the aim of estimating the soil erosion of the single rain event on 23rd June 2011. The sensitive parameters (section 4.3.3.2) were altered for every model run for the single rain. The relative soil saturation index (S) must be pre-defined as an antecedent condition. The S values were set at 0.46 for the Nam Kim and 0.42 for the Nam Khat. The method of accuracy assessment was to estimate the benefit of model simulation based on the Nash and Sutcliffe efficiency (Nash & Sutcliffe, 1970).

Table 4-1. Parameters of the Nam Kim watershed

Plane_ID	Shape_Area	AvgSlope	INT_	Cover	Mann_N	Splash	Rock	Ks	G	Por	Smax	Cv	Fract_sand	Fract_silt	Fract_clay	Dist
3	21.6	0.59	1.68	44.66	0.08	121.91	0.07	5.41	300.91	0.44	0.84	0.52	0.36	0.25	0.39	0.27
5	21.6	0.62	1.47	39.15	0.06	121.89	0.07	5.14	298.69	0.44	0.84	0.53	0.37	0.25	0.38	0.28
9	22.4	0.53	2.01	50.10	0.09	120.13	0.06	4.36	334.32	0.46	0.83	0.50	0.28	0.23	0.48	0.22
11	32.6	0.52	1.71	56.25	0.10	119.26	0.06	4.08	346.43	0.46	0.83	0.50	0.26	0.22	0.51	0.21
12	12.3	0.58	1.65	56.90	0.10	120.15	0.06	5.24	334.99	0.46	0.84	0.51	0.27	0.23	0.50	0.21
13	22.8	0.59	2.03	42.79	0.07	122.46	0.06	6.72	266.34	0.42	0.84	0.58	0.48	0.25	0.27	0.35
14	0.2	0.63	1.80	35.92	0.05	122.94	0.06	8.08	291.95	0.47	0.86	0.56	0.30	0.24	0.46	0.21
16	8.9	0.66	1.48	50.50	0.08	120.71	0.07	4.86	323.63	0.45	0.84	0.51	0.31	0.24	0.46	0.23
17	0.3	0.50	1.65	42.35	0.05	119.93	0.06	4.69	337.11	0.47	0.84	0.52	0.26	0.23	0.51	0.20
18	0.6	0.63	1.21	43.46	0.04	122.64	0.05	7.58	254.08	0.41	0.84	0.61	0.51	0.25	0.23	0.37
19	6.6	0.54	1.51	43.33	0.05	121.03	0.06	6.00	301.30	0.44	0.84	0.56	0.37	0.24	0.39	0.28
22	9.7	0.57	1.63	52.00	0.08	119.98	0.06	4.97	338.77	0.47	0.84	0.52	0.26	0.23	0.51	0.20
23	8.5	0.57	1.75	48.24	0.08	119.07	0.06	3.50	354.30	0.47	0.83	0.49	0.24	0.22	0.54	0.19
24	30.4	0.59	1.64	55.32	0.10	122.32	0.06	6.60	284.45	0.43	0.84	0.54	0.41	0.25	0.33	0.31
25	1.3	0.57	1.72	53.20	0.09	118.39	0.06	3.11	367.13	0.47	0.83	0.49	0.21	0.22	0.57	0.17
26	2.7	0.54	2.21	35.20	0.05	118.81	0.06	2.86	359.16	0.47	0.83	0.49	0.23	0.22	0.55	0.18
27	17.3	0.52	1.80	51.75	0.09	118.57	0.06	3.21	363.51	0.47	0.83	0.49	0.22	0.22	0.56	0.18
28	48.5	0.56	1.72	51.61	0.09	120.18	0.06	4.57	330.62	0.46	0.83	0.51	0.30	0.23	0.47	0.23

Table 4-2. Parameters of the Nam Khat watershed

Plane_ID	Shape_Area	AvgSlope	INT_	Cover	Mann_N	Splash	Rock	Ks	G	Por	Smax	Cv	Fract_sand	Fract_silt	Fract_clay	Dist
2	5.92	0.51	1.65	72.56	0.12	122.07	0.06	7.93	295.79	0.44	0.84	0.55	0.38	0.25	0.37	0.28
4	5.94	0.56	2.18	65.88	0.10	122.27	0.05	7.99	258.82	0.40	0.83	0.59	0.53	0.25	0.22	0.39
7	6.08	0.47	2.28	63.27	0.09	121.38	0.05	7.17	268.12	0.40	0.83	0.59	0.52	0.25	0.23	0.39
9	13.63	0.41	2.21	58.91	0.08	121.18	0.06	6.81	293.34	0.43	0.83	0.59	0.42	0.24	0.34	0.32
12	16.05	0.42	1.67	67.07	0.11	119.45	0.06	5.09	337.19	0.45	0.83	0.53	0.30	0.23	0.48	0.23
13	2.37	0.45	2.64	55.41	0.06	121.54	0.05	6.78	263.00	0.40	0.83	0.60	0.54	0.25	0.21	0.40
14	9.02	0.60	1.88	69.63	0.11	123.16	0.06	8.93	250.57	0.40	0.84	0.58	0.53	0.26	0.21	0.39
15	0.29	0.53	2.73	52.07	0.05	121.54	0.05	6.54	263.00	0.40	0.83	0.60	0.54	0.25	0.21	0.40
16	0.88	0.54	2.67	58.52	0.07	121.54	0.05	7.00	263.00	0.40	0.83	0.60	0.54	0.25	0.21	0.40
17	0.03	0.51	3.00	55.00	0.06	121.54	0.05	6.75	263.00	0.40	0.83	0.60	0.54	0.25	0.21	0.40
18	0.23	0.51	1.97	42.16	0.05	121.54	0.05	5.90	263.00	0.40	0.83	0.60	0.54	0.25	0.21	0.40
19	11.45	0.56	1.92	68.60	0.11	123.34	0.06	8.94	249.20	0.40	0.84	0.58	0.53	0.26	0.21	0.39
20	2.02	0.54	2.21	63.97	0.09	121.54	0.05	7.41	263.00	0.40	0.83	0.60	0.54	0.25	0.21	0.40

Plane_ID presents the identifications of planes (Fig. 4-1), Shape_Area is plane's area (km^2), AvgSlope is the zonal mean slope of the plane element in percent rise, INT_ is interception depth (m), Cover is fraction of surface covered by intercepting cover – the rainfall intensity is reduced by this fraction until the specified interception depth has been accumulated (0-1), Mann-N is Manning's n coefficient, Splash represents rain splash coefficient (0-1), Rock is volumetric rock fraction, G is the mean capillary drive (mm), Por indicates soil porosity ($cm^3\ cm^{-3}$), Smax is maximum relative saturation (%), Cv is coefficient of variation, Fract_sand, silt and clay indicates the fractions of sand silt and clay (0-1) and Dist is pore size distribution index.

4.4 Results

4.4.1 Model Validation

Figure 4-2 shows a good concurrence between the model outflows and gauged data through the Nam Kim outlet. The model was performed with hill slope Ks ranging from 4.3 to 11.5, from 6.1 to 10.7; the S was set at 0.46, 0.42 and N ranging from 0.04 to 0.1, 0.05 to 0.12 for the Nam Kim and Nam Khat, respectively. The agreement is illustrated by the calculated Nash–Sutcliffe efficiency (NSE) of 0.78 for the use of satellite rainfall and 0.71 for the use of radar rainfall data. The errors of the times and the peak values comparing simulated data and observed information were approximately 30 minutes and 10 m^3 s^{-1}, respectively. This would be the result of differences between the coarse time of gauged measurement (1 hour) and the time of model estimation (1 minute).

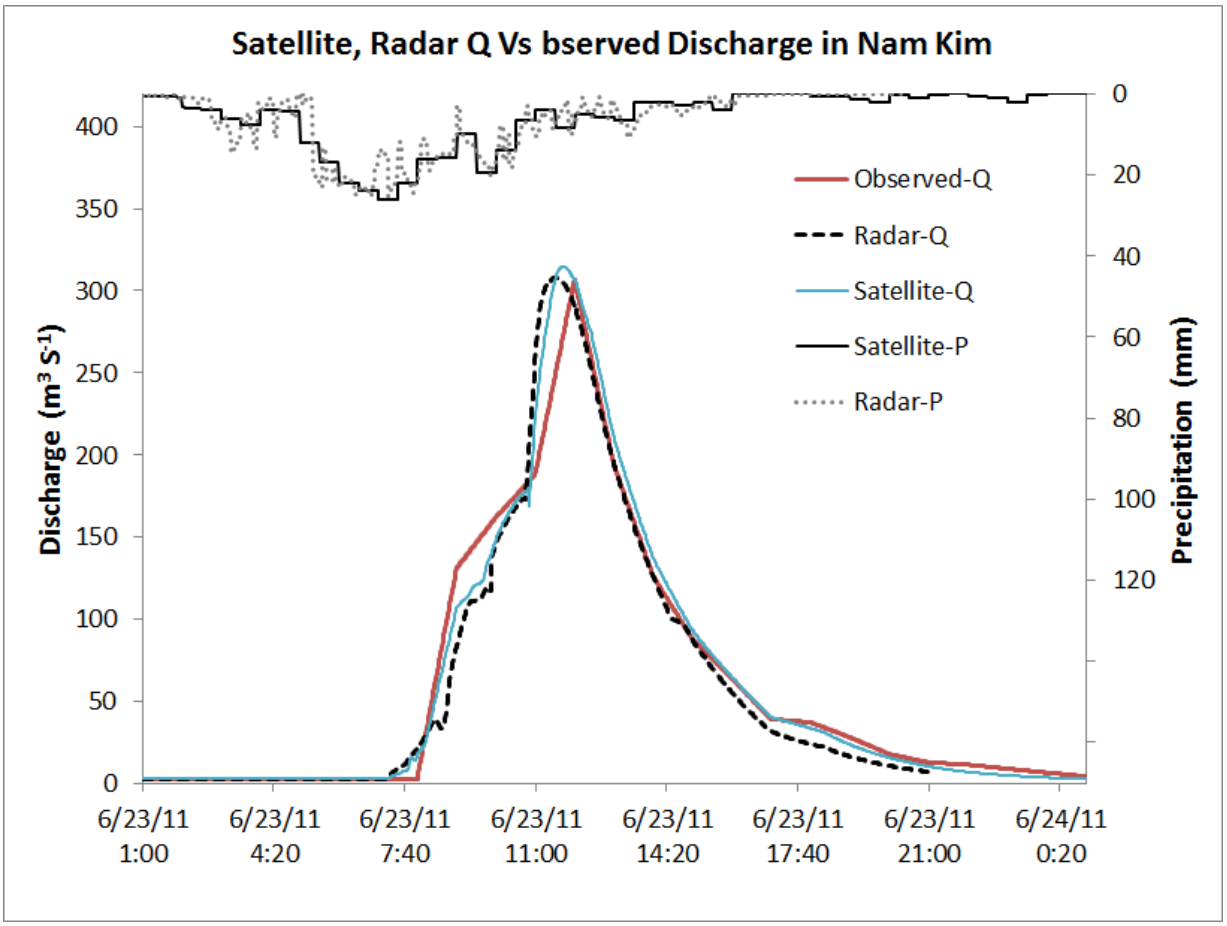

Figure 4-2. Simulated vs observed data through the outlet of the Nam Kim watershed.

4.4.2 Comparisons between Different Rainfall Inputs Effecting Sediment Yield

The remarkable indications shown in the Fig. 4-3 were various patterns of the plane and channel sediment flow (SeF) and the flow volumes. Although, the pattern colours on

individual watersheds (a compares to b, c to d) were not much different, the SeF values of the use of radar rainfall were much lower than the use of satellite rainfall (indicated by the legends). The rainfall is presented in the Figs 4-4 and 5 with outstanding differences of temporal resolutions.

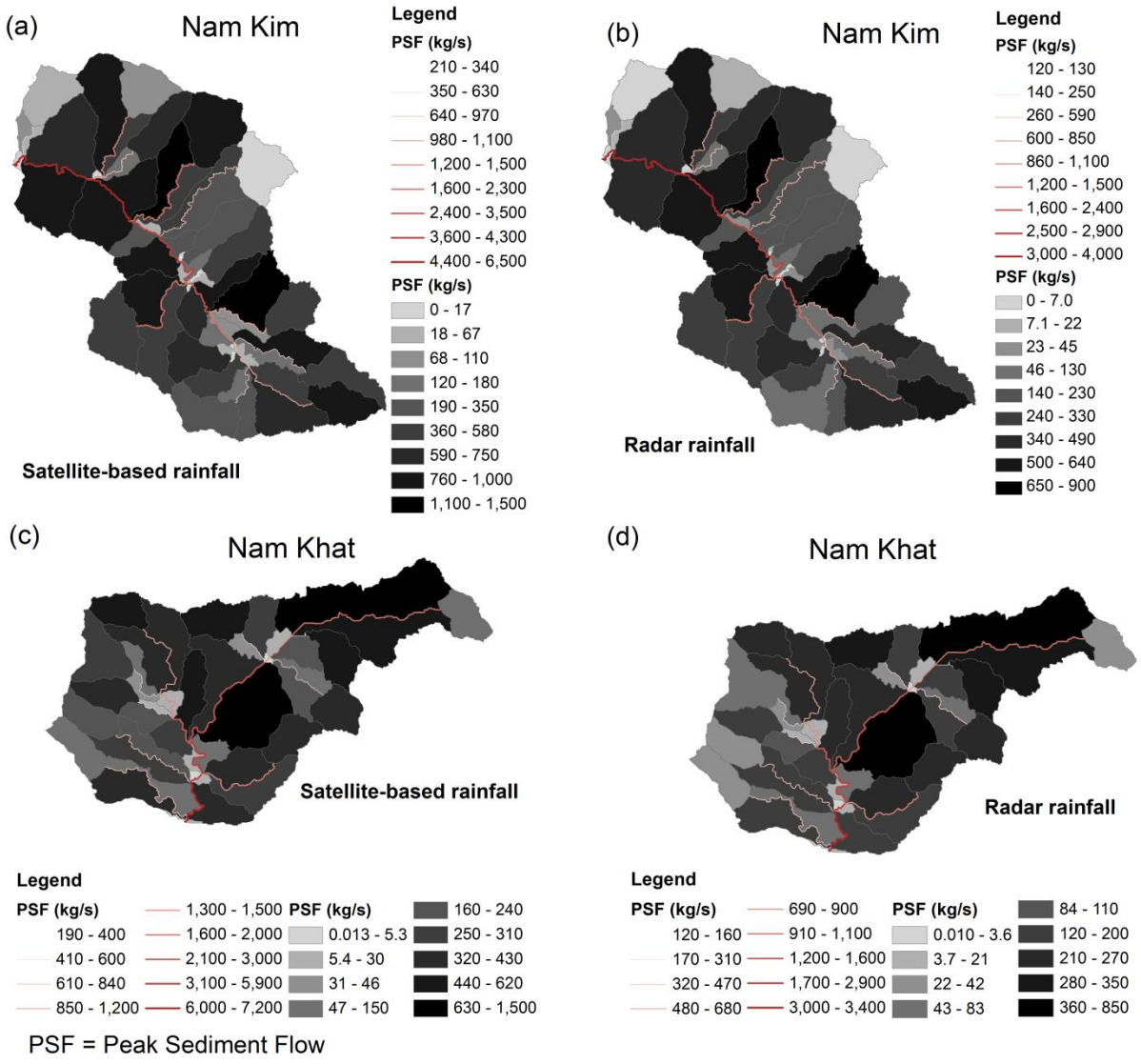

Figure 4-3. Rainfall inputs effect on simulated sediment flows of the Nam Kim and Nam Khat watersheds for the rain event on 23rd June 2011.

4.4.3 Impacts of Soil Saturation Index on Simulated Soil Loss for the Two Watersheds

There were sharp rises (from 17 t s^{-1} to just over 40 t s^{-1} for the Nam Kim and from about 4 t s^{-1} to 13.5 t s^{-1} for the Nam Khat) of peak sediment discharges flowing through the river's outlets while the S was increased from 20% (S2) to 30% (S3) and to 40% (S4) in the Fig. 4-4. The Fig. 4-4 indicated the gradual increase of lag time to peak. However, with the bigger watershed (Nam Kim) this trend was more evident (Fig. 4-5a). It can also be seen that the use

of the satellite rainfall (SAT-rainfall, mm h^{-1}) produced higher sediment discharge than the use of the radar rainfall (Radar-Rainfall, mm h^{-1}).

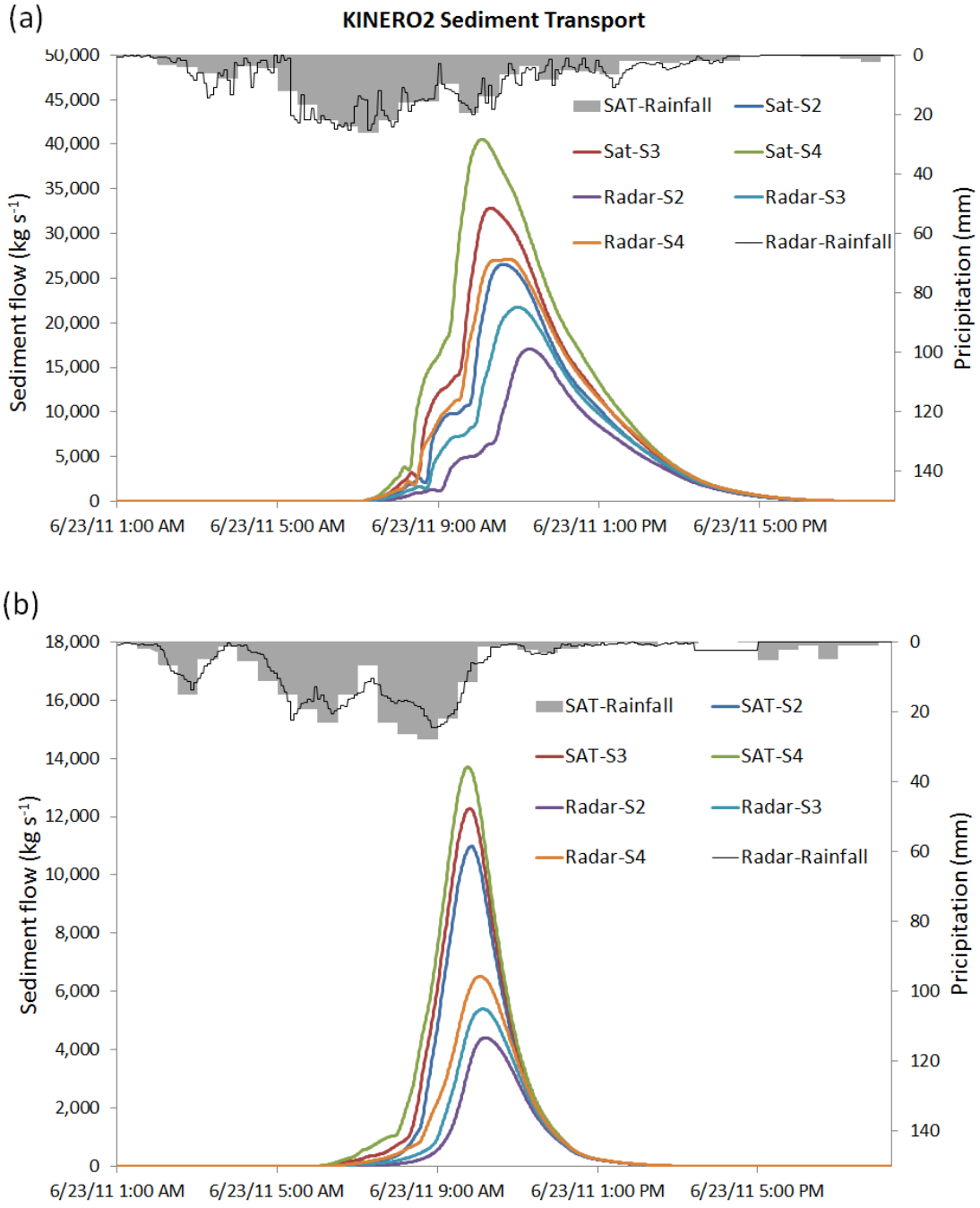

Figure 4-4. Peak sediment flow estimated at the outlets of the Nam Kim (a) and Nam Khat (b) with variations of Soil saturation Indexes (S).

4.4.4 Results of Testing Plane or Hill Slope Roughness Affecting Soil Loss Estimation

The graphs in the Fig. 4-5 showed the impacts of the roughness of the watershed's planes on the computed sediment discharges with multipliers by 2 (R2), 3 (R3) and 4 (R4) in comparison with different climate precipitation data. Both watersheds were sensitive to this

parameter with large scale variations of SeF values. When comparing Fig. 4-5a to Fig. 4-5b, it can be seen that the bigger catchment area of the Nam Kim had a higher volume of the lateral flow (after the peak) while the smaller one of the Nam Khat seemed to more sensitive to small rain at the very start of the whole rain event.

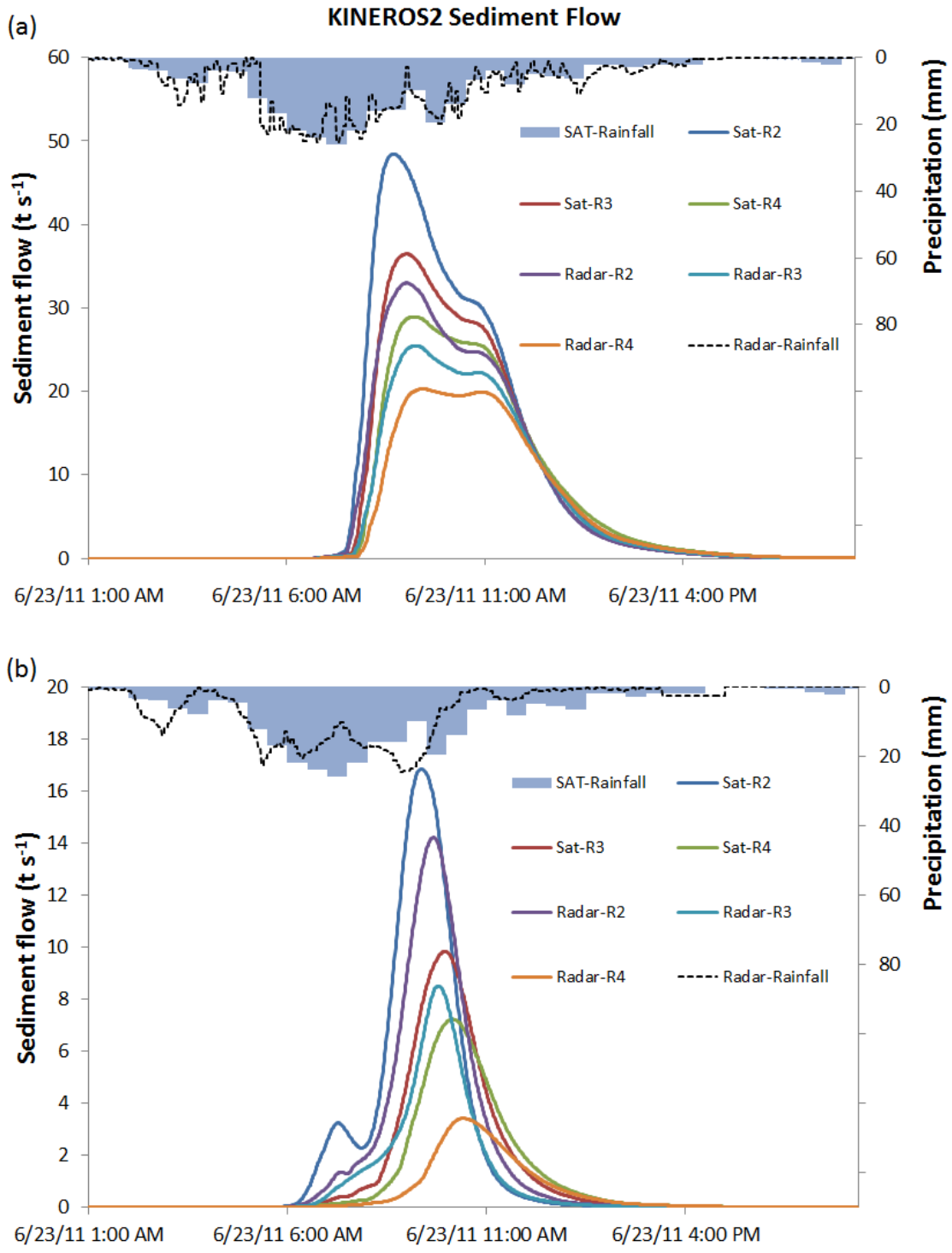

Figure 4-5. Peak sediment flow estimated at the outlets of the Nam Kim (a) and Nam Khat (b) with variations of plane roughness (R).

4.4.5 Effects of Plane Ks on Simulated Soil Loss

By adjusting the saturated hydraulic conductivity (Ks) we had comparisons between total sediment flow (TSeF) through the outlets of the two watersheds in conditions of plus and minus 20% to Ks (Ks−20% and Ks+20% to the Ks values shown within Tables 4-1 and 2). The figure 4-6 indicated that by minus 20% to Ks the TSeF increased significantly, particularly in the middle of the simulation time for both cases. On the other hand, with Ks+20%, there were important sharp declines also for both watersheds. It is also shown on the graphs (Fig. 4-6) that the curves were quite symmetric. This illustrated the dominant influences of Ks alternations on the TSeF volumes and less impact on the peak-time lag.

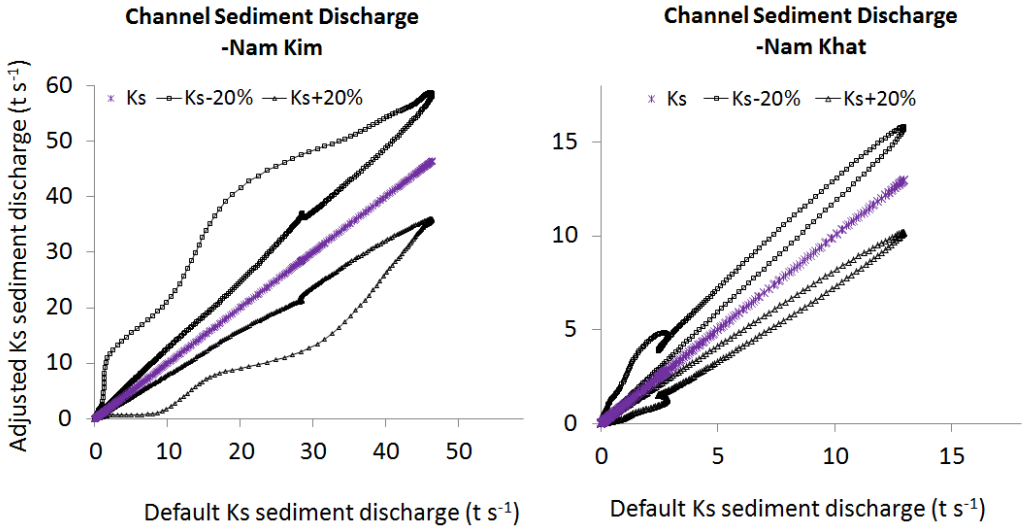

Figure 4-6. Evaluated total channel discharge for the Nam Kim and Nam Khat watersheds with plane Ks alternations and radar rainfall input.

4.4.6 Effects of Model Resolution on Channel and Plane Modelled Sediment Yield

Interesting results of sediment yield (SY) maps are illustrated in the Fig. 4-7. By the watersheds which were discretized into larger components (planes) or bigger critical source areas (CSAs), the estimated sediment yield for the planes was reduced gradually in both cases. Remarkably, the channel SeFs dropped sharply while the CSAs were enlarged. In addition, there was a significant simplification of SY rates in small watershed components (Figs 4-7a and d) into larger ones (c and f) with lower SY rates. The figure also showed that the SY rates were higher in the upper-stream areas (about 30 t ha^{-1} for the Nam Kim and around 6 t ha^{-1} for the Nam Khat) and lower in the down-stream zones (approximately 3 t ha^{-1} for the Nam Kim and 300 kg ha^{-1} for the Nam Khat) for both watersheds.

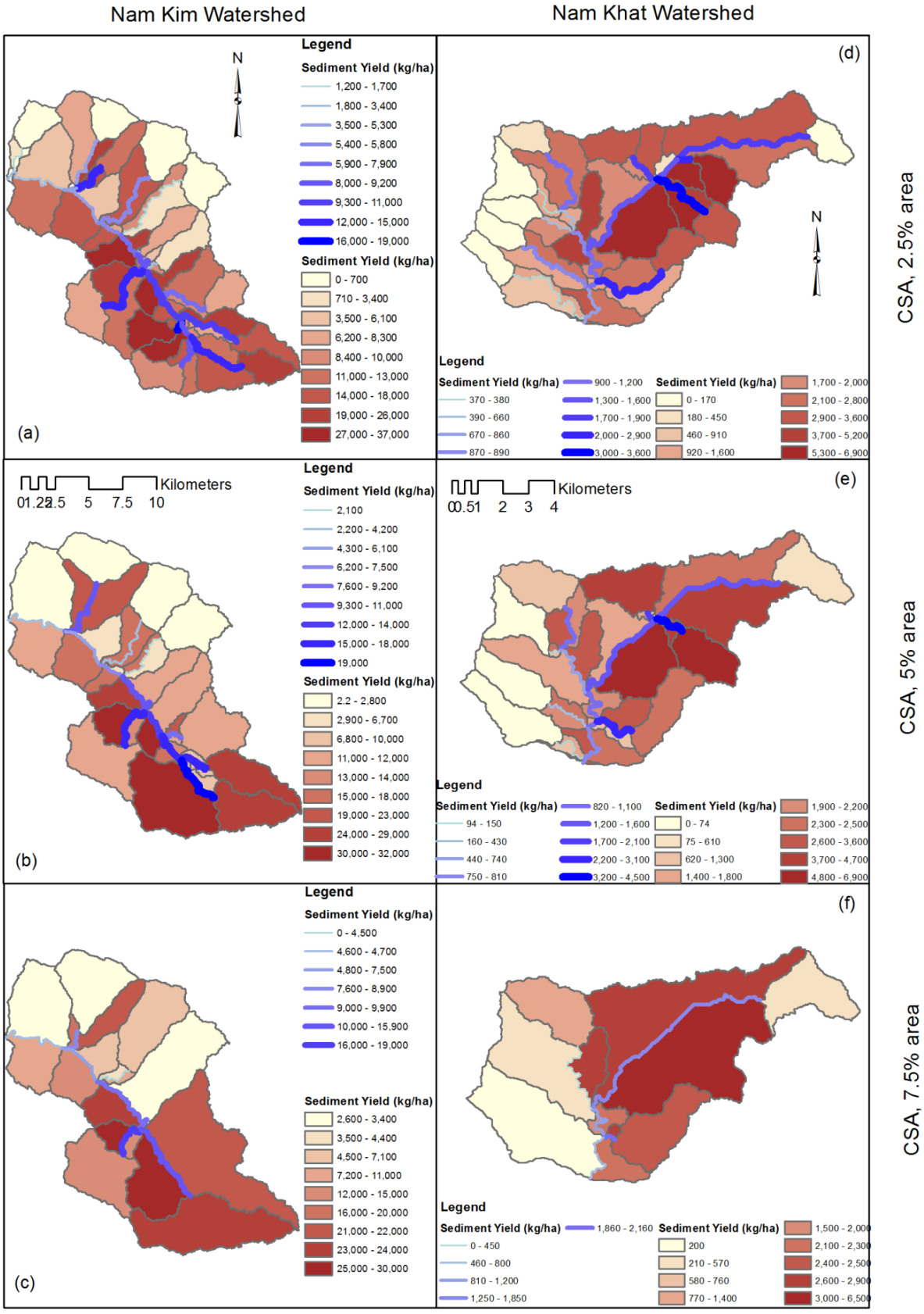

Figure 4-7. Maps of channel and plane sediment yield estimated by KINEROS2 with different geomorphologic resolutions of watershed modelling.

4.4.7 Comparison Different LULC Effect on SY

The reduction of vegetation cover (decline of the forest and increase of shrub, bare and agricultural land) in the five year period (2002 to 2007) was clearly shown when comparing maps (Figs 4-8a and b) of the Nam Kim watershed. In contrast, this was less evident on the maps of the Nam Khat (Figs 4-8d and e). Using the LULC2007, the Nam Kim generated more significant rates of sediment yield than the use of LULC2002 in most areas. In some areas (in red or orange), the soil loss rates increased from 4 t ha^{-1} to 8 t ha^{-1} and there were only small areas in the down-stream zone of the Nam Kim with a decline of SY of 0 to 400 kg ha^{-1}. The sediment yield transport in channels increased in most streams. However, this was not the case for the Nam Khat with the SY rates increasing and sinking alternately.

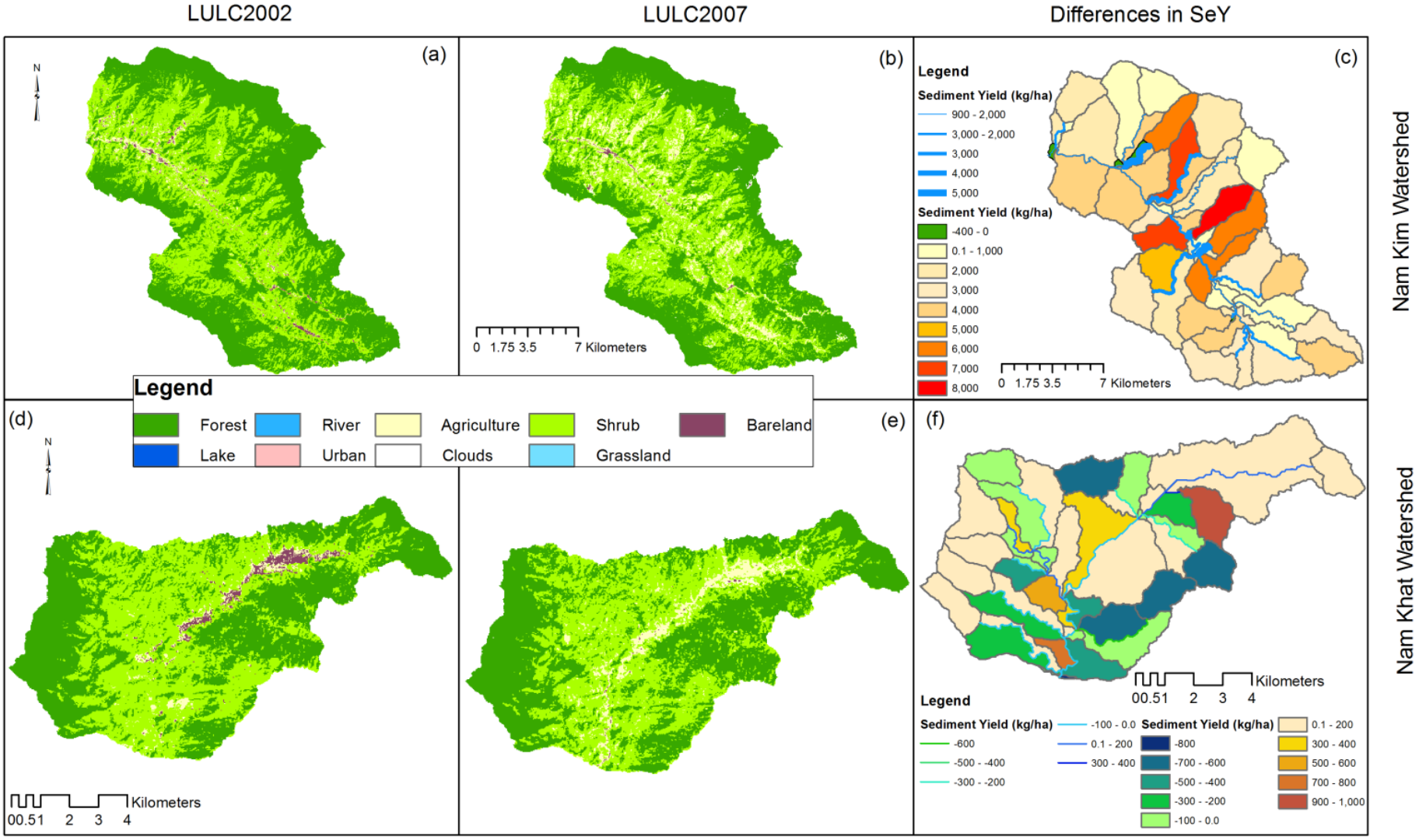

Figure 4-8. Maps of satellite-based LULC (a, b, d and e) and their impacts on SY estimations (c and f) for the rain event 23rd June 2011.

4.5 Discussion

Channel discharge routine in KINEROS2 is treated by the continuity equation for one-dimensional equations presented in (Woolhiser et al., 1990) and (Smith et al., 1995). When this method was applied to this study, we found that the most sensitive parameters to model output of discharge were critical hydraulic conductivity (Ks), Soil saturation index (S) and the Manning's n coefficient (N) which was less sensitive. This point was supported by studies of Al-Qurashi et al., (2008) and Memarian et al., (2013). By the adjustment of these parameters, the KINEROS2 indicated its ability to generate channel discharge close to measured data with different types of rainfall inputs (Fig. 4-2).

The differences in the temporal interval of precipitations derived from satellite and radar sources have had momentous effects on results of sediment flows (Fig. 4-3). Despite the variances of the accumulative rainfalls were negligible (144 and 138 mm for satellite and radar rainfall), the calibrated SeFs using satellite rainfall were nearly double the rates using radar rainfall. This could be explained by the exponential impact of the r factor in the equation (4-3) which has a direct positive influence on the splash erosion. There have been numerous investigations using radar rainfall for modelling river discharge such as (Looper & Vieux, 2012; Unkrich et al., 2010; Versini, 2012; Villarini et al., 2010; Zoccatelli et al., 2010) and others. However, few attempts have analysed the uncertainty of this parameter in terms of comparison with other data sources. Although radar rainfall has some advantages of finer temporal and spatial resolutions (in comparison to satellite rainfall), it is still difficult to judge which of the two is more accurate.

Previous literature has shown that sensitive parameter analyses might be important for hydrological modelling performances due to their common task in modelling performances and being an effective coverage of the model's results to observed data by adjusting them (Duru & Hjelmfelt, 1994). We carried out parameter sensitive analyses for four model variables, namely soil saturation index (S) (section 4.4.3), hill slope roughness (R) (section 4.4.4), hill slope critical hydraulic conductivity (Ks) (section 4.5.5) and the CSAs (section 4.4.6). Every variable had to some extent an influence on the results. However, the Ks was found to be the most important control parameter. The Ks and S had a significant effect on SY magnitude (peaks). The R, on the other hand, reserved lateral flow and lengthened time to peak with the bigger watershed - Nam Kim. A similar topic of CSA assessment was carried out by (Kalin et al., 2003) and we also found a significant drop of estimated SYs while the CSAs were increasing. What value of the CSA is feasible? This is still a tough question. However, it is very much based on areas of modelled watersheds, topographic characters, geomorphologic properties (Helmlinger et al., 1993) and hydrologic responses.

The topic of investigation into changing LULC resulting in soil erosion exaggerations has been a favourite theme for many studies, to name but a few (Anh et al., 2014; Blavet et al., 2009; David et al., 2014). This study employed the LULC 2002-2007 (not in 2011) datasets only for investigation into the extent of how different land use changes resulted in soil loss. These estimations did not necessarily present the factual soil erosion rates of these watersheds. If the LULC condition in 2011 was inputted to the model, the SY rates would be expected to be higher.

As a physics-based distributed model, KINEROS2 has its own advantages and disadvantages over a lumped parameter model (Schmengler, 2010). Based on model input data requirement, scale issues discussed in (Bakimchandra, 2011), model validation and SY generations, we recommend the use of this model for the aim of soil water assessment with individual rain events in the tropics. Nevertheless, this study was limited to the examination of one single rain; more rain events should be tested for the model's verifications. However, some previous researches used this model for similar investigations (Smith et al., 1999) and an event case study in northern Vietnam (Ziegler et al., 2007; Ziegler et al., 2004; Ziegler et al., 2006) but with different perspectives.

4.6 References

Al-Qurashi, A., McIntyre, N., Wheater, H., & Unkrich, C. (2008). Application of the Kineros2 rainfall–runoff model to an arid catchment in Oman. *Journal of Hydrology, 355*(1–4), 91-105. doi: http://dx.doi.org/10.1016/j.jhydrol.2008.03.022

Anh, P. T. Q., Gomi, T., MacDonald, L. H., Mizugaki, S., Van Khoa, P., & Furuichi, T. (2014). Linkages among land use, macronutrient levels, and soil erosion in northern Vietnam: A plot-scale study. *Geoderma, 232–234*(0), 352-362. doi: http://dx.doi.org/10.1016/j.geoderma.2014.05.011

Arnold, J. G., J.R. Williams, R. Srinivasan, K.W. King, and R.H. Griggs. (1994). SWAT: Soil Water Assessment Tool. *U. S. Department of Agriculture, Agricultural Research Service, Grassland, Soil and Water Research Laboratory.* Temple, TX.

Bakimchandra, O. (2011). Integrated Fuzzy-GIS approach for assessing regional soil erosion risks. *Universitsty of Stuttgart, Germany.* PhD thesis.

Blavet, D., De Noni, G., Le Bissonnais, Y., Leonard, M., Maillo, L., Laurent, J. Y., . . . Roose, E. (2009). Effect of land use and management on the early stages of soil water erosion in French Mediterranean vineyards. *Soil & Tillage Research, 106*(1), 124-136. doi: DOI 10.1016/j.still.2009.04.010

Burns, I. S., Scott, S. N., Levick, L. R., Semmens, D. J., Miller, S. N., Hernandez, M., . . . Kepner, W. G. (2008). Automated Geospatial Watershed Assessment (AGWA) Documentation. *U.S. Department of Agriculture, Agricultural Research Service*.

Cooper, J. R., Wainwright, J., Parsons, A. J., Onda, Y., Fukuwara, T., Obana, E., . . . Hargrave, G. H. (2012). A new approach for simulating the redistribution of soil particles by water erosion: A marker-in-cell model. *Journal of Geophysical Research-Earth Surface, 117*. doi: Artn F04027 Doi 10.1029/2012jf002499

da Silva, G. R. V., de Souza, Z. M., Martins, M. V., Barbosa, R. S., & de Souza, G. S. (2012). Soil, Water and Nutrient Losses by Interrill Erosion from Green Cane Cultivation. *Revista Brasileira De Ciencia Do Solo, 36*(3), 963-970.

David, M., Follain, S., Ciampalini, R., Le Bissonnais, Y., Couturier, A., & Walter, C. (2014). Simulation of medium-term soil redistributions for different land use and landscape design scenarios within a vineyard landscape in Mediterranean France. *Geomorphology, 214*(0), 10-21. doi: 10.1016/j.geomorph.2014.03.016

Duru, J. O., & Hjelmfelt, A. T. (1994). Investigating Prediction Capability of Hec-1 and Kineros Kinematic Wave Runoff Models. *Journal of Hydrology, 157*(1-4), 87-103. doi: Doi 10.1016/0022-1694(94)90100-7

Engelund, F., & Hansen, E. (1967). A monograph on sediment transport in alluvial streams. *Technical University of Denmark. Teknisk Vorlag, Copenhagen, 62 pp.*

Guzman, G., Quinton, J. N., Nearing, M. A., Mabit, L., & Gomez, J. A. (2013). Sediment tracers in water erosion studies: current approaches and challenges. *Journal of Soils and Sediments, 13*(4), 816-833. doi: DOI 10.1007/s11368-013-0659-5

Helmlinger, K. R., Kumar, P., & Foufoula-Georgiou, E. (1993). On the use of digital elevation model data for Hortonian and fractal analyses of channel networks. *Water Resources Research 29*, 2599–2613.

Horton, R. E. (1933). The role of infiltration in the hydrologic cycle. *Eos Trans. AGU 14*, 446–460.

Kalin, L., Govindaraju, R. S., & Hantush, M. M. (2003). Effect of geomorphologic resolution on modeling of runoff hydrograph and sedimentograph over small watersheds. *Journal of Hydrology, 276*(1–4), 89-111. doi: http://dx.doi.org/10.1016/S0022-1694(03)00072-6

Kefi, M., Yoshino, K., & Setiawan, Y. (2012). Assessment and mapping of soil erosion risk by water in Tunisia using time series MODIS data. *Paddy and Water Environment, 10*(1), 59-73. doi: DOI 10.1007/s10333-011-0265-3

Kefi, M., Yoshino, K., Setiawan, Y., Zayani, K., & Boufaroua, M. (2011). Assessment of the effects of vegetation on soil erosion risk by water: a case of study of the Batta

watershed in Tunisia. *Environmental Earth Sciences, 64*(3), 707-719. doi: DOI 10.1007/s12665-010-0891-x

Looper, J. P., & Vieux, B. E. (2012). An assessment of distributed flash flood forecasting accuracy using radar and rain gauge input for a physics-based distributed hydrologic model. *Journal of Hydrology, 412*, 114-132. doi: DOI 10.1016/j.jhydrol.2011.05.046

Memarian, H., Balasundram, S. K., Talib, J. B., Teh Boon Sung, C., Mohd Sood, A., & Abbaspour, K. C. (2013). KINEROS2 application for land use/land cover change impact analysis at the Hulu Langat Basin, Malaysia. *Water and Environment Journal, 27*(4), 549-560. Doi: 10.1111/wej.12002

Millington, A. C. (1986). Reconnaissance scale soil erosion mapping using a simple geographic information system in the humid tropics. In: W. Siderius, ed. Land evaluation for land-use planning and conservation in sloping areas. *The Netherlands: ILRI*, 64-81.

Nash, J. E., & Sutcliffe, J. V. (1970). River flow forecasting through conceptual models 1: a discussion of principles. *Journal of Hydrology 10* (3), 282–290.

NCHMF. (2011). Vietnamese National Center for Hydrological Forecasting http://www.nchmf.gov.vn/web/vi-VN/71/29/45/Default.aspx. (accessed on 7th March 2014).

Nearing, M. A., G. R. Foster, L. J. Lane, & Finkner, S. C. (1989). A Process-Based Soil Erosion Model for USDA - Water Erosion Prediction Project Technology. *The American Society of Agricultural Engineers Vol. 32*(5): 09-10.1989

Parsons, A. J., Wainwright, J., Powell, D. M., Kaduk, J., & Brazier, R. E. (2004). A conceptual model for determining soil erosion by water. *Earth Surface Processes and Landforms, 29*(10), 1293-1302. doi: Doi 10.1002/Esp.1096

Pham Thai NAM, D. Y., Shinjiro KANAE, Taikan OKI and Katumi MUSIAKE. (2003). Global Soil Loss Estimate Using RUSLE Model: The Use of Global Spatial Datasets on Estimating Erosive Parameters. *Geoinformatics, vol.14*, no.1, pp.49-53, 2003.

Schmengler, A. C. (2010). Modeling soil erosion and reservoir sedimentation at hill and catchment scale in semi-arid Burkina Faso. *Rheinischen Friedrich-Wilhelms-Universität zu Bonn.* PhD thesis.

Smith, R. E., Goodrich, D. C., & Unkrich, C. L. (1999). Simulation of selected events on the Catsop catchment by KINEROS2: A report for the GCTE conference on catchment scale erosion models. *CATENA, 37*(3–4), 457-475. doi: http://dx.doi.org/10.1016/S0341-8162(99)00033-8

Smith, R. E., Goodrich, D. C., Woolhiser, D. A., & Unkrich, C. L. (1995). KINEROS – A kinematic runoff and erosion model; Chapter 20 in V.P. Singh (editor), Computer

Models of Watershed Hydrology. *Water Resources Publications, Highlands Ranch, Colorado, 1130 pp*.

Tuan, V. V. (1993). Evaluation of the Impact of Deforestation to Inflow Regime of theHoaBinh Reservoir in Vietnam, Hydrology of Warm Humid Regions. *Proceedings of the Yokahama Symposium, July 1993. IAHS Publication 216,* pp. 135–138.

Unkrich, C. L., Michael Schaffner, Chad Kahler, David C. Peter Troch, Hoshin Gupta, Thorsten Wagener, & Yatheendradas, S. (2010). Real-time Flash Flood Forecasting Using Weather Radar and Distributed Rainfall-Runoff Model. *2nd Joint Federal Interagency Conference, Las Vegas, NV.*

Versini, P. A. (2012). Use of radar rainfall estimates and forecasts to prevent flash flood in real time by using a road inundation warning system. *Journal of Hydrology, 416*, 157-170. doi: DOI10.1016/j.jhydrol.2011.11.048

Villarini, G., Krajewski, W. F., Ntelekos, A. A., Georgakakos, K. P., & Smith, J. A. (2010). Towards probabilistic forecasting of flash floods The combined effects of uncertainty in radar-rainfall and flash flood guidance. *Journal of Hydrology, 394*(1-2), 275-284. doi: DOI 10.1016/j.jhydrol.2010.02.014

Williams, J. R. (1995). Chapter 25: The EPIC model. *p. 909-1000. In V.P. Singh (ed.) Computer models of watershed hydrology. Water Resources Publications.*

Woolhiser, D. A., Smith, R. E., & Goodrich, D. C. (1990). KINEROS, A Kinematic Runoff and Erosion Model. Documentation and User Manual. *ARS-77. USDA, ARS, Washington, DC*.

Ziegler, A. D., Giambelluca, T. W., Plondke, D., Leisz, S., Tran, L. T., Fox, J., . . . Tran Duc, V. (2007). Hydrological consequences of landscape fragmentation in mountainous northern Vietnam: Buffering of Hortonian overland flow. *Journal of Hydrology, 337*(1–2), 52-67. doi: http://dx.doi.org/10.1016/j.jhydrol.2007.01.031

Ziegler, A. D., Giambelluca, T. W., Tran, L. T., Vana, T. T., Nullet, M. A., Fox, J., . . . Evett, S. (2004). Hydrological consequences of landscape fragmentation in mountainous northern Vietnam: evidence of accelerated overland flow generation. *Journal of Hydrology, 287*(1–4), 124-146. doi: http://dx.doi.org/10.1016/j.jhydrol.2003.09.027

Ziegler, A. D., Tran, L. T., Giambelluca, T. W., Sidle, R. C., Sutherland, R. A., Nullet, M. A., & Vien, T. D. (2006). Effective slope lengths for buffering hillslope surface runoff in fragmented landscapes in northern Vietnam. *Forest Ecology and Management, 224*(1–2), 104-118. doi: http://dx.doi.org/10.1016/j.foreco.2005.12.011

Zoccatelli, D., Borga, M., Zanon, F., Antonescu, B., & Stancalie, G. (2010). Which rainfall spatial information for flash flood response modelling? A numerical investigation based on data from the Carpathian range, Romania. *Journal of Hydrology, 394*(1-2), 148-161. doi: DOI 10.1016/j.jhydrol.2010.07.019

CHAPTER 5

Flash Flooding Prediction in Regions of Northern Vietnam Using the KINEROS2 Model[6]

"The whole climate is changing: the winds, the ocean currents, the storm patterns, snow packs, snowmelt, flooding, droughts. Temperature is just a bit of it."

-John Holdren

Abstract

Flash flooding (FF) in Vietnam has become an important issue due to increasing loss of property and life. This paper investigates FF prediction using the KINEROS2 model to perform comprehensive analyses to: 1) evaluate the role of initial soil moisture (θ) conditions using the BEACH model; 2) model the discharge (Q) using different rainfall inputs; 3) test the sensitivities of the model to θ and Manning's n coefficient (N) on Q and validate the model; and 4) predict channel discharge (Q_C) using forecasted rainfall (FR). A relative saturation index (R) of 0.46 and N of 0.14 produced the best match of the simulated outflow to measured Q, while the saturated hydraulic conductivity (Ksat) and R had significant effects on the magnitude of flooding. The parameter N had remarkable influences on the volume of flow and its peak time. Surprisingly, the use of radar rainfall data underestimated Q compared to the measured discharge and estimates using satellite rainfall. We conclude that the KINEROS2 model is well equipped to predict FF events in the study area and is therefore suitable as an early warning system when combined with weather forecasts. However, uncertainties grow when the forecasted period expands further into the future.

[6] This paper is accepted on 12 November 2015 for publication in the Hydrology Research, IWA publishing http://hr.iwaponline.com/content/early/2015/12/24/nh.2015.125. DOI: 10.2166/nh.2015.125

5.1 Introduction

Recently, there has been a growing interest in the damage caused by natural hazards (Creutin et al., 2013; Kousky & Walls 2014) and flash floods (FFs). The most devastating floods often cause heavy loss of life (Gupta 2006; Ashley & Ashley 2008; Brauer et al., 2011). In northern Vietnam, the development of flash floods has induced an imperative need to mitigate their impact (NCHMF 2011). Despite this need, few attempts have been made to mitigate floods in the region. This lack of flood mitigation might be explained by the complexity of FFs themselves and by the remaining prevailing uncertainties (Montz & Gruntfest 2002; Estupina-Borrell et al., 2006; Ntelekos et al., 2006). An extensive amount of research has been accumulated worldwide on many aspects of FFs (Montz & Gruntfest 2002; Morin et al., 2009); many of these works suggested that a feasible approach to FF mitigation is to identify their occurrences early (Khavich & Benzvi 1995; Alfieri et al., 2012; Looper & Vieux 2012; Quintero et al., 2012; Versini 2012). We used a modelling method employing the Kinematic Run-off and Erosion Model (KINEROS2) to assess a past FF on 23rd June 2011 (R23rd), the Bridging Event and Continuous Hydrological (BEACH) model to calculate θ as input to the KINEROS2, and the results from some meteorological models, namely the Global Spectral Model (GSM) (Krishnamurti et al., 2006) and the High Resolution Model (HRM) (Majewski 2009), for the forecast stage.

In 11 years, from 1995 to 2005, Vietnam experienced up to 300 FF events that resulted in the following losses: 968 people died, 628 people were injured, and material losses worth €71 million occurred. Most of the FFs were in the north of Vietnam (NCHMF 2011). The north of Vietnam, in general, and Yen Bai province, in particular, are identified as being very prone to FFs, and the people are highly exposed to flash flooding problems. In Yen Bai province (case study area), the R23rd event took four lives in the Nam Khat catchment area. FFs have not only resulted in loss of life and property but also negatively impacted society or had severe social consequences (Ruin et al., 2008). It is believed that for an advanced understanding of FFs, multidisciplinary approaches must be integrated (Villarini et al., 2010). This study focuses on the physical techniques of modelling FFs and their forecast prospects.

FF modelling is complex and linked to the problem of uncertainties (Beven 2001). Although there are large numbers of studies on FFs, their behaviours are not fully understood (Sahoo et al., 2006). Many questions have been addressed, such as questions on the accuracy of model inputs and outputs (Li et al., 2010, 2013; Li & Xu 2014), model structure (Bloschl et al., 2008; Garcia-Pintado et al., 2009; Looper & Vieux 2012), initial conditions and boundary

conditions (Abderrezzak et al., 2009; Vincendon et al., 2009; Seo et al., 2012), temporal and spatial scales (Amengual et al., 2007; Reed et al., 2007; Younis et al., 2008), and threshold-runoff uncertainties (Gupta 2006; Ntelekos et al., 2006). El-Hames & Richards (1998) suggested that, for a successful application of flood prediction, complex and comprehensive techniques are often required. Furthermore, as FFs occur shortly after the onset of rainfall events, hydrological models used for FF forecast must have the ability to evaluate the level of risk in a short time (Janal & Stary 2012).

We used the robust model of KINEROS2 for estimating and predicting Q_C (a complete study framework is presented in the Materials and methods section). The model has already proven to be reliable for such tasks in semi-arid regions (Volkmann et al., 2010). The goal of our study is to evaluate its merits for a more humid sub-tropical environment, to identify the key variables that determine its output, and to assess its suitability to predict FF events based on different precipitation input data.

5.2 Study Site

This study focuses on regions in northern Vietnam featuring similar climatic and morphological conditions of typical tropical, steep and dense drainage-network systems. Some representative watersheds in Yen Bai province were chosen for the actual modelling implementations.

The Nam Kim watershed, shown in Figure 5-1, was chosen for the KINEROS2 model validations using observed data records at its outlet. BEACH daily actual evapotranspiration (ETa) was computed for the three watersheds and compared with the SWAT ETa. Nam Khat experienced the FF event on 23th June 2011, which resulted in the loss of life and property. Many areas in Yen Bai province are prone to flash flooding due to their conditions of annual precipitation of approximately 1,500 mm, average slopes of 28 degrees and a reduction of vegetation cover. The watersheds are located at approximately 1200 meters a.s.l., where most residents belong to an ethnic minority and are potentially exposed to flooding. Ngoi Hut is the largest watershed and was used for testing the application of the KINEROS2 model for a larger watershed.

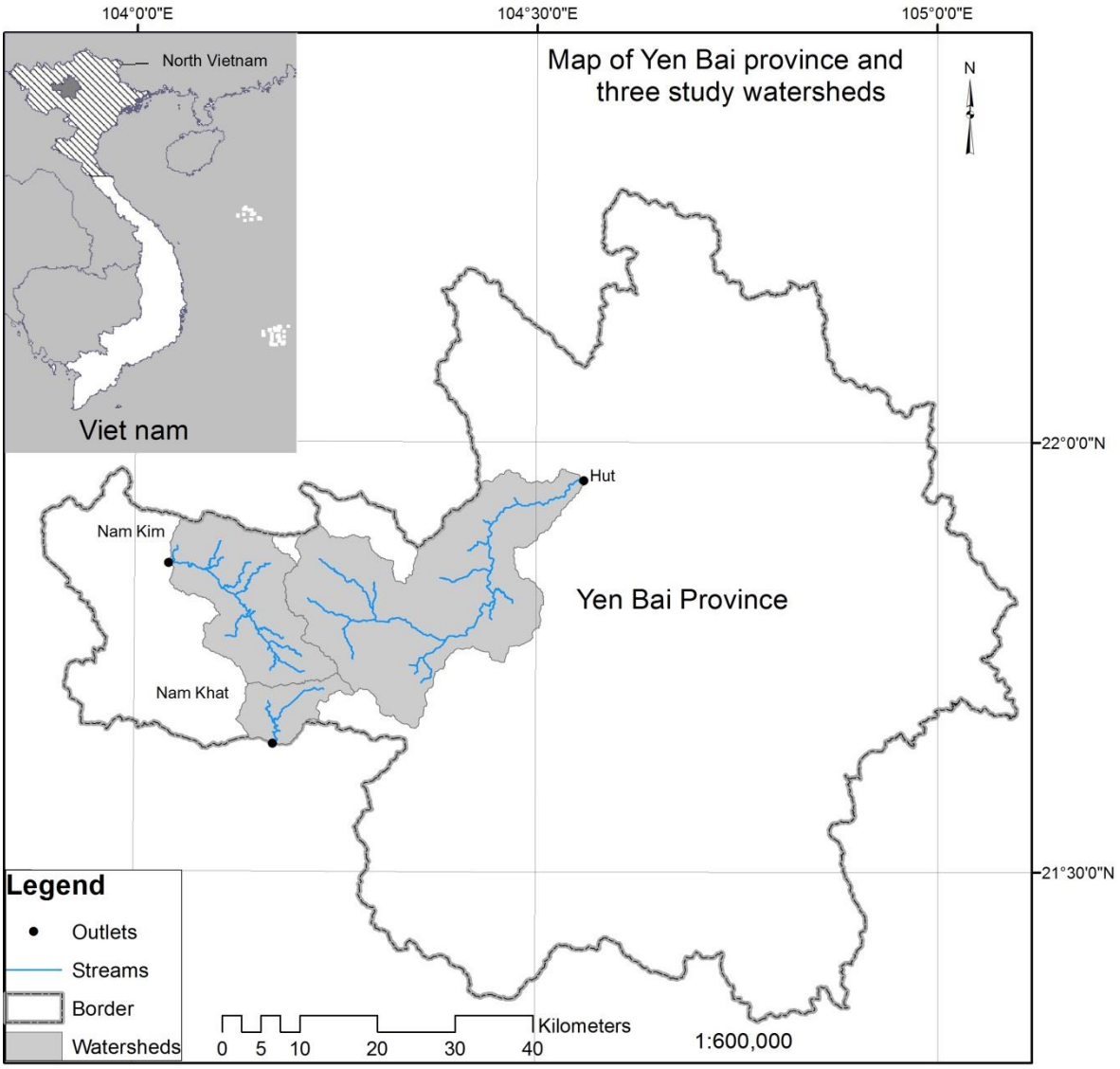

Figure 5-1. Site study of the Nam Kim, Ngoi Hut and Nam Khat watersheds in Yen Bai province, Vietnam.

5.3 Materials and Methods

5.3.1 Study Flowchart

Figure 5-2 provides an overview of the steps to achieve the study objective of flash flooding forecast. Model input preparations, calibrations, validations and connections are presented step-by-step in the following sections.

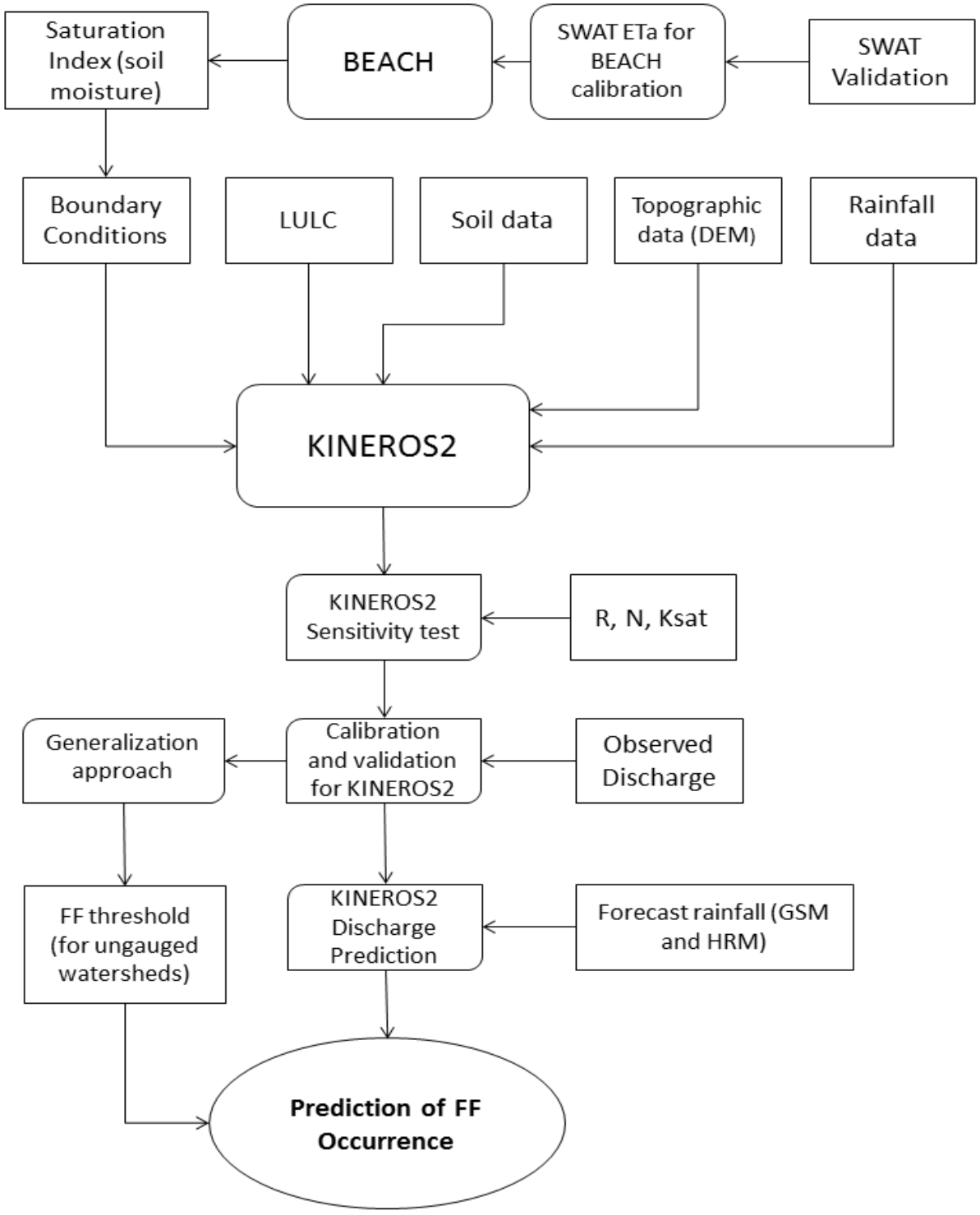

Figure 5-2. Methodological flowchart of flash flood prediction.

5.3.2 Channel Routine Equations

The basic equations of the channel routine were defined comprehensively in Woolhiser et al., (1990) and Smith et al., (1995) or, for the more recent version of KINEROS2, in Semmens et al., (2008). We only present the following kinematic channel equation solved by a four point implicit techniques (Woolhiser et al., 1990).

$$A_{j+1}^{i+1} - A_{j+1}^{i} + A_{j}^{i+1} - A_{j}^{i} + \frac{2\Delta t}{\Delta x}\left\{\theta_w \left[\frac{dQ^{i+1}}{dA}\left(A_{j+1}^{i+1} - A_{j}^{i+1}\right)\right] + (1-\theta_w)\left[\frac{dQ^{i}}{dA}\left(A_{j+1}^{i} - A_{j}^{i}\right)\right]\right\} = 0.5\Delta t\left(q_{cj+1}^{i+1} + q_{cj}^{i+1} + q_{cj+1}^{i} + q_{cj}^{i}\right) \quad (5\text{-}1)$$

where A is the cross-sectional area, q_c is the lateral inflow, θ_w is a weighting parameter (often 0.6 to 0.8) for the x derivatives at the advanced time step (Δt), and Q is the discharge per unit width (L^{-2} T^{-2}); Newton's iteration technique is used to solve for the unknown area $\left[A_{j+1}^{i+1}\right]$.

5.3.3 The BEACH and SWAT Models

Because the event-based KINEROS2 model does not compute inter-storm soil moisture condition (θ), antecedent soil moisture (θ_{ant}) must be provided as the initial condition at the beginning of the model run. The daily soil moisture calculated by the BEACH model could be a good solution.

The BEACH model developed by Sheikh et al., (2009) is a spatially distributed daily basic hydrological model. The model calculates the continuous soil moisture for each cell based on water balance as in the following relation:

$$D\frac{d\theta_i}{dt} = P_i - R_i + \Delta LF_i - E_{ai} - T_{ai} - DP_i \quad (5\text{-}2)$$

where θ is soil moisture content (m^3 m^{-3}), D refers to depth of soil moisture simulation (m), dt is the calculation time-step (day), P and R indicate daily precipitation and surface run-off (m), ΔLF indicates the difference between the lateral inflow (in the cell) and the lateral outflow (out of the cell) (m) and E_a, T_a and DP are the actual evaporation and transpiration (m) and the leakage or deep percolation (m), respectively.

The BEACH model estimates actual evaporation as in following relationship (Allen et al., 1998):

$$E_a = \left(\frac{\theta_t - \theta_{dr}}{\theta_{fc} - \theta_{dr}}\right) * (K_{cmax} - K_{cb}) * ET_0 \quad (5\text{-}3)$$

$$K_{cmax} = max\left[\left\{1.2 + [0.04(U_2 - 2) - 0.004(RH_{min} - 45)] * \left(\frac{h}{3}\right)^{0.3}\right\}; \{K_{cb} + 0.05\}\right] \quad (5\text{-}4)$$

where E_a is actual evaporation (mm day^{-1}); θ_t, θ_{dr}, θ_{fc} are actual soil moisture content, moisture content of air-dry soil and soil moisture content at field capacity (m^3 m^{-3}), respectively; K_{cmax} indicates an upper limit to the evaporation and transpiration from any cropped surface (1.05 to 1.30); K_{cb} presents crop transpiration (mm day^{-1}) and ET_0 presents the reference evapo-transpiration rate based on Penman–Monteith (FAO56) (Allen et al., 1998); U_2 is wind speed (m s^{-1}); RH_{min} refers to minimum air relative humidity (%) and h is maximum crop high (m).

We used E_a values estimated by the SWAT model to validate the BEACH E_a. The SWAT model also calculates the actual evaporation if the ET_0 is determined. When the model is calculating E_a, it removes storage water as much as possible in canopy (Neitsch et al., 2009). When the potential evapotranspiration (ET_0) is smaller than the amount of free water stored in the canopy (R_{INT}), E_a is calculated equally as evaporation from free water (E_{can}):

$$E_a = \left(R_{INT(i)} - R_{INT(f)}\right) = ET_0 \text{ with } E_{can} = R_{INT(i)} - R_{INT(f)} \quad (5\text{-}5)$$

If ET_0 is greater than R_{INT}, then $E_{can} = R_{INT(i)}$ and $R_{INT(f)}$ = 0.

where $R_{INT(i)}$ and $R_{INT(f)}$ are initial and final free water held in canopy is (mm H_2O) (for more details see Neitsch et al., 2009).

5.3.4 Soil, Land Use/Land Cover (LULC) and DEM

The LULC of Yen Bai province was mapped using Landsat 5 TM scenes (30 × 30 m resolution) acquired in 2009. The map consists of six classes, including forest, shrub, agricultural land, grassland, water bodies and bare land. The soils of the regions are categorized into six major soil groupings: fluvisols, calcisols, ferralsols, alisols, acrisols and gleysols. The soils were derived from a custom soil map produced by the Environment and Resource Centre-Agricultural Institute of Plan and Design, Vietnam. The DEM used for geomorphological inputs was provided by the Vietnam Resources and Environment Corporation and produced in 2009 using the Aerial Photogrammetric technology of the Intergraph Corporation, USA.

5.3.5 Rainfall Data

We used several rainfall sources for this research including satellite-based (Sat-P), radar rainfalls (Rad-P), gauged and FR. All the data were provided by the Vietnamese National Centre for Hydrological Forecasting (NCHMF).

The Sat-P of the R23rd event and the rainfall event on 30th June 2011 (R30th) was derived from 70 images. We developed a model (called SATAS) using the Model Builder application running within the ArcMap environment. The model extracts the rainfall from the original images.

Radar precipitation was derived from the data of two ground radar stations at Viet Tri and Phu Lien for the R23rd event and processed similarly together with the Sat-P using the SATAS. The spatial resolution of a radar scan was two kilometres, and the scanning-time interval was five minutes. The Rad-P was estimated using the conventional method of Marshall et al., (1947), as in the following relation:

$$z = 200R^{1.6} \tag{5-6}$$

where R (mm h^{-1}) is the rain rate, and z is the radar reflectivity factor.

Daily gauged-3-hour rainfall (Gau-P) was recorded by the rain gauge in Nam Kim (Fig. 5-1) and extracted for the KINEROS2 validation of the rainfall on the 8th (R8th) and 31st (R31st) of July 2011. These data were accumulated to daily values and used as input for the SWAT model.

As the forecasted rainfall is a prerequisite for the FF prediction, we used the FR from the numerical weather prediction (NWP) of GSM (3.5 day forecast) and of HRM (5.5 day forecast). The GSM and HRM are operated in local watersheds at times of 00:00, 06:00, 12:00 and 18:00 and at times of 00:00 and 12:00, respectively. The Thiessen approach (Thiessen, 1911) can be applied for generating distributed forecasting precipitation.

5.3.6 Stream Gauged Discharge

The in-situ measured Q (daily and hourly) recorded by the stream gauges (Fig. 5-1) was available for Nam Kim and Ngoi Hut. The daily data were used for the SWAT, and the hourly data were used for the KINEROS2 model.

5.3.7 SWAT Calibration and Validation

The model was calibrated over the five years from 2001 to 2005 for Nam Kim and Ngoi Hut. Some sensitive parameters were adjusted, as summarized in Table 5-1. Note that some final values were averaged from the values of hydrologic response units (HRUs). Model validation was applied after every calibration from 2006 to 2012. The goodness of agreement between the simulated data and the observed data were evaluated using the coefficient of

determination (R^2), the Nash–Sutcliffe simulation efficiency coefficient (NSE) and graphical methods. These methods were also applied for BEACH and KINEROS2.

Table 5-1. Top ten SWAT sensitive parameters and final values

Sensitivity order	Parameter	Description	Unit	Range	Initial value	Final value
1	CN2	Curve number condition 2	–	35–98	35	54.1
2	Alpha_Bf	Baseflow recession constant	days	0–1	0.04	0.4
3	Ch_K2	Effective hydraulic conductivity in channel	mm hr^{-1}	−0.01–500	50	75
4	Sol_K	Saturated hydraulic conductivity	mm hr^{-1}	0–2,000	2	4.30
5	Ch_N2	Manning's n value for the main channel	–	−0.01–0.3	0.015	0.05
6	Surlag	Surface runoff lag coefficient	–	1–24	4	2.5
7	Sol_Awc	Available water capacity	mm mm^{-1}	0–1	0.22	0.31
8	Gw_Revap	Revap coefficient	–	0.02–0.2	0.02	0.2
9	Esco	Soil evaporation compensation factor	–	0-1	0	0.95
10	Gwqmin	Threshold water level in shallow aquifer for base flow	mm	0–5,000	0	0.50

5.3.8 BEACH Calibration

The BEACH calibrated parameters are represented in Table 5-2, based on the results of the calibration and validation of SWAT. As the BEACH estimates ETa for different types of crops, the SWAT ETa was calculated for each HRU representing the corresponding crop class for these comparisons.

Table 5-2. BEACH input variables and parameters

Variables	Notations	Unit	Grass	Shrub	Industrial plants	Rice	Thin forest	Forest
Curve number condition 2	CN_2	–	80	60	65	75	50	45
Initial basal crop coefficient	$K_{cb\,\mathrm{ini}}$	–	0.03	0.20	0.17	0.15	0.30	0.40
Median basal crop coefficient	$K_{cb\,\mathrm{mid}}$	–	0.30	0.80	1.10	0.85	1.20	1.50
End basal crop coefficient	$K_{cb\,\mathrm{end}}$	–	0.15	0.25	0.25	0.85	0.85	0.70
Light use efficiency	μ	–	0.25	0.50	0.45	0.30	0.60	0.75
Maximum crop height	$H_{\max}$	m	0.30	1.10	1.10	0.40	2.50	10.0
Maximum leaf area index	$LAI_{\max}$	$m^2\ m^{-2}$	0.06	2.00	3.20	1.50	5.00	6.0
Maximum root depth	$RD_{\max}$	m	0.30	1.70	1.50	0.50	1.70	2.50
Saturated hydraulic conductivity in surface layer	$K_{sat\,1}$	$m\ d^{-1}$	0.06	0.10	0.10	0.09	0.10	0.11
Saturated hydraulic conductivity in second layer	$K_{sat\,2}$	$m\ d^{-1}$	0.26	0.26	0.26	0.26	0.31	0.36
Soil evaporation depth	D_e	m	0.15	0.15	0.15	0.15	0.15	0.15
Soil moisture at saturation in surface layer	θ_1	$m^3\ m^{-3}$	0.45	0.50	0.55	0.55	0.55	0.60
Soil moisture at saturation in second layer	θ_2	$m^3\ m^{-3}$	0.50	0.60	0.65	0.55	0.65	0.70
Soil moisture at field capacity in surface layer	$\theta_{\mathrm{fc}\,1}$	$m^3\ m^{-3}$	0.15	0.23	0.20	0.25	0.30	0.40
Soil moisture at field capacity in second layer	$\theta_{\mathrm{fc}\,2}$	$m^3\ m^{-3}$	0.20	0.25	0.22	0.27	0.35	0.45
Soil moisture at wilting point	θ_{wp}	$m^3\ m^{-3}$	0.11	0.13	0.13	0.12	0.14	0.15
Subsurface flow coefficient	C	d^{-1}	0.25	0.25	0.25	0.25	0.25	0.25
Water stress sensitivity	P	–	0.55	0.55	0.55	0.45	0.75	0.85

5.3.9 KINEROS2 Calibration and Validation

The KINEROS2 model was calibrated for the R23rd event using the hourly gauged Q and Sat-P. Some significant changes of parameters were implemented in the calibration stage to make the model an acceptable simulator of the real hydrological system. These parameters are summarized in Table 5-3. Afterwards, the model validation was performed for the R30th (using Sat-P), R8th and R31st (employing Gau-P) events.

Table 5-3. KINEROS2 parameters calibrated for the R23rd event

Parameter	Description	Unit	Range		Initial value		Optimal value[a]	
			Plane	Channel	Plane	Channel	Plane	Channel
ksat	Saturated hydraulic conductivity	mm h^{-1}	0–10	20–50	3.7	41.7	4.46	45.5
s	Initial saturation	–	0–0.9	0–0.9	0.2	0.45	0.46	0.85
n	Manning's n coefficient	–	0.01–1	0.01–1	0.035	0.036	0.07	0.14
ϕ	Soil porosity	–	–	–	0.1	0.44	0.47	0.44
g	Capillary length scale	mm	0-500	0-500	0	0	367.13	101
w	Woolhiser coefficient (channel microtopography)	–	NA	–	NA	0.15	NA	0.15
i	Interception depth	mm	–	–	2	NA	1.51	NA
p	Plant cover	–	–	NA	1	NA	0.52	NA
slp	Slope factor	–	0.5–1	NA	1	NA	0.66	NA
spl	Splash coefficient	s m^{-1}	25–150	NA	25	NA	121.37	NA

[a] Averaged values; NA = not applicable.

5.4 Results

Compared to the daily observed data, significant overestimates of Q for Nam Kim and underestimates for Ngoi Hut exist before the calibration of the models (NSE ≈ −0.35) (Figs 5-3a and c). In contrast, the simulated discharge after calibration and validation matched closely to the measured data in both watersheds, with average R^2 of 0.79 and NSE of 0.65.

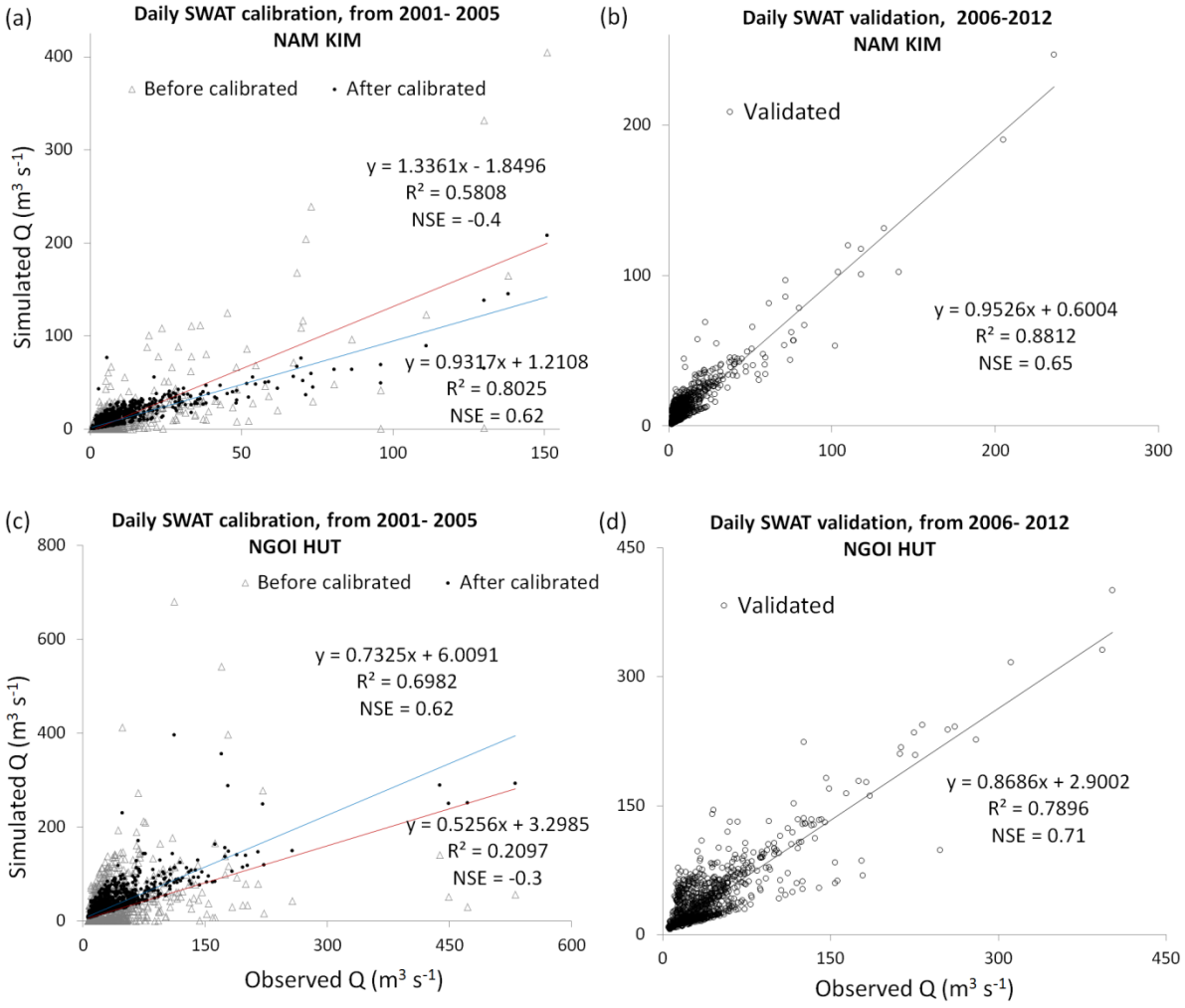

Figure 5-3. Comparison between the gauged and the SWAT discharge in the Nam Kim and Ngoi Hut watersheds.

5.4.1 Results of KINEROS2 Calibration and Validation

In the first model run using the default parameters, θ of 46% and channel Manning's n coefficient (Nc) of 0.035, KINEROS2 simulated the Q as being much higher than in the observed data, and its peak was nearly double the gauged peak. The gap was reduced after the calibration stage, mostly due to increases in N and reductions in Ksat. This trend remained in the validations. The goodness of agreement is graphically depicted in Fig. 5-4, with a mean

R^2 of 0.93. The best correlation between simulated and observed Q was found for the R23rd event, and less agreement was found for the R31st event.

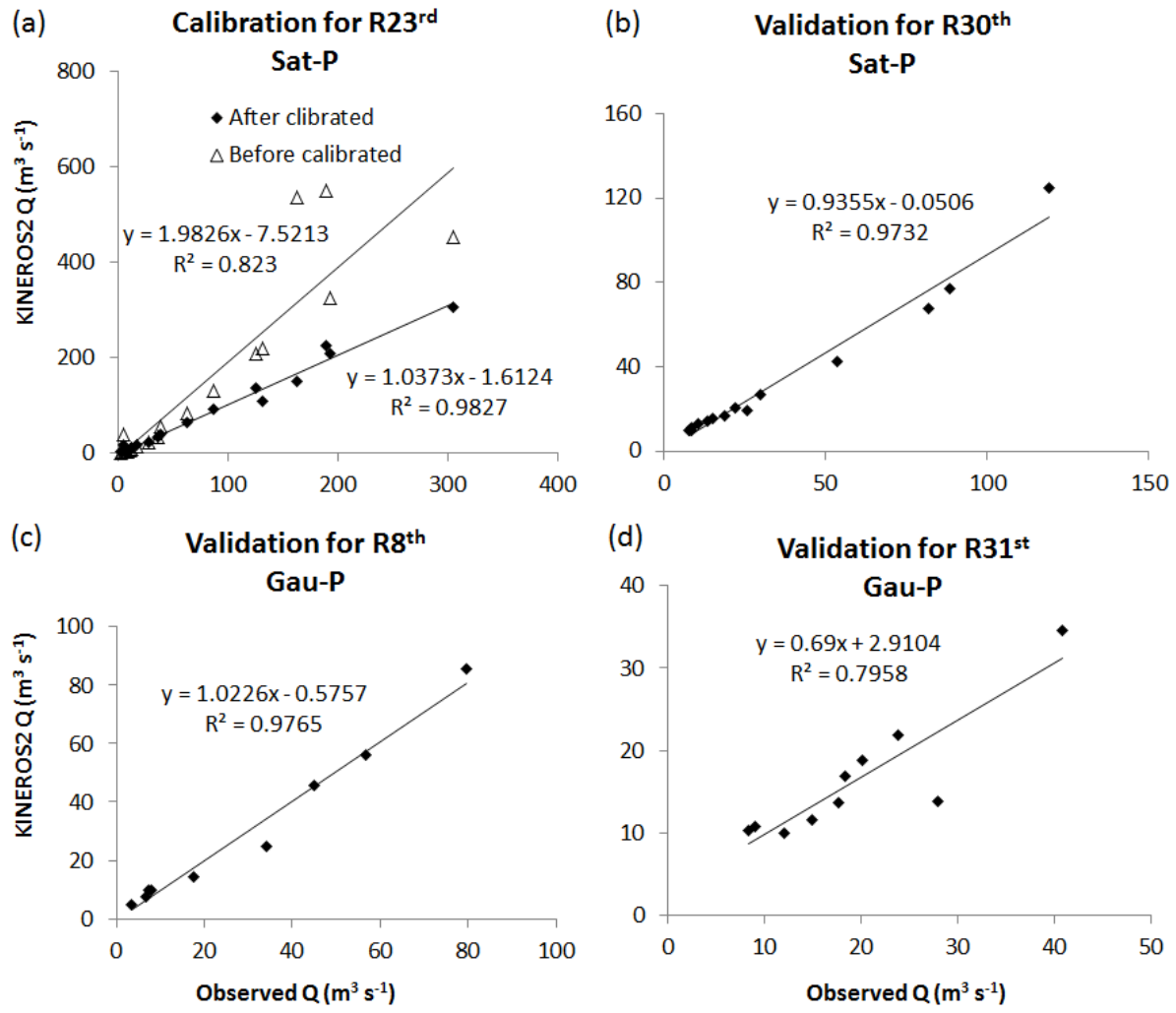

Figure 5-4. Scatter plots of the KINEROS2 calibration and validation for the R23rd, R30th, R8th and R31st events.

5.4.2 Comparing SWAT and BEACH ETa

Figure 5-5 indicates the positive correlation between evapotranspiration of the two models calculated for the watersheds in 2011, with a NSE of 0.6 for both Nam Kim and Ngoi Hut watersheds and 0.62 for the Nam Khat watershed. The differences were greater from mid-January to mid-March. In all cases, the ETa peaked around 25th March at above 10 mm d^{-1}. From May to November, the ETa varied by approximately 2 mm d^{-1}. Correlations between the daily rainfall and evapotranspiration were also observed. On rainy days, the ETa values were low; however, on the subsequent dry days, they rose sharply.

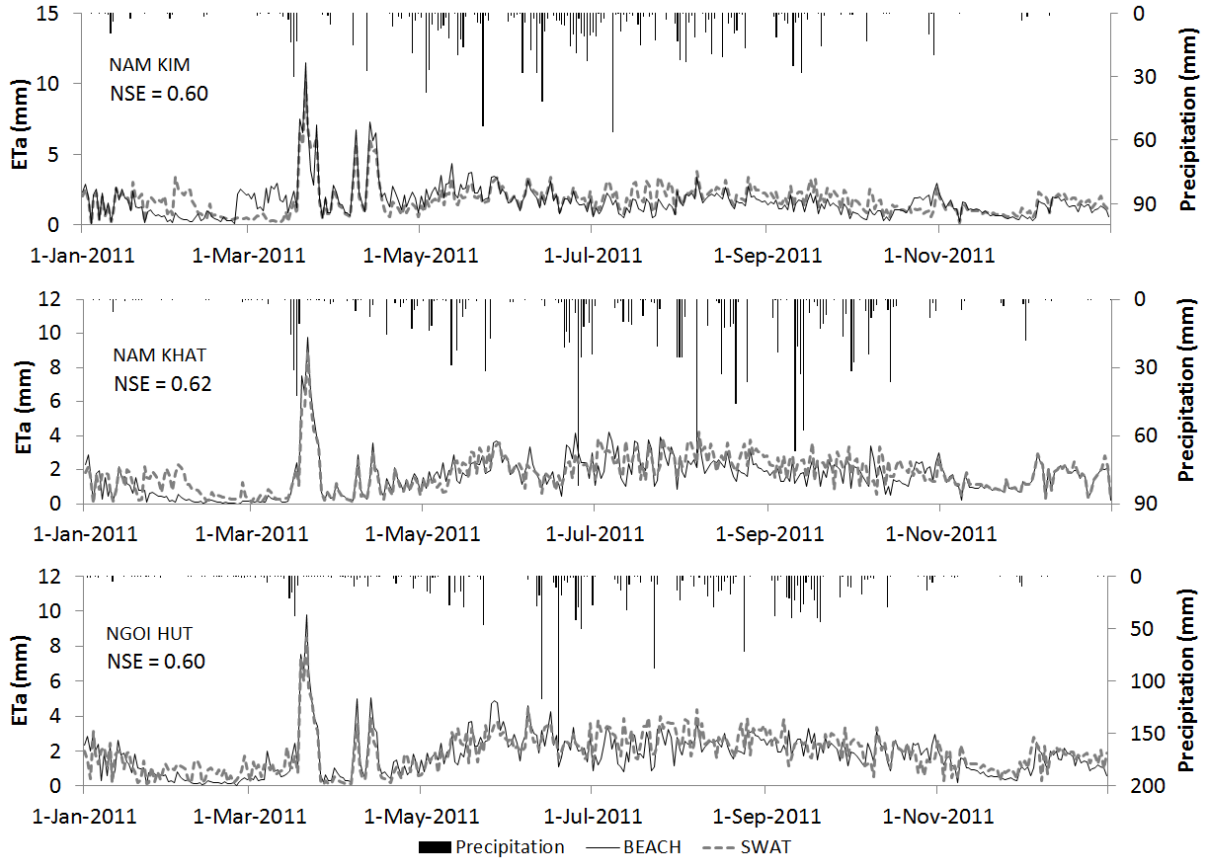

Figure 5-5. Comparison of the mean daily ETa values of the BEACH and SWAT simulations for the Nam Kim, Nam Khat and Ngoi Hut watersheds.

5.4.3 BEACH Soil Moisture

Figure 5-6 illustrates that the forest land was the wettest land, in contrast to the plant industrial zone. The differences between θ of forest land and the mean values (calculated considering area-weightings) were minimal because of the dominance of the forest area in Nam Kim. In both watersheds, from 25th February to 20th March, the soil was the driest. In contrast, from May to October, the soil was wet, with the conditions gradually becoming drier. The mean θ on 22nd of June 2011 was marked at 46% for the Nam Kim watershed and at 42% for the Nam Khat watershed and was used for the KINEROS2 modelled R23rd event.

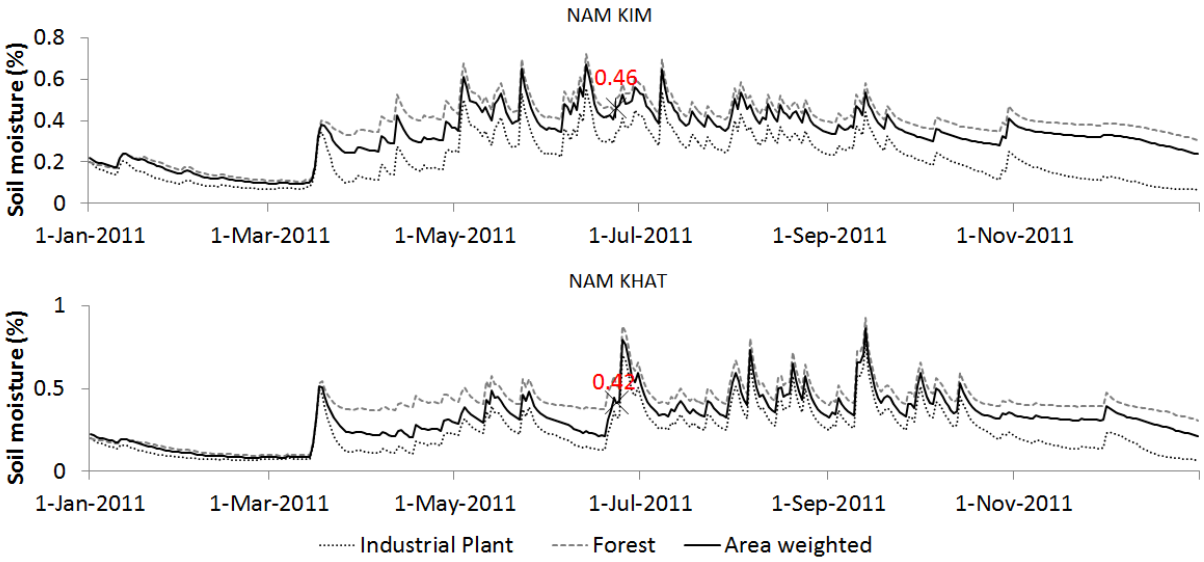

Figure 5-6. Daily BEACH soil moisture.

5.4.4 Results of the KINEROS2 Model

5.4.4.1 Model Parameter Sensitivity Tests

The graphs (Figs 5-7a and c) show the impacts of changing θ_{ant} conditions on the estimated KINEROS2 outflow through the watershed outlets. The reduction of θ_{ant} from 50% to 20% resulted in declines of the peaks from 845 to 535 $m^3\ s^{-1}$ in the Nam Kim watershed and from 355 to 279 $m^3\ s^{-1}$ in the Nam Khat watershed. However, the reduction had no impact on the time to peak. In addition, the graphs (Figs 7b and d) presented the changes of both Q values and the time to peak while the Nc values were increased and θ_{ant} was kept unchanged. The peaks and the lags in Nam Kim (268 km^2) reduced sharply while the Nc was decreased. However, less sensitivity was found for Nam Khat (74 km^2), with Q declines of 60 $m^3\ s^{-1}$ and lags of 30 minutes. The model predicted the Q fitting best to the observed flow at the θ conditions of 46% and the Nc of 0.14 (Fig. 5-7b, S4.6N4).

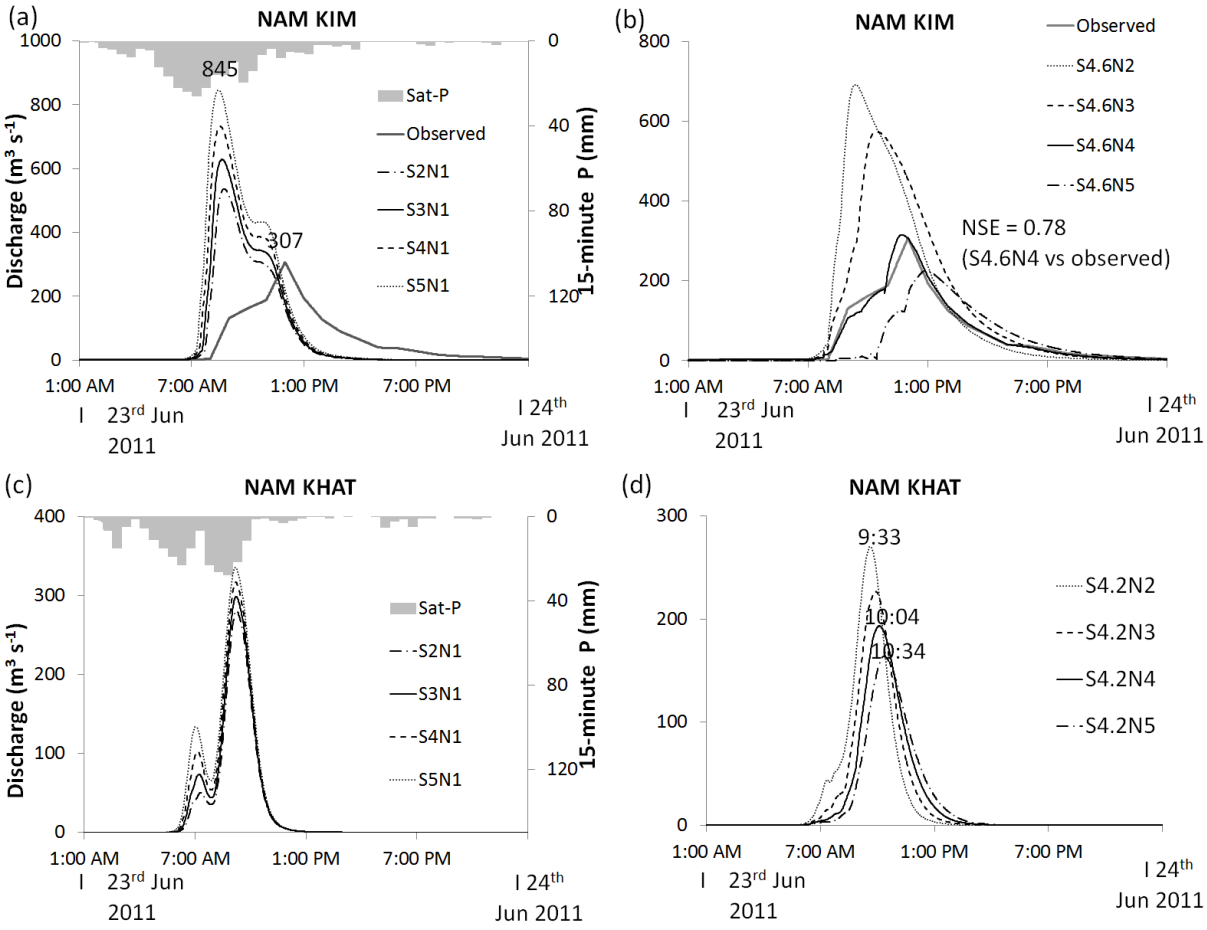

Figure 5-7. Effects of antecedent soil moisture and N on discharges (P denotes precipitation. S2, S3, S4, S5, S4.6 and S4.2 represent soil moisture conditions at 20%, 30%, 40%, 50%, 46% and 42%, respectively; N1, N2, N3, N4 and N5 indicate Manning's n roughness coefficients of 0.035, 0.07, 0.10, 0.140 and 0.175, respectively).

5.4.4.2 Ksat Sensitivity Test

The Ksat represents the most sensitive parameter of KINEROS2: with an increase or decrease of only 20% from the initial values (see Table 5-3), great changes in simulated Q are found in the graphs compared to the results of the initial input (the continuous lines in the middle in Fig. 5-8). However, the plane Ksat was more sensitive than the channel Ksat. In addition, the size of the watershed played a remarkable role in the impact of the Ksat, as depicted by the 'plump' graph of Nam Kim and the 'slender' one of Nam Khat.

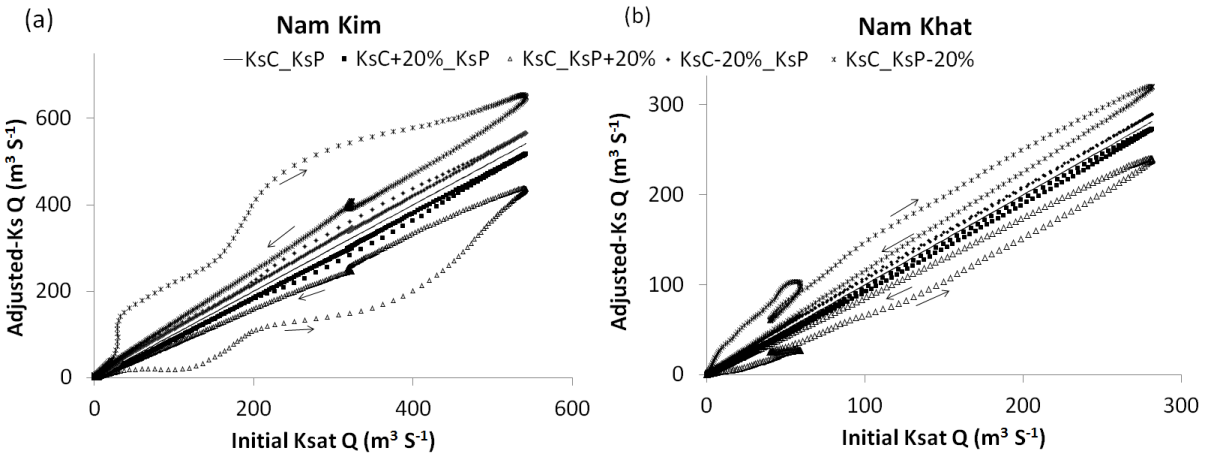

Figure 5-8. Effects of Ksat on the discharge simulated for the R23rd event (KsC and KsP refer to the channel and plane Ksat).

5.4.4.3 Comparing Discharge Using Sat-P and Rad-P

While other inputs, such as θ and N, were kept unchanged, in general, using Rad-P produced lower peaks than using the Sat-P (≈ observed) in both of the watersheds (Table 5-4). Although the total Sat-P and Rad-P rainfalls were not much different, the estimated time to peak of the Rad-P was 0.73 hours later than that using Sat-P in Nam Kim and 0.26 hours later than that in Nam Khat.

Table 5-4. Comparing the simulated discharge using the Sat-P and Rad-P for the R23rd event

Parameters/ Watersheds	**Peak discharge (m^3 s^{-1})**			**Lags (hour)**		**θ (%)**	**Accumulative rainfall (mm)**	
	Sat-P	Rad-P	Observed	Sat-P	Rad-P		Sat-P	Rad-P
NAM KIM	314.3	189.2	306.2	4.4	5.13	46	144.4	133.3
NAM KHAT	191.5	108.7	–	1.67	2.02	42	135.5	113.1

5.4.4.4 KINEROS2 Stream Discharges

The Nam Kim and Nam Khat watersheds were modelled using KINEROS2 and Sat-P, with an Nc of 0.14 and an S of 0.46 and 0.42, respectively. The peak flows of the streams and planes are presented in Fig. 5-9. Obviously, the flow volumes were positively proportional to the areas of the model elements. The new version of KINEROS2 is linked to the ArcMap interface and allows users to view hydrographs of any reach. A combination of the hydrographs and the maps could be extremely helpful for quickly identifying the reaches and planes that have large amounts of discharge.

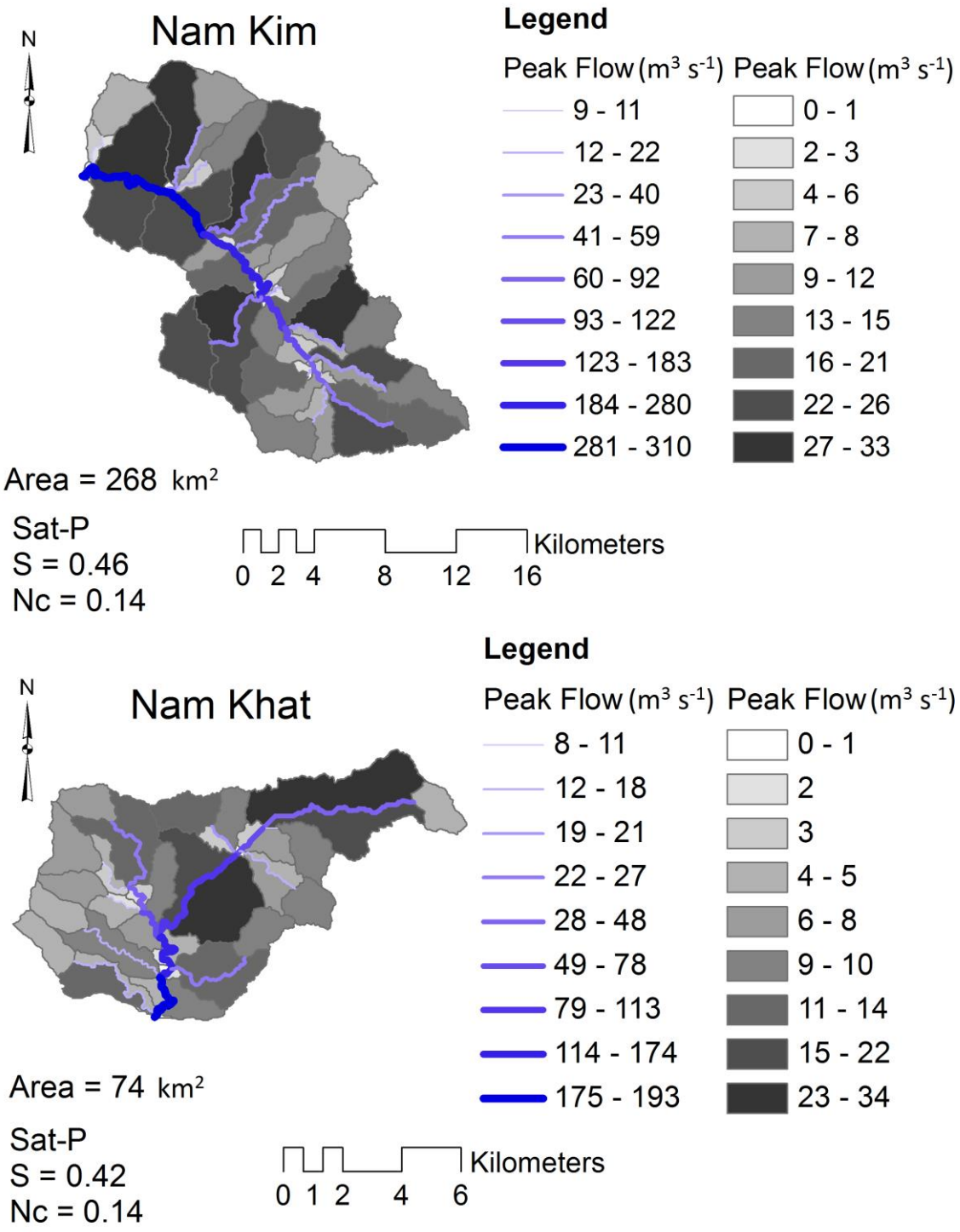

Figure 5-9. Modelled stream and overland flow using KINEROS2.

5.4.4.5 Forecast KINEROS2 Discharge Using the HRM and GSM

Using the forecast rainfall provides an opportunity to issue flash flooding warning relying on the modelling Q. The merit of the model was presented by the fitness of the simulated Q with the observed Q and the agreement between using Sat-P and the GSM and HRM rainfalls (Fig.

5-10). However, some false alarms (marked by the circles) and overestimates at approximately 6 a.m. on the 26th June were found.

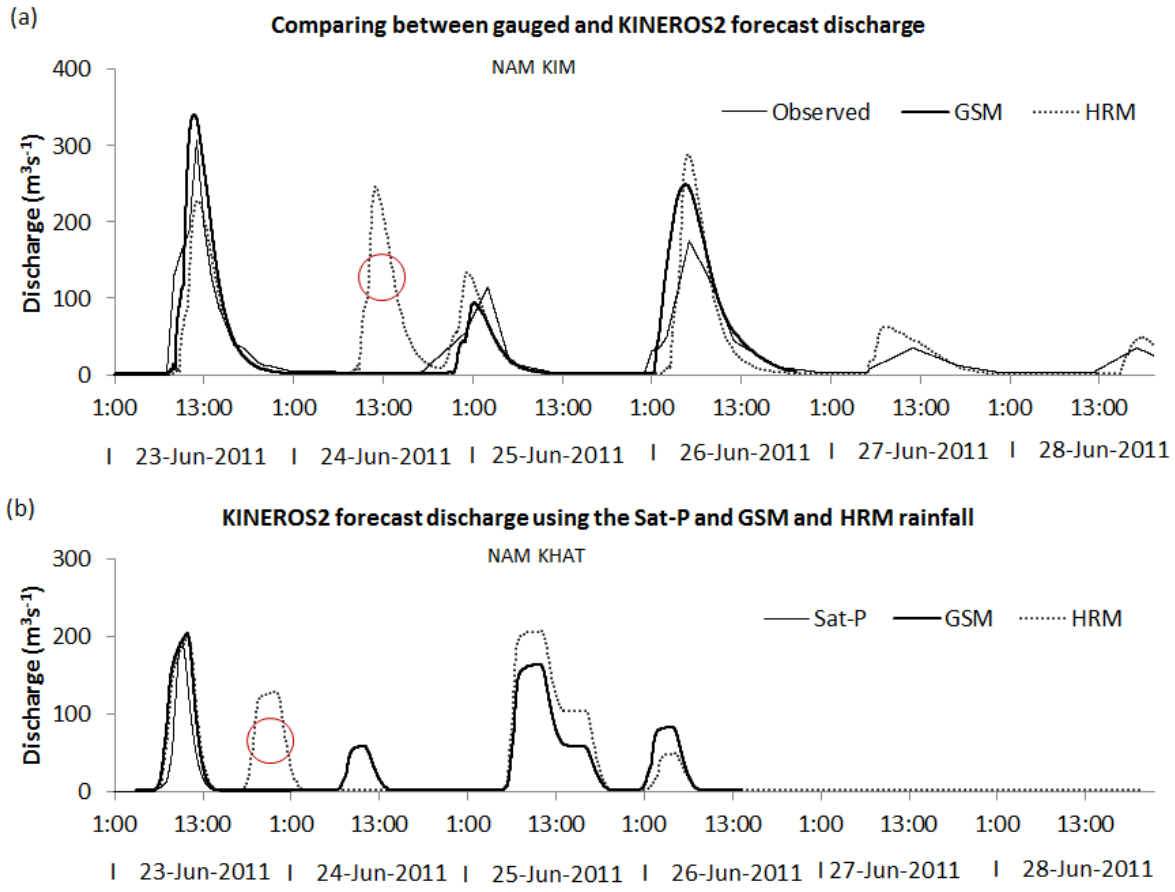

Figure 5-10. Forecast Q_C using the GSM and HRM rainfall at the outlets of Nam Kim (a) and Nam Khat (b).

5.5 Discussion

In performing FF prediction, we face great challenges and uncertainties concerning the input data and model structure (Montz & Gruntfest, 2002). Although it is difficult to overcome these obstacles (Beven, 2001), it is certainly not impossible. Many previous studies have failed to predict the stream runoff due to insufficient θ condition information (Ntelekos et al., 2006; Javelle et al., 2010; Marchi et al., 2010). Hence, the result of the certified BEACH model might play an important role to address this issue. In addition, all other inputs used for this study, such as the DEM, soil map, or LULC, were produced following the national norms or evaluated using a thorough accuracy assessment.

Concerning the model structure and parameter evaluations, all models were calibrated and validated. In particular, KINEROS2 was tested with several rainfall inputs; such testing had

not been performed in many other works. This difference gives us opportunities to compare and contrast the outcomes. Some similarities of using the Gau-P and Sat-P outputs were found, whereas the supervised output of Rad-P underestimating the observed data was found. However, we do not judge that the Rad-P is less accurate than the Sat-P. It might be a question of the old radar generation used in Vietnam. As FFs often occur a short time after rains (4–6 hours) (Austin, 2002), a good FF warning system should provide timely information (Lin et al., 2002). This requirement is for the computational operation of models as well. KINEROS2 was validated using an Intel core™ i3, 2GB RAM computer, which only required approximately 20 seconds to run (at Nam Kim). This short run was one of the reasons for choosing this robust model. Only new updated FR is required for an up-coming forecast operation. Other parameters, such as the LULC, are recommended to be updated seasonally, and the soils and DEM are renewed in decades if significant changes are found.

Manual parameter calibration is a time-consuming implementation. Thus, the results of model parameter sensitivity tests might be significant for this work and for future studies as well. These study findings of substantial sensitivities of the Ksat, S and N to the model outputs are consistent with those of Martínez-Carreras et al., (2007) and Memarian et al., (2013). An important point is that this result of model calibration could be applied to ungauged 'neighbour' watersheds (Nam Khat for example) using a so-called 'regionalization approach' or similar methods already applied by Boughton and Chiew (2007), Makungo et al., (2010) and Servat & Dezetter (1993). Therefore, previously unresolved questions of flooding threshold determination for ungauged catchments might be answered. In addition, Carpenter et al., (1999) considered that the FF threshold is an essential part of FF warning systems. Unfortunately, the FF threshold varies naturally from watershed to watershed; as a result, traditional methods of evaluating the threshold using statistical reports were often not convincing (considering impacts of climate change) and inapplicable for ungauged catchments.

The uncertainties of a hydrological model's outputs are directly linked to rainfall estimations (Villarini et al., 2010). Currently, Adjei et al., (2015), Castro et al., (2014) and Xu et al., (2015) have introduced the newest rainfall estimation for tropical regions using satellite techniques. In addition, Finsen et al., (2014), Kang & Merwade (2014) and Wu et al., (2015) have made efforts to improve radar rainfall and to provide hydrological models with near or real-time data as well. Altogether, the above-described work gives more accurate rainfall availability for hydrological modellers. However, for operational flash flooding prediction,

very precise precipitation forecasts are needed at any given time. The GSM and HRM rainfalls were not expected to be the most suitable, but were the only ones available at the time of this study in Vietnam. Because most parameters of the NWP models are highly nonlinear and naturally inconsistent (Majewski, 2009; JMA, 2013), uncertainties grow when the forecasted period expands further into the future. This might limit the average goal of the USA FF warning systems of 65% of correct alarms (Smith et al., 2005). As such, much work is required to improve the forecast of rainfall particularly with regard to extremes and the consequence of the prediction of FFs.

5.6 Conclusions

The θ_{ant} conditions were found to be extremely important for predicting the flooding magnitude and are therefore very helpful for providing flash flood guidance. However, unlike discharge and precipitation data, θ data are not routinely observed over a long period. Hence, the use of BEACH for E_a estimates is a promising approach. The Ksat was found to be the most sensitive parameter to determine the simulated Q_C. Although the variance of S and the Ksat had no impact on the time of Q's peak, changes in both parameters had significant effects on Q's volume. KINEROS2 represented a dynamic, robust hydrological model with the capability to simulate discharges (hydrographs) that fitted well to measured data using different rainfall sources. Therefore, we conclude KINEROS2 could be an appropriate model for the purpose of predicting the Q_C and thus for use in forecasts. The applications of the KINEROS2 model with the FR (from GSM and HRM) revealed the possibility to predict the time, magnitude and location of approaching FFs.

5.7 References

Abderrezzak, K. E., Paquier, A. & Mignot, E. 2009 Modelling flash flood propagation in urban areas using a two-dimensional numerical model. *Nat. Hazards* 50(3), 433–460. doi: 10.1007/s11069-008-9300-0

Adjei, K. A., Ren, L., Appiah-Adjei, E. K., & Odai, S. N. (2015). Application of satellite-derived rainfall for hydrological modelling in the data-scarce Black Volta trans-boundary basin. *Hydrology Research, 46*(5), 777-791. Doi: 10.2166/nh.2014.111

Alfieri, L., Thielen, J. & Pappenberger, F. 2012 Ensemble hydro-meteorological simulation for flash flood early detection in southern Switzerland. *J. Hydrol. 424*, 143–153. doi: 10.1016/j.jhydrol.2011.12.038

Amengual, A., Romero, R., Gomez, M., Martin, A. & Alonso, S. 2007 A hydrometeorological modeling study of a flash-flood event over Catalonia, Spain. *J. Hydrometeorol. 8*(3), 282–303. doi: 10.1175/Jhm577.1

Ashley, S. T. & Ashley, W. S. 2008 Flood fatalities in the United States. *J. Appl. Meteor. Climatol. 47*, 806–818.

Austin, G. S. (2002). Advanced hydrologic prediction services – Concept of services and operations. *Report U.S. Department of Commerce* – NOAA – NWS.

Beven, K. 2001 How far can we go in distributed hydrological modelling? *Hydrol. Earth Syst. Sci. 5*(1), 1–12.

Bloschl, G., Reszler, C. & Komma, J. 2008 A spatially distributed flash flood forecasting model. *Environ. Modell. Softw. 23*(4), 464–478. doi: 10.1016/j.envsoft.2007.06.010

Boughton, W. & Chiew, F. 2007 Estimating runoff in ungauged catchments from rainfall, PET and the AWBM model. *Environ. Modell. Softw. 22*(4), 476–487. doi: http://dx.doi.org/10.1016/j.envsoft.2006.01.009

Brauer, C. C., Teuling, A. J., Overeem, A., van der Velde, Y., Hazenberg, P., Warmerdam, P. M. M. & Uijlenhoet, R. 2011 Anatomy of extraordinary rainfall and flash flood in a Dutch lowland catchment. *Hydrol. Earth Syst. Sci. 15*, 1991–2005. doi: 10.5194/hess-15-1991-2011

Carpenter, T. M., Sperfslage, J. A., Georgakakos, K. P., Sweeney, T. & Fread, D. L. 1999 National threshold runoff estimation utilizing GIS in support of operational flash flood warning systems. *J. Hydrol. 224*(1–2), 21–44. doi: 10.1016/s0022-1694(99)00115-8

Castro, L. M., Salas, M. & Fernández, B. 2014 Evaluation of TRMM Multi-satellite precipitation analysis (TMPA) in a mountainous region of the central Andes range with a Mediterranean climate. *Hydrol. Res. 46*(1), 89–105. doi:10.2166/nh.2013.096

Creutin, J. D., Borga, M., Gruntfest, E., Lutoff, C., Zoccatelli, D. & Ruin, I. 2013 A space and time framework for analyzing human anticipation of flash floods. *J. Hydrol. 482*, 14–24. doi: http://dx.doi.org/10.1016/j.jhydrol.2012.11.009

El-Hames, A. S. & Richards, K. S. 1998 An integrated, physically based model for arid region flash flood prediction capable of simulating dynamic transmission loss. *Hydrol. Process. 12*(8), 1219–1232. doi:10.1002/(Sici)1099-1085(19980630)12:8<1219::Aid-Hyp613>3.0.Co;2-Q

Estupina-Borrell, V., Dartus., D. & Ababou, R. 2006 Flash flood modeling with the MARINE hydrological distributed model. *Hydrol. Earth Syst. Sci..3*, 3397–3438.

Finsen, F., Milzow, C., Smith, R., Berry, P. & Bauer-Gottwein, P. 2014 Using radar altimetry to update a large-scale hydrological model of the Brahmaputra river basin. *Hydrol. Res. 45*(1), 143–164.

Garcia-Pintado, J., Barbera, G. G., Erena, M. & Castillo, V. M. 2009 Calibration of structure in a distributed forecasting model for a semiarid flash flood: Dynamic surface storage and channel roughness. *J. Hydrol. 377*(1–2), 165–184. doi: 10.1016/j.jhydrol.2009.08.024

Gupta, H. 2006 Development of a site-specific flash flood forecasting model for the Western Region- Final Report for COMET proposal. *University of Arizona:* Tucson, AZ, USA. Available online: http://www.comet.ucar.edu/outreach/abstract_final/0344674_AZ.pdf (accessed on 20th November 2014)

Janal, P. & Stary, M. 2012 Fuzzy model used for the prediction of a state of emergency for a river basin in the case of a flash flood - Part 2. *J. Hydrol. Hydromech. 60*(3), 162–173. doi: 10.2478/v10098-012-0014-3

Javelle, P., Fouchier, C., Arnaud, P. & Lavabre, J. 2010 Flash flood warning at ungauged locations using radar rainfall and antecedent soil moisture estimations. *J. Hydrol. 394*(1–2), 267–274. doi: http://dx.doi.org/10.1016/j.jhydrol.2010.03.032

JMA. 2013 Outline of the Operational Numerical Weather Prediction at the Japan Meteorological Agency. *Appendix to WMO Technical Progress Report on the Global Data-processing and Forecasting System (GDPFS) and Numerical Weather Prediction (NWP) Research.* Available online: http://www.jma.go.jp/jma/jma-eng/jma-center/nwp/outline2013-nwp/pdf/outline2013_all.pdf (accessed on 1st September 2014).

Kang, K. & Merwade, V. 2014 The effect of spatially uniform and non-uniform precipitation bias correction methods on improving NEXRAD rainfall accuracy for distributed hydrologic modeling. *Hydrol. Res. 45*(1), 23–42.

Khavich, V. & Benzvi, A. 1995 Flash-flood forecasting-model for the Ayalon Stream, Israel. *Hydrol. Sci. J.* 40(5), 599–613. doi: 10.1080/02626669509491447

Kousky, C. & Walls, M. 2014 Floodplain conservation as a flood mitigation strategy: Examining costs and benefits. *Ecol. Econ. 104*, 119–128. doi: http://dx.doi.org/10.1016/j.ecolecon.2014.05.001

Krishnamurti, T. N., Bedi, H. S., Hardiker, V. M. & Ramaswamy, L. 2006 An Introduction to Global Spectral Modeling. 2nd Revised and Enlarged Edition, *Springer, Atmospheric and Oceanographic Sciences Library*.

Li, L., Xia, J., Xu, C.-Y. & Singh, V. P. 2010 Evaluation of the subjective factors of the GLUE method and comparison with the formal Bayesian method in uncertainty assessment of hydrological models. *J. Hydrol. 390*, 210–221.

Li, L., Xu, C.-Y. & Engeland, K. 2013 Development and comparison in uncertainty assessment based Bayesian modularization method in hydrological modeling. *J. Hydrol. 486*, 384–394.

Li, L. & Xu, C.-Y. 2014 The comparison of sensitivity analysis of hydrological uncertainty estimates by GLUE and Bayesian method under the impact of precipitation errors. *Stoch. Env. Res. Risk. A.28*(3),491–504.

Lin, C. A., Wen, L., Beland, M. & Chaumont, D. 2002 A coupled atmospheric-hydrological modeling study of the 1996 Ha! Ha! River basin flash flood in Quebec, Canada. *Geophys. Res. Lett. 29*(2). 13-1–13-4. doi: 10.1029/2001gl013827

Looper, J. P. & Vieux, B. E. 2012 An assessment of distributed flash flood forecasting accuracy using radar and rain gauge input for a physics-based distributed hydrologic model. *J. Hydrol. 412*, 114–132. doi: 10.1016/j.jhydrol.2011.05.046

Majewski, D. 2009 HRM – User's Guide for the HRM with the SSO scheme (Vrs. 2.5 and higher). *Deutscher Wetterdienst, Press and Public Relations*: Offenbach, Germany. Available online: http://www.dwd.de/SharedDocs/downloads/DE/modelldokumentationen/nwv/hrm/HRM_users_guide.pdf?__blob=publicationFile&v=2 (accessed on 4th November 2014)

Makungo, R., Odiyo, J. O., Ndiritu, J. G. & Mwaka, B. 2010 Rainfall–runoff modelling approach for ungauged catchments: A case study of Nzhelele River sub-quaternary catchment. *Phys. Chem. Earth, Parts A/B/C*, *35*(13–14), 596–607. doi: http://dx.doi.org/10.1016/j.pce.2010.08.001

Marchi, L., Borga, M., Preciso, E. & Gaume, E. 2010 Characterisation of selected extreme flash floods in Europe and implications for flood risk management. *J. Hydrol. 394*(1–2), 118–133. doi: http://dx.doi.org/10.1016/j.jhydrol.2010.07.017

Marshall, J. S., Langille, R. C. & Palmer, W. M. K. 1947 Measurement of rainfall by radar. *J. Meteorol. 4*(6), 186–192. doi: 10.1175/1520-469(1947)004<0186:MORBR>2.0.CO;2

Martínez-Carreras, N., Soler, M., Hernández, E. & Gallart, F. 2007 Simulating badland erosion with KINEROS2 in a small Mediterranean mountain basin (Vallcebre, Eastern Pyrenees). *Catena 71*(1), 145–154. doi: http://dx.doi.org/10.1016/j.catena.2006.05.013

Memarian, H., Balasundram, S. K., Talib, J. B., Teh Boon Sung, C., Mohd Sood, A., & Abbaspour, K. C. (2013). KINEROS2 application for land use/cover change impact analysis at the Hulu Langat Basin, Malaysia. *Water and Environment Journal, 27*(4), 549-560. Doi: 10.1111/wej.12002

Montz, B. E. & Gruntfest, E. 2002 Flash flood mitigation: recommendations for research and applications. *Global Environ. Change B Environ. Hazard. 4*(1), 15–22. doi: 10.1016/s1464-2867(02)00011-6

Morin, E., Jacoby, Y., Navon, S. & Bet-Halachmi, E. 2009 Towards flash-flood prediction in the dry Dead Sea region utilizing radar rainfall information. *Adv. Water Resour. 32*(7), 1066–1076. doi: 10.1016/j.advwatres.2008.11.011

NCHMF. 2011 Vietnam National Centre for Hydro-Meteorological Forecasting. Available at: http://www.nchmf.gov.vn/web/vi-VN/71/29/45/Default.aspx (accessed on 7th March 2014).

Neitsch, S. L., Arnold, J. G., Kiniry, J. R. & Williams, J. R. 2009 Soil and Water Assessment Tool Theoretical Documentation, Version 2009. *Texas Water Resources Institute Technical Report* No. 406.

Ntelekos, A. A., Georgakakos, K. P. & Krajewski, W. F. 2006 On the uncertainties of flash flood guidance: Toward probabilistic forecasting of flash floods. *J. Hydrometeorol.* 7(5), 896–915. doi: 10.1175/jhm529.1

Quintero, F., Sempere-Torres, D., Berenguer, M. & Baltas, E. 2012 A scenario-incorporating analysis of the propagation of uncertainty to flash flood simulations. *J. Hydrol. 460*, 90–102. doi: 10.1016/j.jhydrol.2012.06.045

Reed, S., Schaake, J. & Zhang, Z. Y. 2007 A distributed hydrologic model and threshold frequency-based method for flash flood forecasting at ungauged locations. *J. Hydrol. 337*(3–4), 402–420. doi: 10.1016/j.jhydrol.2007.02.015

Ruin, I., Creutin, J. D., Anquetin, S. & Lutoff, C. 2008 Human exposure to flash floods - Relation between flood parameters and human vulnerability during a storm of September 2002 in Southern France. *J. Hydrol. 361*(1–2), 199–213. doi: 10.1016/j.jhydrol.2008.07.044.

Sahoo, G. B., Ray, C. & De Carlo, E. H. 2006 Use of neural network to predict flash flood and attendant water qualities of a mountainous stream on Oahu, Hawaii. *J. Hydrol. 327*(3–4), 525–538. doi: 10.1016/j.jhydrol.2005.11.059

Semmens, D. J., Goodrich, D. C., Unkrich, C. L., Smith, R. E., Woolhiser, D. A. & Miller, S. N. 2008 KINEROS2 and the AGWA modeling framework. In: H. S. Wheater, S. Sorooshian and K. D. Sharma (Eds.). *Hydrological Modelling in Arid and Semi-arid Areas.* Cambridge University Press, Cambridge, pp. 41–48.

Seo, D., Lakhankar, T., Mejia, J., Cosgrove, B. & Khanbilvardi, R. 2012 Evaluation of Operational National Weather Service Gridded Flash Flood Guidance Over the Arkansas Red River Basin. *Journal of the American Water Resources Association (JAWRA) 1-12*. DOI: 10.1111/jawr.12087.

Servat, E. & Dezetter, A. 1993 Rainfall-runoff modelling and water resources assessment in northwestern Ivory Coast. Tentative extension to ungauged catchments. *J. Hydrol. 148*(1–4), 231–248. doi: http://dx.doi.org/10.1016/0022-1694(93)90262-8

Sheikh, V., Visser, S. & Stroosnijder, L. 2009 A simple model to predict soil moisture: Bridging Event and Continuous Hydrological (BEACH) modelling. *Environ. Modell. Softw. 24*(4), 542–556. doi: http://dx.doi.org/10.1016/j.envsoft.2008.10.005

Smith, P. L., Barros, A., Chandrasekar, V., Forbes, G., Gruntfest, E., Krajewski, W. & Galinis, E. 2005 Flash Flood Forecasting over Complex Terrain with an Assessment of the Sulphur Mountain NEXRAD in Southern California. *The National Academies Press*, Washington DC. Available at: www.nap.edu

Smith, R. E., Goodrich, D. C., Woolhiser, D. A. & Unkrich, C. L. 1995 KINEROS – A kinematic runoff and erosion model. In: V. P. Singh (Ed), *Computer Models of Watershed Hydrology*. Water Resources Publications, Highlands Ranch, CO, 1130 pp.

Thiessen, A. H. 1911 Precipitation averages for large areas. *Monthly Weather Rev. 39*(7), 1082–1089. doi: 10.1175/1520-0493(1911)39<1082b:PAFLA>2.0.CO;2

Versini, P. A. 2012 Use of radar rainfall estimates and forecasts to prevent flash flood in real time by using a road inundation warning system. *J. Hydrol. 416*, 157–170. doi: 10.1016/j.jhydrol.2011.11.048

Villarini, G., Krajewski, W. F., Ntelekos, A. A., Georgakakos, K. P. & Smith, J. A. 2010 Towards probabilistic forecasting of flash floods: The combined effects of uncertainty in radar-rainfall and flash flood guidance. *J. Hydrol. 394*(1–2), 275–284. doi: http://dx.doi.org/10.1016/j.jhydrol.2010.02.014

Vincendon, B., Ducrocq, V., Dierer, S., Kotroni, V., Le Lay, M., Milelli, M. & Steiner, P. 2009 Flash flood forecasting within the PREVIEW project: value of high-resolution hydrometeorological coupled forecast. *Meteor. Atmos. Phys. 103*(1–4), 115–125. doi: 10.1007/s00703-008-0315-6

Volkmann, T. H. M., Lyon, S. W., Gupta, H. V. & Troch, P. A. 2010 Multicriteria design of rain gauge networks for flash flood prediction in semiarid catchments with complex terrain. *Water Resour. Res. 46,* W11554. Doi: 10.1029/2010wr009145

Woolhiser, D. A., Smith, R. E. & Goodrich, D. C. 1990 KINEROS, A kinematic runoff and erosion model. Documentation and User Manual. *ARS-77. USDA, ARS, Washington DC.*

Wu, S.-J., Lien, H.-C., Hsu, C.-T., Chang, C.-H. & Shen, J.-C. 2015 Modeling probabilistic radar rainfall estimation at ungauged locations based on spatiotemporal errors which correspond to gauged data. *Hydrol. Res. 46*(1), 39–59.

Xu, H., Xu, C.-Y., Sælthun, N.-R., Zhou, B. & Xu, Y. P. 2015 Evaluation of reanalysis and satellite-based precipitation datasets in driving hydrological models in a humid region of Southern China. *Stoch. Environ. Res. Risk Assess. 29*(8), 2003–2020. doi: 10.1007/s00477-014-1007-z

Younis, J., Anquetin, S. & Thielen, J. 2008 The benefit of high-resolution operational weather forecasts for flash flood warning. *Hydrol. Earth Syst. Sci. 12*, 1039–1051.

CHAPTER 6

Flash Flood Prediction by Coupling KINEROS2 and HEC-RAS Models for Tropical Regions of Northern Vietnam[7]

"A property in the 100-year floodplain has a 96 percent chance of being flooded in the next hundred years without global warming. The fact that several years go by without a flood does not change that probability."

-Earl Blumenauer

Abstract

Northern Vietnam is a region prone to heavy flash flooding events. These often have devastating effects on the environment, cause economic damage and, in the worst case scenario, cost human lives. As their frequency and severity are likely to increase in the future, procedures have to be established to cope with this threat. As the prediction of potential flash floods represents one crucial element in this circumstance, we will present an approach that combines the two models KINEROS2 and HEC-RAS in order to accurately predict their occurrence. We used a documented event on 23rd June 2011 in the Nam Khat and the larger adjacent Nam Kim watershed to calibrate the coupled model approach. Afterward, we evaluated the performance of the coupled models in predicting flow velocity (FV), water levels (WL), discharge (Q) and streamflow power (P) during the 3–5 days following the event, using two different precipitation datasets from the global spectral model (GSM) and the high resolution model (HRM). Our results show that the estimated Q and WL closely matched observed data with a Nash–Sutcliffe simulation efficiency coefficient (NSE) of around 0.93 and a coefficient of determination (R^2) at above 0.96. The resulting analyses reveal strong relationships between river geometry and FV, WL and P. Although there were some minor errors in forecast results, the model-predicted Q and WL corresponded well to the gauged data.

[7] This paper is published on 17th November 2015 in the Hydrology, MDPI-Open Assess Publishing. http://www.mdpi.com/2306-5338/2/4/242. DOI:10.3390/hydrology2040242

6.1 Introduction

Unlike paleoflood, flash floods (FF) occur in small streams (Ruiz-Villanueva et al., 2010) and are linked to short, but extreme rainfall events (Zanon et al., 2010). However, they have been categorized into fatal and costly natural disasters (Seo et al., 2012; Masoud, 2011; Rozalis et al., 2010). Northern Vietnam is one of the regions most affected by FF in Vietnam and likely to suffer more frequently due to the impacts of climate change (Nguyen Van Tai et al., 2009). Thus, there exists an urgent requirement for FF-related studies. Much previous research has suggested approaches to mitigate the impacts of FFs through the early identification of FF occurrences (time and location) or their forecast (Montz & Gruntfest, 2002; Naulin et al., 2013; Smith et al., 2005; Tao & Barros, 2013; Villarini et al., 2010; Vincendon et al., 2009). This is crucial information for the local people; as such information will help them to protect themselves from these floods (Vinet, 2008). In this study, we modelled and predicted the occurrence of a specific FF event that took place on 23 June 2011 in the Nam Khat watershed and extended the modelling to the adjacent watershed of Nam Kim, Yen Bai province, Vietnam. This work was done by coupling the KINEROS2 (kinematic runoff and erosion) and HEC-RAS (the Hydraulic Engineering Center River Analysis System) models employing satellite-based and forecast rainfall.

Numerous attempts have been made to forecast FF occurrence using modelling approaches for different conditions of complex terrain (Abderrezzak et al., 2009; Smith et al., 2005; Volkmann et al., 2010; Yates et al., 2000), urban and rural areas (Abderrezzak et al., 2009; Snell and Gregory, 2002), ungauged zones (Javelle et al., 2010; Norbiato et al., 2009; Reed et al., 2007) or in the tropics (Liu & Wu, 2011; Tao & Barros, 2013). Other studies have taken advantage of the finer resolution of radar rainfall and operated in real or near real time (Morin et al., 2009; Rozalis et al., 2010; Unkrich et al., 2010; Younis et al., 2008), though several other options exist using satellite-derived precipitation data (Ahmed et al., 2010; Wardah et al., 2008). Defining FF is difficult (Montz & Gruntfest, 2002). However, an FF is recognized by its physical characteristics of massive power (energy), fast flows (velocity) (Montz & Gruntfest, 2002; Rozalis et al., 2010) and high discharge stage (water level) (Borga et al., 2014). In our modelling implementations, we focused more on these physical characteristics (not the social impacts) of FFs and predicted them based on forecast rainfall inputs. When FFs are identified at an early stage, this information is extremely helpful for flash flooding warning systems (Krzysztofowicz, 2014).

Prior warning of FFs is very complicated, not only because of the complexity of the system (physical processes, short leading time), but also the output uncertainty (related to scant available data, methodology) (Georgakakos, 1986; Ntelekos et al., 2006; Estupina-Borrell, 2006). Therefore, many researchers have attempted to analyse the uncertainty sources (Quintero et al., 2012; Villarini et al., 2010; Yatheendradas, 2008). One major issue in early FF research concerned the forecast uncertainty and its significant dependence on meteorological inputs (rainfall) (Morin et al., 2009). Our result accuracy relied on the merit of two robust models and validated observed data utilizing the method by Nash and Sutcliffe (1970).

The aim of this study is to use the two well-known hydrological models, firstly, for calibrating and validating the models and making sure that the models work properly; secondly, for modelling the past flooding event and analysing the hydraulic response by looking at river discharge, flow velocity and power and their relationships; thirdly, for running the models in forecast mode using forecast rainfall data and comparing the model outputs with observed information. In the forecast stage, the three important aspects of flow stage, flow velocity (FV) and streamflow force were analysed, as well.

To achieve the study goals, we designed a practical framework with a combination of the well-known robust models (in terms of precision and computational efficiency). The benefit of coupling the two models is to solve the data scarcity problem when the finer input data required by the HEC-RAS were not available. In addition, there have been some studies using the KINEROS2 model alone for the aim of FF prediction (Volkmann et al., 2010; Yatheendradas, 2008) and Gupta (2006) and Mudd (2006) also recommended the use of it. However, the KINEROS2 does not accurately estimate the river water level and flow force (two important criteria for identifying the FF), but the use of HEC-RAS afterwards could be a good solution. As the FFs often occur within six hours of causative rains (Austin, 2002) or a shorter event of a few hours (Kourgialas et al., 2012), the total model operation time (including preparing new model inputs, model runs and the result display and analyses) should meet this time criterion. Otherwise, the information provided by the model for FF warning might be too late for the warning system in a real-time operation. With an Intel core™ i3, 2 GB RAM computer, the models need less than one minute to run the modelling of the bigger watershed of Nam Kim (268.5 km^2). Only new updated forecast rainfall and input discharge for HEC-RAS are needed to re-input for forecast operation. The time for preparing these inputs is assumed to depend on the skill of the operators, and for this study,

approximately 30 min were needed. We recommend seasonal updating for land use and land cover for KINEROS2, and the less dynamic parameters of topography, river and soil profiles could be renewed in a few decades if significant changes are found.

6.2 Study Site

This study focuses on the region of North Vietnam, which has tropical climatic conditions, steep terrain and an increase in intensive land use (Anh et al., 2014; Ranzi et al., 2012). The region is considered to have a scarcity of data available, with 108 metrological gauges in the whole region and only three gauges in Yen Bai province. The north of Vietnam has an annual average rainfall ranging from 800 to 1500 mm and annual mean temperature varying from 20 °C to 24 °C (Nguyen Van Tai et al., 2009). Nam Kim and Nam Khat, located in the red ellipse (Fig. 6-1) within Yen Bai province, were chosen as the representative watersheds of the region.

Both Nam Kim and Nam Khat are classified as medium-sized watersheds. The elected reaches (in the green circles) for HEC-RAS simulation have no construction along them, such as bridges, embankments or dams. Local people cross the rivers on foot or on footbridges (illustrated in Fig. 6-2). Dominant local residents are Tay and Dao ethnicities and are considered to be very vulnerable to flash floods. Nam Kim was chosen for the case study because observational data were available (recorded at the outlet) for model validation and has also experienced flash flooding, but not severe. Nam Khat was additionally selected due to its flash flooding incidence on 23 June 2011, when four lives were lost (the reach in the green circle in Nam Khat in Fig. 6-1).

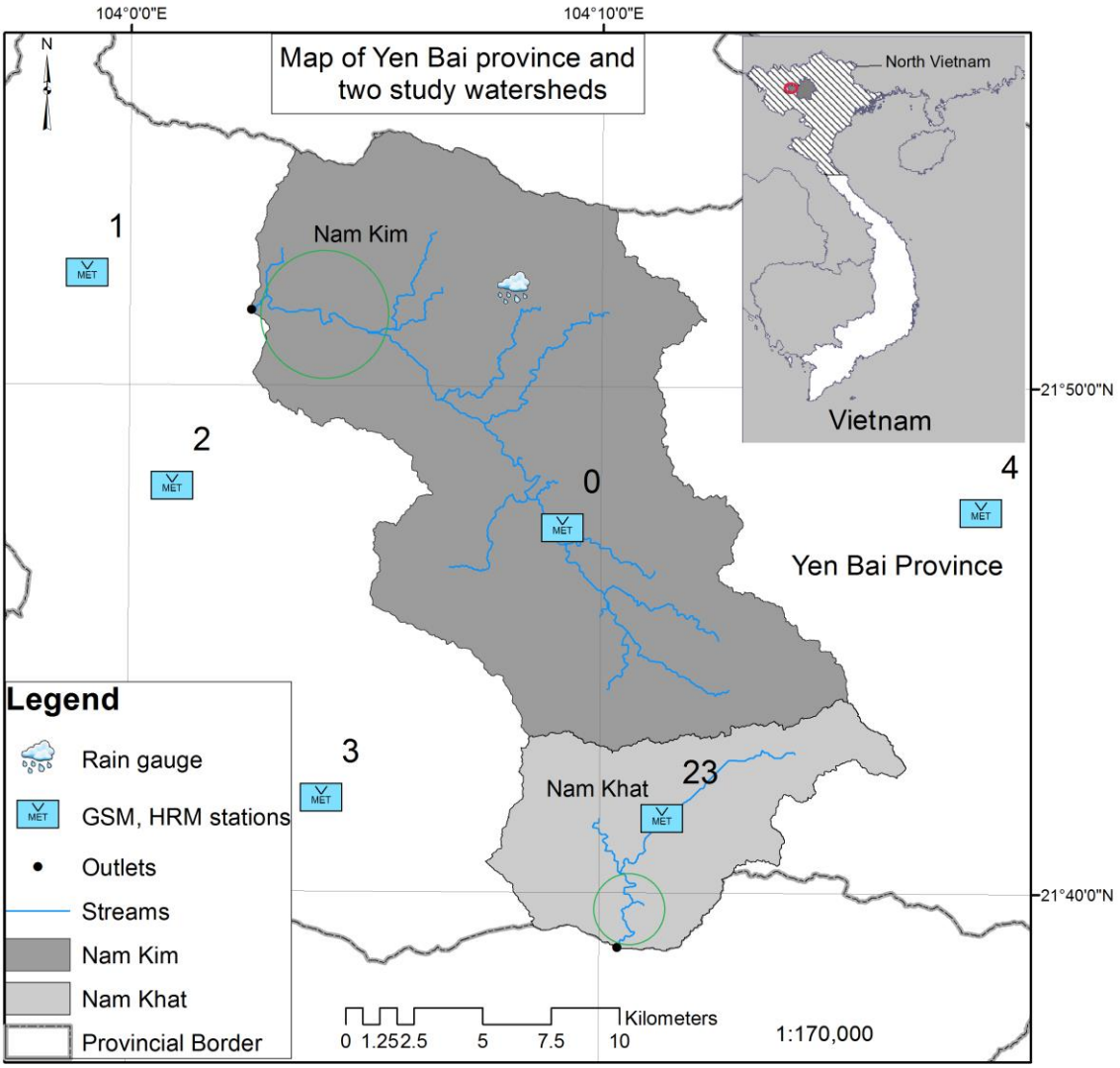

Figure 6-1. Study site of the Nam Kim and Nam Khat watersheds. GSM, global spectral model; HRM, high resolution model.

Figure 6-2. Pupils crossing the river on their way to the school (a) and a typical footbridge (b) in rural areas in Vietnam (source: http://tuyensinh.nld.com.vn and http://kienthuc.net.vn, respectively).

6.3 Methodology and Materials

6.3.1 Study Flowchart

The study framework was designed to accomplish the study objective, as shown in Fig. 6-3. It is important to note that the forecast rainfall by means of the KNIEROS2 model (Smith et al., 1999; Smith et al., 1995) will produce the forecast river hydrographs, depth and initial flow, which will be used as inputs for the HEC-RAS and generate the forecast water levels or stages (WLs), flow velocity (FV) and energy curves for the FF forecast strategy.

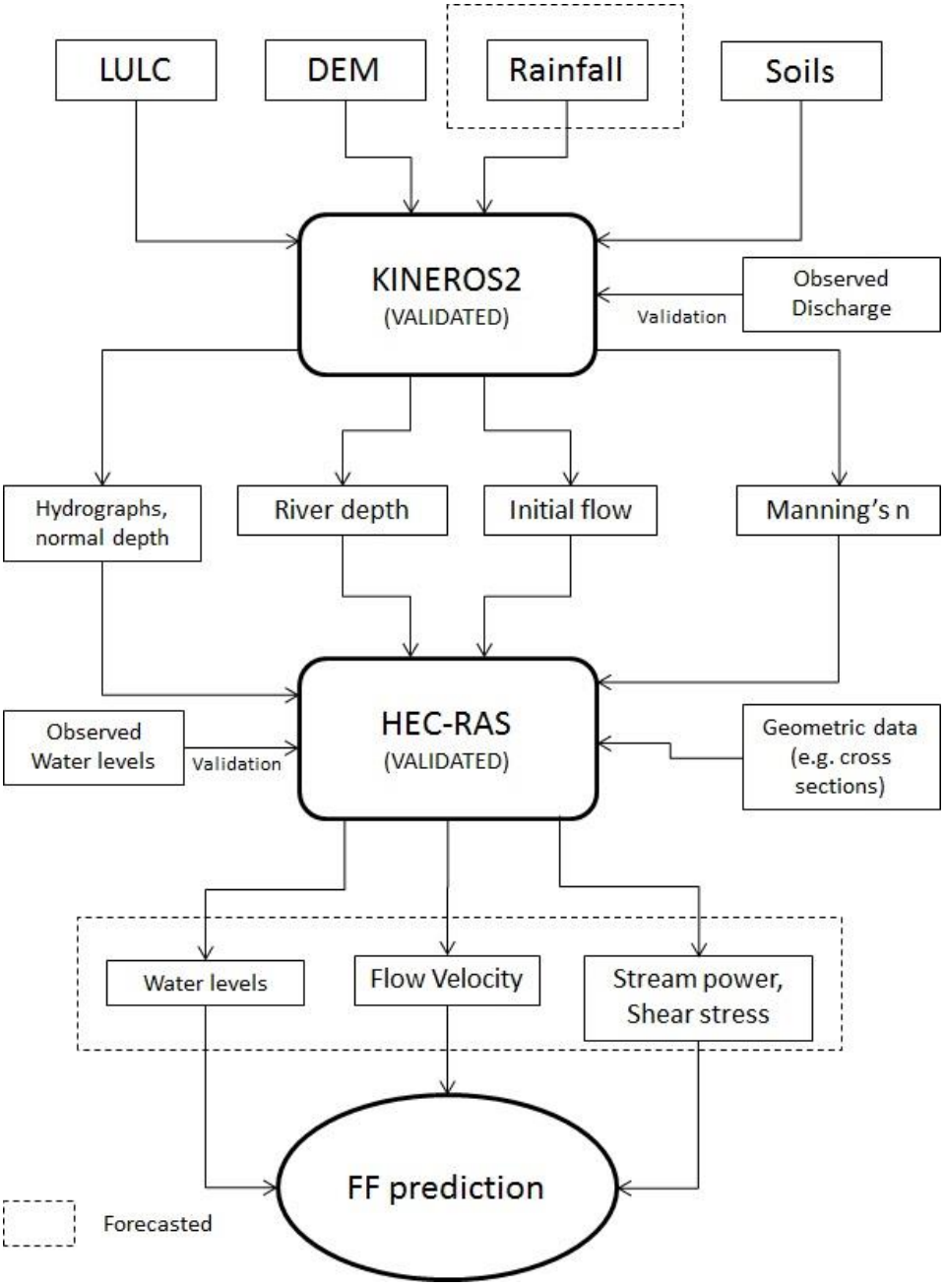

Figure 6-3. The study flowchart.

6.3.2 Model Description

6.3.2.1 KINEROS2

KINEROS2 is the improved version of KINEROS (Woolhiser et al., 1990) and a dynamic, distributed simulation model. Most model features were written by Smith et al., (1995). The model requires four types of datasets to operate, namely topographic, rainfall, soil and land use data. Some of the useful features for the later HEC-RAS inputs will be presented as follows.

KINEROS2 treats the channel routine discharge (Q) using a four-point implicit technique. Manning's n roughness coefficient can be retreated in the kinematic wave approximation equation (for more details, see Woolhiser et al., (1990)).

The hydraulic depth is estimated in KINEROS2 by approximating the channel cross-sections as trapezoidal or circular, as shown in Fig. 6-4 and in the following equation:

$$h_D = D\left[\frac{\theta_c - \sin\theta_c}{\sin(\theta_c/2)}\right]/8 \qquad (6\text{-}1)$$

where h_D presents the hydraulic depth (m) and D is the diameter of the channel conduit.

When the channel cross-section is approximated as trapezoidal, the depth is calculated as in the following relationship:

$$p_e = \min\left[\frac{h}{0.15\sqrt{BW}}, 1.0\right] \times p \qquad (6\text{-}2)$$

where h is the depth, p_e presents the effective wetted perimeter for infiltration, p indicates the channel wetted perimeter at depth h and BW is the channel bottom width, as in Fig. 6-4. Equation (6-2) indicates that the p_e is smaller than the p until a threshold depth is reached, and at depths greater than the threshold depth, the two values are identical.

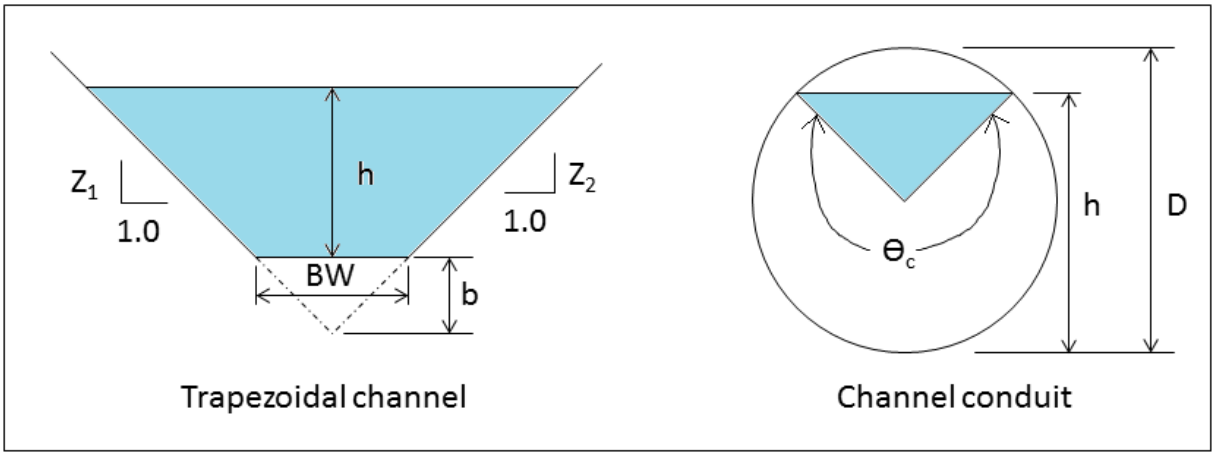

Figure 6-4. Channel and conduit cross-sections.

6.3.2.2 HEC-RAS

The U.S. Army Corps of Engineers' River Analysis System (HEC-RAS) is software that allows users to perform one-dimensional steady and unsteady flow river hydraulics calculations (Brunner, 2010). In this study, the latter method was applied. The equations of one-dimensional steady and unsteady flow are described by (Horritt & Bates, 2002). The following features are the main relationships that are important for FF identification. The model estimates the channel depth in unsteady flow based on momentum equations expressed by Newton's second law as in the following expression:

$$\sum \boldsymbol{F_x} = \frac{\boldsymbol{d\vec{M}}}{\mathrm{dt}} \tag{6-3}$$

where $\sum \boldsymbol{F_x}$ is the accumulative momentum applied in the x-direction, $\boldsymbol{d\vec{M}}$ indicates the momentum flux, which is the velocity vector in the flow direction, and dt presents the fluid mass times. The pressure, gravity and boundary drag are considered as three forces.

The channel depth can be inferred from the pressure force equation (Shames, 1962):

$$F_p = \int_0^h \rho g(h-y)\, T(y)\, \mathrm{dy} \tag{6-4}$$

where F_p is the pressure force in the x-direction, h is the depth, y is the distance above the channel invert and $T(y)$ presents the width function, which links the width of the cross-section to the distance above the channel invert (for more details, see Brunner (2010)).

The FV at the discrete cross-section is computed in the HEC-RAS by solving the continuity, energy and flow resistance equation (Brunner, 2002):

$$Y_2 + Z_2 + \frac{\alpha_2 V_2^2}{2g} = Y_1 + Z_1 + \frac{\alpha_1 V_1^2}{2g} + h_e \tag{6-5}$$

in which Y is water depth, Z indicates channel elevation, V represents the mean velocity, α is a velocity weighting coefficient, g is the gravitational acceleration, h_e represents energy head loss and subscripts 1 and 2 signify Cross-sections 1 and 2, respectively.

To achieve the above outputs, the river geometric, unsteady flow data (boundary and initial conditions) have to be supplied. The boundary condition includes a stage/flow hydrograph (or both) and normal depth derived from KINEROS2.

6.3.3 Coupling of KINEROS2 and HEC-RAS

We coupled the KINEROS2 and the HEC-RAS models by using the KINEROS2 outputs for the HEC-RAS inputs; however, internally, the two models were performed separately. The discharges (using satellite-based, gauged and forecasted rainfalls), river depths, initial flow and Manning's n coefficient were used for the inputs and for defining the initial conditions in the HEC-RAS, as well. All of these KINEROS2 parameters were derived from the validated calibration stage, and they are, hence, realizable. We applied the unsteady flow analysis approach.

6.3.4 Model Calibration and Validation

KINEROS2 and HEC-RAS calibrations for Nam Kim were made for the rain event on 23 June 2011 (R23rd) using observed discharge and water levels from each model respectively. In these stages, the hydraulic conductivity (Ksat) and relative saturation index (S) were adjusted for the KINEROS2, and Manning' n coefficient (N) was altered for the HEC-RAS calibration.

Other rain events on 30 June (R30th), 8 (R8th) and 31 (R31st) July 2011 were elected for model validations employing field measurements of the hydraulic gauge at the Nam Kim outlet. The implementations of the models were investigated by using statistical values of the Nash–Sutcliffe simulation efficiency coefficient (NSE) (Nash & Sutcliffe, 1970), the coefficient of determination (R^2) and graphical approaches of comparing simulated with observed information. Unfortunately, there was no gauged data recorded for the validation in Nam Khat. However, due to the similar conditions of the two watersheds, the model calibration for Nam Kim could be transposed to the ungauged Nam Khat, a method that has been applied in several studies, such as (Blöschl, 2005; Javelle et al., 2010; Naulin et al., 2013; Norbiato et al., 2009).

6.3.5 Data for KINEROS2

6.3.5.1 Rainfall

Precipitation data were derived from three sources of satellite-based (MSAT-Japan), ground rain gauges and the Numerical Weather Prediction (NWP) models of the global spectral model (GSM) (Krishnamurti et al., 2006) and the high resolution model (HRM) (Majewski, 2009). All of this rainfall data were supplied by the National Center for Hydro-Meteorological Forecasting, Vietnam.

The temporal and spatial resolutions of the satellite-based rainfall are 30 min and 4 × 4 km, respectively. The accumulative distributed rainfall (the maps in Fig. 6-5) and the 30-min rain density (the graphs in Fig. 6-5) of the R23rd and R30th were assessed for Nam Kim and Nam Khat.

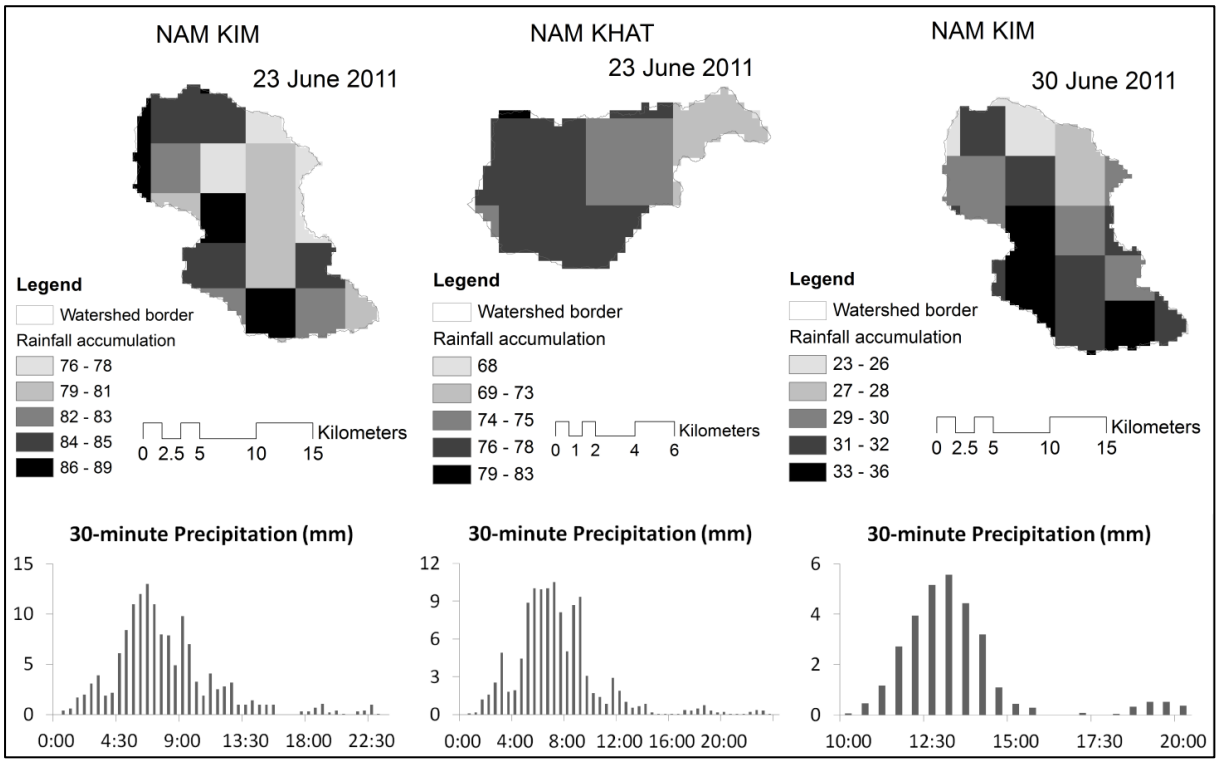

Figure 6-5. Satellite-based rainfall.

We also used gauged rainfall recorded every three hours on 8 July (R8th) and 30 to 31 (R31st) July 2011 by the rain gauge established at Nam Kim (Fig. 6-1) for validations of the models. The development of the rain is represented in the section 6.4.1.1 (in Fig. 6-7).

The 6-h, accumulated rainfall of GSM (84-h forecast) and HRM (132-h forecast) was the forecasted observation at 00:00 on 23 June 2011 (Fig. 6-6) at Stations 0 and 23 (locations shown in the study site figure). Both of the models have the ability to operate at large, meso- and small (grid) scales and take about 50 min for each operation. The GSM was operating four times a day at 00:00, 06:00, 08:00 and 12:00, and the HRM was operating at 00:00 and at 12:00.

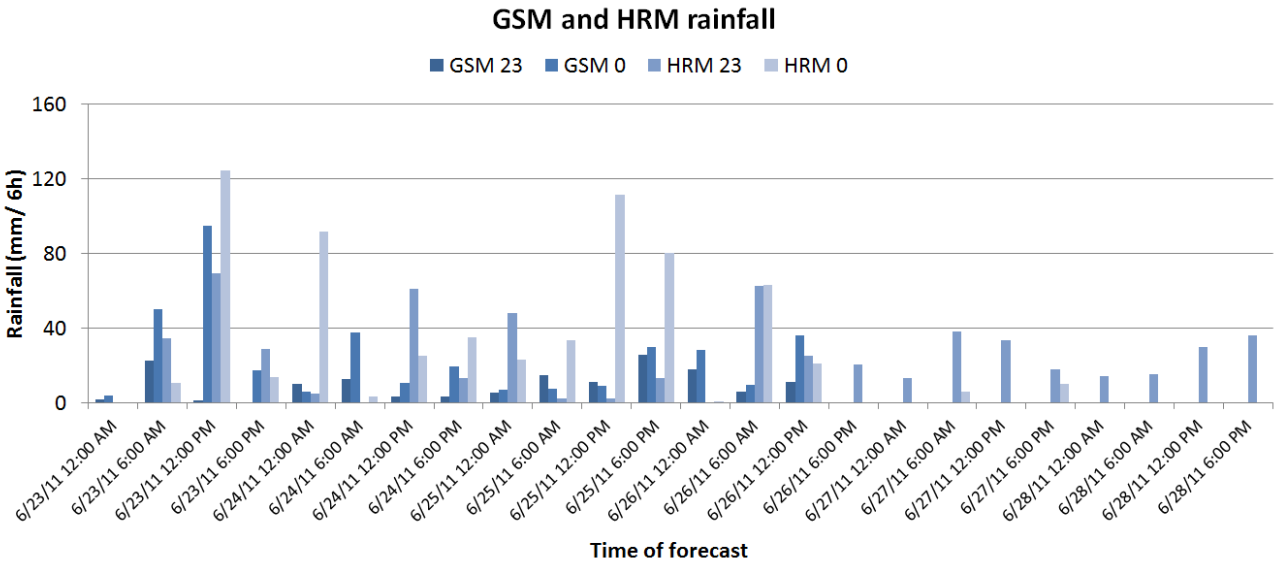

Figure 6-6. Forecasted rainfall by GSM and HRM of the designed stations 23 and 0.

6.3.5.2 Land Use, Digital Elevation Model, Soil and Discharge Data

The LULC map was mapped from the Landsat scene with a 30 × 30 m spatial resolution acquired in 2009. The forest, shrub, agricultural land, grassland, water bodies and bare land are classified as the six major land uses. The accuracy of the LULC map was examined using the producer accuracy (76.5%), user accuracy (76.7%) and kappa statistics (0.74), as well.

A 10 × 10 m grid-based DEM was used for the KINEROS2 morphologic parameterizations. It was provided by the Vietnam Resources and Environment Corporation in 2009.

The dominant soil groups of Fluvisols, Calcisols, Ferralsols, Alisols, Acrisols and Gleysols were categorized on a custom soil map and employed as soil data for the model. The map was produced by the Resource Centre-Agricultural Institute of Plan and Design, Vietnam in 1996 (NIAPP, 1996).

Finally, we employed the hourly discharge and WLs measured at the outlet of Nam Kim provided by National Centre for Hydro-Meteorological Forecasting (NCHMF, 2011) for the calibration and validation of the two models.

6.3.6 Data for HEC-RAS

6.3.6.1 Geometric Data

River cross-sections (RS) were built at points (up to 50 meters above the river banks), which were directly measured on the Aerial Photogrammetry Station of the Intergraph Corporation,

USA, with absolute geometric errors of less than one meter. The river depths were derived from the KINEROS2 results. We used the trapezoidal channel to define the channel shape. The Nam Kim reach (Table 6-1) (3.5 km) was defined by sixteen RSs and Nam Khat (Table 6-2) (1.2 km) by twelve RSs. The distance between cross-sections is chosen based on the changes in river slope. The elevation of the river banks was derived from a geodatabase of Yen Bai province, and these banks were *in situ* field measurements.

Table 6-1. Geometric profiles of the Nam Kim reach

(Chl = channel, W.S. = water surface and E.G. = energy gradeline for calculated W.S.)

River Stations	Min Chl Elevation (m)	W.S. Elevation (m)	E.G. Elevation (m)	E.G. Slope (m/m)	Flow Area (m^2)	Top Width (m)
101	904.2	907.0	907.4	0.0014	121.3	53.3
102	903.4	906.0	906.9	0.0043	85.4	53.6
103	901.0	903.9	906.1	0.0089	54.0	31.2
104	899.3	903.4	903.7	0.0007	155.0	56.3
105	899.5	902.8	903.4	0.0021	90.1	34.7
106	898.8	901.9	903.0	0.0040	67.9	26.4
107	899.3	901.7	902.2	0.0022	101.4	46.8
108	898.5	900.6	901.9	0.0075	67.8	44.3
109	896.9	899.2	900.3	0.0053	70.5	38.4
110	896.0	897.8	898.7	0.0066	76.3	52.7
111	893.8	896.3	899.6	0.0188	51.3	39.9
112	890.7	892.4	893.9	0.0109	57.8	37.5
113	888.0	889.5	891.8	0.0269	46.8	45.1
114	880.6	883.5	884.6	0.0044	69.2	30.6
115	880.4	882.6	883.3	0.0039	83.9	45.0
116	879.0	882.7	882.9	0.0004	195.6	61.0

Table 6-2. Geometric profiles of the Nam Khat reach

River Stations	Min Chl Elevation (m)	W.S. Elevation (m)	E.G. Elevation (m)	E.G. Slope (m/m)	Flow Area (m^2)	Top Width (m)
101	1250.5	1252.5	1253.1	0.0184	62.2	34.7
102	1247.2	1249.5	1250.0	0.0229	65.0	44.2
103	1245.4	1246.8	1247.6	0.0239	54.6	42.1
104	1239.3	1243.2	1244.1	0.0186	53.1	20.3
105	1236.9	1240.2	1241.0	0.0173	63.6	36.3
106	1235.1	1237.9	1238.4	0.0194	70.3	36.0
107	1233.9	1236.0	1236.6	0.0152	67.9	48.6
108	1228.1	1232.7	1233.4	0.0189	66.9	24.0
109	1226.2	1230.5	1231.2	0.0136	68.7	26.2
110	1223.8	1228.0	1229.2	0.0198	50.5	18.6
111	1220.1	1224.1	1225.3	0.0164	46.9	16.8
112	1216.0	1220.1	1220.8	0.0126	63.7	28.4

6.3.6.2 On-Site Measured River Discharge and Water Levels

Hourly (two-hour recordings for the cases of R8th and R31st) discharge and river stages were recorded during the R23rd, R30th, R8th and R31st at the outlet of the Nam Kim River by the NCHMF (2011). These data were used for the calibrations and validations of the models (see the study flowchart).

6.3.7 Regionalization Technique

We used the regionalization technique, defined as a method of transferring model parameters from calibrated catchments to ungauged ones of similar characteristics (Makungo et al., 2010), for Nam Khat. The two watersheds are neighbours (Fig. 6-1) and located in the same climatic zone (Nguyen Van Tai et al., 2009). The Humic Ferralsols and Humic Acrisols are both major soils in the watersheds. LULC is also similar to the major classes of forest, shrub and agricultural land, and both watersheds have complex and mountainous terrain (statistics from the inputs).

6.4 Results and Discussion

To accomplish the study objective of flash flood prediction, the FV, the WLs and the flow energy (all related to peak discharge) are considered to be influential with respect to FF occurrence (Lumbroso & Gaume, 2012; Marchi et al., 2010; Villarini et al., 2010). KINEROS2 was calibrated and validated, and the outputs were used for HEC-RAS. Next, we investigated the capacity of the HEC-RAS model to accurately estimate these factors. Then, we applied the model for the prediction stage by using forecasted discharge from

KINEROS2. HEC-RAS also offers a module to map the flooding plains. However, due to the very steep riverbanks of the study areas, the flooding areas are of less importance to our study compared to the factors mentioned above.

6.4.1 Model Calibration and Validation

6.4.1.1 KINEROS2

The results of KINEROS2 calibration for the R23rd in the Nam Kim watershed can be seen as represented by the hydrographs in Fig. 6-7a as a result of changing the most sensitive parameters of the saturation index of the soil (initial value of 0.2 and final value of 0.46) and the Ksat (average initial value of 5.16 and final value of 4.12). Additionally, the Nash–Sutcliffe simulation efficiency (NSE) and coefficient of determination (R^2) were above 0.95 comparing the observed data with the discharge calibrated after.

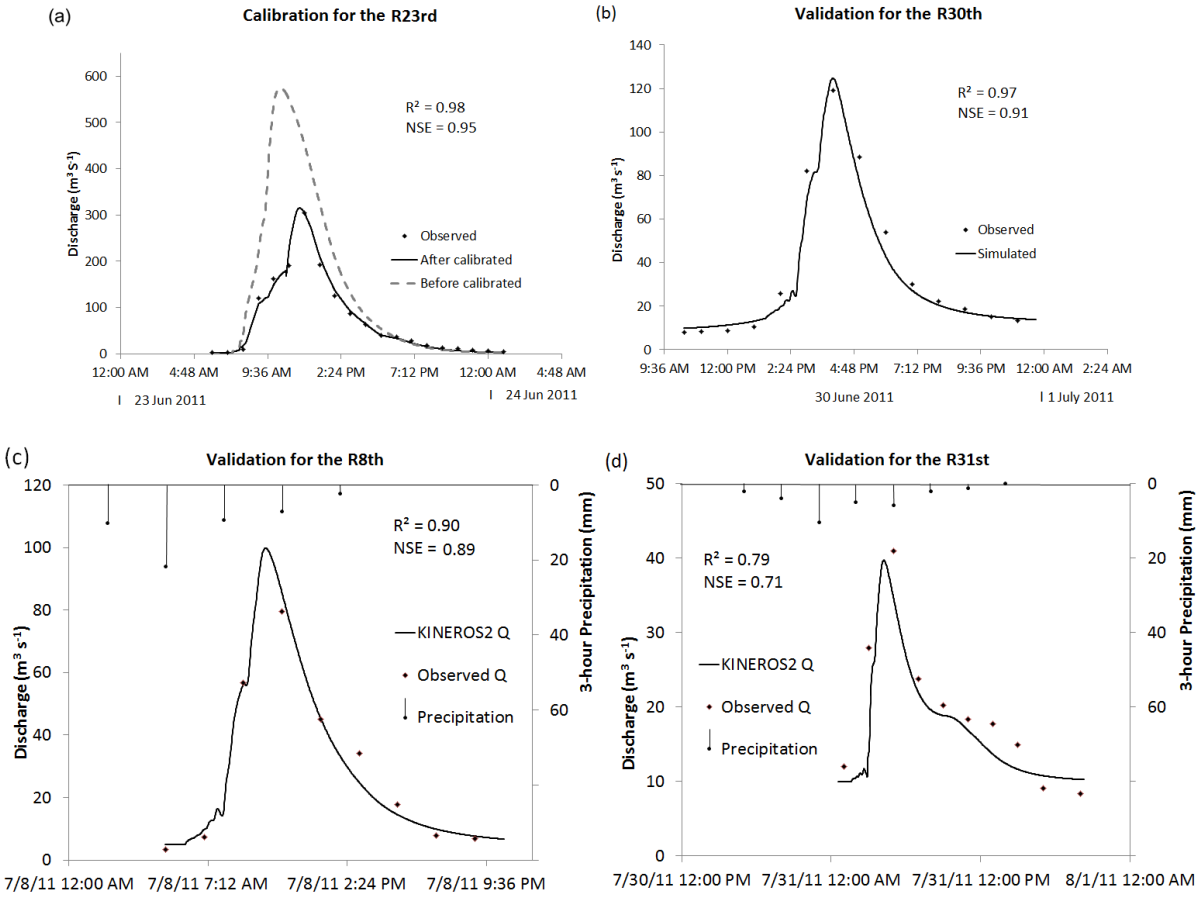

Figure 6-7. KINEROS2 results of calibration and validation:
(a) for the rain event on 23 June; (b) on 30 June; (c) on 8 July; and (d) on 31 July 2011.

The model appeared very stable in the validation stage, with the R30th illustrating great accuracy (R^2 = 0.97 and NSE = 0.91) in Fig. 6-7b. A slightly reduction of agreement between simulated and observed discharges has been found in the validation for gauged rains on 8 July 2011 with R^2 of 0.90 and NSE of 0.89 and on 30–31 July 2011 with R^2 of 0.79 and NSE of 0.71 (Figs 6-7c and d). This accurate reduction could be a result of different rain types (satellite and gauged) being used and the variation of rain intensity, as well. In general, although there was a different temporal resolution of the simulated (a minute) and recorded (an hour) data, graphically, they matched each other well.

6.4.1.2 HEC-RAS

What is interesting in the calibration hydrographs shown in Fig. 6-8a is that in the simulation phase, there was an overestimate of WL compared to the field measured data. However, the time of the peak was accurately computed. On the other hand, according to after the calibration, they match the observed information almost perfectly. However, the calibrated stage was still lower by the end of the day.

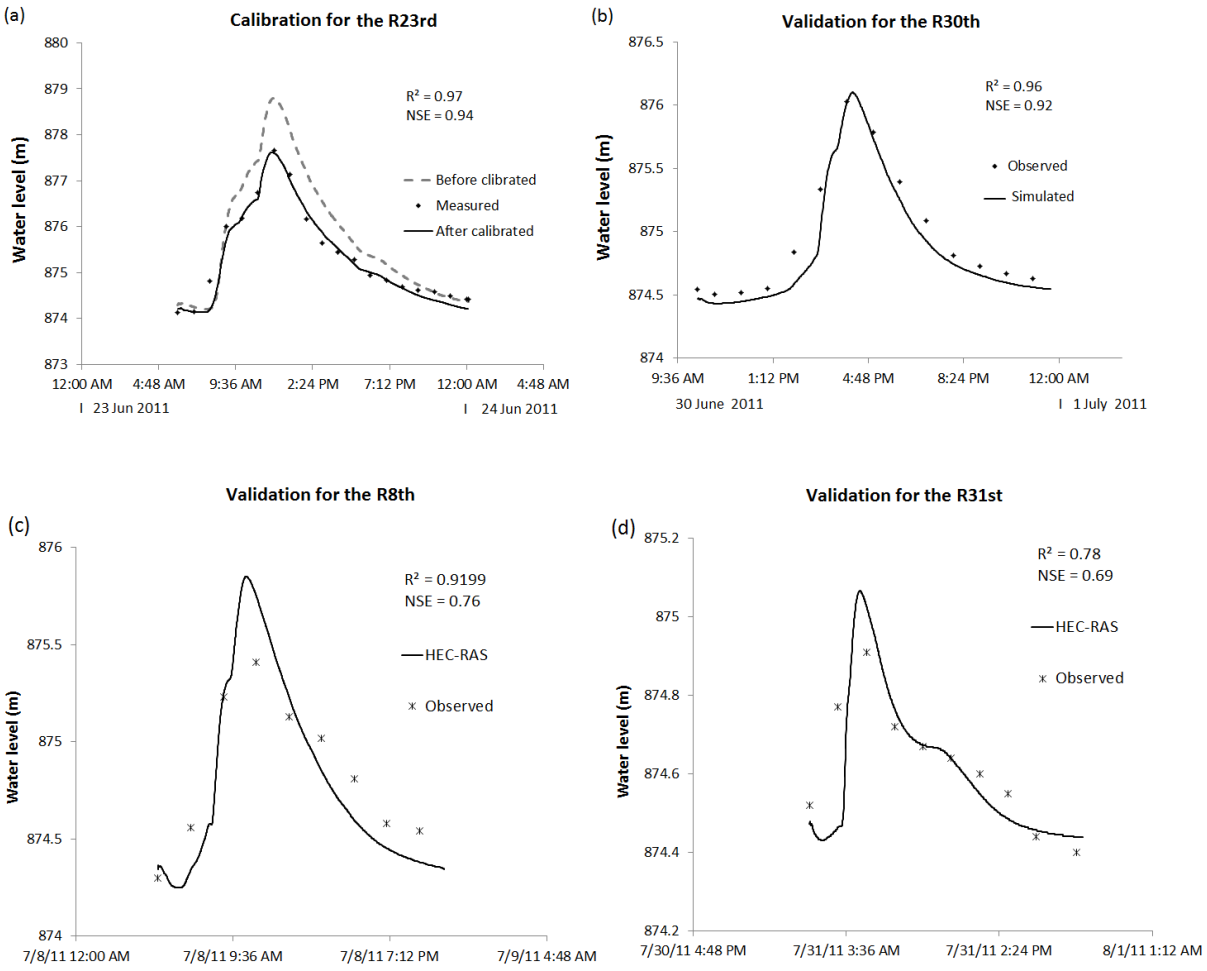

Figure 6-8. Results of calibration and validation for HEC-RAS: (a,b) using satellite based rainfall; (c,d) using gauged rainfall.

Less accurate simulation was found in the validation for the R30th with the R^2 of 0.96 and NSE of 0.92 compared to the R^2 of 0.97 and NSE of 0.94 in the model calibration. A similar scenario of water levels predicted by the HEC-RAS also can be seen in Figs 6-8c and d, with a slight decrease of both the R^2 and NSE. In addition, the model might overestimate the peaks of water levels, or this could be a result of the difference in the temporal resolution of the estimated and observed WL. Otherwise, this performance was affirmed to be a fine implementation. This dependence has also been shown in several other study results (Klimes et al., 2014; Rodriguez et al., 2008; Sarhadi et al., 2012).

6.4.2 Relationship between HEC-RAS Discharge and Water Level

Correlations between flow value and water level were modelled at the outlets (RS101) and upstream RSs (116 and 112) for the R23rd in the Nam Kim and Nam Khat reaches and the R30th in Nam Kim (no significance was found in Nam Khat). Graphically, strong relationships are shown in Fig. 6-9 for all of the RSs and the rains (all R^2 are greater than 0.9). Originally, the simulation time interval was one minute, but the rating curves were sustained for up to one hour (the lozenges and crosses) for the graphic presentation with the trends and their equations added. The outstanding ratings were the highest values of flow and stage (the peaks) compared to the elevation of the banks (the red dotted lines). Important riverbank overflows of the R23rd were found in both rivers. On the other hand, the R30th made no serious warning at the upper RS115 of Nam Kim and only a 0.5 m riverbank overflow of the water level at the outlet (RS101). The accurate estimated peaks of discharge water level are considered to be very important for determining the occurrences of FFs (Looper & Vieux, 2012; Pekarova et al., 2012; Versini, 2012) and, as such, helpful for FF warning systems (Alfieri et al., 2012). Furthermore, Carpenter et al., (1999) asserted that FFs likely happen when the river discharge (directly related to WL and FV) slightly exceed flow thresholds. They also introduced the method to calculate FF runoff thresholds on a national scale using GIS, and similar work was done by Kourgialas et al., (2012).

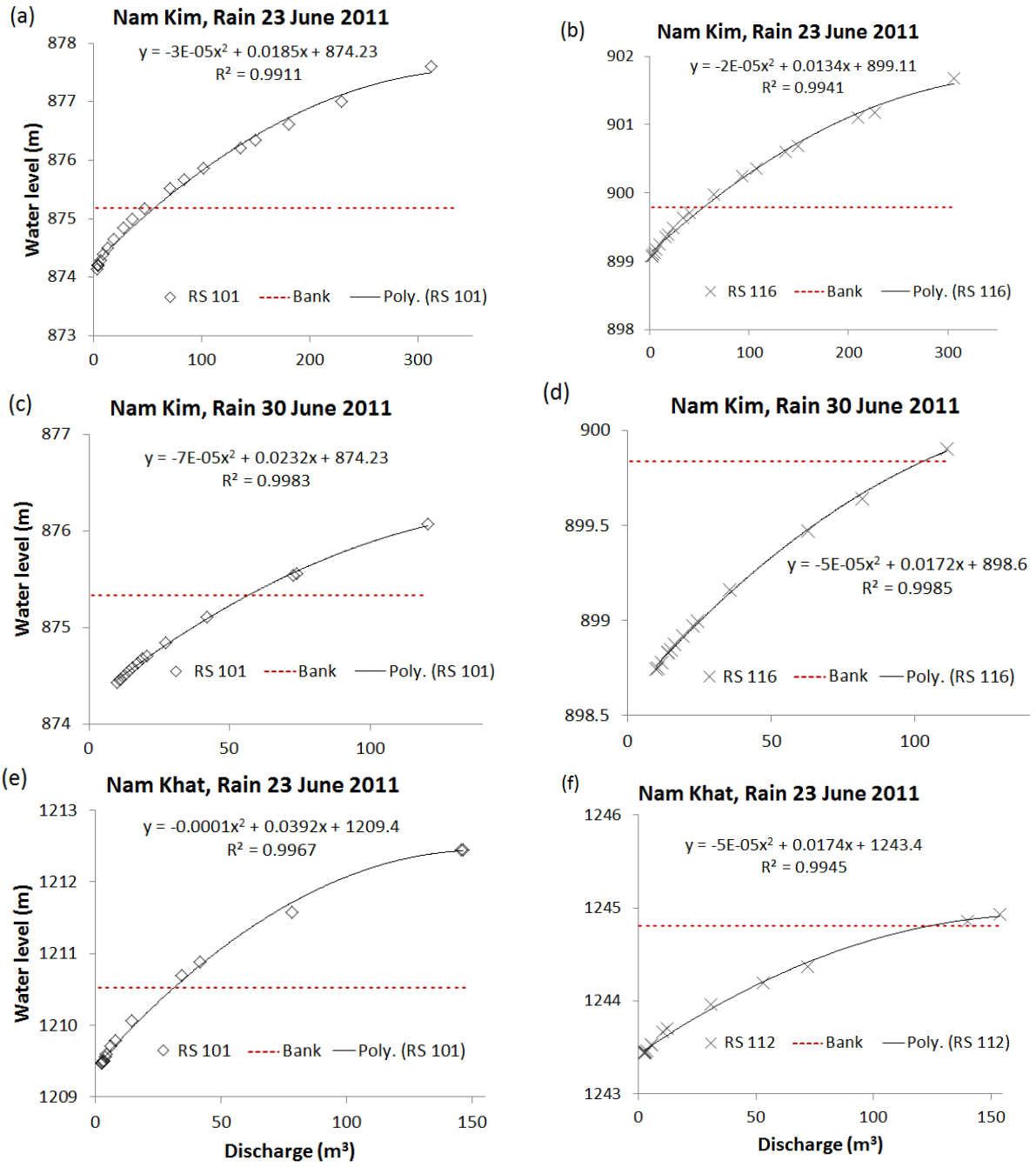

Figure 6-9. Modelled rating curves compared to river banks:
(a) for Nam Kim, the rain event on 23 June at RS 101; (b) at 116; (c) on 30 June 2011 at RS 101; (d) at 116; (e) for Nam Khat, the rain event on 23 June 2011 at RS 101; and (f) at 112. RS, river cross-section.

6.4.3 Relationship between HEC-RAS Flow Velocity, Channel Slope and Top Width

Figures 6-10a and b indicate a positive correlation (positive slope of the equations) between modelled-max FV flowing through the RSs 16 and 12 of Nam Kim and Nam Khat, respectively, for the R23rd with their slope gradients. It was indicated that the velocity varied widely ranging from 1.8 to 8 m s^{-1} in Nam Kim and from 3.1 to 4.8 m s^{-1} in the Nam Khat

reach. However, FV is not only dependent on slope (Borga et al., 2014; Masoud, 2011), but also on top width, flow area and discharge, as well. For example, the RS of Nam Kim, which had the biggest slope value, did not produce the highest FV, whereas the second biggest slope gradient did (Fig. 6-10a).

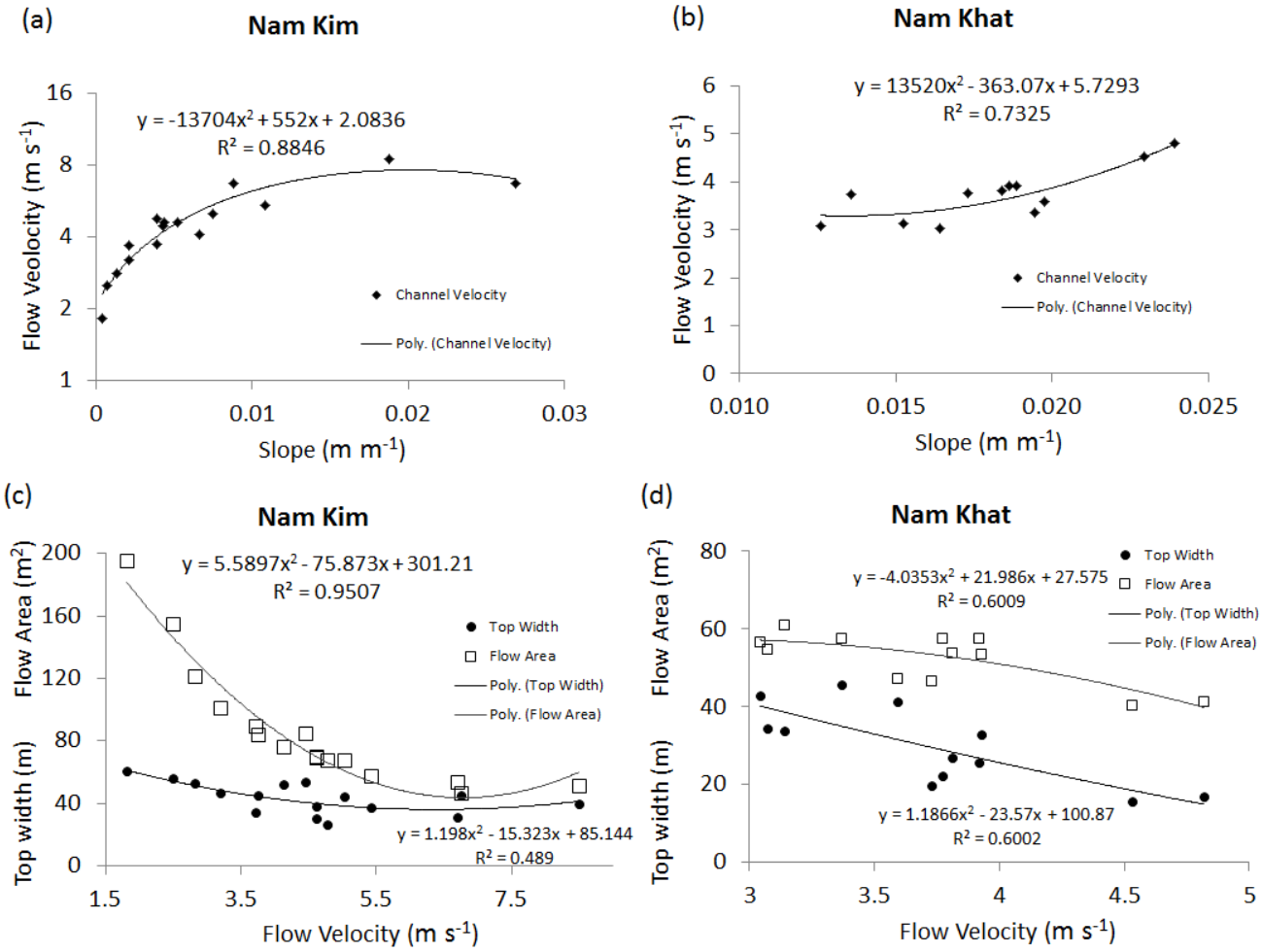

Figure 6-10. Modelled flow velocity (FV) for the rain event of 23 June 2011 (R23rd) compared to: (a) channel slope of Nam Kim; (b) of Nam Khat; (c) top width and flow area of Nam Kim; and (d) of Nam Khat.

On the other hand, Figs 6-10c and d represents an inverse proportion of FV to the river top and flow area. In addition, it appeared that the bigger and longer reach of Nam Kim had a stronger relationship (R^2 = 0.95) than the smaller and shorter one of Nam Khat (R^2 = 0.6). In fact, the total flow area is calculated from the top width and the river depth (according to Brunner (2002)), and thus, although the trends (the Polys of the Figs 6-10c and d) were similar, the FL was also driven by the river depth input using the KINEROS2 results. The better the estimated river depth by KINEROS2, the better the FV simulated by HEC-RAS would be. Altogether, the estimated FV had a close relationship to the slope, shape and

roughness (Marchi et al., 2010). This factor is believed to be important for identifying the FF (Ancona et al., 2014; Lumbroso & Gaume, 2012).

6.4.4 HEC-RAS Modelling Stream Power and Shear Stress Compared to FV

The total power of the flow, shear stress and average channel velocity values at RSs of the reaches (Table 6-3) was computed for the R23rd (133 mm of rain accumulation). The flooding event on 23 June 2011 in Nam Khat appeared to be a devastating FF with a great force of around 2000 N m^{-1} s^{-1} and shear stress of 530 N m^{-2}, particularly at RS102, 103 and 110. On the other hand, although the R23rd (144 mm of rain accumulation) in Nam Kim was a little heavier than in Nam Khat, the flow was much less violent. This trend could be explained by the linkage of the channel slope factor to flow power (El-Magd et al., 2010) (Nam Khat had larger slopes than Nam Kim; see Tables 6-1 and 2 and Figs 6-10a and b). Additionally, based on Newton's second law of motion and the shear Reynolds number (presented in (Brunner, 2002)), the streamflow and shearing forces also have a positive correlation with the channel and friction slope.

The FV distinguishes FFs from other kinds of inundation floods based on the short leading time and its spatial scale (a small scale as compared to paleoflood) (Pekarova et al., 2012; Rozalis et al., 2010; Versini, 2012), and this is directly linked to slope, as well. The maximum FVs on the channel water surface were considered to be very high, around 8.5 m s^{-1} at RS106 of Nam Kim and 4.8 m s^{-1} at RS103 of Nam Khat. However, in ungauged regions, FFs might be recognized through our realization, for example the WL and FV in Nam Kim (also see the discussion above) were higher than in Nam Khat, but no FF was identified, because no lives and property were lost there due to this event. The important information in Table 6-3 is the overview of the FV and forces distributions within the reaches of Nam Kim and Nam Khat, as they are assumed to be useful for identifying the location of FFs, as well as their degree of danger.

Table 6-3. Estimated total flow power, shear stress and average channel FV for Nam Kim and Nam Khat.

Watershed\RS		101	102	103	104	105	106	107	108	109	110	111	112	113	114	115	116
Nam Kim	Power (N	19	257	411	1794	858	1370	380	404	507	138	416	175	37	807	239	77
Nam Khat	m^{-1} s^{-1})	1131	2159	2072	865	844	995	707	1037	1500	1856	1056	1070				
Nam Kim	Shear (N	12.0	69.3	91.5	269.5	159.2	225.6	93.0	91.4	110.5	44.8	90.6	50.5	18.2	139.8	66.2	30.0
Nam Khat	m^{-2})	370.4	530.6	520.7	302.1	294.6	348.2	261.9	337.4	422.9	531.9	363.2	355.5				
Nam Kim	Velocity	1.8	3.8	4.6	6.8	5.4	8.5	4.1	4.6	5.0	3.2	4.8	3.7	2.5	6.7	4.5	2.8
Nam Khat	(m s^{-1})	3.8	4.5	4.8	3.9	3.8	3.4	3.1	3.9	3.7	3.6	3.0	3.1				

6.4.5 HEC-RAS Forecast Flood Stage and Discharge

Figure 6-11 provides the intercorrelations between the HEC-RAS discharge and stage fluctuations during the forecast time (3.5 and 5.5 days by GSM and HRM) in the Nam Kim (top graph) and in the Nam Khat (lower graph) channels at the outlets (RS101). The remarkable features were that the forecast Q and WL of the first rain (starting at 6 a.m. on 23 June 2011) corresponded well with hydrological gauged data, changing in WL proportionally well with the changes of flow values and the wrong predictions (marked by the red crosses and identified by means of a comparison with observed data in Nam Kim and the differences between GSM and HRM stage and flow in Nam Khat). Interestingly, when we compare the peaks of the two graphs, those of Nam Khat were intuitively not very natural (less smooth than expected) compared to the peaks of Nam Kim. This could be explained by the coarse temporal resolution of the forecast precipitation (6 h), which had stronger impacts on the predicted Q and WL in the smaller watershed of Nam Khat than in the bigger one of Nam Kim. When it comes to FF prediction, the question of hydrological and meteorological uncertainty is well known and has often been discussed (Montz & Gruntfest, 2002). The agreements between the GSM- and HRM-based flows presented in Fig. 6-11a were illustrated using the Nash–Sutcliffe efficiency (NSE) (Nash & Sutcliffe, 1970) for the predicted discharge of GSM and HRM rainfalls, which were 0.6 and 0.4, respectively. Based on the NSEs, using GSM precipitation appeared to perform better compared to using HRM, though satisfactory performances were observed for the first rain on 23 June 2011. On the other hand, there were some differences between forecasts and measured data for both cases on 26 June 2011 (red circle). In addition, by comparing the different uses of forecast rainfall, some false alarms and missing forecast (red crosses) likely could be seen on the graph. However, it is still difficult to conclude whether the uncertainties came from the hydrological models or from the rainfall models. We might need more calibrations for both rainfall models. The estimate accuracy could greatly benefit from rainfall data of higher quality (Looper & Vieux, 2012); possibly, rainfall from newer radar generations would be a good option. Unfortunately, there was no available on-site measured discharge and stage data for testing the forecast flow and stage for the Nam Khat reach.

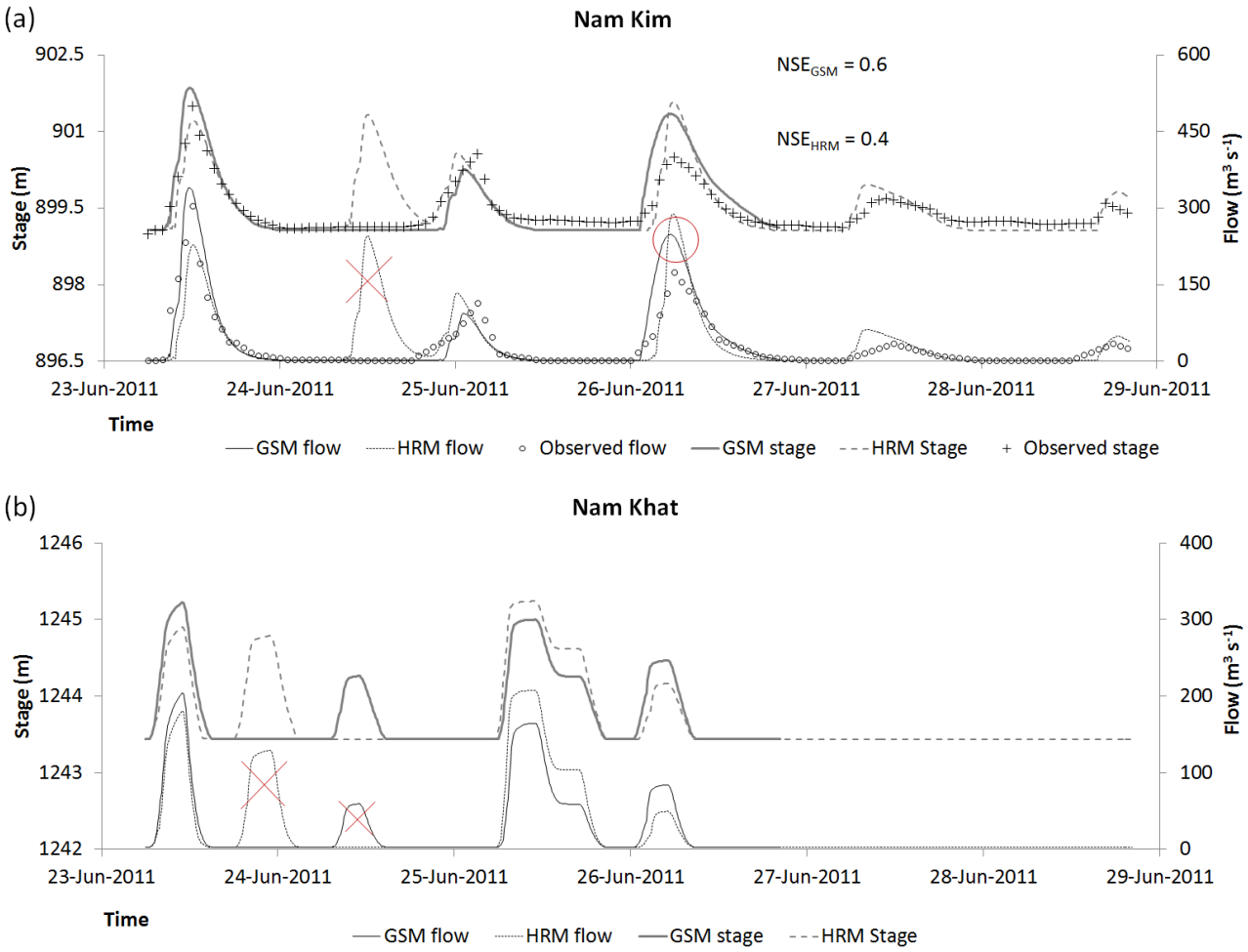

Figure 6-11. HEC-RAS forecast flow discharge and stages using observations at 6 a.m. 23 June 2011 of GSM and HRM: (a) for Nam Kim; and (b) for Nam Khat.

6.4.6 HEC-RAS Forecast Channel Velocity, Flow Power and Shearing Force

The total streamflow, shearing forces and velocity at individual RS (including interpolated RSs) were forecasted for 3.5 and 5.5 days using GSM and HRM rainfall, respectively, and the starting time of the forecast was at 6:00 on 23 June 2011. Furthermore, their relationships were presented by the power curves, equations and the R^2 values (Fig. 6-12). The shearing power varied greatly from 10 to 350 in Nam Kim using GSM precipitation (the peaks were a little lower compared to using HRM) and from about 220 to 750 N m^{-2} in Nam Khat (for both GSM and HRM). Similarly, the flows were very powerful (ranging from 50 to 2500 in Nam Kim, from 650 to 3400 N m^{-1} s^{-1}), and there was not much difference between using GSM and HRM rainfall. The interesting point is that the strong correlations between streamflow power and shearing force were explicitly shown for all of the cases (all $R^2 \approx 0.99$; Figs 6-12a, c, e and g).

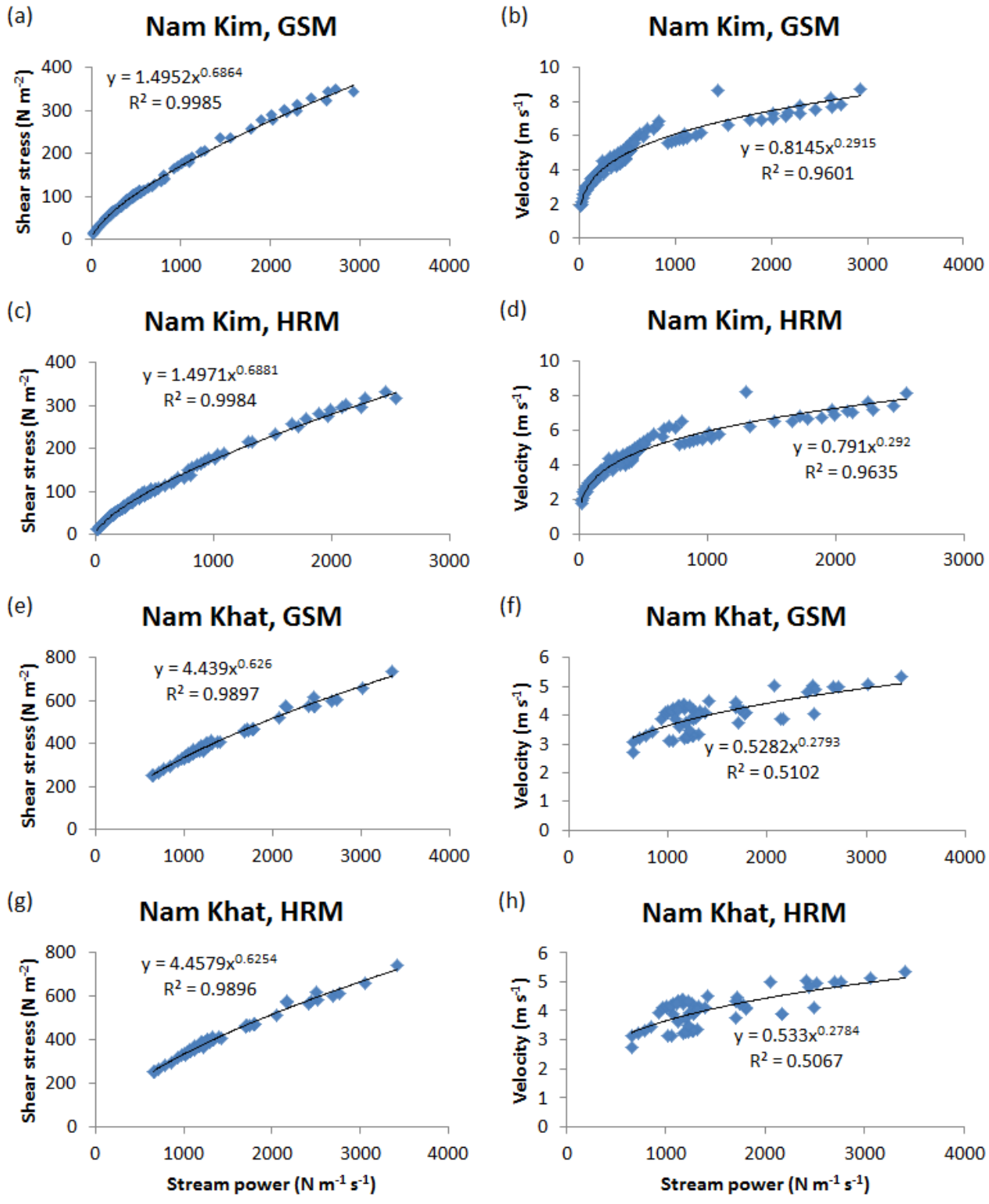

Figure 6-12. Forecasted stream power in the Nam Kim channel compared to: (a) Shear stress using the GSM rainfall; (b) velocity using the GSM rainfall; (c) shear stress employing the HRM rainfall; and (d) velocity using the HRM rainfall. Forecasted stream power in the Nam Khat channel compared to. (e) Shear stress employing the GSM rainfall; (f) velocity using the GSM rainfall; (g) shear stress using the HRM rainfall; and (h) velocity employing the HRM rainfall.

The mean streamflow speed was also predicted for all of the RSs of the two streams using GSM and HRM rainfall and scattered with the flow forces (Figs 6-12b, d, f and h). The flow speeds reached approximately 8 m s^{-1} at some RSs in Nam Kim and about 5 m s^{-1} in Nam Khat. Better velocity-stream power linkages were found with the prediction for Nam Kim (R^2 ≈ 0.96), and there was less connection for Nam Khat (R^2 ≈ 0.51). However, the FV values were more important when predicted at high speed and might exceed the FF threshold and cause flash flooding, as Vinet (2008) asserted, namely that FFs are likely to occur when the flow velocities are several meters per second.

6.5 Summary and Conclusions

The findings of the study show that by coupling the two models, both the estimated water levels and discharge, using satellite and forecast rainfall by KINEROS2 and HEC-RAS agreed well with the field-measured data. The merits of the models were verified not only by the validations, but also by the precise, applicable outputs for FF prediction, such as peak discharge, flow stage, velocity and power. By using the GSM and HRM forecast rainfall, the models produced some errors in the prediction phase. We assert that the models performed well, but the error source likely came from the forecast rainfall data. Therefore, we suggest an improvement in the accuracy of GSM and HRM production for the aim of providing an FF warning system with accurate rainfall. Although total time (about one hour) of the hydrological and NWP model calculations was still sufficient for providing timely forecasted Q, in the near future, it will be quickly improved due to the advancement of information technology. Additionally, combining the two models could accumulate errors from the models. Especially this problem is significant when the first model has large uncertainties. However, as hydrological models require various data sources for the inputs, this sources of uncertainty are important, as well.

We also found close relationships between river geometry (slope, top width and flow area) and hydrological responses and between those of hydraulic behaviour (velocity, streamflow power and shearing forces). From the result analyses, we found reasonable outcomes for the ungauged watershed of Nam Khat using the so-called traditional concept of spatial proximity invented by Blöschl (2005). This is meaningful for the enlargement of this approach to other poorly-gauged and ungauged watersheds in North Vietnam. Especially, FFs could occur in any watershed from small to large, even in subwatersheds, and usually, not all watersheds are gauged. This approach of proximity was supported by some similar studies of Makungo et al., (2010), Servat and Dezetter (1993) and Boughton and Chiew (2007).

6.6 References

Abderrezzak, K. E., Paquier, A., & Mignot, E. (2009). Modelling flash flood propagation in urban areas using a two-dimensional numerical model. *Natural Hazards, 50*(3), 433-460. doi: DOI 10.1007/s11069-008-9300-0

Ahmed M. Y, Biswajeet P, & Abdallah M. H. (2010). Flash flood risk estimation along the St. Katherine road, southern Sinai, Egypt using GIS based morphometry and satellite imagery. *Environ Earth Sci 62*:611–623.

Alfieri, L., Thielen, J., & Pappenberger, F. (2012). Ensemble hydro-meteorological simulation for flash flood early detection in southern Switzerland. *Journal of Hydrology, 424*, 143-153. doi: DOI 10.1016/j.jhydrol.2011.12.038

Ancona, M., Corradi, N., Dellacasa, A., Delzanno, G., Dugelay, J. L., Federici, B., . . . Zolezzi, G. (2014). On the Design of an Intelligent Sensor Network for Flash Flood Monitoring, Diagnosis and Management in Urban Areas Position Paper. *Procedia Computer Science, 32*(0), 941-946. doi: http://dx.doi.org/10.1016/j.procs.2014.05.515

Anh, P. T. Q., Gomi, T., MacDonald, L. H., Mizugaki, S., Van Khoa, P., & Furuichi, T. (2014). Linkages among land use, macronutrient levels, and soil erosion in northern Vietnam: A plot-scale study. *Geoderma, 232–234*(0), 352-362. doi: http://dx.doi.org/10.1016/j.geoderma.2014.05.011

Austin, G. S. (2002). Advanced hydrologic prediction services – Concept of services and operations. *Report U.S. Department of Commerce* – NOAA – NWS.

Blöschl, G. (2005). Rainfall–runoff modelling of ungauged catchments. *In: Anderson, M.G.E. (Ed.), Encyclopedia of Hydrological Sciences. John Wiley & Sons, Chichester,* pp. 2061–2080.

Borga, M., Stoffel, M., Marchi, L., Marra, F., & Jakob, M. (2014). Hydrogeomorphic response to extreme rainfall in headwater systems: Flash floods and debris flows. *Journal of Hydrology, 518, Part B,* 194-205. doi: http://dx.doi.org/10.1016/j.jhydrol.2014.05.022

Boughton, W., & Chiew, F. (2007). Estimating runoff in ungauged catchments from rainfall, PET and the AWBM model. *Environmental Modelling & Software, 22*(4), 476-487. doi: http://dx.doi.org/10.1016/j.envsoft.2006.01.009

Brunner, G. W. (2002). River Analysis System: Hydraulic Reference Manual. *US Army Corps of Engineers Hydrologic Engineering Center, Davis, CA.*, Version 3.1 November 2002 (Approved for Public Release. Distribution Unlimited. CPD-69).

Brunner, G. W. (2010). HEC-RAS, River Analysis System Hydraulic Reference Manual. *Hydrological Engineering Center, US Army Corps of Engineers, Davis, CA, Version 4.1 January 2010* (Approved for Public Release. Distribution Unlimited. CPD-69).

Carpenter, T. M., Sperfslage, J. A., Georgakakos, K. P., Sweeney, T., & Fread, D. L. (1999). National threshold runoff estimation utilizing GIS in support of operational flash flood warning systems. *Journal of Hydrology, 224*(1–2), 21-44. doi: 10.1016/s0022-1694(99)00115-8

El-Magd, I. A., Hermas, E., & Bastawesy, M. E. (2010). GIS-modelling of the spatial variability of flash flood hazard in Abu Dabbab catchment, Red Sea Region, Egypt. *The Egyptian Journal of Remote Sensing and Space Science, 13*(1), 81-88. doi: 10.1016/j.ejrs.2010.07.010

Estupina-Borrell ,V., D. D., and R. Ababou. (2006). Flash flood modeling with the MARINE hydrological distributed model. *Hydrology and Earth System Sciences. Discuss., 3*, 3397–3438

Georgakakos, K. P. (1986). On the design of national, real-time warning systems with capability for site-specific, flash-flood forecasts. *Bulletin of the American Meteorological Society, 67*(10)(1233–1239).

Gupta, H. 2006 Development of a site-specific flash flood forecasting model for the Western Region- Final Report for COMET proposal. *University of Arizona: Tucson, AZ, USA.* Available online: http://www.comet.ucar.edu/outreach/abstract_final/0344674_AZ.pdf (accessed on 20th November 2014)

Horritt, M. S., & Bates, P. D. (2002). Evaluation of 1D and 2D numerical models for predicting river flood inundation. *Journal of Hydrology, 268*(1–4), 87-99. doi: http://dx.doi.org/10.1016/S0022-1694(02)00121-X

Javelle, P., Fouchier, C., Arnaud, P., & Lavabre, J. (2010). Flash flood warning at ungauged locations using radar rainfall and antecedent soil moisture estimations. *Journal of Hydrology, 394*(1–2), 267-274. doi: http://dx.doi.org/10.1016/j.jhydrol.2010.03.032

Klimes, J., Benesova, M., Vilimek, V., Bouska, P., & Rapre, A. C. (2014). The reconstruction of a glacial lake outburst flood using HEC-RAS and its significance for future hazard assessments: an example from Lake 513 in the Cordillera Blanca, Peru. *Natural Hazards, 71*(3), 1617-1638. doi: DOI 10.1007/s11069-013-0968-4

Kourgialas, N. N., Karatzas, G. P., & Nikolaidis, N. P. (2012). Development of a thresholds approach for real-time flash flood prediction in complex geomorphological river basins. *Hydrological Processes, 26*(10), 1478-1494. doi: Doi 10.1002/Hyp.8272

Krishnamurti, T. N., Bedi, H. S., Hardiker, V. M., & Ramaswamy, L. (2006). An Introduction to Global Spectral Modeling. 2nd Revised and Enlarged Edition, *Springer, Atmospheric and Oceanographic Sciences Library*.

Krzysztofowicz, R. (2014). Probabilistic flood forecast: Exact and approximate predictive distributions. *Journal of Hydrology, 517*(0), 643-651. doi: http://dx.doi.org/10.1016/j.jhydrol.2014.04.050

Liu, W. C., & Wu, C. Y. (2011). Flash flood routing modeling for levee-breaks and overbank flows due to typhoon events in a complicated river system. *Natural Hazards, 58*(3), 1057-1076. doi: DOI 10.1007/s11069-010-9711-6

Looper, J. P., & Vieux, B. E. (2012). An assessment of distributed flash flood forecasting accuracy using radar and rain gauge input for a physics-based distributed hydrologic model. *Journal of Hydrology, 412*, 114-132. doi: DOI 10.1016/j.jhydrol.2011.05.046

Lumbroso, D., & Gaume, E. (2012). Reducing the uncertainty in indirect estimates of extreme flash flood discharges. *Journal of Hydrology, 414–415*(0), 16-30. doi: http://dx.doi.org/10.1016/j.jhydrol.2011.08.048

Majewski, D. 2009 HRM – User's Guide for the HRM with the SSO scheme (Vrs. 2.5 and higher). *Deutscher Wetterdienst, Press and Public Relations:* Offenbach, Germany. Available online: http://www.dwd.de/SharedDocs/downloads/DE/modelldokumentationen/nwv/hrm/HRM_users_guide.pdf?__blob=publicationFile&v=2 (accessed on 4th November 2014)

Makungo, R., Odiyo, J. O., Ndiritu, J. G., & Mwaka, B. (2010). Rainfall–runoff modelling approach for ungauged catchments: A case study of Nzhelele River sub-quaternary

catchment. *Physics and Chemistry of the Earth, Parts A/B/C, 35*(13–14), 596-607. doi: http://dx.doi.org/10.1016/j.pce.2010.08.001

Marchi, L., Borga, M., Preciso, E., & Gaume, E. (2010). Characterisation of selected extreme flash floods in Europe and implications for flood risk management. *Journal of Hydrology, 394*(1–2), 118-133. doi: http://dx.doi.org/10.1016/j.jhydrol.2010.07.017

Masoud, A. A. (2011). Runoff modeling of the wadi systems for estimating flash flood and groundwater recharge potential in Southern Sinai, Egypt. *Arabian Journal of Geosciences, 4*(5-6), 785-801. doi: DOI 10.1007/s12517-009-0090-9

Montz, B. E., & Gruntfest, E. (2002). Flash flood mitigation: recommendations for research and applications. *Global Environmental Change Part B: Environmental Hazards, 4*(1), 15-22. doi: 10.1016/s1464-2867(02)00011-6

Morin, E., Jacoby, Y., Navon, S., & Bet-Halachmi, E. (2009). Towards flash-flood prediction in the dry Dead Sea region utilizing radar rainfall information. *Advances in Water Resources, 32*(7), 1066-1076. doi: DOI 10.1016/j.advwatres.2008.11.011

Mudd, S. M. (2006). Investigation of the hydrodynamics of flash floods in ephemeral channels: Scaling analysis and simulation using a shock-capturing flow model incorporating the effects of transmission losses. *Journal of Hydrology, 324*(1–4), 65-79. doi: 10.1016/j.jhydrol.2005.09.012

Nash, J. E., & Sutcliffe, J. V. (1970). River flow forecasting through conceptual models 1: a discussion of principles. *Journal of Hydrology 10 (3), 282–290.*

Naulin, J. P., Payrastre, O., & Gaume, E. (2013). Spatially distributed flood forecasting in flash flood prone areas: Application to road network supervision in Southern France. *Journal of Hydrology, 486*(0), 88-99. doi: http://dx.doi.org/10.1016/j.jhydrol.2013.01.044

NCHMF. (2011). Vietnamese National Center for Hydrological Forecasting. Available online:http://www.nchmf.gov.vn/web/vi-VN/71/29/45/Default.aspx. (accessed on 7 March 2014).

Nguyen Van Tai, Kim Thi Tuy Ngoc, Phan Tuan Hung, Le Thi Le Quyen, Nguyen Thi Ngoc Anh, Anna Stabrawa, . . . Cuong, N. M. (2009). Vietnam Assessment Report on Climate Change *Institute of Strategy and Policy on natural resources and environment, Viet Nam Van hoa - Thong tin Publishing House: 318-2009/CXB/16-28/VHTT*, 112-115.

Norbiato, D., Borga, M., & Dinale, R. (2009). Flash flood warning in ungauged basins by use of the flash flood guidance and model-based runoff thresholds. *Meteorological Applications, 16*(1), 65-75. doi: Doi 10.1002/Met.126

Ntelekos, A. A., Georgakakos, K. P., & Krajewski, W. F. (2006). On the Uncertainties of Flash Flood Guidance: Toward Probabilistic Forecasting of Flash Floods. *Journal of Hydrometeorology, 7*(5), 896-915. doi: 10.1175/jhm529.1

Pekarova, P., Svoboda, A., Miklanek, P., Skoda, P., Halmova, D., & Pekar, J. (2012). Estimating Flash Flood Peak Discharge in Gidra and Parna Basin: Case Study for the 7-8 June 2011 Flood. *Journal of Hydrology and Hydromechanics, 60*(3), 206-216. doi: DOI 10.2478/v10098-012-0018-z

Quintero, F., Sempere-Torres, D., Berenguer, M., & Baltas, E. (2012). A scenario-incorporating analysis of the propagation of uncertainty to flash flood simulations. *Journal of Hydrology, 460*, 90-102. doi: DOI 10.1016/j.jhydrol.2012.06.045

Ranzi, R., Le, T. H., & Rulli, M. C. (2012). A RUSLE approach to model suspended sediment load in the Lo river (Vietnam): Effects of reservoirs and land use changes.

Journal of Hydrology, 422–423(0), 17-29. doi: http://dx.doi.org/10.1016/j.jhydrol.2011.12.009

Reed, S., Schaake, J., & Zhang, Z. Y. (2007). A distributed hydrologic model and threshold frequency-based method for flash flood forecasting at ungauged locations. *Journal of Hydrology, 337*(3-4), 402-420. doi: DOI 10.1016/j.jhydrol.2007.02.015

Rodriguez, L. B., Cello, P. A., Vionnet, C. A., & Goodrich, D. (2008). Fully conservative coupling of HEC-RAS with MODFLOW to simulate stream–aquifer interactions in a drainage basin. *Journal of Hydrology, 353*(1–2), 129-142. doi: http://dx.doi.org/10.1016/j.jhydrol.2008.02.002

Rozalis, S., Morin, E., Yair, Y., & Price, C. (2010). Flash flood prediction using an uncalibrated hydrological model and radar rainfall data in a Mediterranean watershed under changing hydrological conditions. *Journal of Hydrology, 394*(1-2), 245-255. doi: DOI 10.1016/j.jhydrol.2010.03.021

Ruiz-Villanueva, V., Díez-Herrero, A., Stoffel, M., Bollschweiler, M., Bodoque, J. M., & Ballesteros, J. A. (2010). Dendrogeomorphic analysis of flash floods in a small ungauged mountain catchment (Central Spain). *Geomorphology, 118*(3–4), 383-392. doi: 10.1016/j.geomorph.2010.02.006

Sarhadi, A., Soltani, S., & Modarres, R. (2012). Probabilistic flood inundation mapping of ungauged rivers: Linking GIS techniques and frequency analysis. *Journal of Hydrology, 458–459*(0), 68-86. doi: http://dx.doi.org/10.1016/j.jhydrol.2012.06.039

Seo, D., Lakhankar, T., Mejia, J., Cosgrove, B. & Khanbilvardi, R. 2012 Evaluation of Operational National Weather Service Gridded Flash Flood Guidance Over the Arkansas Red River Basin. *Journal of the American Water Resources Association (JAWRA) 1-12*. DOI: 10.1111/jawr.12087.

Servat, E., & Dezetter, A. (1993). Rainfall-runoff modelling and water resources assessment in northwestern Ivory Coast. Tentative extension to ungauged catchments. *Journal of Hydrology, 148*(1–4), 231-248. doi: http://dx.doi.org/10.1016/0022-1694(93)90262-8

Shames, I. H. (1962). Mechanics of Fluids. *McGraw-Hill Book Company, NY*.

Smith, P. L., Ana Barros, v. Chandrasekar, Greg Forbes, Eve Gruntfest, Witold Krajewski, . . . Galinis, E. (2005). Flash flood forecasting over complex terrain With An Assessment Of The Sulphur Mountain NEXRAD In Southern California. *The National Academies Press, DC 20001; 800*-624-6242.

Smith, R. E., Goodrich, D. C., & Unkrich, C. L. (1999). Simulation of selected events on the Catsop catchment by KINEROS2: A report for the GCTE conference on catchment scale erosion models. *CATENA, 37*(3–4), 457-475. doi: http://dx.doi.org/10.1016/S0341-8162(99)00033-8

Smith, R. E., Goodrich, D. C., Woolhiser, D. A., & Unkrich, C. L. (1995). KINEROS – A kinematic runoff and erosion model; Chapter 20 in V.P. Singh (editor), Computer Models of Watershed Hydrology. *Water Resources Publications, Highlands Ranch, Colorado, 1130 pp*.

Snell, S., & Gregory, K. (2002). A Flash Flood Prediction Model for Rural and Urban Basins in New Mexico. Technical Complete Report. Account Number 01345694. *Department of Geography University of NewMexico*.

Tao, J., & Barros, A. P. (2013). Prospects for flash flood forecasting in mountainous regions – An investigation of Tropical Storm Fay in the Southern Appalachians. *Journal of Hydrology, 506*(0), 69-89. doi: http://dx.doi.org/10.1016/j.jhydrol.2013.02.052

Unkrich, C. L., Michael Schaffner, Chad Kahler, David C. Peter Troch, Hoshin Gupta, Thorsten Wagener, & Yatheendradas, S. (2010). Real-time Flash Flood Forecasting Using Weather Radar and Distributed Rainfall-Runoff Model. *2nd Joint Federal Interagency Conference, Las Vegas, NV*.

Versini, P. A. (2012). Use of radar rainfall estimates and forecasts to prevent flash flood in real time by using a road inundation warning system. *Journal of Hydrology, 416*, 157-170. doi: DOI 10.1016/j.jhydrol.2011.11.048

Villarini, G., Krajewski, W. F., Ntelekos, A. A., Georgakakos, K. P., & Smith, J. A. (2010). Towards probabilistic forecasting of flash floods The combined effects of uncertainty in radar-rainfall and flash flood guidance. *Journal of Hydrology, 394*(1-2), 275-284. doi: DOI 10.1016/j.jhydrol.2010.02.014

Vincendon, B., Ducrocq, V., Dierer, S., Kotroni, V., Le Lay, M., Milelli, M., . . . Steiner, P. (2009). Flash flood forecasting within the PREVIEW project: value of high-resolution hydrometeorological coupled forecast. *Meteorology and Atmospheric Physics, 103*(1-4), 115-125. doi: DOI 10.1007/s00703-008-0315-6

Vinet, F. (2008). Geographical analysis of damage due to flash floods in southern France: The cases of 12–13 November 1999 and 8–9 September 2002. *Applied Geography, 28*(4), 323-336. doi: 10.1016/j.apgeog.2008.02.007

NIAPP. (1996). Yen Bai Soil Map Report. National Institute of Agricultural Planning and Projection (NIAPP)-*Centre for Resources and Environment*, NIAPP: Hanoi, Vietnam.

Volkmann, T. H. M., Lyon, S. W., Gupta, H. V., & Troch, P. A. (2010). Multicriteria design of rain gauge networks for flash flood prediction in semiarid catchments with complex terrain. *Water Resources Research, 46*. doi: Artn W11554. Doi: 10.1029/2010wr009145

Wardah, T., Abu Bakar, S. H., Bardossy, A., & Maznorizan, M. (2008). Use of geostationary meteorological satellite images in convective rain estimation for flash-flood forecasting. *Journal of Hydrology, 356*(3-4), 283-298. doi: DOI 10.1016/j.jhydrol.2008.04.015

Woolhiser, D. A., Smith, R. E., & Goodrich, D. C. (1990). KINEROS, A Kinematic Runoff and Erosion Model. Documentation and User Manual. *ARS-77. USDA, ARS, Washington, DC*.

Yates, D. N., Warner, T. T., & Leavesley, G. H. (2000). Prediction of a flash flood in complex terrain. Part II: A comparison of flood discharge simulations using rainfall input from radar, a dynamic model, and an automated algorithmic system. *Journal of Applied Meteorology, 39*(6), 815-825. doi: Doi 10.1175/1520-0450(2000)039<0815:Poaffi>2.0.Co;2

Yatheendradas, S. W., T. Gupta, H. Unkrich, C. Goodrich, D. Schaffner, M. Stewart, A. (2008). Understanding uncertainty in distributed flash flood forecasting for semiarid regions. *Water Resources Research, 44*(5). Doi 10.1029/2007wr005940

Younis, J., S. A., and J. Thielen. (2008). The benefit of high-resolution operational weather forecasts for flash flood warning. *Hydrology and Earth System Sciences, 12*, 1039–1051.

Zanon, F., Borga, M., Zoccatelli, D., Marchi, L., Gaume, E., Bonnifait, L., & Delrieu, G. (2010). Hydrological analysis of a flash flood across a climatic and geologic gradient: The September 18, 2007 event in Western Slovenia. *Journal of Hydrology, 394*(1–2), 182-197. doi: 10.1016/j.jhydrol.2010.08.020

CHAPTER 7

Modelling Surface Runoff and Evapotranspiration Using SWAT and BEACH for a Tropical Watershed in North Vietnam, Compared to MODIS Products[8]

"Just as human activity is upsetting Earth's carbon cycle, our actions are altering the water cycle."

-David Suzuki

Abstract

Accurate estimation of surface runoff (Q) and evapotranspiration (ET) is a challenging task but an important research topic because both Q and ET play vital roles in the study of the hydrological cycle, of climate change, water resources, and flood management etc. In this paper we will present the modelling method to estimate the daily Q and ET for a medium-sized watershed in the tropical region of the North of Vietnam using the Soil and Water Assessment Tool (SWAT) and Bridging Event and Continuous Hydrological (BEACH) models. The models were calibrated and validated for the river discharge for SWAT and evaporation (E) for BEACH in a 12-year period from 2001 to 2012. The simulated ETs by the models were compared with the satellite-based ET of MODIS products. Our simulation results show that the SWAT and BEACH models are capable of satisfactorily reproducing (with the NSE > 0.62 and R^2 > 0.78) the stream-gauged river discharge and the observed E, respectively. Daily ET varied from 0.3 to 14 mm day^{-1} and was highest from May to August and lowest from December to March. Although the monthly and yearly MODIS ETs were slightly higher than those of SWAT and BEACH, a strong relationship between them was found with a standard deviation ranging from three to 40 mm. A light decrease of ET values in the 12 years can be seen in the result analyses; however a longer simulation time might be needed to ensure this trend.

[8] This paper is published on 17th November 2015 in the International Journal of Advanced Remote Sensing and GIS, Cloud Publications

http://technical.cloud-journals.com/index.php/IJARSG/article/view/Tech-493

7.1 Introductions

Currently, there has been growing interest in hydrological connectivity processes (Lopez-Vicente et al., 2013) such as surface runoff (Q) and evapotranspiration (ET) (Boegh et al., 2009; Camporese et al., 2014; Dias et al., 2015 and Liu et al., 2012). Both these two processes are significant components in the water balance circle and linked to numerous environmental problems, for example excessive rainfall runoff causes soil erosion and water pollution (Lenzi & DiLuzio, 1997; Marttila & Klove, 2010) land degradation (Mchunu & Chaplot, 2012), flooding (Rogger et al., 2012; Tripathi et al., 2014) etc. and changing ET might be the result of changes in weather (Petković et al., 2015), particularly in surface soil moisture and temperature (Almorox et al., 2015; Sun et al., 2012) and land cover changes (Dias et al., 2015). Surface runoff is defined as that part of the rainfall which is not observed by soil infiltration and which flows overland called overland-flow flowing in streams to the sea, all of which is dependent on the amount of rainfall, rainfall intensity and infiltration capacity (Horton, 1933). The evapotranspiration is considered as the total water loss to the atmosphere (Sawano et al., 2015) by evaporation both from the vegetative and non-vegetative surfaces and transpiration from plants (Kisi et al., 2015; Petković et al., 2015). Since the *in situ* measurements of surface runoff and ET for large areas are time consuming, costly and extremely difficult (Camporese et al., 2014), indirect estimations of Q and ET using the modelling approach and satellite-based products are necessary (Velpuri et al., 2013), particularly for sparse data-available areas such as in northern Vietnam.

Although many studies have been conducted using the modelling method at watershed scale for estimating Q, to name some of them (Casali et al., 2008; Guber et al., 2014; Linde et al., 2008; Tibebe, 2011) employing the SWAT, KINEROS2 and the HBV and VIC models, little attention has been paid to tropical regions using the SWAT model such as (Fukunaga et al., 2015 and Ndomba et al., 2008) and for regions of Vietnam (Vu et al., 2012). Similarly with studies on surface runoff, there is a large amount of literature available on research into ET including direct or *in situ* measurement (Connan et al., 2015; Howell et al., 2015) and indirect methods (referring to modelling (Camporese et al., 2014; Kisi et al., 2015) and using satellite technology (Consoli & Vanella, 2014; Tian et al., 2013)), from watershed/catchment scales (Jaksa & Sridhar, 2015; Sun et al., 2009) to the global scale (Hu et al., 2015; Mu et al., 2007a and 2011) and others. Surprisingly, despite many scientific works having been conducted on ET elsewhere in the world as mentioned above, few or even no previous studies on that topic were found for the case study in Yen Bai province or in North Vietnam.

As mentioned at the very beginning, the importance of surface runoff and ET information and the lack of Q and ET literature on the study region have motivated the study objective of modelling and estimating that information. In addition, data scarcity has been reduced thanks to more ground-based hydrologic and meteorological stations being established in the region (for model calibration and validation). In addition satellite data (MODIS, Landsat etc.) have become more available to reduce the lack of temporal and spatial data in ungauged regions (Westerhoff, 2015) and to be used for model validation (Immerzeel & Droogers, 2008) as well. The interesting point is that both large-scale *in situ* Q and ET measurements are difficult, expensive and time consuming (Almorox et al., 2015) but the modelling approach could be appropriate to deal with this challenge. Finally, the study results might be helpful for research into other fields such as Q information for flood, ground/surface water management and ET for cropping irrigation, drought detection and management etc., particularly rapid change in climate, water and the increasing population have all become a great concern both for the environment and society (Mu et al., 2007a).

In summary five main outcomes of expertise could be identified to cope with this study topic: (i) calibrating and validating daily river discharge and evaporation for the SWAT and BEACH model respectively, (ii) estimating daily ET by the two models, (iii) comparing SWAT, BEACH discharge and with observed data, (iv) comparing monthly ETs and analysing their trend in the 2001-2012 period and, (v) mapping SWAT and MODIS annual accumulative ET. Our results elucidate the abilities of the two models to produce surface runoff and evaporation closely to field measured data, the strong relationships between SWAT, BEACH and MODIS ET and a slightly decreasing trend of ET in the simulating time.

7.2 Study Site

The study watershed is Nam Kim located in western Yen Bai province (Fig. 7-1) has its centre coordinate as104°07'51.3"E and 21°49'10.7"N. The mean elevation is 1571 m above sea level and the area of the watershed is about 268 km^2. The main land use land covers (LULC) are forest, agricultural (rice) and shrub lands with contributions of 40, 33 and 23% of the watershed area, respectively. The yearly mean air temperature varies from 20 to 24 ^oC (Nguyen Van Tai et al., 2009) and annual mean precipitation is 1695 mm (2001-2012 statistic from the rain gauge presented on the map). The dominant soils are Humic Ferralsols, Humic Acrisols and Humic Alisols and the cropping system is mainly rice and cassava harvested twice a year in May and October. There are three gauges established for measurements of rainfall, discharge and other meteorological data.

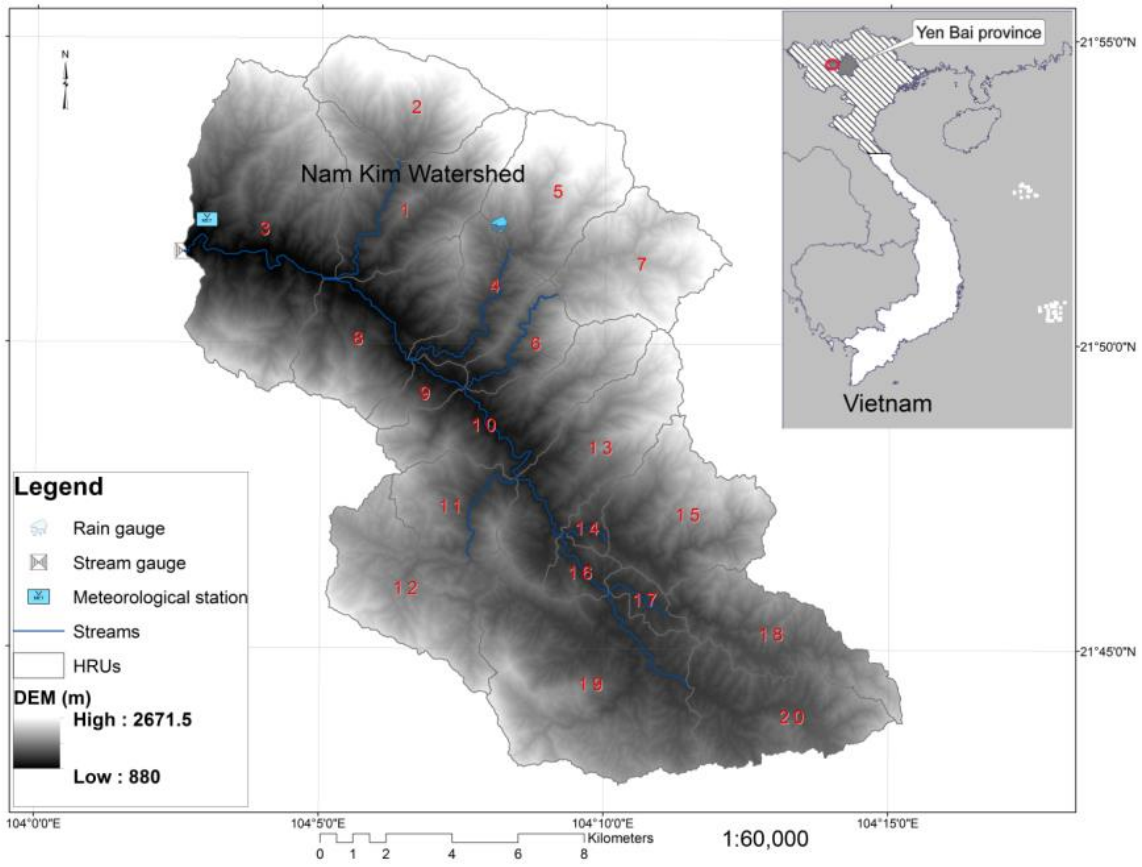

Figure 7-1. Map of site study and stations for data collection.

7.3 Method and Materials

7.3.1 The Soil and Water Assessment Tool (SWAT)

SWAT is a physically based, continuous model and is computationally efficient, enabling users to study long-term impacts and is a long-term yield model (Neitsch et al., 2009). The model simulates surface runoff volumes and peak runoff rates for each hydrologic response unit (HRU) using a modification of the SCS curve number method (USDA-SCS, 1972) or the Green & Ampt infiltration method (Green, 1911). The evaporation from soils and plants are computed separately by the method described in (Ritchie, 1972). Wherein, the potential evapotranspiration (PET) is the ET rate of a large area completely and uniformly covered with growing vegetation and an unlimited supply of soil water. In addition, the micro-climatic processes such as advection or heat-storage should not have effects on PET. The model uses the Hargreaves (1985), Priestley and Taylor (1972) and Penman-Monteith approaches for the estimation of PET.

7.3.2 The Bridging Event and Continuous Hydrological (BEACH)

The BEACH is a simple two-layer soil water balance model developed by Sheikh et al., (2009) using freely available GIS and programming language, PCRaster. It is a spatially distributed daily basic hydrological model and has the ability to predict antecedent soil moisture, actual E and ET as its primary objective. The model also estimates the infiltration and runoff using either the Bucket or CN approach (for more details see Sheikh et al., (2009)). Although the BEACH model offers two options of calculating runoff, the study results of Sheikh et al., (2009) showed that the CN approach performed better than the Bucket. That is reason for selecting the CN approach for simulating Q by the BEACH in this study.

In this model, the ET is separated into evaporation and transpiration and calculated based on the Penman-Monteith (FAO56) method (Allen et al., 1998). Based on an assumption of a hypothetical grass cover with an assumed height of 0.12 m, a surface resistance of 70 s m^{-1} and an albedo of 0.23, the FAO56 computes a reference evapotranspiration rate (ET_0). The PET of the other surface is calculated by multiplying the ET_0 with a crop-specific coefficient (K_c).

The BEACH was developed for only one year (2004) hydrologic assessments, but for this study objective of long-term hydrological modelling (12 years) we recoded the code and made the model adapt to the requirement with an assumption that the crop harvesting seasons have not changed in the computational time.

7.3.3 MODIS Evapotranspiration

We used the MODIS ET of the improved algorithm (Mu et al., 2011) from the old algorithm (Mu et al., 2007a) calculated as the sum of the E from moist soil, the transpiration from vegetation during the daytime, intercepted canopy precipitation and ET in the night-time. Some other improvements are the vegetation cover fraction (F_c), the soil heat flux (G), the wet surface fraction (F_{wet}), evaporation from the wet canopy surface (E_{wet_C}), plant transpiration (E_{trans}) etc. (more details see Mu et al., (2011)).

The total daily ET is calculated as in following relation:

$$\lambda E = \lambda E_{wet\_C} + \lambda E_{trans} + \lambda E_{SOIL} \quad (7\text{-}1)$$

where λE_{SOIL} is the actual daily soil evaporation.

The monthly ET is summarized from daily ETs.

7.3.4 SWAT Input

SWAT requires four groups of input data including topography, LULC, soils and climatic data.

- The topographic dataset commonly used is a Digital Elevation Model (DEM) which is employed to generate drainage network, flow directions, flow accumulation etc. for the topographical model's parameterization. We used a Triangulated Irregular Network (TIN) extracted from Yen Bai geodatabase (provided by the Vietnam Resources and Environment Corporation, Hanoi Vietnam) for generating the 30 × 30 m DEM for the study area (Fig. 7-1).
- The Land use/land cover (LULC) map (Fig. 7-2) of nine classes (including cloud) was produced from Landsat scenes acquired in 2009 with 30 × 30 m spatial resolution, seven bands of reflections. The map was classified using the supervised method in ENVI 4.7 software. The ground truth data was derived from the Yen Bai geodatabase. The accuracy of the classification was examined by calculating the user, producer accuracy and Kappa statistics for categorized classes (Table 7-1). The data shown within the table indicates the precision of the classification is at a good level with an overall accuracy of 78.6% and the Kappa coefficient of 0.73.

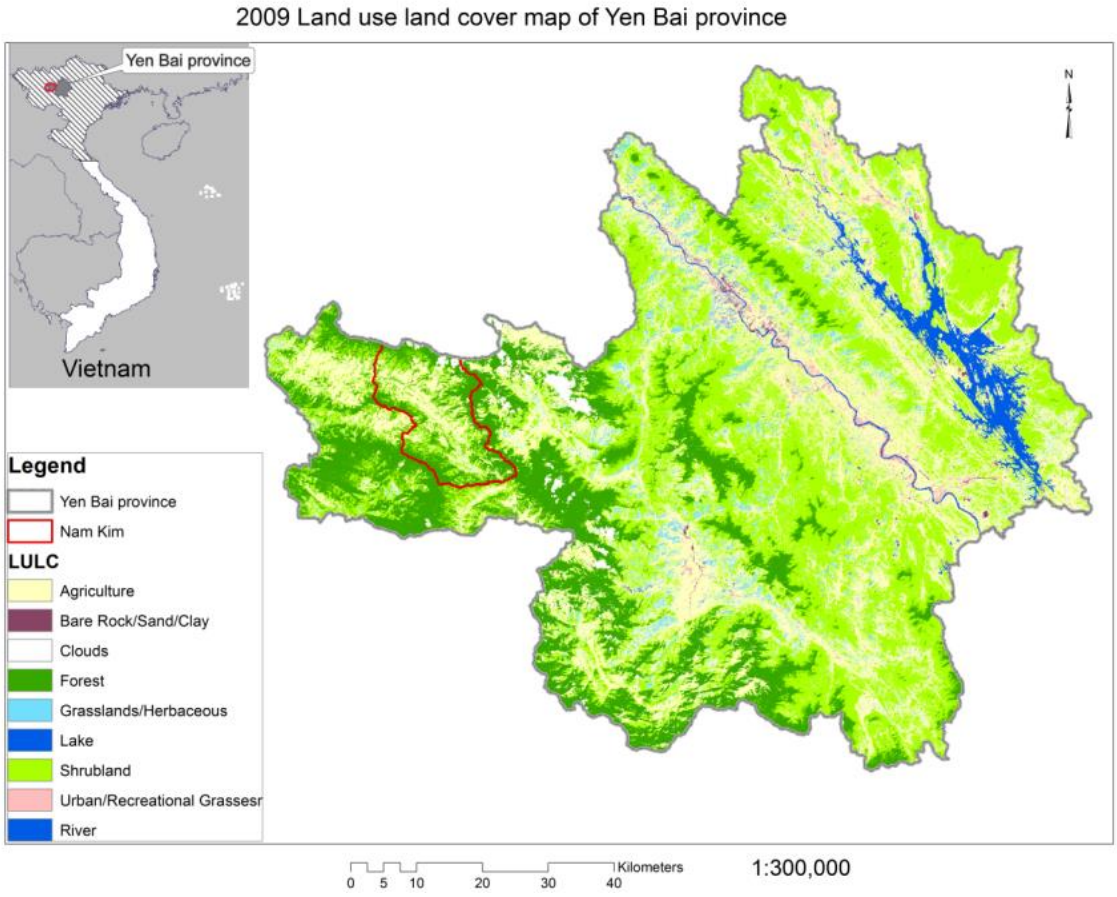

Figure 7-2. Landsat LULC map of Yen Bai in 2009.

Table 7-1. LULC classification accuracy assessment

LULC (year)	P/U (%)	Forest	Lake	River	Urban	Agriculture	Shrubland	Grassland	Barren	O (%)	Kappa
2009	P	86.2	88.8	76.3	72.3	73.4	73.8	64.0	74.7	76.8	0.73
	U	86.5	82.7	74.7	75.2	68.8	73.1	73.3	78.7		

P= Producer accuracy, U= User accuracy, O= Overall accuracy, and Kappa is the kappa statistic or kappa coefficient.

- Various physical and hydrological properties of soils are required by the model such as texture, hydraulic conductivity, bank density etc. Distribution of the soils was derived from a digital soil map of Yen Bai province produced in 1996 with six major soil groupings of fluvisols, calcisols, ferralsols, alisols, acrisols and gleysols.
- Climatic data required by the model includes daily rainfall, minimum and maximum temperature, wind speed, relative humidity, solar radiation and dew point temperature. This data can be read from measured data set or generated by a weather generator

algorithm. We collected this data from the gauges (Fig. 7-1) recorded from 1st January 2011 to 31st December 2012.

7.3.5 BEACH Inputs

Similar to SWAT, BEACH requires four main groups of input data: (i) topography, (ii) lands use, (iii) soil physical properties and (iv) climatic data. For the land use information, we need extra crop-specific information that could be obtained from literature of FAO paper no. 56 (Allen et al., 1998). The overview of input for BEACH was indicated in the Table 7-2.

Table 7-2. Input requirements of BEACH

Type	Data resolution	Input variables and parameters	Unit	Source
Topography	Constant	Slope map	m m^{-1}	DEM
	Constant	Drainage direction	-	DEM
	Constant	Wetness index (W)	-	DEM
Land use	Seasonally	Land use map	-	Satellite
	Constant	Maximum leaf area index (LAI_{max})	m^2 m^{-2}	Literature
	Constant	Maximum crop height (H_{max})	m	Literature (FAO56)
	Constant	Maximum crop depth (RD_{max})	m	Literature (FAO56)
	Constant	Light use efficiency (μ)	-	Literature
	Constant	Sowing and harvesting date	-	Literature
	Constant	Growing stages	-	Literature (FAO56)
	Constant	Basel crop coefficient (K_{cb})	-	Literature (FAO56)
	Constant	Water stress sensitivity (p)	-	Literature (FAO56)
Soil	Constant	Yen Bai soil map	-	Database, field survey
	For each layer	Layer depth (D)	m	Soil map
	Constant	Soil evaporation depth (D_e)	m	User specified
	For each layer	Subsurface flow coefficient (c)	d^{-1}	User specified
	For each layer	Drainage coefficient (γ)	-	User specified
	For each layer	Soil moisture at saturation (Θ_{sat})	m^3 m^{-3}	Literature
	For each layer	Saturated hydraulic conductivity (K_{sat})	m d^{-1}	Soil map, literature
Climate	Daily	Reference evapotranspiration (ET_0)	m	Weather station
	Daily	Minimum relative humidity (RH_{min})	%	Weather station
	Daily	Wind speed (U_2)	m s^{-1}	Weather station
	Daily	Precipitation (P)	m	Weather station

7.3.6 Model Calibration, Validation and Simulation

- SWAT: Before model calibration, the watershed was modelled by dividing it into 20 HRUs (Fig. 7-1) and parameterized with the inputs of topography, LULC and soils. The

parameters were summarized in Table 7-3. Climatic parameterization was separately implemented and written to climatic datasets.

Table 7-3. SWAT parameters for the Nam Kim watershed

HRUs	Area (km^2)	MeanElev (m)	AvgSlope ($m\ m^{-1}$)	MaxFlowLen (m)	Main soils	CN	Cover
1	17	1573	0.65	10522	Humic Ferralsols	47.4	46.4
2	14	2026	0.57	5909	Humic Alisols	37.0	46.2
3	35	1468	0.59	11203	Humic Acrisols	47.2	47.7
4	8	1360	0.63	9076	Humic Ferralsols	50.6	44.6
5	14	2008	0.61	7509	Humic Alisols	34.7	36.4
6	6	1447	0.67	6766	Humic Acrisols	47.6	49.0
7	14	1988	0.57	7979	Humic Alisols	43.1	65.0
8	16	1343	0.56	7364	Humic Ferralsols	49.1	48.5
9	3	1300	0.51	3233	Humic Ferralsols	49.7	52.8
10	16	1484	0.58	10179	Humic Ferralsols	48.8	45.8
11	9	1484	0.54	8726	Humic Ferralsols	49.5	40.6
12	17	1717	0.53	6295	Humic Ferralsols	46.8	52.9
13	16	1561	0.56	9042	Humic Alisols	47.7	47.1
14	2	1260	0.49	3970	Humic Ferralsols	51.9	41.2
15	16	1626	0.58	8837	Humic Ferralsols	47.6	50.0
16	3	1232	0.52	3649	Humic Ferralsols	49.1	50.3
17	2	1219	0.43	3752	Humic Ferralsols	50.0	45.2
18	13	1506	0.57	11914	Humic Ferralsols	46.1	61.9
19	31	1469	0.51	10366	Humic Ferralsols	47.6	54.6
20	14	1412	0.51	8403	Humic Ferralsols	46.9	55.9

MeanElve is average elevation, AvgSlope means average slope, MaxFlowLen is Maximum flow length, CN indicates area-weighted curve number based on soil type and land cover, and Cover is fraction of surface covered by intercepting cover.

In the model calibration stage, the CN, infiltration and base flow recession parameter were adjusted to generate the estimated discharge close to observed discharge measured from 2001 to 2005. The model validation was done with observed discharge for a period of seven years from 2006 to 2012.

- BEACH: The model was set up with the four crops of forest, shrub, rice (agriculture) and grass and calibrated with four-year measured E from 2001 to 2004. The calibrated model's input variables and parameters were tabularized in Table 7-4. As the observed E is the point measurement and based on the LULC map, we made average estimated E of the surrounding land use (shrub and rice) for comparison with *in situ* data. The model validation was run for the 2005-2012 period.

Table 7-4. Variables of input and parameters (calibrated)

Input	Unit	Rice	Grass	Shrub	Forest
$\Theta_{sat\ 1}$	$m^3\ m^{-3}$	0.36	0.42	0.36	0.40
$\Theta_{sat\ 2}$	$m^3\ m^{-3}$	0.40	0.40	0.40	0.65
$K_{sat\ 1}$	$m\ d^{-1}$	0.01	0.01	0.03	0.15
$K_{sat\ 2}$	$m\ d^{-1}$	0.03	0.03	0.03	0.45
c	d^{-1}	0.25	0.25	0.25	0.25
D_e	M	0.15	0.15	0.15	0.15
LAI_{max}	$m^2\ m^{-2}$	2.50	2.50	4.50	6.00
H_{max}	M	0.80	0.40	2.50	10.0
RD_{max}	M	0.60	0.50	1.20	2.50
μ	-	0.45	0.40	0.30	0.75
$K_{cb\ ini}$	-	1.05	0.40	0.50	0.40
$K_{cb\ mid}$	-	1.20	0.90	0.95	1.50
$K_{cb\ end}$	-	0.90	0.70	0.75	0.7
p	-	0.55	0.55	0.50	0.65
CN_2	-	75	60	65	50

Both the models simulated the ET values from 2001 to 2012 and the model performances were examined by calculating the coefficient of determination (R^2) and Nash–Sutcliffe efficiency (NSE) (Nash & Sutcliffe, 1970). We used a simple averaging method (to average ET from all crops appearing in the HRU 3) to calculate the mean BEACH ET for HRU 3 and then compared it with SWAT and MODIS ET (used zonal statistics) for this HRU.

7.3.7 MODIS Evapotranspiration

Monthly MODIS ET datasets with 1-km spatial resolution generated based on the MOD16 algorithm in Mu et al., (2011) from 2001 to 2012 were used to extract actual ET. These ET was verified by comparing with measured data of both globally and locally at 46 eddy flux towers presented in the study of Mu et al., (2011). We developed a simple model in the ModelBuilder of ArcMap-ArcInfo to extract the monthly and yearly ET using ArcGIS functions as in the Fig. 7-3.

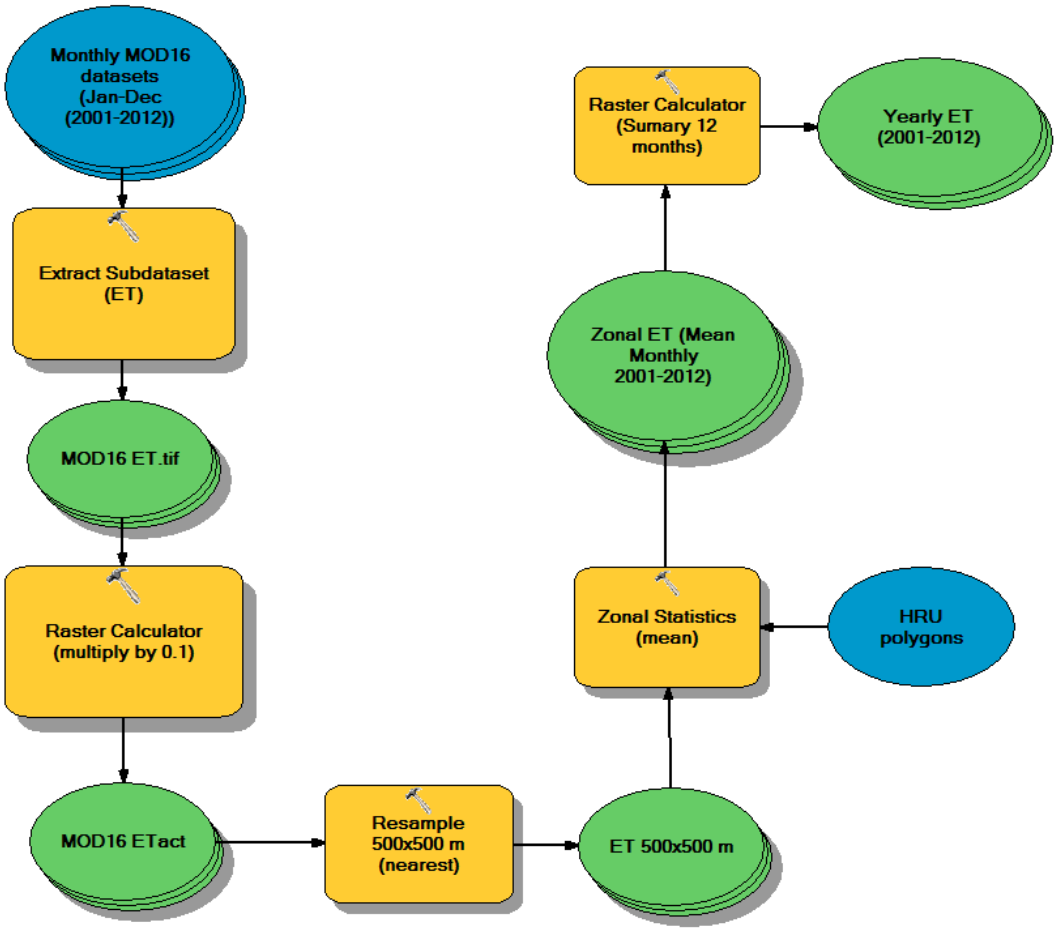

Figure 7-3. Model flow work for monthly and yearly ET calculation using MODIS datasets: Wherein, the blue ellipses are the model's inputs, the yellow rounded rectangles perform the model's functions, and the green ellipses are the temporal and final outputs.

7.4 Results and Discussion

7.4.1 SWAT Calibration and Validation for Surface Runoff

Overestimates of before calibrated discharge values (computing from 1st January 2001 to 31st December 2005) compared to gauged data (more triangles above the red linear and value of Y axis larger than X axis as well) have been shown in the Fig. 7-4a and the R^2 and NSE were assumed to be low, 0.58 and −0.4, respectively. However, after adjusting the model parameters (mentioned in the method section) the model simulated Q (after calibration) matched the stream-gauged information (NSE = 0.62 and R^2 = 0.80) well.

Figure 7-4b shows the good agreement between SWAT simulated and observed discharge values in the validated stage performing from 1st June 2001 to 31st December 2012 with R^2 of 0.88 and NSE of 0.65. Although there were still some over/underestimates of river discharge at some peaks, the results of model calibration and validation revealed the important

capability of SWAT to produce the Q matching closely to measured data in a medium-size tropical watershed (SWAT was developed for arid/semi-arid river catchments). In addition, this point was supported by some similar previous studies of Fukunaga et al., (2015), Ndomba et al., (2008) and Tibebe (2011) even for a case study in Vietnam such as Vu et al., (2012).

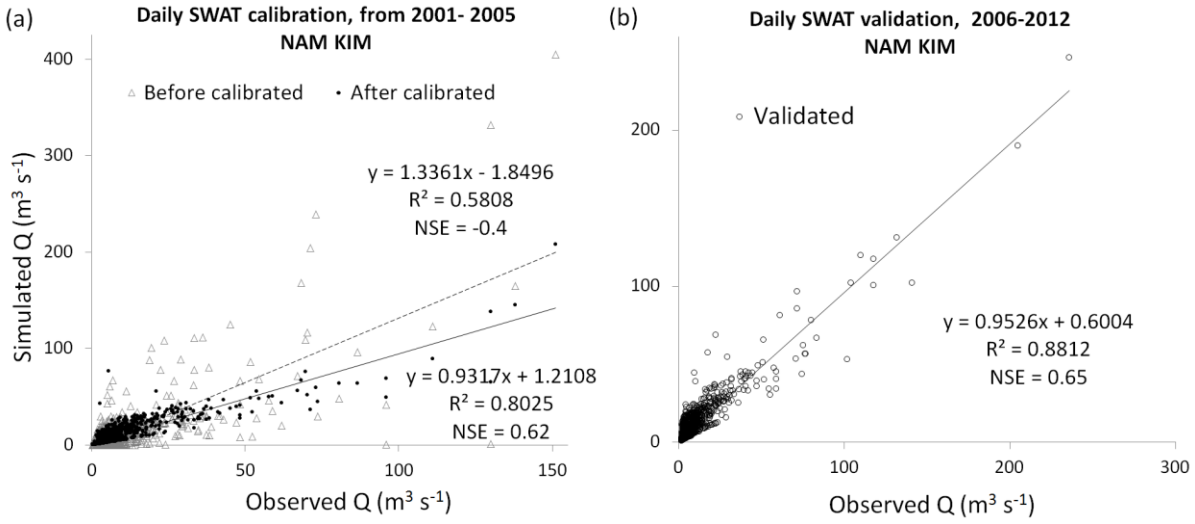

Figure 7-4. Scatted plots of SWAT calibration (a) and validation (b) for runoff.

7.4.2 BEACH Calibration and Validation for Evaporation

The BEACH started calibrating for a 2001-2004 period for four types of crops (mentioned in Table 7-4) and the before-calibrated simulated E (averaged from rice and shrub E) was much lower compared to observed E (R^2 = 0.23 and NSE = −0.22). Especially in some periods such as in December 2001 and 2003 the simulated E was a large uncertainty but after consideration of the sowing dates of the rice crop (December is the irrigation time of the winter-spring season) we adjusted the rice sowing and harvesting dates and increased the K_c and a good agreement was found after calibration (Fig. 7-5b) with R^2 of 0.76 and NSE of 0.62, except for some underestimates of some peaks. For the daily simulation, these values of R^2 and NSE are asserted at a good level and also certified by Moriasi et al., (2007) and Santhi et al., (2001).

Model validation was done for an eight-year period from 2005 to 2015 and the result was illustrated in the Fig. 7-5c with acceptable agreement between calculated E and field measured E (R^2 = 0.71 and NSE = 0.65). Furthermore, the figure indicated the variations (0.1 to 12 mm) of E values in the validated period. In general, the E values were highest from March to May and lower from June to September. Besides the climatic aspects such as humidity, wind, radiation and precipitation, the cropping irrigation, crop growing (Jaksa & Sridhar, 2015) and land use changes (Dias et al., 2015) have important effects on E and ET. For this case study, some differences between simulated and observed E might come from

changes in crop and land use because we kept the cropping sowing dates and land use unchanged over the simulation period. To improve the model performance, an updated crop type and time might be needed, however for long-term observation it is very time consuming.

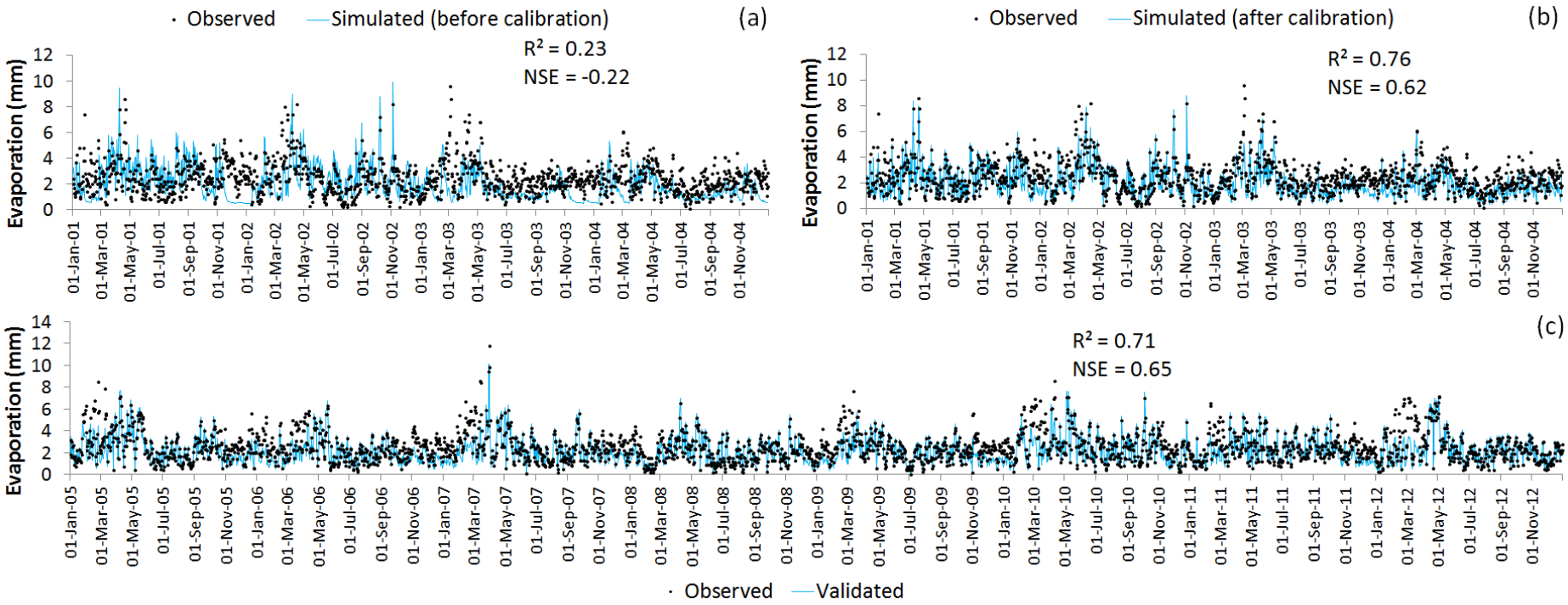

Figure 7-5. Daily before (a) after (b) calibrated and validated (c) evaporation compared to measured evaporation.

7.4.3 Comparing SWAT and BEACH Daily ET (of HRU3 from 2001 to 2012)

The time series daily actual evapotranspiration values calculated by SWAT (for HRUs) and BEACH (averaged from the four crop's ET) and measured rainfall were presented and compared to each other by the line graph (Fig. 7-5). The graph indicated not only the variations of ET (0.3 to 14 mm day^{-1}) and rainfall but also the yearly routine of ET. The ET values appeared very high before rainy seasons (May to August) and lowest in winter (December to March). The changing in ET is basically related to stand density (number of trees per hectare) and also incoming solar radiation (referring to season) (Vanderhoof & Williams, 2015). A better understanding of the ET routine and trends might help to predict the ET in the future but a longer time of simulation is needed (instead of 12 years). There were two periods May to September 2003 and 2004 with large differences in ETs estimated by SWAT and BEACH. Unfortunately, without the *in situ* measured ETs for comparison we did not know whether the SWAT ET was more accurate than the BEACH ET or the reverse. However, based on the good relationship between BEACH E and observed E (discussed in the section 7.4.2) the BEACH ET (lower value) would be more reliable in these computational times.

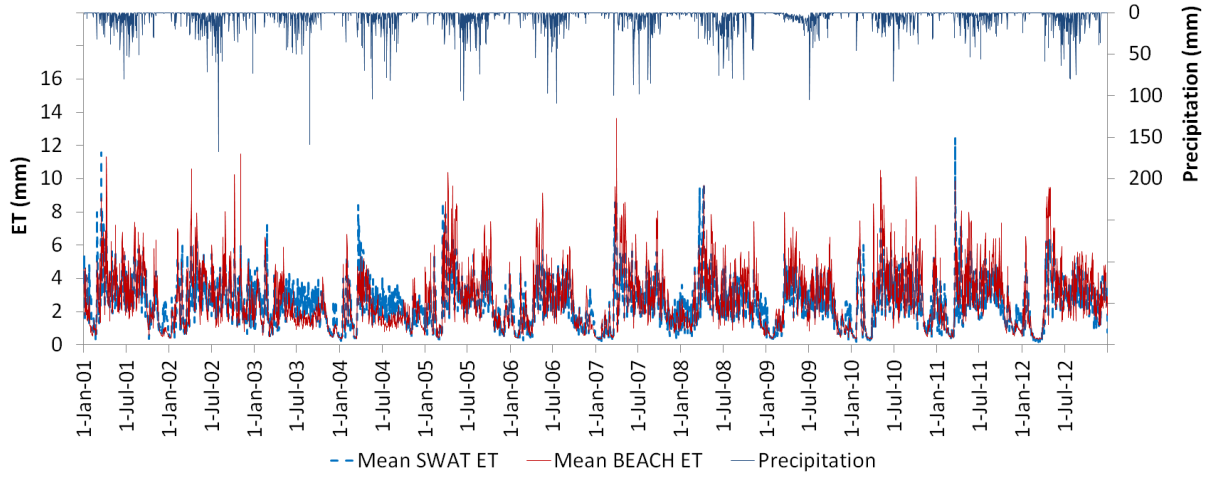

Figure 7-6. Line graph of time series SWAT and BEACH ET (calculated for HRU 3) and measured rainfall.

We analysed the relationship between the two estimates of ET represented in the Fig. 7-7 with the moderate correlation (R^2 of 0.73). However, both models predicted ETs closely together when the rates were low (< 4 mm). These rates consisted of more than 90% of the estimates. The interesting correlation between measured daily rainfall and SWAT ET was also indicated in the figure. Basically, the wet days (with precipitation > 0 mm day^{-1}) had ET rates from one to four mm day^{-1}. On the other hand, all the ET values are higher than six mm

day^{-1} generated in dry days (no rainfall). The ET of 0.3 to one mm day^{-1} and rainfall less than 10 mm day^{-1} were calculated for the winter time. This relationship could provide helpful information for cropping irrigation (Immerzeel & Droogers, 2008), the drought season (Vicente-Serrano et al., 2015), particularly when we could forecast the ET values (Ballesteros et al., 2016), and for improved understanding of the interactions between land surfaces and the atmosphere (Hong et al., 2009 and Mu et al., 2007a).

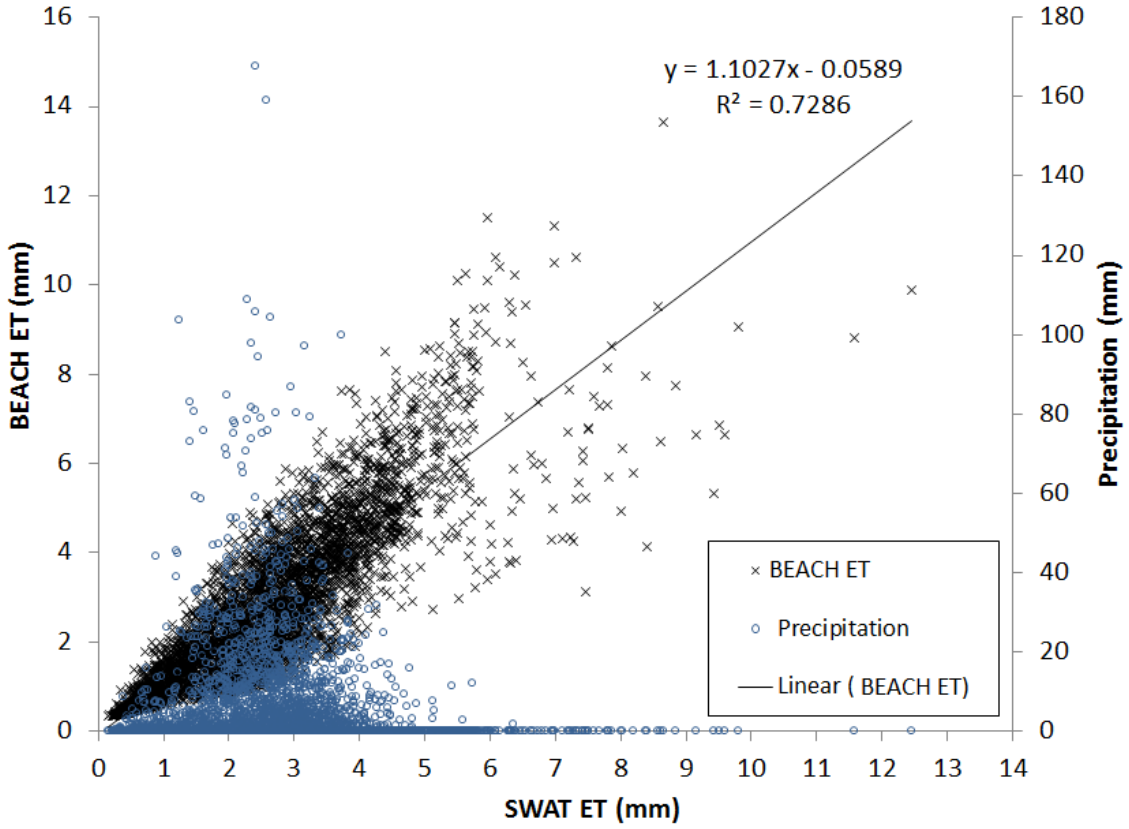

Figure 7-7. Relationship between daily SWAT and BEACH ET, SWAT ET and rainfall.

7.4.4 Comparing SWAT and BEACH (CN) Daily Runoff (2001-2012)

Figure 7-8 shows the daily discharge values generated by the SWAT and BEACH models from 2001 to 2012 compared with the daily measured data at the watershed outlet. There were some peaks of discharge captured by the models, varying from 100 to 240 m^3 s^{-1} and most values ranged from 0 to 50 m^3 s^{-1}. The SWAT appeared to predict the discharge closer to observed information than the BEACH with NSE of 0.67 and 0.61 for the models, respectively. Generally, both models slightly underestimated the discharge. However, close relationships between simulated and field measured discharge can be seen in the figure in both cases with R^2 of 0.81 for the SWAT and 0.83 for the BEACH.

Although the two models use the same CN method (USDA-SCS, 1986) to simulate the discharge value, many reasons could be explained for the differences of Q values shown in the Fig. 7-8 such as the difference in model structure, in inputs etc. Many previous studies found that the modelled runoff is sensitive to CN values (Singh et al., 2004; Shen et al., 2009 and Tibebe, 2011), we altered the CN value of each land use class (of crops for the case of the BEACH) in oder to calculate to discharge close to the observed data.

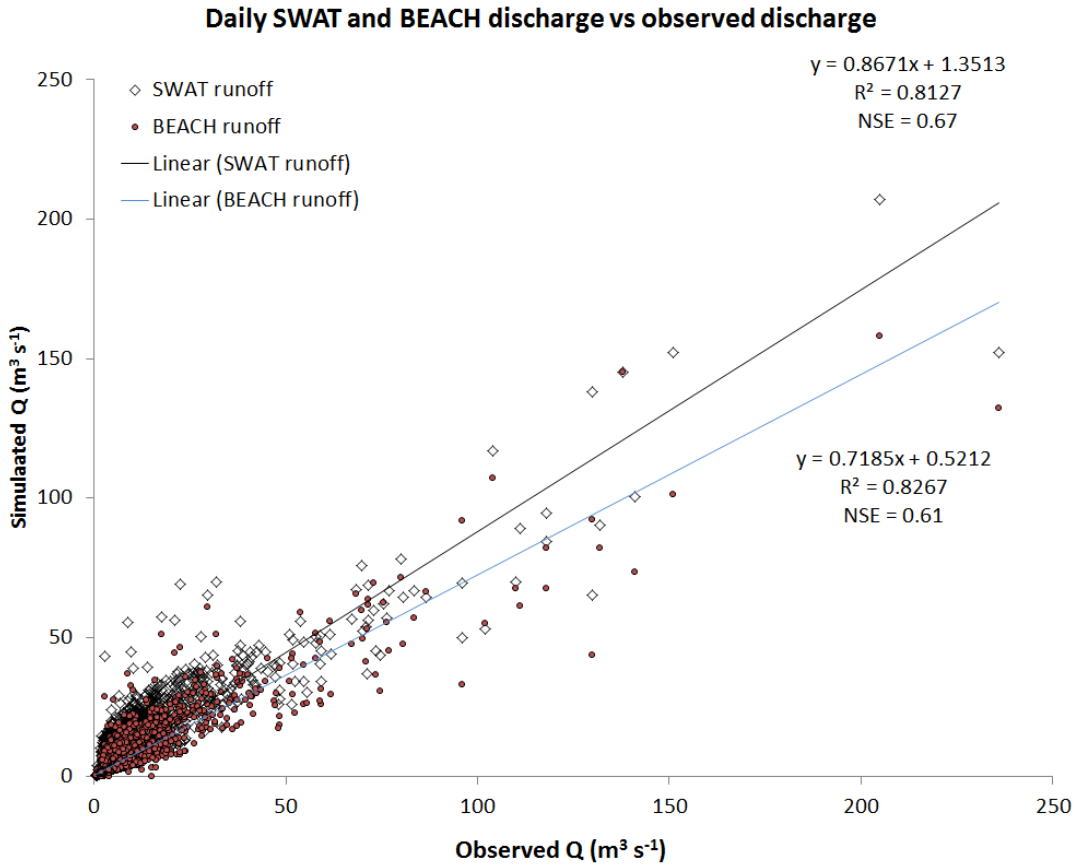

Figure 7-8. Relationship between daily SWAT, BEACH and observed discharge from 2001 to 2012.

7.4.5 Monthly SWAT and BEACH vs MODIS ET of HRU 3 from 2001-2012

The variations of monthly ET calculated from MODIS scenes, from the SWAT and BEACH models and their standard deviations from 2001 to 2012 are presented in the bar graph of Fig. 7-9. Although the ET from all estimates was highest from May to October and lowest from December to February, the MODIS ET varied gradually over the twelve years. Both the SWAT and BEACH estimated the ET in 2003 and 2004 much lower than the MODIS ET. The MODIS ET was estimated higher than the BEACH ET and the SWAT ET was lowest in general. The standard deviations of the three ET sources calculated for each month fluctuated from three to 40 mm and the average value was 17. 5 mm. The MODIS ET was estimated

using the improved ET algorithm at global scale (global parameters) (Mu et al., 2011) and compared to the watershed scale in this study we assert that the agreement between the three estimated ETs was at a good level.

The monthly ET varied over different seasons and the most driving factors on ET found in the study of Petković et al., (2015) were relative humidity and wind speed at two meters high. Both the SWAT and BEACH models thoroughly take into account these two factors but the algorithm for MODIS ET does not include wind speed and topographic influences (elevation, slope and aspect) (Hu et al., 2015).

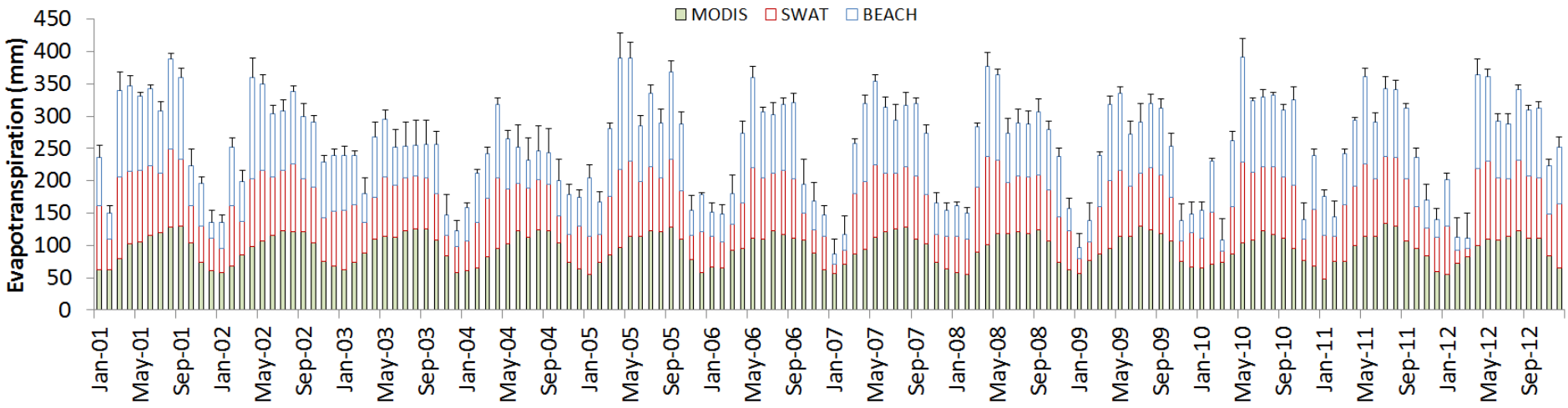

Figure 7-9. Monthly ET extracted from MODIS product, estimated by the SWAT and BEACH models in 2001-2012 periods.

7.4.6 ET Trend Analyses

The slightly downward trend of ET in the 2001-2012 periods has been shown in the Fig. 7-10 for all cases of estimations illustrated by the negative slope line of the equations. However, in the first four years the ET decreased gradually but in the rest of the years the rates were more stable. While all data sources represented the decrease of monthly ET, the 12 years of simulation might be too short to come to a conclusion that the annual ET in the study region is currently declining and will in the future. Therefore, longer term assessment could be needed (40 years or more) and the reasons for this trend were also out of this paper's scope.

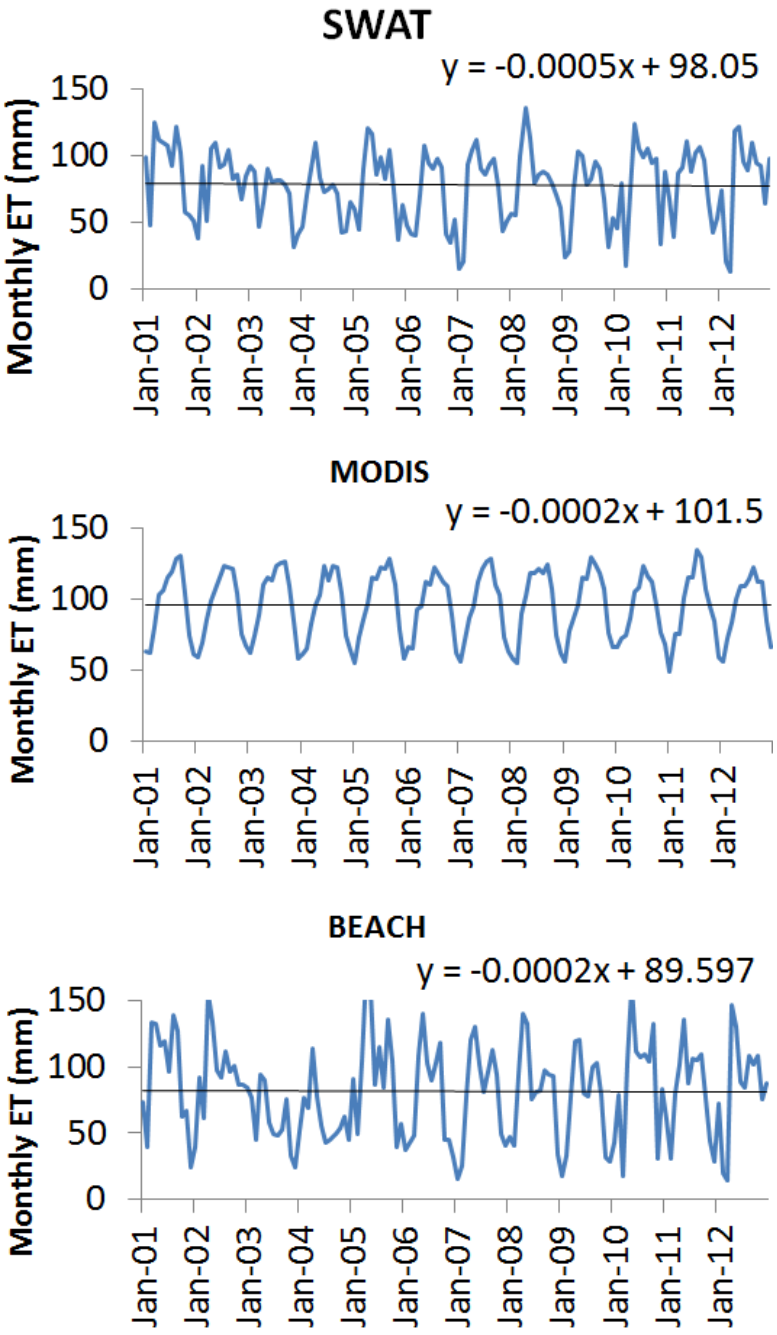

Figure 7-10. SWAT, BEACH and MODIS ET trends.

7.4.7 SWAT and MODIS ET Spatial Distributions

The yearly ET accumulations of the SWAT and BEACH were mapped for twenty HRUs (1-20) of the Nam Kim watershed with two-year intervals from 2002 to 2012 (Fig. 7-11). Crossed comparison can be made between the maps of the SWAT ET, MODIS ET and between the SWAT and MODIS ET maps. Among the SWAT ET maps, the 2004 one had the highest ET rate of 1069 to 1086 mm year^{-1} (mm y^{-1}) following by 2008, 2002, 2012, 20010 and 2006 had the lowest rate ranging from 751 to 773 mm y^{-1}. Among the MODIS maps, the

map 2006 had the highest rate of 1050 to 1192 mm y^{-1} following by 2004, 2002, 2012, 2008 and 2010 had the lowest rate of 950 to 1150 mm y^{-1}. In general, the MODIS maps had higher ET rates than SWAT maps. The yearly ET calculated for the HRUs also varied over time in all the maps. Some similarities in the maps can be seen in the HRUs such as HRU 7, 8, 10, 13, 14 and 20 (except the year 2004) with lower ET and 1, 5, 11 and 19 with higher ET. Differences between SWAT and MODIS distributed ET appeared in the figure as well, for example the HRU 12, 16 and 14 with lower ET in MODIS maps and higher ET in the SWAT ones. These dissimilarities were thought to be normal because the results were estimated from different approaches and scales. However, the agreements were dominant.

The changes of ET patterns might be related to changes in land use/land cover for example the decrease in canopy interception causes a decrease in ET and percolation and increase in runoff (Dias et al., 2015 and Lin et al., 2015). In addition, as discussions in the section 7.4.6 that SWAT used distributed soil and topographic inputs, therefore the SWAT ET might be more precise than MODIS due to the fact that global satellite products generally contain noises (Westerhoff, 2015).

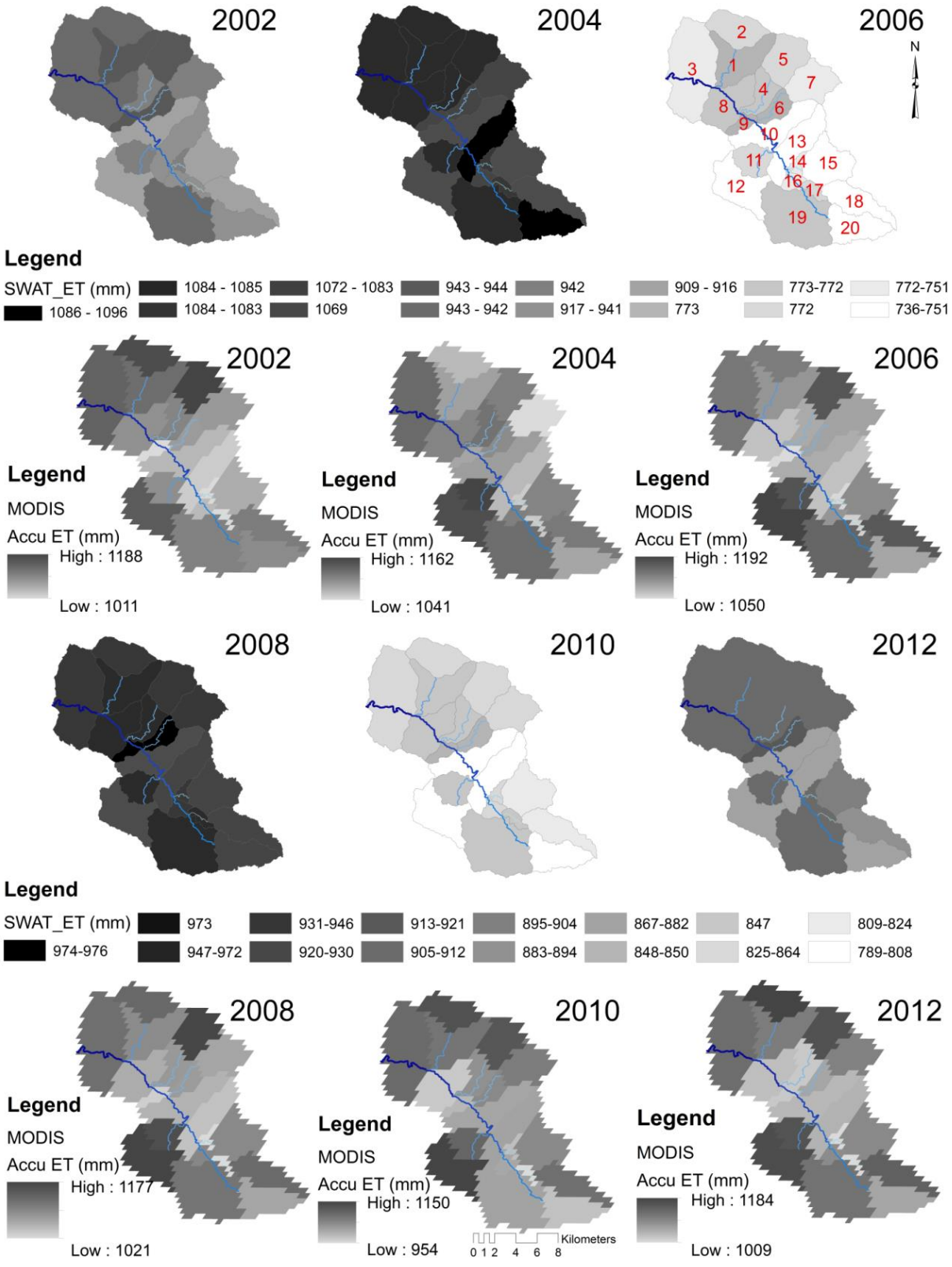

Figure 7-11. Yearly spatial ET distribution modelled by SWAT and derived from MODIS products (Accu stands for accumulative; the MODIS maps were results of the model, Fig. 7-3, built in ArcMap discussed in the method section).

7.5 Summary and Conclusions

Daily discharge and evaporation were calculated and validated by SWAT for the 268 km^2 watershed in the tropical region in North Vietnam with acceptable agreement between simulated and observed data verified by the NSE and R^2 values. This might reveal a possible application of the two hydrological models for tropical regions. The good correlations between discharges produced by the models were also represented in the study results as well.

Although the daily estimated ETs by the SWAT and BEACH models were not validated, they matched well with each other and the monthly ETs were compared with the published MODIS product. Despite the SWAT and BEACH ETs being slightly lower than the MODIS ET, basically a close correlation between them can be seen in the study results (analysed using standard deviations) and also all the monthly ETs showed the slight downward trend in the simulation time (2001-2012).

The results of zonal statistics applied for the yearly MODIS and SWAT ETs were mapped, providing interesting information of temporal and distributed ET patterns in the watershed. Both differences and similarities could be found in the map but the correspondence between them was dominant. We conclude that the MODIS ET was very helpful for verifying the smaller scale of ET estimation by the two models.

7.6 References

Allen, R. G., Pereira, L. S., Raes, D., & Smith, M. (1998). Crop evapotranspiration: guidelines for computing cropwater requirements. In: *Irrigation and Drainage. Paper 56*. FAO, Rome.

Almorox, J., Quej, V. H., & Martí, P. (2015). Global performance ranking of temperature-based approaches for evapotranspiration estimation considering Köppen climate classes. *Journal of Hydrology, 528,* 514-522. doi: http://dx.doi.org/10.1016/j.jhydrol.2015.06.057

Ballesteros, R., Ortega, J. F., & Moreno, M. Á. (2016). FORETo: New software for reference evapotranspiration forecasting. *Journal of Arid Environments, 124,* 128-141. doi: http://dx.doi.org/10.1016/j.jaridenv.2015.08.006

Boegh, E., Poulsen, R. N., Butts, M., Abrahamsen, P., Dellwik, E., Hansen, S., . . . Soegaard, H. (2009). Remote sensing based evapotranspiration and runoff modeling of agricultural, forest and urban flux sites in Denmark: From field to macro-scale. *Journal of Hydrology, 377*(3–4), 300-316. doi: http://dx.doi.org/10.1016/j.jhydrol.2009.08.029 Singh

Camporese, M., Daly, E., Dresel, P. E., & Webb, J. A. (2014). Simplified modeling of catchment-scale evapotranspiration via boundary condition switching. *Advances in Water Resources, 69,* 95-105. doi: http://dx.doi.org/10.1016/j.advwatres.2014.04.008

Casali, J., Gastesi, R., Alvarez-Mozos, J., De Santisteban, L. M., de Lersundi, J. D., Gimenez, R., . . . Doneezar, M. (2008). Runoff, erosion, and water quality of agricultural watersheds in central Navarre (Spain). *Agricultural Water Management, 95*(10), 1111-1128. doi: DOI 10.1016/j.agwat.2008.06.013

Connan, O., Maro, D., Hébert, D., Solier, L., Caldeira Ideas, P., Laguionie, P., & St-Amant, N. (2015). In situ measurements of tritium evapotranspiration (3H-ET) flux over grass and soil using the gradient and eddy covariance experimental methods and the FAO-56 model. *Journal of environmental radioactivity, 148,* 1-9. doi: http://dx.doi.org/10.1016/j.jenvrad.2015.06.004

Consoli, S., & Vanella, D. (2014). Comparisons of satellite-based models for estimating evapotranspiration fluxes. *Journal of Hydrology, 513,* 475-489. doi: http://dx.doi.org/10.1016/j.jhydrol.2014.03.071

Dias, L. C. P., Macedo, M. N., Costa, M. H., Coe, M. T., & Neill, C. (2015). Effects of land cover change on evapotranspiration and streamflow of small catchments in the Upper Xingu River Basin, Central Brazil. *Journal of Hydrology: Regional Studies, 4, Part B,* 108-122. doi: http://dx.doi.org/10.1016/j.ejrh.2015.05.010

Fukunaga, D. C., Cecílio, R. A., Zanetti, S. S., Oliveira, L. T., & Caiado, M. A. C. (2015). Application of the SWAT hydrologic model to a tropical watershed at Brazil. *CATENA, 125*(0), 206-213. doi: http://dx.doi.org/10.1016/j.catena.2014.10.032

Green, W. H., & Ampt, G. A., 1911. Studies on soil physics, 1. The flow of air and water through soils. *Journal of Agricultural Sciences 4:*11-24.

Guber, A. K., Pachepsky, Y. A., Yakirevich, A. M., Shelton, D. R., Whelan, G., Goodrich, D. C., & Unkrich, C. L. (2014). Modeling runoff and microbial overland transport with KINEROS2/STWIR model: Accuracy and uncertainty as affected by source of infiltration parameters. *Journal of Hydrology, 519, Part A*(0), 644-655. doi: http://dx.doi.org/10.1016/j.jhydrol.2014.08.005

Hargreaves, G. L., Hargreaves, G. H., Riley, J. P., Irrig, J., & Drain. (1985). Agricultural benefits for Senegal River Basin. *J. Irrig. Drain Eng. 1985.111*(2):113-124.

Hong, S.-h., Hendrickx, J. M. H., & Borchers, B. (2009). Up-scaling of SEBAL derived evapotranspiration maps from Landsat (30 m) to MODIS (250 m) scale. *Journal of Hydrology, 370*(1–4), 122-138. doi: http://dx.doi.org/10.1016/j.jhydrol.2009.03.002

Horton, R. E. (1933). The role of infiltration in the hydrologic cycle. *Eos Trans. AGU 14,* 446–460.

Howell, T. A., Evett, S. R., Tolk, J. A., Copeland, K. S., & Marek, T. H. (2015). Evapotranspiration, water productivity and crop coefficients for irrigated sunflower in the U.S. Southern High Plains. *Agricultural Water Management, 162,* 33-46. doi: http://dx.doi.org/10.1016/j.agwat.2015.08.008

Hu, G., Jia, L., & Menenti, M. (2015). Comparison of MOD16 and LSA-SAF MSG evapotranspiration products over Europe for 2011. *Remote Sensing of Environment, 156,* 510-526. doi: http://dx.doi.org/10.1016/j.rse.2014.10.017

Immerzeel, W. W., & Droogers, P. (2008). Calibration of a distributed hydrological model based on satellite evapotranspiration. *Journal of Hydrology, 349*(3–4), 411-424. doi: http://dx.doi.org/10.1016/j.jhydrol.2007.11.017

Jaksa, W. T., & Sridhar, V. (2015). Effect of irrigation in simulating long-term evapotranspiration climatology in a human-dominated river basin system. *Agricultural*

and Forest Meteorology, 200, 109-118. doi: http://dx.doi.org/10.1016/j.agrformet.2014.09.008

Singh, J., Knapp, H. V., Arnold, J., & Demissie, M. (2005). Hydrological modeling of the Iroquois River watershed using HSPF and SWAT. *Journal of the American Water Resources Association, 41*(2), 343-360.

Kisi, O., Sanikhani, H., Zounemat-Kermani, M., & Niazi, F. (2015). Long-term monthly evapotranspiration modeling by several data-driven methods without climatic data. *Computers and Electronics in Agriculture, 115,* 66-77. doi: http://dx.doi.org/10.1016/j.compag.2015.04.015

Lenzi, M. A., & DiLuzio, M. (1997). Surface runoff, soil erosion and water quality modelling in the Alpone watershed using AGNPS integrated with a Geographic Information System. *European Journal of Agronomy, 6*(1-2), 1-14. doi: Doi 10.1016/S1161-0301(96)02001-1

Lin, B., Chen, X., Yao, H., Chen, Y., Liu, M., Gao, L., & James, A. (2015). Analyses of landuse change impacts on catchment runoff using different time indicators based on SWAT model. *Ecological Indicators, 58,* 55-63. doi: http://dx.doi.org/10.1016/j.ecolind.2015.05.031

Linde, A. H. t., Aerts, J. C. J. H., Hurkmans, R. T. W. L., & Eberle, M. (2008). Comparing model performance of two rainfall-runoff models in the Rhine basin using different atmospheric forcing data sets. *Hydrol. Earth Syst. Sci., 12,* 943–957, 2008.

Liu, M., Tian, H., Lu, C., Xu, X., Chen, G., & Ren, W. (2012). Effects of multiple environment stresses on evapotranspiration and runoff over eastern China. *Journal of Hydrology, 426–427,* 39-54. doi: http://dx.doi.org/10.1016/j.jhydrol.2012.01.009

Lopez-Vicente, M., Poesen, J., Navas, A., & Gaspar, L. (2013). Predicting runoff and sediment connectivity and soil erosion by water for different land use scenarios in the Spanish Pre-Pyrenees. *CATENA, 102,* 62-73. doi: DOI 10.1016/j.catena.2011.01.001

Marttila, H., & Klove, B. (2010). Managing runoff, water quality and erosion in peatland forestry by peak runoff control. *Ecological Engineering, 36*(7), 900-911. doi: DOI 10.1016/j.ecoleng.2010.04.002

Mchunu, C., & Chaplot, V. (2012). Land degradation impact on soil carbon losses through water erosion and CO2 emissions. *Geoderma, 177,* 72-79. doi: DOI 10.1016/j.geoderma.2012.01.038

Monteith, J. L. (1965). Evaporation and the environment. In The state and movement of water in living organisms. 19th Symposia of the Society for Experimental Biology. *Cambridge Univ. Press, London, U.K.,* p. 205-234. .

Moriasi, D. N., Arnold, J. G., Van Liew, M. W., Bringer, R. L., Harmel, R. D., & Veith, T. L. (2007). Model evaluation guidelines for systematic quantification of accuracy in watershed simulations. *Am. Soc. Agric. Biol. Eng. 50* (3), 885–900.

Mu, Q., Heinsch, F. A., Zhao, M., & Running, S. W. (2007a). Development of a global evapotranspiration algorithm based on MODIS and global meteorology data. *Remote Sensing of Environment, 111,* 519−536.

Mu, Q., Zhao, M., & Running, S. W. (2011). Improvements to a MODIS global terrestrial evapotranspiration algorithm. *Remote Sensing of Environment, 115*(8), 1781-1800. doi: http://dx.doi.org/10.1016/j.rse.2011.02.019

Nash, J. E., & Sutcliffe, J. V. (1970). River flow forecasting through conceptual models 1: a discussion of principles. *Journal of Hydrology 10* (3), 282–290.

Ndomba, P., Mtalo, F., & Killingtveit, A. (2008). SWAT model application in a data scarce tropical complex catchment in Tanzania. *Physics and Chemistry of the Earth, Parts A/B/C, 33*(8–13), 626-632. doi: http://dx.doi.org/10.1016/j.pce.2008.06.013

Neitsch, S. L., J.G. Arnold, J.R. Kiniry , & Williams, J. R. (2009). Soil and Water Assessment Tool Theoretical Documentation, Version 2009. *Texas Water Resources Institute* Technical Report No. 406.

Nguyen Van Tai, Kim Thi Tuy Ngoc, Phan Tuan Hung, Le Thi Le Quyen, Nguyen Thi Ngoc Anh, Anna Stabrawa, . . . Cuong, N. M. (2009). Vietnam Assessment Report on Climate Change Institute of Strategy and Policy on natural resources and environment, *Viet Nam Van hoa - Thong tin Publishing House: 318-2009/CXB/16-28/VHTT*, 112-115.

Petković, D., Gocic, M., Trajkovic, S., Shamshirband, S., Motamedi, S., Hashim, R., & Bonakdari, H. (2015). Determination of the most influential weather parameters on reference evapotranspiration by adaptive neuro-fuzzy methodology. *Computers and Electronics in Agriculture, 114*, 277-284. doi: http://dx.doi.org/10.1016/j.compag.2015.04.012

Priestley, C. H. B., & Taylor, R. J. (1972). On the assessment of surface heat flux and evaporation using large-scale parameters. *Mon. Weather Rev.* 100:81-92.

Ritchie, J. T. (1972). A model for predicting evaporation from a row crop with incomplete cover. *Water Resour. Res. 8*:1204-1213.

Rogger, M., Kohl, B., Pirkl, H., Viglione, A., Komma, J., Kirnbauer, R., . . . Blöschl, G. (2012). Runoff models and flood frequency statistics for design flood estimation in Austria – Do they tell a consistent story? *Journal of Hydrology, 456–457*(0), 30-43. doi: http://dx.doi.org/10.1016/j.jhydrol.2012.05.068

Santhi, C., Arnold, J. G., Williams, J. R., Dugas, W. A., Srinivasan, R., & Hauck, L. M. (2001). Validation of the SWAT model on a large river basin with point and nonpoint sources. *J. Am. Water Resour. Assoc. 37* (5), 1169–1188.

Sawano, S., Hotta, N., Tanaka, N., Tsuboyama, Y., & Suzuki, M. (2015). Development of a simple forest evapotranspiration model using a process-oriented model as a reference to parameterize data from a wide range of environmental conditions. *Ecological Modelling, 309–310*, 93-109. doi: http://dx.doi.org/10.1016/j.ecolmodel.2015.04.011

Sheikh, V., Visser, S., & Stroosnijder, L. (2009). A simple model to predict soil moisture: Bridging Event and Continuous Hydrological (BEACH) modelling. *Environmental Modelling & Software, 24*(4), 542-556. doi: http://dx.doi.org/10.1016/j.envsoft.2008.10.005

Shen, Z. Y., Gong, Y. W., Li, Y. H., Hong, Q., Xu, L., & Liu, R. M. (2009). A comparison of WEPP and SWAT for modeling soil erosion of the Zhangjiachong Watershed in the Three Gorges Reservoir Area. *Agricultural Water Management, 96*(10), 1435-1442. doi: DOI 10.1016/j.agwat.2009.04.017

Sun, J., Salvucci, G. D., & Entekhabi, D. (2012). Estimates of evapotranspiration from MODIS and AMSR-E land surface temperature and moisture over the Southern Great Plains. *Remote Sensing of Environment, 127*, 44-59. doi: http://dx.doi.org/10.1016/j.rse.2012.08.020

Sun, Z., Wang, Q., Matsushita, B., Fukushima, T., Ouyang, Z., & Watanabe, M. (2009). Development of a Simple Remote Sensing EvapoTranspiration model (Sim-ReSET): Algorithm and model test. *Journal of Hydrology, 376*(3–4), 476-485. doi: http://dx.doi.org/10.1016/j.jhydrol.2009.07.054

Tian, F., Qiu, G., Yang, Y., Lü, Y., & Xiong, Y. (2013). Estimation of evapotranspiration and its partition based on an extended three-temperature model and MODIS products. *Journal of Hydrology, 498*, 210-220. doi: http://dx.doi.org/10.1016/j.jhydrol.2013.06.038

Tibebe, D. B., W. (2011). Surface Runoff and Soil Erosion Estimation Using the Swat Model in the Keleta Watershed, Ethiopia. *Land Degradation & Development, 22*(6), 551-564. doi: Doi 10.1002/Ldr.1034

Tripathi, R., Sengupta, S. K., Patra, A., Chang, H., & Jung, I. W. (2014). Climate change, urban development, and community perception of an extreme flood: A case study of Vernonia, Oregon, USA. *Applied Geography, 46*(0), 137-146. doi: http://dx.doi.org/10.1016/j.apgeog.2013.11.007

USDA-SCS (United States Department of Agriculture–Soil Conservation Service). (1972). *National Engineering Handbook, Section 4 Hydrology.* Washington, DC.

USDA-SCS. (1986). Technical Release 55, Urban hydrology for small watersheds. (Chapter 9 and 10). *United States Department of Agriculture, Soil Conservation Service.* http://www.wcc.nrcs.usda.gov/hydro//hydro-tools-models-tr55.html.

Vanderhoof, M. K., & Williams, C. A. (2015). Persistence of MODIS evapotranspiration impacts from mountain pine beetle outbreaks in lodgepole pine forests, south-central Rocky Mountains. *Agricultural and Forest Meteorology, 200*, 78-91. doi: http://dx.doi.org/10.1016/j.agrformet.2014.09.015

Velpuri, N. M., Senay, G. B., Singh, R. K., Bohms, S., & Verdin, J. P. (2013). A comprehensive evaluation of two MODIS evapotranspiration products over the conterminous United States: Using point and gridded FLUXNET and water balance ET. *Remote Sensing of Environment, 139*, 35-49. doi: http://dx.doi.org/10.1016/j.rse.2013.07.013

Vicente-Serrano, S. M., Van der Schrier, G., Beguería, S., Azorin-Molina, C., & Lopez-Moreno, J.-I. (2015). Contribution of precipitation and reference evapotranspiration to drought indices under different climates. *Journal of Hydrology, 526*, 42-54. doi: http://dx.doi.org/10.1016/j.jhydrol.2014.11.025

Vu, M. T., Raghavan, S. V., & Liong, S. Y. (2012). SWAT use of gridded observations for simulating runoff - a Vietnam river basin study. *Hydrology and Earth System Sciences, 16*(8), 2801-2811. doi: DOI 10.5194/hess-16-2801-2012

Westerhoff, R. S. (2015). Using uncertainty of Penman and Penman–Monteith methods in combined satellite and ground-based evapotranspiration estimates. *Remote Sensing of Environment, 169*, 102-112. doi: http://dx.doi.org/10.1016/j.rse.2015.07.021

"Global warming creates volatility. I feel it when I'm flying. The storms are more volatile. We are paying the price in more hurricanes and tornadoes."

-Debbie Stabenow

8.1 Summary

In this thesis, the three main objectives of water-induced soil erosion, flash flood prediction and assessment of evapotranspiration have been accomplished step-by-step using a unique approach of modelling. The thesis will be summarized in the form of its goals.

a. The natural problems of WSE and FF have drawn social, media, and scientific attention to them. A general introduction to the issues, basic concepts, thesis outlines and study area are discussed in the first two chapters.

b. The annual water-driven soil erosion (WSE) rate of 4.1 t ha^{-1} y^{-1} was estimated using the SWAT model for the Yen Bai province (including 32 sub-watersheds). Although this rate is considered to be moderate, some steep, non-vegetative areas were suffering serious soil loss of approximately 26 t ha^{-1} y^{-1}. Due to a lack of literature on WSE, the estimated WSE was compared with the soil erosion map (good agreement) for verifying the accuracy of the estimation. The SWAT model presented its ability to generate river discharge matched closely to the observed data verified by accepted R^2 and NSE values. Using different LULC conditions in most of the HRUs in the province, the WSE rates were found to have increased from 0.2 to 3.3 t ha^{-1} y^{-1}. In contrast, few HRUs had a decreasing rate of from −0.1 to −1.9 t ha^{-1} y^{-1}. It was found that the DEM mesh size and the CSA values (defining the spatial watershed model resolutions) had some impacts on estimated WSE patterns and rates. Finally, close correlations were found between surface runoff and precipitation and between surface runoff and estimated soil loss.

c. Event-based sediment load/flow rates of the Nam Kim and Nam Khat watersheds were computed for model planes and channels using the KINEROS2 model with satellite-based and radar rainfalls. The model was calibrated and validated for both kinds of rainfalls (satellite and radar) for an event on 23rd June 2011. The hydraulic conductivity, soil moisture condition were the most sensitive parameters to the simulated sediment yield. The model resolutions (affected by the CSAs) and LULC conditions also had important influences on the model outcomes. In general, using the LULC2007 condition

produced higher SY rates than using the LULC2002. Although, there was no *in situ* SY measurement of this event for validating the simulated SY rate, this study contributed crucial knowledge to understanding the hydrological processes at finer temporal and spatial scales on slopes and in channels.

d. Simple assembled models of the SWAT, BEACH and KINEROS2 were made for the aim of flash flood prediction using several rainfall sources of the satellite, radar, NWP. Based on the results and represented in literature and since the KINEROS2' outputs are very sensitive to the antecedent soil moisture condition, the BEACH model was used to obtain this data. The governing parameters of the three models were calibrated using observed data. The results of the model's calibrations and validations were evaluated at a good level based on the R^2 and NSE values, more than 0.8 and 0.6, respectively. The modelled forecast discharge for planes and channels revealed an opportunity to predict flash flood occurrences. Model uncertainty and computational efficiency were intensively discussed. As the KINEROS2 model showed some limitations of not computing the flow velocity, power and accurate water level, the HEC-RAS model was used for the further flash flood prediction stage.

e. The method of coupling the KINEROS2 and HEC-RAS models showed its advancement in the prediction of the four important characteristics of Q, FV, WL and P. These are considered to be important in shaping the FF occurrences. The crossed relationships between these factors and river geometry like channel slope, top width, flow area were thoroughly analyzed as well. The regionalization method was also applied for ungauged (also poorly gauged) watersheds such as the Nam Khat. Using outputs of a model to serve as input to another is thought to be helpful in solving the data scarcity problem. Once again, much discussion of uncertainty has been addressed in FF forecast, concluding that errors likely came from predicted rainfalls.

f. In the penultimate chapter, long-term (2001-2012) ETs, Q were calculated by the SWAT and BEACH models and they were compared with each other (a good agreement was found with average $R^2 \approx 0.78$ and NSE ≈ 0.64). Monthly and yearly MODIS ETs were also extracted from MODIS datasets based on the MOD16 algorithm. Afterwards, the ETs were compared temporally and spatially with the SWAT and BEACH ETs. Basically, the MODIS ET was computed at higher rates than the SWAT and BEACH ETs. However, a common downward trend of the ET in the 2001-2012 periods was found in all three ET sources.

8.2 Contributions and Limitations

a. Study Contributions

- As there is still a high demand for research into WSE in the tropics using the SWAT model (the SWAT model was developed for arid/semi-arid regions), the calibrated model parameters could establish cornerstones for future similar studies in the tropics.
- Using the method of transferring model parameters from calibrated watersheds to ungauged ones (it has not been done by many others) revealed a capability to model ungauged areas hydraulically. The modelled WSE information might be helpful for later usages (there was no *in situ* soil loss measurement in the study area).
- Most WSE modelling works have focused on large scales. However, this application of KINEROS2 provided an in-depth look into the hydrological processes in single and series rainfall events including sediment transport. Therefore, a better understanding of the processes could be gained.
- Based on current search engines, this study is one of very first studies into this problem of FF prediction *for the region (North Vietnam)*. This part of the research not only provides a flash flood guidance system with timely, spatially predicted discharge for flooding planes and streams, but also precise soil moisture data. This information is crucial for other purposes of hydrological modelling and extremely difficult to obtain accurately in large areas.
- Coupling and assembled series of models could be a good approach in producing quick responses to some kinds of natural hazards such as flash flooding. This method has been done in this research and could be valuable for wider applications in the scientific community.
- The in-depth analyses of flooding behavior in streams using a hydrological engineering model (HEC-RAS) could help to understand FFs and also their indicators better. Frequent discussions on the uncertainty, error sources and computational efficiency have been provided.
- The penultimate chapter provides valuable data of runoff and evapotranspiration for the local area. The decreasing trend of ET might reveal something interesting about the significant changes in the water cycle of the region.

b. Limitations

- As the SWAT model was simulated for a 12-year period, a longer model simulation *could* produce better outputs (previous literature has suggested a 20 year period).
- Due to lack of *in situ* soil loss observation in the study area, the modelled soil loss rates were only compared to the rates from the large scale soil erosion map.
- The method of transferring model parameters from calibrated watersheds to ungauged ones has its limitation of unequal precision in the whole model. This means the errors in an uncalibrated watershed are likely to be larger than in calibrated ones.
- Assembled and coupling models have both advantages and disadvantages. The final model outputs might have cumulative errors from all the applied models, particularly the significant effects in regard to the first model's errors in the assembly.
- The results of FF prediction showed some false alarms and this was discussed and linked to the NWP models. This research might need more accurate forecasted rainfalls in order to gain better results.

8.3 Recommendations

Learning from the research limitations, some corresponding recommendations are suggested for continuous future work on the topic as follows:

- As the SWAT was developed for arid, semi-arid river basins, when applied to the tropics, more parameter calibrations and a longer simulation time would improve the model adaptation.
- More work on accurate field measurement of WSE or on other methods is still needed for more precise calibrations and validations for the modelled sediment yield.
- Currently, world-wide data is available (remote sensing, global scale models). The ungauged watersheds could be validated using these data sources.
- The hydrological modelling framework using assembled models would be an appropriate approach for natural disaster adaptation or mitigation. However, it is recommended that all the models should be verified and certified and the model's inputs must also be examined.
- Improving precipitation estimates and forecast could be an interesting topic for future studies. Rainfall from a new radar generation is suggested as a good data source for such research. However, to set up new radar stations needs a great deal of investment and sometimes politics. Therefore, much work needs to be done in connection with this.

Academic Curriculum Vitae
Nguyen Hong Quang

1. Personal Information

Name:	Nguyen Hong Quang
Date and Place of Birth:	1977 / Thai Binh, Vietnam
Gender:	Male
Email:	hongquang116@yahoo.com

2. Employment

Geodesy engineering	Full time	2000- current	Vietnam Natural Resources and Environment Corporation

3. Education

Ph.D. Research in Remote Sensing and GIS	Full time	2012-2016	Dept. Cartography, GIS and Remote Sensing, University of Göttingen, Germany
M.Sc. in Geodesy	Full time	2004-2007	Hanoi University of Mining and Geology
B.Sc. in Land survey	Full time	1995-1999	Hanoi University of Mining and Geology

4. Publications

1) Nguyen, Hong Quang, Degener, Jan, & Kappas, Martin. (2015). Flash Flood Prediction by Coupling KINEROS2 and HEC-RAS Models for Tropical Regions of Northern Vietnam. *Hydrology, 2(4),* 242-265; doi:10.3390/hydrology2040242
2) Nguyen, Hong Quang, & Kappas, Martin. (2015). Modeling Surface Runoff and Evapotranspiration using SWAT and BEACH for a Tropical Watershed in North Vietnam, Compared to MODIS Products. *International Journal of Advanced Remote Sensing and GIS, Vol. 4.* 1367-1384
3) Nguyen, Hong Quang, Degener, Jan, & Kappas, Martin. (2015). Flash flooding prediction in regions of northern Vietnam using the KINEROS2 model. *Hydrology Research, IWA Publishing* (accepted on 12-11-2015)
4) Nguyen, Hong Quang, & Kappas, Martin. (2015). Event-based, Water-induced Soil Erosion Modelling for Medium Watersheds in Yen Bai Province, Vietnam Using the KINEROS2 Model. *Conference proceedings, FIG Conference,* May 2015, Sofia, Bulgaria.